

## 5-1 INTRODUCTION

Using steam to provide mechanical work probably owes its birth to the need for pumping water from coal mines. The very first successful attempt at this was a "pumping engine" built by Thomas Savery (1650-1715) in England. In Savery's engine, steam at pressures between 50 and 100 psig (4.5 to 8 bar) acted directly upon the surface of water in a chamber to force it up through a pipe. A crude check valve prevented reverse flow. After the chamber was cleared of water, steam supply was manually cut off and cold water was applied over the chamber, thus condensing the steam inside and creating a vacuum that sucked in more water. The direct contact between steam and water caused large condensation losses, and the lack of safety valves was responsible for many explosions.

At about the same time, Denis Papin (1647-1712), who invented the safety valve, conceived of the idea of separating the steam and water by a piston, and Thomas Newcomen (1663-1729) designed and built an engine with one. In it low-pressure steam was admitted to a vertical cylinder, where it pushed the piston upwards. The steam left in the cylinder was then condensed by a jet of outside cold water, creating a vacuum in the cylinder. The outside atmospheric pressure pushed the piston back on the working stroke, hence the name "atmospheric engine." The piston was attached to one end of a beam that had a fulcrum about midpoint. A piston in a separate pumping cylinder was attached to the other end. The pump piston was smaller in diameter than the steam piston, so a greater water pressure than steam pressure was obtained. The various valves of Newcomen's engine were operated manually at first. Automatic operation, the first on record, was conceived by a small lad who was hired to operate

the valves. Being smaller and lazier than the others, as the story goes, he noticed the regular pattern of beam and valve operation and rigged up a string mechanism that allowed the beam to actuate the valves. Newcomen's engine used one-third less coal per hph than Savery's.

It was not until some 60 years later that James Watt\* developed the ideas of the "modern" reciprocating steam engine. Working as an instrument maker, he was called upon one day in 1764 to repair a Newcomen engine and noticed the waste of steam condensed in the cylinder. In 1765 he conceived of the idea of a separate condenser, and subsequently ideas such as the working stroke caused by steam expansion, the double-acting cylinder, the flyball throttling governor, the conversion of reciprocating to rotary motion (in 1781), and other important features. His now-famous engine was a major contributor to the industrial revolution. Watt's engine used 60 percent less coal than Newcomen's and 75 percent less than Savery's.

The next major improvement was made by Corliss (1817-1888), who developed the quick-closing intake valves that bear his name which reduce throttling during closing. The Corliss engine used about half as much coal as Watt's but still four or five times as much as modern steam-turbine powerplants. Next came Stumpf (1863-?), who developed the "uniflow engine," which was designed to further reduce condensation losses.

The reciprocating steam engine reached its pinnacle in size when it was called upon to drive the then-giant 5-MW electric generators early in the twentieth century. No larger engines were built then or after, although performance continued to improve mainly with the uniflow engine. But about that time electric generators were capable of getting bigger with no reciprocating engines large enough to drive them. Enter the steam turbine, not a new idea by any means, for the need for it was foreseen by many inventors in the late 1800s. Like many great inventions, it became practical when the world needed it.

Actually, history's first recorded steam turbine was one built by Hero of Alexandria about the first century A.D. It consisted of a hollow sphere that was free to turn about a horizontal axis between two fixed tubes that connected it to a caldron or boiler (Fig. 5-1). Steam, generated in the caldron, enters the sphere and exits to the atmosphere tangentially via two nozzles situated in the plane perpendicular to the axis of rotation and pointing in opposite directions. The steam leaving the nozzles causes the sphere to rotate in a manner similar to that of water ejecting from a lawn sprinkler. Hero's turbine thus operated on the *reaction principle* (Sec. 5-3). Much later, about 1629, a steam turbine used a jet of steam that impinged on blades projecting from a wheel.

\* James Watt (1736-1819) was a Scottish self-educated instrument maker and inventor. Besides his famous engine, he is credited with the first meaningful research on the properties of steam. He ran into considerable financial difficulties that necessitated borrowing money from benefactors before his engine became a financial success. In 1769 he took a patent for "A New Invented Method of Lessening the Consumption of Steam and Fuel in Fire Engines." In 1775 he went into partnership with Matthew Boulton, a manufacturer in Birmingham. The partnership lasted 25 years. Unlike many great inventors, his achievements were recognized during his lifetime. He was awarded a doctor of laws degree from Glasgow University in 1806, was made a foreign associate of the French Academy of Sciences in 1814, and was offered a baronetcy, which he declined because of modesty.

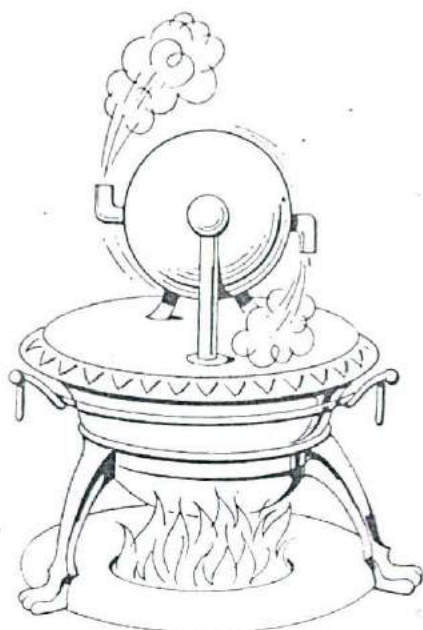


Figure 5-1 The aeolipile of Hero of Alexandria (from *Aeolus*, "god of the winds," and *pila*, a "ball") the first recorded steam turbine in history.

thus causing it to rotate. This turbine operated on the *impulse principle* (Sec. 5-2). Later yet, in 1831, William Avery of the United States built the first steam turbines, which were used commercially in sawmills and woodcutting shops, with at least one tried on a locomotive. The Avery turbine had similarities to Hero's in that it used a hollow shaft with two 2.5-ft-long hollow arms attached to it at right angles with a small opening at the end of each and each pointing in opposite directions. Steam supplied through the hollow shaft exited through the openings and caused the shaft to rotate. Avery's, like Hero's, was therefore a reaction turbine. The turbines, though claiming similar efficiencies as contemporary reciprocating steam engines, were abandoned because of high noise level, difficult regulation, and frequent breakdowns.

The turbines that were destined to take over from the reciprocating engine, however, came about late in the nineteenth century as a result of the efforts of a handful of men, the most prominent of whom were Gustav de Laval\* of Sweden and Charles Parsons† of England. de Laval first developed a small, high-speed (42,000 r/min)

\* Carl Gustav Patrick de Laval (1845-1913), an engineering graduate of the University of Upsala, Sweden, was an inventor whose main income came from a cream separator and was spent on various other unprofitable inventions. The turbine he invented was intended for a cream separator. Also active in public affairs, he became a member of both houses of parliament and was honored repeatedly for his contributions to technology.

† Sir Charles Algernon Parsons (1854-1931), an upper-class Englishman, was motivated by the need to find a steam drive for ships. He is credited with developing the *reaction-stage principle*.

reaction turbine but did not consider it practical and so turned to the development of a reliable single-stage impulse turbine, which bears his name until today. He is also credited with being the first to employ a convergent-divergent nozzle for use in that turbine. The first unit was tested in 1890 and the first commercial unit, 5 hp, went into service in 1891. In 1892 he built a 15-hp turbine with two wheels for ships: one for forward and one for astern propulsion. Parsons developed the multistage reaction turbine, a low-speed machine for use in ships. The first Parsons turbine was built in 1884. The first ship ever to use a turbine was launched in 1895 and, naturally, was called the "Turbinia." It also had two sets of elements, one for forward and one for astern propulsion. Later on some turbine-generator sets were installed in both ships and powerplants.

In addition to de Laval and Parsons, C. E. A. Rateau of France developed the multistage impulse principle (pressure staging), Charles G. Curtis of the United States developed the velocity-compounded impulse stage, and George Westinghouse, also of the United States, secured American rights to the Parson's turbine and installed the first U.S. commercial units of 400-kW capacity at the Westinghouse Air Brake Co., Wilmerding, Pennsylvania.

Shortly after the turn of the century, steam turbines began to replace reciprocating steam engines in powerplants. Rapid development ensued. By 1909 12-MW units were installed in the Fisk powerplant in Chicago. The turbine performance and efficiency exceeded those of the reciprocating engine and allowed the use of superheated steam on an expanding scale. This led to the use of cast steel rather than cast iron in turbines. Capacities rose steadily. A 208-MW unit was installed in New York in 1929. The rise was helped in 1937 by the use of hydrogen-cooled, 3600-r/min electric generators. By the late 1950s capacities reached 450 MW. In the post-World War II era, capacities rose beyond 1000 MW and 3600 r/min became a standard in the United States for 60-Hz current (3000 for 50-Hz current in most of the rest of the world) for high-pressure units and 1800 r/min (1500 non-U.S.) for the low-pressure units used in water-cooled nuclear reactors. The steam turbine today is the mainstay of electric-power generation and promises to continue in that role for the foreseeable future.

Gas turbines are as old as windmills since a windmill is essentially a gas (air) turbine. An early gas device called the *smokejack* was operated by hot gases rising through a fireplace chimney. The smokejack is believed to have been first sketched by Leonardo da Vinci and later described by John Wilkins, an English clergyman, in his book *Mathematical Magick* in 1648. Other attempts followed, including work by John Barber of England, who received a patent in 1871 for a device that compressed air and produced gas in a cylinder and then burned and directed the mixture to a turbine wheel through nozzles. The first significant advance was by F. Stolze of Germany, whose turbine consisted of components similar to those of today's gas turbines: a separately fired combustion chamber and a multistage axial-flow compressor coupled directly to a multistage reaction turbine. The efficiencies of compressor and turbine and the gas temperatures, however, were too low to permit successful operation. The first successful gas turbine was built in 1903 in France. It consisted of a multistage reciprocating compressor, combustion chamber, and a two-row impulse turbine. It had a thermal efficiency of about 3 percent. Further progress was slow.

In more modern times, during World War II developers in Switzerland, a country isolated by the war, developed the technology for power generation by gas turbines. Sir Frank Whittle of England was one of many who recognized the applicability of gas turbines for jet propulsion of aircraft. Such efforts led to the development of the jet fighter and subsequently jet transport in many countries.

The gas turbine is now used in the utility industry mainly as a peaking unit (to deliver excess power during periods of high demand), for powering isolated locations, on oil pipeline routes, and more recently, in combined-cycle (gas and steam) powerplants (Chap. 8).

## 5-2 THE IMPULSE PRINCIPLE

Before discussing the impulse turbine, a review of the *impulse principle* may be useful. Consider a horizontal fluid jet impinging in the  $+x$  direction on a fixed vertical flat plate (Fig. 5-2a). That fluid will spread out along the plate, its velocity in the direction of the jet reduced to zero, and will impart to it a horizontal force  $F$  in the  $+x$  direction. This force is called an *impulse* and is equal to the change in momentum of the jet in the  $+x$  direction

$$F = \frac{m}{g_c} (V_x - 0) = \frac{\dot{m}}{g_c} V_x \quad (5-1)$$

- where
- $F$  = force or impulse,  $\text{lb}_f$  or  $\text{N}$
  - $\dot{m}$  = mass-flow rate of the jet,  $\text{lb}_m/\text{s}$  or  $\text{kg}/\text{s}$
  - $V_x$  = velocity in the horizontal direction,  $\text{ft}/\text{s}$  or  $\text{m}/\text{s}$
  - $g_c$  = conversion factor,  $32.2 \text{ lb}_m \cdot \text{ft}/(\text{lb}_f \cdot \text{s}^2)$  or  $1 \text{ kg} \cdot \text{m}/(\text{N} \cdot \text{s}^2)$

Now consider that the plate is free to move in the horizontal direction (Fig. 5-2b) with a velocity  $V_B$ .  $V_x - V_B$  will be the velocity of the jet relative to the plate. Now the force on the plate is

$$F = \frac{\dot{m}}{g_c} (V_x - V_B) \quad (5-2)$$

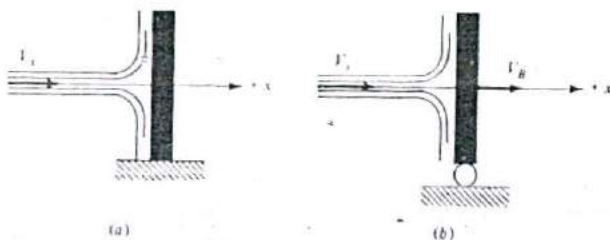


Figure 5-2 The impulse of a fluid jet on (a) a fixed flat plate and (b) a moving flat plate.

and because the plate is moving, work is being done on it equal to the product of force and distance. In a unit time, that distance is  $V_B$ , so that the work done per unit time, or the power, in  $\text{ft} \cdot \text{lb}_f/\text{s}$  or watts, is

$$\dot{W} = FV_B = \frac{\dot{m}}{g_c} V_B (V_1 - V_B) \quad (5-3)$$

The efficiency of the flat plate is obtained by dividing the work, Eq. (5-3), by the initial power of the jet  $\dot{m}V_1^2/2g_c$  (kinetic energy per unit time). Thus

$$\eta_{\text{plate}} = 2 \left[ \frac{V_B}{V_1} - \left( \frac{V_B}{V_1} \right)^2 \right] \quad (5-4)$$

where  $\dot{W}$  = work per unit time, a power,  $\text{ft} \cdot \text{lb}_f/\text{s}$  or watts. Note the power is zero if  $V_B$  is zero (fixed plate) or if  $V_B = V_1$ , since no force will be exerted by the jet. Thus there is an optimum plate velocity  $V_B$  which maximizes the power. It is found by differentiating  $\dot{W}$  with respect to  $V_B$  and equating the derivative to zero, or

$$\frac{d}{dV_B} \left[ \frac{\dot{m}}{g_c} (V_1 V_B - V_B^2) \right] = \frac{\dot{m}}{g_c} (V_1 - 2V_B) = 0$$

Thus the optimum plate velocity is half the jet velocity

$$V_{B,\text{opt}} = \frac{V_1}{2} \quad (5-5)$$

and the maximum power is

$$\dot{W}_{\text{max}} = \frac{\dot{m}V_1^2}{4g_c} \quad (5-6)$$

which also happens to be half the power or kinetic energy per unit time of the jet. Thus the maximum efficiency of converting the jet energy to the plate is 50 percent, as can be verified from Eq. (5-4).

Now, instead of a flat plate, consider a cylindrical blade that allows the jet to reverse direction (Fig. 5-3). Again the jet enters the blade with a *relative velocity*  $V_1 - V_B$ . Consider further that the blade is frictionless and that there is neither expansion nor contraction of the fluid between blade entry and exit. The fluid relative exit velocity is therefore also  $V_1 - V_B$ . The absolute velocity of the jet at exit in the  $+x$  direction will now be  $V_B - (V_1 - V_B) = (2V_B - V_1)$ . The impulse equal to the change in momentum is then equal to

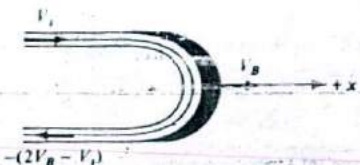


Figure 5-3 The impulse of a fluid jet on a 180° curved blade.

$$F = \frac{\dot{m}}{g_c} [V_i - (2V_B - V_i)] = \frac{2\dot{m}}{g_c} (V_i - V_B) \quad (5-7)$$

and the work per unit time is  $FV_B$  or

$$\dot{W} = 2 \frac{\dot{m}}{g_c} V_B (V_i - V_B) \quad (5-8)$$

We shall now define a *blade efficiency*  $\eta_b$  as the ratio of the power, Eq. (5-8), to the initial power of the jet,  $\dot{m}V_i^2/2g_c$ , or

$$\eta_b = 4 \left[ \frac{V_B}{V_i} - \left( \frac{V_B}{V_i} \right)^2 \right] \quad (5-9)$$

and  $F$ ,  $\dot{W}$ , and  $\eta_b$ , Eqs. (5-7) to (5-9), for the blade are twice the values for the flat plate, Eqs. (5-2) to (5-4).

To find the optimum blade velocity that results in maximum power, again differentiate  $\dot{W}$  with respect to  $V_B$  and equate to zero, also giving

$$V_{B,\text{opt}} = \frac{V_i}{2} \quad (5-10)$$

and

$$\dot{W}_{\text{max}} = \frac{\dot{m}V_i^2}{2g_c} \quad (5-11)$$

The optimum blade velocity is half the jet velocity, the same as for the flat plate, but the maximum power is twice that for the flat plate and equal to the total kinetic energy (per unit time) of the jet. In other words, the *maximum blade efficiency* as can be verified from Eq. (5-9) is

$$\eta_{B,\text{max}} = 100\% \quad (5-12)$$

Because the blade moves away from the jet, continuous power can be obtained only if a series of blades were mounted on the circumference of a wheel so that as the wheel rotates they continually face the jet. A high-speed jet needs a nozzle which has physical dimensions so that it is impossible to have the jet impinging on the blades in their direction of motion but at a shallow angle  $\theta$  (Fig. 5-4). The blade-entrance angle also cannot be zero from horizontal because it should correspond nearly to the relative fluid direction. The blade-exit angle also cannot be zero from horizontal or

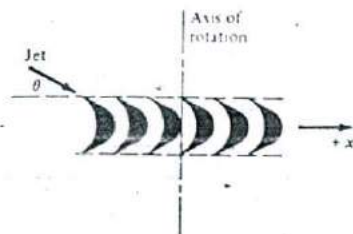


Figure 5-4 Top view of a row of impulse blades on wheel.

else the fluid would not be able to leave the row of successive blades. The practical blade, therefore, is turned around an angle less than  $180^\circ$ .

### The Velocity Diagram

To evaluate the work on the blade, which is in the direction of motion, one then needs to construct a velocity vector diagram, shown for a single blade in Fig. 5-5. Figure 5-5a shows the velocity diagram in relation to the blade. Figure 5-5b and c shows simplified versions of it, called "extended" diagrams, with the blade shape removed. In these diagrams

$V_{r1}$  = absolute velocity of fluid leaving nozzle

$V_B$  = blade velocity

$V_{r1}$  = relative velocity of fluid (as seen by an observer riding on the blade)

$V_{r2}$  = relative velocity of fluid leaving blade

$V_{r2}$  = absolute velocity of fluid leaving blade

$\theta$  = nozzle angle

$\phi$  = blade entrance angle

$\gamma$  = blade exit angle

$\delta$  = fluid exit angle

The work on the blade may be obtained from impulse-momentum principles as above or from first-law principles. Both methods yield numerically identical results.

From *impulse momentum*, the force, a vector quantity in the direction of motion of the blade, is equal to the change in momentum of the fluid in the direction of motion, or

$$F = \frac{\dot{m}}{g_c} (V_{r1} \cos \theta - V_{r2} \cos \delta) \quad (5-13a)$$

The component of the steam velocity in the direction of blade motion is called the *velocity of whirl*. Thus  $V_{r1} \cos \theta$  is the entrance velocity of whirl  $V_{w1}$ , and  $V_{r2} \cos \delta$  is the exit velocity of whirl  $V_{w2}$  and the force may be written as

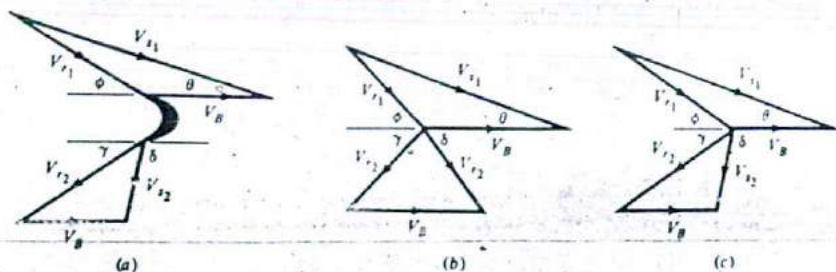


Figure 5-5 Velocity diagrams on a single-stage impulse blade.



$$F = \frac{\dot{m}}{g_c} (V_{w1} - V_{w2}) \quad (5-13b)$$

The work per unit time (power) is equal to the product of force and distance traveled by the blade in unit time or the product of force and velocity. Thus

$$\dot{W} = \frac{\dot{m}V_B}{g_c} (V_{x1} \cos \theta - V_{x2} \cos \delta) \quad (5-14)$$

Note that if both  $\theta$  and  $\delta$  are 0,  $V_{x2} = V_B - (V_{x1} - V_B)$  in the  $+x$  direction (for frictionless, nonexpansion or noncontraction flow), and Eq. (5-14) reverts to Eq. (5-8). Note also that  $\cos \delta$  is positive if  $\delta$  is less than  $90^\circ$  (Fig. 5-5b) and negative if  $\delta$  is greater than  $90^\circ$  (Fig. 5-5c), so that the work is greater if  $\delta$  is greater.

The blade efficiency again is defined as the ratio of the blade work, Eq. (5-14), to the initial energy of the jet  $\dot{m}V_{x1}^2/2g_c$  or

$$\eta_B = 2 \left[ \left( \frac{V_B}{V_{x1}} \right) \cos \theta - \left( \frac{V_B}{V_{x1}} \right) \left( \frac{V_{x2}}{V_{x1}} \right) \cos \delta \right] \quad (5-15)$$

*Optimum blade speed.* By analogy with the  $180^\circ$  blade, the relative velocity of fluid entering blade in the  $+x$  direction is  $V_{x1} \cos \theta - V_B$ . With no friction, expansion, or contraction, that is also the relative velocity leaving the blade but in the  $-x$  direction. The absolute velocity of the fluid leaving the blade in the  $+x$  direction,  $V_{x2} \cos \delta$ , is therefore  $V_B - (V_{x1} \cos \theta - V_B) = (2V_B - V_{x1} \cos \theta)$ . Equation (5-14) can thus be written in the form

$$\dot{W} = \frac{2\dot{m}V_B}{g_c} (V_{x1} \cos \theta - V_B) \quad (5-16)$$

The optimum blade speed that yields maximum work is again obtained by differentiating  $\dot{W}$  with respect to  $V_B$  and equating the derivative to zero, giving

$$V_{B,\text{opt}} = \frac{V_{x1} \cos \theta}{2} \quad (5-17)$$

The maximum work is obtained by substituting Eq. (5-17) into Eq. (5-16), giving

$$\dot{W}_{\text{max}} = \frac{\dot{m}}{2g_c} (V_{x1} \cos \theta)^2 = \frac{2\dot{m}}{g_c} V_{B,\text{opt}}^2 \quad (5-18)$$

The maximum blade efficiency is obtained by dividing  $\dot{W}_{\text{max}}$  by  $\dot{m}V_{x1}^2/2g_c$ , giving

$$\eta_{B,\text{max}} = (\cos \theta)^2 \quad (5-19)$$

An examination of the velocity diagram shows that in ideal flow where  $V_{r1} = V_{r2}$  and when  $\phi = \gamma$ , the optimum blade velocity which results in maximum work also results in  $\delta = 90^\circ$ , or absolute exit velocity straight in the axial direction. In that case  $V_{x2} \cos \delta$ , the exit velocity of whirl, is zero. Equations (5-17) to (5-19) revert to Eqs. (5-10) to (5-13) for  $\theta = 0$ .

From the *first-law principles*, with no change in potential energy and no heat

transfer, the work is equal to the decrease in enthalpies and absolute kinetic energies of the fluid

$$\dot{W} = (H_1 - H_2) + \dot{m} \left( \frac{V_{r1}^2}{2g_c} - \frac{V_{r2}^2}{2g_c} \right) \quad (5-20)$$

where  $H_1$  and  $H_2$  are the enthalpies of the fluid entering and leaving the blade, respectively.  $H_1 - H_2$  is obtained by considering fluid flow relative to the blade (as seen by an observer riding on the blade), where only relative velocities and no work are observed. Thus

$$H_1 - H_2 = \left( \frac{V_{r2}^2}{2g_c} - \frac{V_{r1}^2}{2g_c} \right) \quad (5-21)$$

Combining with Eq. (5-20) gives

$$\dot{W} = \frac{\dot{m}}{2g_c} [(V_{s1}^2 - V_{s2}^2) - (V_{r1}^2 - V_{r2}^2)] \quad (5-22)$$

This is a *general* equation for the work in *any* blade, i.e., including friction, expansion, or contraction of the fluid through the blade passage. In the case of a *pure* impulse blade, where none of these effects is present,  $H_1 = H_2$ ,  $V_{r1} = V_{r2}$ , and

$$\dot{W}_{\text{pure impulse}} = \frac{\dot{m}}{2g_c} (V_{s1}^2 - V_{s2}^2) \quad (5-23)$$

Values of  $V_{s1}$  and  $V_{s2}$  are obtained from the nozzle equation,  $V_B$  and the various blade angles. In an impulse blade with friction, the usual method of describing the effect of friction is by the use of a *velocity coefficient*  $k_v$ , less than one and given by

$$k_v = \frac{V_{r2}}{V_{r1}} \quad (5-24)$$

We shall now define *stage efficiency*  $\eta_{\Delta H}$ . This is the work of the blade divided by the total enthalpy drop of the fluid for the whole stage, i.e., including nozzle and blade, if expansion of the fluid were reversible and adiabatic,  $\Delta H_s$

$$\eta_{\Delta H} = \frac{\dot{W}}{\Delta H_s} = \frac{\dot{W}}{\dot{m} \Delta h_s} \quad (5-25)$$

**Example 5-1** 100 lb<sub>m</sub>/s of steam enter and leave the nozzle of an impulse turbine stage at 400 psia and 500°F, and 200 psia, respectively. The nozzle efficiency is 90 percent. The nozzle angle is 20°. The blade is symmetrical, travels at optimum velocity, and has a velocity coefficient of .97. Calculate the blade angle, stage power in horsepower and megawatts, and the blade and stage efficiencies.

**SOLUTION** From the steam tables, App. A, steam conditions entering nozzle (Fig. 5-6) are  $h_n = 1307.4$  Btu/lb<sub>m</sub>,  $s_n = 1.5901$  Btu/(lb<sub>m</sub> · °R). Steam conditions

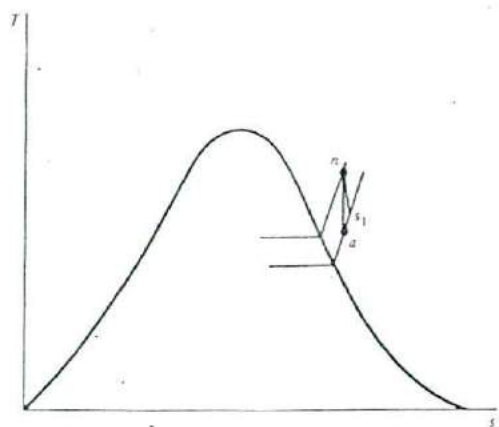


Figure 5-6  $T$ - $s$  diagram for nozzle of Example 5-1.

leaving nozzle if it were adiabatic reversible at  $a$  are  $s_a = 1.5901 \text{ Btu}/(\text{lb}_m \cdot ^\circ\text{R})$  and by interpolation at 200 psia,  $h_a = 1237.2 \text{ Btu}/\text{lb}_m$ .

$$\text{Nozzle isentropic enthalpy drop} = 1307.4 - 1237.2 = 70.2 \text{ Btu}/\text{lb}_m$$

$$\text{Nozzle actual enthalpy drop} = 0.9 \times 70.2 = 63.18 \text{ Btu}/\text{lb}_m$$

$$V_{s1} = \sqrt{2 \times 32.2 \times 778.16 \times 63.18} = 1779.4 \text{ ft/s}$$

Refer to Fig. 5-5

$$\text{where } \theta = 20^\circ, V_{s1} \cos \theta = 1672.1 \text{ ft/s}$$

$$V_{B, \text{opt}} = V_{s1} \cos \theta/2 = 836.05 \text{ ft/s}$$

$$V_{r1} \sin \phi = V_{s1} \sin \theta = 608.6 \text{ ft/s}$$

$$V_{r1} \cos \phi = V_{s1} \cos \theta - V_B = 836.05 \text{ ft/s}$$

$$\text{from which } V_{r1} = 1034.1 \text{ ft/s and } \phi = 36.05^\circ$$

$$V_{r2} = k V_{r1} = 1034.1 \times 0.97 = 1003.1 \text{ ft/s}$$

$$V_{r2} \sin \gamma = V_{r2} \sin \delta, \gamma = \phi$$

$$V_{r2} \cos \gamma + V_{r2} \cos \delta = V_B$$

$$\text{from which } V_{r2} = 590.8 \text{ ft/s, } \delta = 87.57^\circ$$

Refer to Eq. (5-14)

$$\begin{aligned} \dot{W} &= \frac{1000 \times 836.1}{32.17} (1672.1 - 25.1) = 4.28 \times 10^7 \text{ ft} \cdot \text{lb}_f/\text{s} \\ &= 77,818 \text{ hp} = 58.03 \text{ MW} \end{aligned}$$

Refer to Eq. (5-22)

$$\begin{aligned}\dot{W} &= \frac{1000}{2 \times 32.17} [(1779.4^2 - 590.8^2) + (1003.1^2 - 1034.1^2)] \\ &= 4.28 \times 10^7 \text{ ft} \cdot \text{lb}_f/\text{s}\end{aligned}$$

which confirms Eq. (5-14).

$$\begin{aligned}\text{Blade efficiency} &= \frac{\dot{W}}{(\dot{m}V_{s1}^2/2g_c)} = \frac{4.28 \times 10^7 \times 2 \times 32.17}{1000 \times 1779.4^2} \times 100 \\ &= 86.97\%\end{aligned}$$

$$\begin{aligned}\text{Stage efficiency} &= \frac{\dot{W}}{\dot{m}(h_n - h_a)} = \frac{4.28 \times 10^7}{1000 \times 70.2 \times 778.16} \times 100 \\ &= 78.35\%\end{aligned}$$

### 5-3 IMPULSE TURBINES

Impulse turbines or turbine stages are simple, single-rotor or multirotor (compounded) turbines to which impulse blades are attached. Impulse blades can be recognized by their shape. They are usually symmetrical and have entrance and exit angles,  $\phi$  and  $\gamma$  respectively, around  $20^\circ$ . Because they are usually used in the entrance high-pressure stages of a steam turbine, when the specific volume of steam is low and requires much smaller flow areas than at lower pressures, the impulse blades are short and have constant cross sections.

Impulse turbines are also characterized by the fact that most or all of the enthalpy, and hence the pressure, drop occurs in the nozzles (or fixed blades that act as nozzles) and little or none in the moving blades. What pressure drop occurs in the moving blade is a result of friction that gives rise to the velocity coefficient  $k_v$ , discussed above. Single-rotor and compounded impulse steam turbines will now be discussed.

#### The Single-Stage Impulse Turbine

The *single-stage impulse turbine*, also called the *de Laval turbine* after its inventor (see Introduction, Sec. 5-1), consists of a single rotor to which impulse blades are attached. The steam is fed through one or several convergent-divergent nozzles which do not extend completely around the circumference of the rotor, so that only part of the blades are impinged upon by the steam at any one time. The nozzles also allow governing of the turbine by shutting off one or more of them.

The velocity diagram for a single-stage impulse turbine has been shown in Fig. 5-5. Figure 5-7 shows the overall pressure and absolute steam-velocity changes in the nozzle and blade passages for an ideal turbine. As can be seen the pressure drop occurs in the nozzle and not in the blades. Maximum velocity, and hence kinetic energy, of

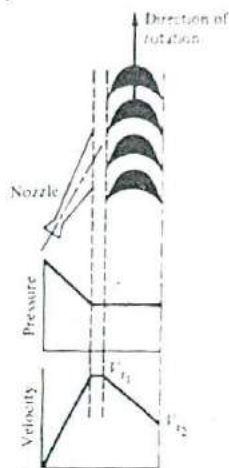


Figure 5-7 Overall steam pressure and absolute steam-velocity changes in an ideal single-stage impulse (deLaval) turbine.

the steam occurs at nozzle exit and decreases from  $V_{r1}$  to  $V_{r2}$  in the blades. The linear changes in pressure and velocity shown are only schematic and do not represent the actual processes.

### Compounded-Impulse Turbines

It has been shown that the optimum blade speed in a single-stage impulse turbine is  $0.5 V_{r1} \cos \theta$  or roughly one-half of the incoming absolute steam velocity,  $\theta$  being small. Steam expanding from modern boiler conditions, say 2400 psia and 1000°F to the condenser pressure of 1 psia (or even to atmospheric pressure) in a single nozzle stage, will have velocities of about 5400 ft/s (1645 m/s), meaning a blade speed of 2700 ft/s (820 m/s). Such a speed is far beyond the maximum allowable safety limits because of centrifugal stresses on the rotor material. In addition, the large steam velocities result in large friction losses (proportional to the square of the velocity) and a reduction in turbine efficiency. The high rotor speeds would also necessitate large and bulky reduction gearing to the electric generator. To overcome these difficulties, two methods have been utilized, both called *compounding* or *staging*. One is the *velocity-compounded* turbine, and the other the *pressure-compounded* turbine.

#### The Velocity-Compounded Impulse Turbine

The velocity-compounded turbine was first proposed by C. G. Curtis (see Introduction) to solve the problems of a single-stage impulse turbine for use with high pressure and temperature steam. The *Curtis stage* turbine, as it came to be called, is composed of one stage of nozzles as the single-stage turbine, followed by two rows of moving blades instead of one. These two rows are separated by one row of fixed blades attached to the turbine stator, which has the function of redirecting the steam leaving the first

row of moving blades to the second row of moving blades. A Curtis stage impulse turbine is shown in Fig. 5-8 with schematic pressure and absolute steam-velocity changes through the stage. In the Curtis stage, the total enthalpy drop and hence pressure drop occur ideally in the nozzles so that the pressure remains constant in all three rows of blades. The kinetic energy of the steam leaving the nozzle at  $V_{r1}$ , however, is utilized in both rows of moving blades instead of a single row as before. The absolute velocity of the steam decreases from  $V_{r1}$  to  $V_{r2}$  in the first row of moving blades, remains essentially constant in the fixed blades, enters the second row of moving blades at  $V_{r3}$ , and leaves at  $V_{r4}$ . Ideally  $V_{r2} = V_{r3}$ , but actually there is a loss as a result of friction in the fixed blades so that  $V_{r3} < V_{r2}$  and they are related by a velocity coefficient  $k_v$  similar to that of Eq. (5-24).

The velocity diagram for a Curtis stage, with friction in moving and fixed blades, is shown in Fig. 5-9. The procedure for constructing that diagram is the same as that for the single-stage impulse turbine (Fig. 5-5). In the diagram, because of friction

$$\begin{aligned} V_{r2} < V_{r1} & \quad \frac{V_{r2}}{V_{r1}} = k_{v1} \\ V_{r3} < V_{r2} & \quad \frac{V_{r3}}{V_{r2}} = k_{v2} \\ V_{r4} < V_{r3} & \quad \frac{V_{r4}}{V_{r3}} = k_{v3} \end{aligned} \quad (5-26)$$

Using an analysis similar to that used for the single-stage impulse turbine, it is easy to write expressions for the work of the Curtis stage using either a momentum-impulse or first law analysis. The latter yields

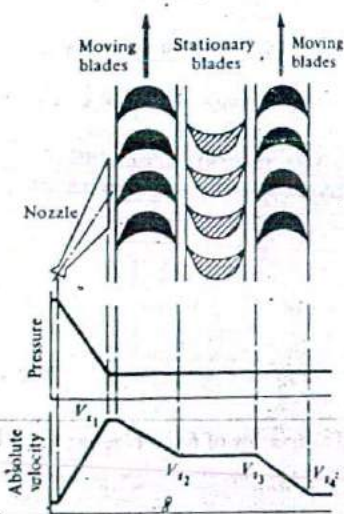


Figure 5-8 Overall steam pressure and absolute steam velocity changes in an ideal velocity-compounded impulse turbine (a Curtis stage).

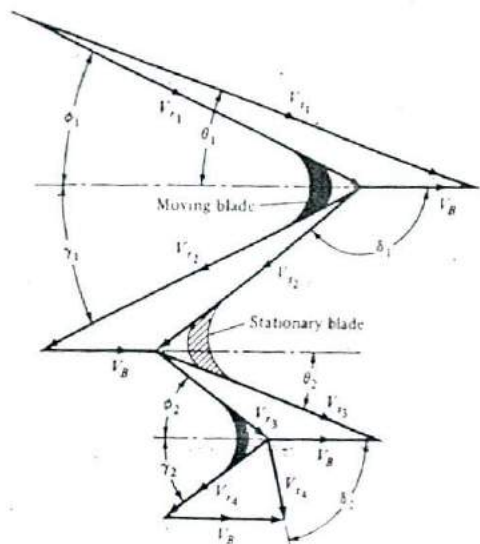


Figure 5-9 Velocity diagram for a Curtis stage, drawn with  $V_B$  the same in both moving blades and with friction taken into account. Note the effect of velocity change on blade angles.

$$\dot{W} = \frac{\dot{m}}{2g_c} \{ [(V_{11}^2 - V_{12}^2) + (V_{22}^2 + V_{21}^2)] + [(V_{13}^2 - V_{14}^2) + (V_{24}^2 - V_{23}^2)] \} \quad (5-27)$$

where the quantities between the two sets of brackets are due to the work of the first and second rows of moving blades, respectively. The blade efficiency of the Curtis stage turbine is obtained, as usual, by dividing  $\dot{W}$  from Eq. (5-17) by  $\dot{m}(V_{11}^2/2g_c)$ , and the efficiency of the stage is obtained by dividing  $\dot{W}$  by the adiabatic reversible enthalpy drop for the stage.

Although the Curtis stage is composed of two rows of moving blades, a velocity-compounded turbine can be composed of any number of such rows, all sharing in the kinetic energy of the incoming steam at  $V_{11}$ . Such staging usually is built with successively increasing blade angles, which results in flatter and thinner blades toward the last row (Fig. 5-10), constructed for three rows of moving blades. An expression for the work of a three-stage turbine may be easily obtained by extending the terms in brackets in Eq. (5-27) to three.

An expression for the optimum velocity may be derived for an ideal frictionless turbine. It shows

$$V_{B,opt} = \frac{V_{11} \cos \theta_1}{2n} \quad (5-28)$$

where  $\theta_1$  is the nozzle angle and  $n$  the number of stages (rows of moving blades). The exit velocity of whirl (due to  $V_{2n}$ ) is zero. Notice that the optimum blade velocity is  $\frac{1}{n}$ th that of a single-stage impulse. In the actual turbine with friction,  $V_{B,opt}$  is slightly less than that given by Eq. (5-28) [37].

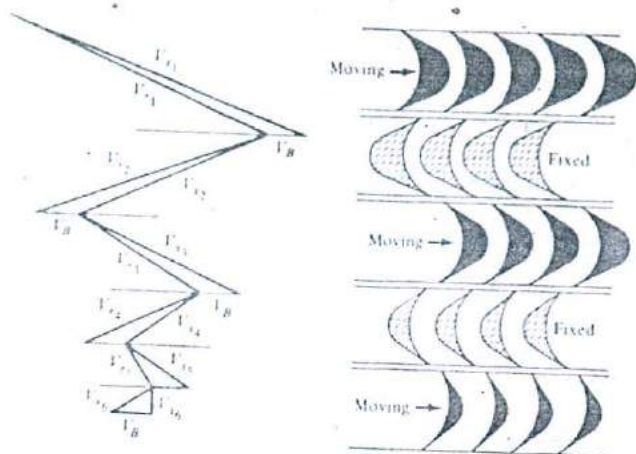


Figure 5-10 velocity diagram and blades for a velocity-compounded impulse turbine with three rows of moving blades.

The work ratio of the highest-to-lowest-pressure stages, in an ideal turbine, can be found to have the ratio 3:1 for a two-stage turbine (Curtis), 5:3:1 for a three-stage turbine, 7:5:3:1 for a four-stage turbine, and so on. This points to one of the major drawbacks of velocity compounding, namely that the lower-pressure stages produce such little work that staging beyond two stages (Curtis) is uneconomical. Another drawback is the still-high steam velocities that result in large friction, especially in the high pressure stages.

If blade speeds must be reduced below that afforded by two stages, the second method of compounding is resorted to.

### The Pressure-Compounded Impulse Turbine

To alleviate the problem of high blade velocity in the single-stage impulse turbine, the total enthalpy drop through the nozzles of that turbine are simply divided up, essentially equally, among many single-stage impulse turbines in series. Such a turbine is called a *Rateau turbine*, after its inventor. Thus the inlet steam velocities to each stage are essentially equal and due to a reduced  $\Delta h$ . From the nozzle equation, ignoring inlet velocities to the nozzles

$$V_{s1} = V_{s2} = \dots = \sqrt{2gc \frac{\Delta h_{tot}}{n}} \quad (5-29)$$

where  $\Delta h_{tot}$  is the total specific enthalpy drop of the turbine and  $n$  the number of stages.

A two-stage pressure-compounded turbine is shown in Fig. 5-11. Note that although the enthalpy drops per stage are the same, the pressure drops are not. An examination of a Mollier steam chart shows, for example, that if we were to divide



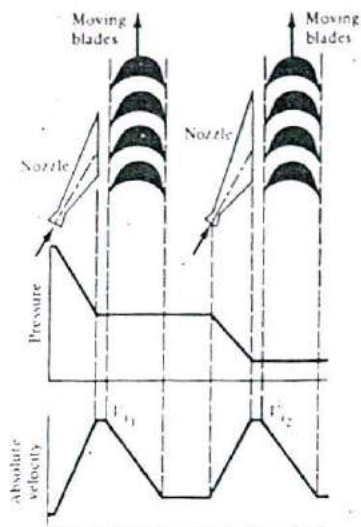


Figure 5-11 A two-stage pressure-compounded impulse turbine (Rateau).

the total enthalpy drop from 1000 psia and 1000°F to 1 psia in isentropic expansion, approximately 580 Btu/lb<sub>m</sub>, into four equal parts, approximately 145 Btu/lb<sub>m</sub>, the pressure drops in the first to fourth stages would roughly be 650, 260, 75, and 15 psi, respectively.

Figure 5-12 shows a velocity diagram of a three-stage pressure-compounded impulse turbine with friction so that  $V_{r2} < V_{r1}$ , etc. The individual triangles are constructed in the identical manner of the single-stage impulse and the equations for that turbine

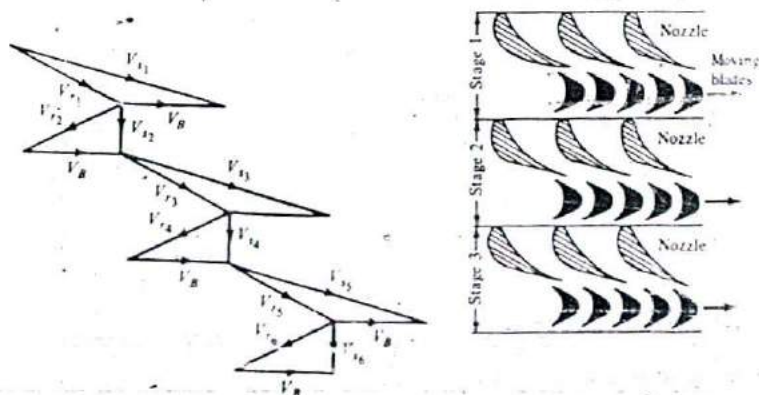


Figure 5-12 Velocity diagrams and nozzles and blades for a three-stage pressure-compounded impulse (Rateau) turbine.

are applicable here, with the exception that  $\Delta h$  per stage is much reduced. In Fig. 5-12 the exit velocities of whirl for all stages are zero, corresponding to optimum. Note also that in calculating  $V_{3s}$ , the kinetic energy in  $V_{2s}$  may not be ignored as was done in Eq. (5-29), because the nozzles of each stage must receive the steam discharged by the preceding stage, expand it, and redirect it to the moving blades. The pressure-compounded impulse turbine has the advantages of reduced blade velocities, reduced steam velocities (and hence friction) and equal work among the stages, or work distribution among the stages as desired by the designer. The disadvantages are the pressure drop across the fixed rows of nozzles, which require leak-tight diaphragms to avoid steam leakage, and the large number of stages. Thus pressure-compounded turbines are ordinarily used for large turbines where efficiency is more important than capital cost.

#### 5-4 THE REACTION PRINCIPLE

A fixed nozzle, a rocket, a whirling lawn sprinkler, and Hero's turbine (Fig. 5-1) are devices that cause a fluid to exit at high speeds. The fluid, beginning with zero velocity inside, creates a force in the direction of motion  $F$  equal to

$$F = \dot{m} \frac{V}{g} \quad (5-30)$$

and there is a corresponding and equal force tending to move the devices in the opposite direction. This force is called *reaction*. The devices mentioned above are, therefore, reaction machines that may have to hold stationary (the nozzle), move in a straight line (the rocket), or in a rotary fashion (the sprinkler and Hero's turbine). In all these, the pressure drop (caused by enthalpy drop) that causes the high velocities occurs inside the devices.

In the impulse turbine, no pressure drop (except that caused by friction) occurs in the moving blades. If now we can imagine a blade passage through which there will be a pressure drop, the blade would have a reaction force moving it in an opposite direction. Because, however, a blade passage is not a reservoir of steam, or a place where steam has zero velocity, a pure reaction blade does not exist. The blades in the so-called reaction turbine are in reality part impulse and part reaction.

A *reaction turbine*, therefore, is one that is constructed of rows of fixed and rows of moving blades. The fixed blades act as nozzles. The moving blades move as a result of the impulse of steam received (caused by change in momentum) and also as a result of expansion and acceleration of the steam relative to them. In other words, they also act as nozzles. The enthalpy drop per stage of one row fixed and one row moving blades is divided among them, often equally. Thus a blade with a 50 percent degree of reaction, or a 50 percent reaction stage, is one in which half the enthalpy drop of the stage occurs in the fixed blades and half in the moving blades. The pressure drops will not be equal; however. They are greater for the fixed blades and greater for the high-pressure than the low-pressure stages, as explained for the pressure-compounded impulse turbine.

The term reaction turbine is used despite the fact that pure reaction turbines are not built. (Some European writers prefer the terms *equal-pressure* and *unequal-pressure turbines* for the impulse and reaction turbines, respectively.)

## 5-5 REACTION TURBINES

Reaction turbines, originally invented by C. A. Parsons, are illustrated by Fig. 5-13 with three stages, each composed of a row of fixed blades and a row of moving blades. The stationary blades are designed in such a fashion that the passages between them form the flow areas of nozzles. They are therefore nozzles with *full steam admission* around the rotor periphery.

The moving blades of a reaction turbine are easily distinguishable from those of an impulse turbine in that they are not symmetrical and, because they act partly as nozzles, have a shape similar to that of the fixed blades, although curved in the opposite direction.

The schematic pressure line (Fig. 5-13) shows that pressure continually drops through all rows of blades, fixed and moving, though the pressure change is greater the greater the pressure. The absolute steam velocity changes within each stage as shown and repeats from stage to stage.

Figure 5-14 shows a typical velocity diagram for two-reaction stages. To construct such a diagram, the  $\Delta h$  per stage is determined, say by dividing the total enthalpy drop of the turbine by the number of stages. This  $\Delta h$  is further divided among the fixed  $\Delta h_f$  and moving  $\Delta h_m$  rows of each stage, each typically half  $\Delta h$ .  $V_{31}$  is calculated

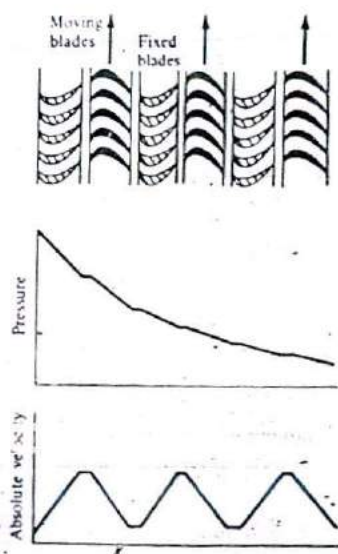


Figure 5-13 Three stages of reaction turbine with overall steam pressures and absolute velocities.

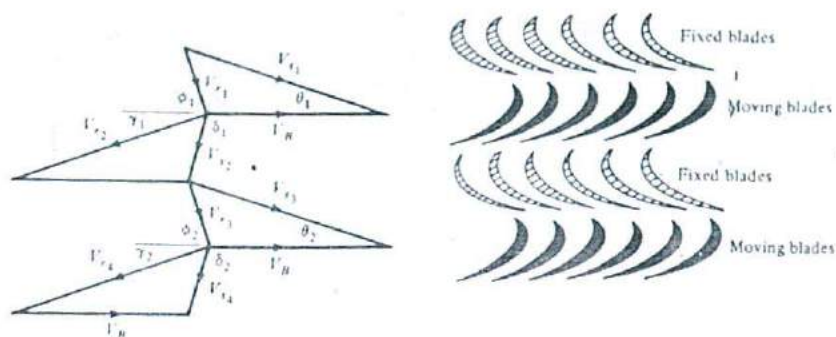


Figure 5-14 Velocity diagram for a two-stage reaction turbine.

from  $\Delta h_f$ . A blade speed  $V_B$  is chosen, say, to correspond to optimum conditions equal to  $V_{r1} \cos \theta$  (compared with  $V_{r1} \cos \theta/2$  for the impulse turbine).  $V_{r1}$  is then found. Note that  $\gamma$  is nearly equal to  $\theta$  but is much less than  $\phi$  here.

The second half of the enthalpy drop  $\Delta h_m$  occurs in the moving blade. This results in increasing the velocities *relative* to the blades. In other words,  $\Delta h_m$  in the moving blades increases its relative velocity. Thus  $V_{r1}$  is increased to  $V_{r2}$  (in the impulse turbine  $V_{r2}$  was equal to or less than  $V_{r1}$  because of friction). For the same  $V_B$ , get the new  $V_{r2}$ , which enters the next row of fixed blades to be increased to  $V_{r3}$ , and so on. Thus

$$\frac{V_{r3}^2 - V_{r2}^2}{2g_c} = \Delta h_f \quad (5-31)$$

and

$$\frac{V_{r4}^2 - V_{r3}^2}{2g_c} = \Delta h_m \quad (5-32)$$

The work of a reaction stage can also be obtained from momentum-impulse or first-law principles. The change in momentum on the blade in the direction of motion  $+x$  is due to the change in the components of the relative velocities  $V_{r1}$  and  $V_{r2}$  in that direction. For one reaction stage in general

$$F = \frac{\dot{m}}{g_c} (V_{r1} \cos \phi + V_{r2} \cos \gamma) \quad (5-33)$$

but as  $V_{r1} \cos \phi = V_{r1} \cos \theta - V_B$

$$F = \frac{\dot{m}}{g_c} (V_{r1} \cos \theta - V_B + V_{r2} \cos \gamma)$$

The rate of work, or power,  $\dot{W} = FV_B$

$$\dot{W} = \dot{m} \frac{V_B}{g_c} (V_{r1} \cos \theta - V_B + V_{r2} \cos \gamma) \quad (5-34)$$

From first-law principles, Eq. (5-22), repeated here, applies.

$$\dot{W} = \frac{\dot{m}}{2g_c} [(V_{s1}^2 - V_{s2}^2) - (V_{r1}^2 - V_{r2}^2)] \quad (5-22)$$

### Optimum Blade Speed

The optimum blade speed can be easily obtained for the case where the fixed moving blades are similar, so that  $\theta = \gamma$ , and Eq. (5-34) is written in the form

$$\dot{W} = \frac{\dot{m} V_B}{g_c} (2V_{s1} \cos \theta - V_B)$$

Again differentiating  $\dot{W}$  with respect to  $V_B$  and equating to zero

$$\frac{d\dot{W}}{dV_B} = 2V_{s1} \cos \theta - 2V_B = 0$$

$$\text{or} \quad V_{B,\text{opt}} = V_{s1} \cos \theta \quad (5-35)$$

$$\text{and} \quad \dot{W}_{\text{max}} = \frac{\dot{m}}{g_c} (V_{s1} \cos \theta)^2 = \frac{\dot{m}}{g_c} (V_B)_{\text{opt}}^2 \quad (5-36)$$

The efficiency of a reaction stage is dependent upon the efficiency of the fixed blades (nozzles) and the efficiency of the moving blades. These are explained with the help of Figs. 5-14 and 5-15, which is a Mollier chart representation of Fig. 5-14.

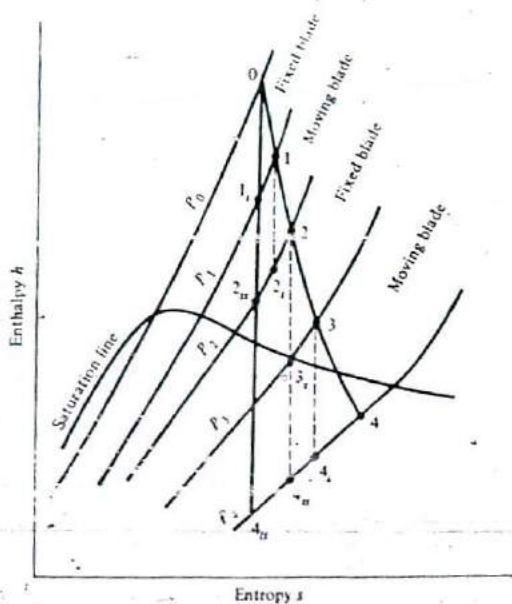


Figure 5-15 Condition curve for a two-stage reaction turbine, drawn on the Mollier (enthalpy-entropy) chart.

Lines  $P_0, P_1$ , etc., represent constant pressure lines, which diverge to the right on the Mollier chart. The actual expansion line 0-1-2-3-4 represents the actual condition of the steam in the two stages and is called a *condition curve*.

The *fixed-blade, or nozzle, efficiency*  $\eta_N$  is the ratio of the kinetic energy change to the adiabatic reversible (isentropic) energy change across the fixed blade. For the first fixed blade

$$\eta_N = \frac{(1/2g_c)(V_{21}^2 - V_{30}^2)}{\Delta h_{f,1}} = \frac{h_0 - h_1}{h_0 - h_{1s}} \quad (5-37)$$

The *moving-blade efficiency*  $\eta_B$  is the work of the blade, Eqs. (5-22) or (5-34), divided by the total energy available to that blade, which consists of the kinetic energy of the incoming steam at  $V_{11}$  plus adiabatic reversible (isentropic) enthalpy drop across it. Note that the latter is greater than  $\Delta h_m$  because of the friction (irreversibility) in the blade, which causes an increase in entropy. Thus

$$\eta_B = \frac{\dot{W}}{\dot{m}(V_{11}/2g_c) + \Delta h_{ms}} = \frac{\dot{W}}{\dot{m}[(V_{11}^2/2g_c) + (h_1 - h_{2s})]} \quad (5-38)$$

The *stage efficiency*  $\eta_{\text{stage}}$  of a reaction stage is the work of the moving blade in the stage divided by the adiabatic reversible (isentropic) enthalpy drop for the entire stage, including fixed and moving blades. Thus

$$\eta_{\text{stage}} = \frac{\dot{W}}{\dot{m} \Delta h_s} = \frac{\dot{W}}{\dot{m}(h_0 - h_{2s})} \quad (5-39)$$

where, as shown in Eqs. (5-37) to (5-39)

$$\begin{aligned} \Delta h_{f,1} &= \text{isentropic enthalpy drop across fixed blade} \\ &= h_0 - h_{1s} \text{ (first stage), } = h_2 - h_{3s} \text{ (second stage), etc.} \\ \Delta h_{ms} &= \text{isentropic enthalpy drop across moving blade} \\ &= h_1 - h_{2s} \text{ (first stage), } = h_3 - h_{4s} \text{ (second stage), etc.} \\ \Delta h_s &= \text{isentropic enthalpy drop across entire stage} \\ &= h_0 - h_{2s} \text{ (first stage), } = h_2 - h_{4s} \text{ (second stage), etc.} \end{aligned}$$

Note that because of the divergence of the constant pressure lines, the isentropic enthalpy drop charged to a row or stage is greater than that for a succession of rows or stages or for an entire turbine. In other words

$$\begin{aligned} h_1 - h_{2s} &> h_{1s} - h_{2s} \\ (h_0 - h_{2s}) + (h_2 - h_{4s}) &> h_0 - h_{4s} \end{aligned}$$

The reaction turbine is an efficient machine that is suited for large capacities. For a given blade speed, limited by material centrifugal stresses, the steam velocity in a reaction turbine is about half that in a pressure-compounded impulse turbine [compare Eqs. (5-35) and (5-17)], resulting in low-friction losses. On the other hand, its work, for the same  $V_B$ , is about half that of an impulse stage [Eqs. (5-36) and (5-18)].

Contrary to an impulse stage, a reaction stage has a pressure drop across the

moving blades. This makes it less suitable for work in the high-pressure stages where  $\Delta P$  per unit enthalpy drop is high, which results in steam leakage around the tips of the blades, which in turn leads to throttling and a loss of availability. It follows then that impulse staging is preferable in the entrance stages of a turbine, when the pressures are high, steam specific volumes are low, and the blade height is small so that steam velocities would be correspondingly low. In the low-pressure stages, reaction stages are preferred because the  $\Delta P$  across the moving blades is less; the blades become progressively longer so that the tip clearance becomes smaller relative to the blade height, i.e., relative to the steam volume. With large reaction blading,  $V_B$  is larger, negating the disadvantage of lower power per stage than an impulse stage of the same  $V_B$ .

### Axial Thrust

Turbine rotors are subjected to an axial thrust as a result of pressure drops across the moving blades and changes in axial momentum of the steam between entrance and exit. This axial thrust must be counteracted to keep the rotor in place.

In *impulse turbines*, there is no pressure drop across the moving blades if the turbine is ideal and little pressure drop caused by friction in a real turbine. In addition there is an axial force on the row because of the change in the axial component of momentum of the steam from entrance to exit. This is given by (see Fig. 5-5)

$$F_{\text{axial}} = \frac{m}{g_c} (V_{r1} \sin \phi - V_{r2} \sin \gamma) \quad (5-40)$$

This axial thrust results in no work. In the case of pure symmetrical impulse blades,  $V_{r1} = V_{r2}$ ,  $\phi = \gamma$  and that thrust is zero. The total axial thrust on an impulse turbine rotor is, in any case, small and poses no severe problems.

The case of the *reaction turbine* is different. The axial components of the steam entering and leaving a reaction turbine are nearly equal (see Fig. 5-14), so that the axial thrust due to the change in axial momentum of the steam is, like an impulse turbine, essentially zero. There is, however, a large and continual pressure drop across the moving blades. Although that pressure drop decreases in the low-pressure stages, the effect is counterbalanced by an increasing blade height and hence area. The resulting axial thrust is quite large and must be coped with. In small turbines, this is done by a thrust bearing on the rotor shaft or by one or more dummy pistons (discs) inside the casing of sufficient area with high-pressure steam on one face only, the other face sealed by a labyrinth packing.

In modern large utility steam turbines, the common solution is to have double-flow turbines or turbine sections in which steam enters in the center, expands both left and right, and leaves to the next lower-pressure section or to the condenser at opposite ends. This gives the turbine an X shape (Fig. 5-16) with each side's axial thrust canceling the other. It also results in dividing up the blade heights and hence areas and axial thrusts in two and reduces blade tip speeds.

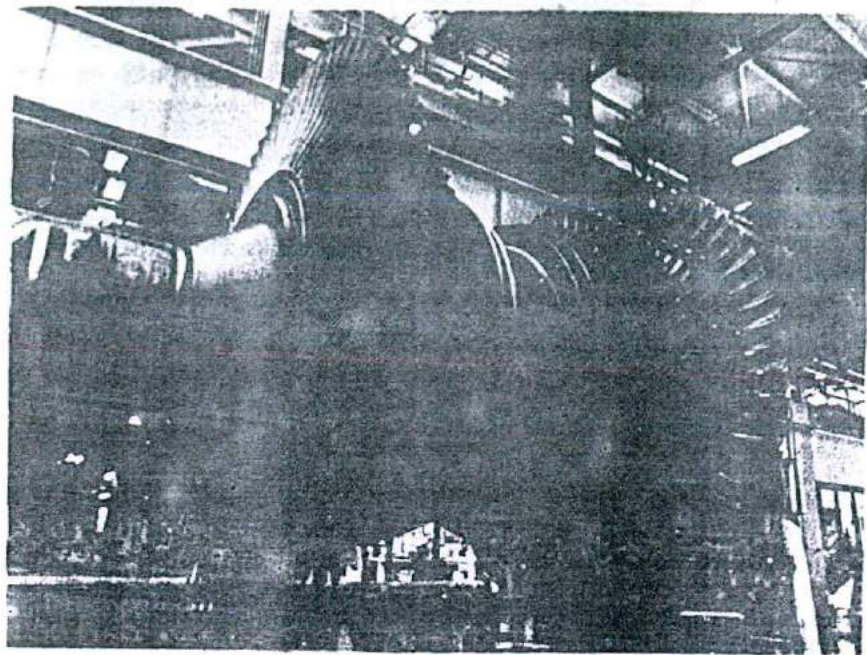


Figure 5-16 A double-flow low-pressure turbine section rotor.

### Twisted Blades

Reaction blades are high, especially in the latter stages. Their height, often one-third of the mean blade diameter, reaches 43 in. (about 1.1 m) in some cases (refer to Table 5-2). The velocity diagrams constructed so far in this chapter assumed constant blade speeds  $V_B$ , given by

$$V_B = \pi DN \quad (5-41)$$

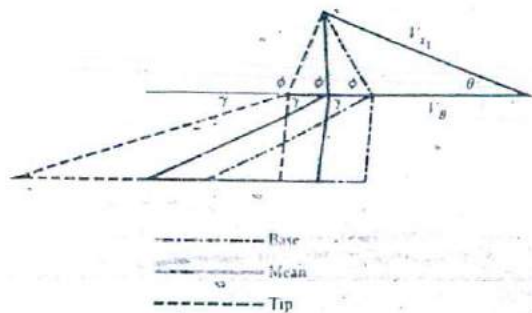


Figure 5-17 Effect of reaction blade height on entrance and exit angles, necessitating a warped radial shape. Drawn for same  $V_1$ ,  $\theta$ , and same exit whirl.



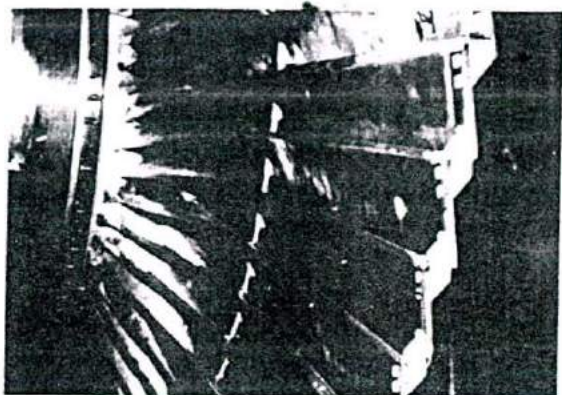


Figure 5-18 33 1/2-in. reaction blading showing twisted construction [38].

where  $D$  is the diameter of the blade and  $N$  the number of revolutions per unit time. Although  $N$  is constant,  $D$  for a high blade obviously is not (high-pressure impulse blades, if used, are so short compared with the rotor shaft diameter that  $V_n$  for them can be considered constant).

Thus  $V_n$  increases with radius from base to tip of the blade, resulting in changes in the shapes of the velocity diagrams along the blade length, as shown in Fig. 5-17, which is drawn for optimum conditions at midpoint. It can be seen that, assuming  $V_{11}$  and  $\theta$  do not vary in the radial direction, the blade entrance angle  $\phi$  increases, and exit angle  $\gamma$  decreases, from base to tip, which necessitates giving the blade a twisted shape. It can also be seen that the degree of reaction varies from base to tip with the blade somewhat resembling an impulse blade at the base and having maximum reaction at the tip. Such blades are called *twisted*, *warped*, or *vortex blades*. Figure 5-18 shows a turbine wheel with 33 1/2-in.-long reaction blades with this characteristic [38]. See also Fig. 5-21.

## 5-6 TURBINE LOSSES

### Supersaturation

When steam expands *rapidly* from a superheated state across the saturated vapor line (point 1, Fig. 5-19), a condition of *metastable equilibrium* exists in which the steam does *not immediately* condense upon crossing point 1. Instead there is no change in the character of the steam, which continues to follow the laws governing superheated steam for some distance past point 1 until a certain lower pressure is reached. At that point condensation suddenly takes place, and the condition of the system is once again in *thermodynamic equilibrium*, which has a quality dictated by the pressure and specific

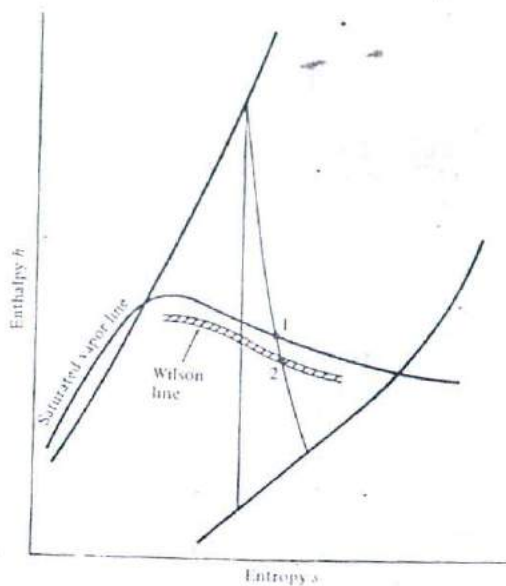


Figure 5-19 Supersaturation condition and the Wilson line, shown on the Mollier ( $h$ - $s$ ) diagram.

volume (or entropy) at point 2. The phenomenon occurs in both turbines and nozzles, where rapid expansion occurs.

Steam in the region 1-2 is called *supersaturated*, or *undercooled*, steam. The locus of points 2 at various pressures, really a band or a zone, is called the *Wilson line* (Fig. 1-19). It is about 60 Btu below the saturated-vapor line on the Mollier chart.

Initial condensation results in liquid droplets of very small diameters and thus large curvature (inversely proportional to diameter). The vapor pressure of a highly curved surface is greater than that of a flat or less-curved surface at the same temperature because a molecule on a highly curved surface is freer to leave that surface as it is restrained by fewer adjacent molecules. Droplet diameters below which this effect is pronounced are believed to be around  $10 \text{ \AA}$  (1 angstrom  $\text{\AA} = 10^{-10} \text{ m}$ ). Conversely, for the same vapor pressure a small drop will be at a lower temperature than a larger one or than the saturation temperature corresponding to that pressure. Thus when expansion occurs rapidly to a given pressure and no condensation takes place, a lower temperature will be reached before the first droplets form. Once they form and grow, thermodynamic equilibrium returns to the system.

This phenomenon is further illustrated by the use of a modified Mollier chart (Fig. 5-20) that represents the region of most interest in steam-turbine supersaturation. In thermodynamic equilibrium, a two-phase mixture at a given temperature has one and only one corresponding saturation pressure (e.g., 4.74 psia and  $160^\circ\text{F}$ ). In supersaturation, the steam behaves somewhat like a gas and the temperature lines in the superheat region extend into the two-phase region, as shown by the dashed lines in the figure. At any given pressure then a supersaturated fluid such as at  $b$  has a lower temperature, about  $105^\circ\text{F}$ , than if it were in thermodynamic equilibrium ( $160^\circ\text{F}$ ). In

other words, the steam is undercooled. The ratio of actual pressure to the pressure corresponding to the lower temperature is called the *degree of supersaturation*, or *degree of undercooling*.

**Example 5-2** Compare the final conditions and the steady-flow work when superheated steam at 11.5 psia and 240°F expands (1) isentropically to 4.74 psia when expansion occurs to a supersaturated state or (2) slowly and thermodynamic equilibrium is maintained. Assume supersaturated vapor obeys  $PV^{1.32} = \text{constant}$ .

**SOLUTION** The initial conditions (point *a*, Fig. 5-20) from the steam tables are  $h_a = 1165.0$  Btu/lb<sub>m</sub>,  $v_a = 35.88$  ft<sup>3</sup>/lb<sub>m</sub>, and  $s_a = 1.8047$  Btu/(lb<sub>m</sub> · °R).

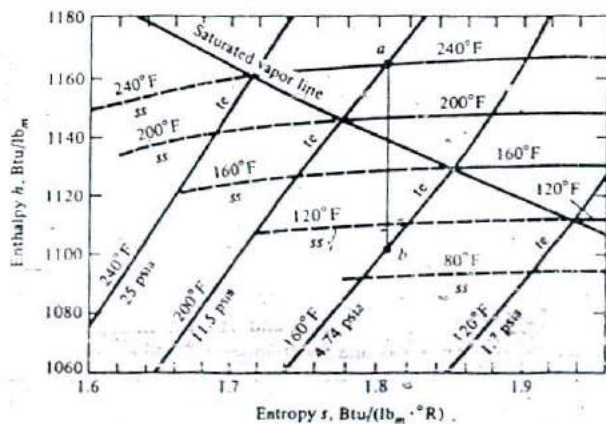
This steam expands isentropically to point *b*. If it does so rapidly and becomes supersaturated, it will behave as a gas and obey  $PV^{1.32} = \text{constant}$ . Thus

$$v_b = v_a \left( \frac{P_a}{P_b} \right)^{1/1.32} = 35.88 \left( \frac{11.5}{4.74} \right)^{0.7575} = 70.22 \text{ ft}^3/\text{lb}_m$$

$$T_b = T_a \left( \frac{P_b}{P_a} \right)^{(1.32 - 1)/1.32} = (240 - 460) \left( \frac{4.74}{11.5} \right)^{0.2424} = 564.6^\circ\text{R} = 104.6^\circ\text{F}$$

From Table 1-3

$$\begin{aligned} \text{Steady-flow work } w_{if} &= \frac{n}{1-n} (P_b v_b - P_a v_a) \\ &= \frac{1.32 \times 144}{1 - 1.32} \left( \frac{4.74 \times 70.22 - 11.5 \times 35.88}{778.16} \right) \\ &= 60.1 \text{ Btu/lb}_m \end{aligned}$$



**Figure 5-20** Modified Mollier chart showing supersaturation (*ss*, dashed lines) and thermodynamic equilibrium (*te*, solid lines).

Therefore

$$h_b = h_a - w_{sf} = 1165.0 - 60.1 = 1104.9 \text{ Btu/lb}_m$$

If the steam expands slowly and maintains thermodynamic equilibrium, the conditions at  $b$  are obtained from the steam tables at 4.74 psia and  $s_b = s_a = 1.8047 \text{ Btu/lb}_m$ , giving  $x_b = 0.9728$ ,  $h_b = 1102.9 \text{ Btu/lb}_m$ , and  $v_b = 75.18 \text{ ft}^3/\text{lb}_m$ . The steady-flow work  $w_{sf} = h_a - h_b = 1165.0 - 1102.9 = 62.1 \text{ Btu/lb}_m$ . The solution is summarized in Table 5-1.

It can be seen that supersaturation results in a lower temperature, justifying the dual name "undercooling," lower volume, and reduced work.

When expansion crosses the Wilson line, it reverts to thermodynamic equilibrium by sudden condensation. This releases the enthalpy of vaporization of the condensed vapor and results in a sudden pressure rise and reduction in specific volume and velocity. The phenomenon is called *condensation shock*, which is similar, though not identical, to normal shocks that occur in supersonic nozzles. It is an irreversible process that results in further loss in availability.

### Fluid Friction

Fluid friction is the biggest cause of all turbine losses. It occurs throughout the turbine. There is, to begin with, friction in the steam nozzles. Next there is blade friction, which we tried to minimize by decreasing steam velocities by compounding, etc. Also there is turbulence in the blades when the blade shape does not possess the proper entrance angle for steam at other than design loads. There is also friction between the steam and the rotor discs that carry the blades. Here rotor design is important (Sec. 5-8). In addition, the rotor and blade rotation impart a centrifugal action on the steam, thus causing part of it to flow radially to the casing and be dragged along by the moving blades. In case of less-than-full steam admission to the moving blades, such as for an impulse stage, there is churning in the moving blades. This is called a *fanning* loss.

Fluid friction losses can amount to about 10 percent of all the energy available to the turbine.

Table 5-1 Comparison of supersaturation and thermodynamic equilibrium for the data from Example 5-2

Properties	$P$ , psia	$T$ , °F	$s$ , Btu/(lb <sub>m</sub> · R)	$h$ , Btu/lb <sub>m</sub>	$v$ , ft <sup>3</sup> /lb <sub>m</sub>	$w_g$ , Btu/lb <sub>m</sub>
Initial	11.5	240.0	1.8047	1165.0	35.88	
Final, ss*	4.74	104.6	1.8047	1104.9	70.27	60.1
Final, te*	4.74	160.0	1.8047	1102.9	75.18	62.1

\* ss = supersaturation, te = thermodynamic equilibrium.

## Leakage

Steam leakage can occur within and to the outside of a turbine. Within the turbine steam can leak between the tips of moving blades and the casing when there is a pressure drop across them, such as in a reaction turbine. This leakage is greater the greater the pressure drop, i.e., in the higher-pressure stages, and the greater the ratio of tip clearance to blade height. The leaking steam is throttled and represents a loss of available energy. In a pressure-compounded (Rateau) impulse turbine, leakage occurs between the base of the stationary diaphragms that carry the nozzles and the shaft.

Leakage can also occur to the outside of the turbine at the various shaft bearings. This is minimized by the use of proper seals or packings, such as a *labyrinth packing*.

Leakage loss can account for about 1 percent of the total energy available to a turbine.

## Moisture Loss

Besides the losses encountered as a result of supersaturation in the two-phase region (above), the presence of liquid droplets causes further losses. These droplets have both a size and velocity distribution, not unlike those in a liquid nozzle spray. Some low-speed droplets splash against the moving blades, i.e., strike them at off-design angles, and thus reduce the mechanical work of the rotor. Others are accelerated by the steam and remove some of its energy through momentum exchange. The result is that turbine sections that operate in the two-phase region are substantially less efficient than those that operate in the superheat region.

Turbines are usually designed to operate with exit-moisture content of no more than about 12 percent (88 percent minimum quality). Higher moisture content (often coupled with high oxygen content in boiling-water reactors) cause blade erosion as a result of the impingement of water droplets on the blades, surface washing, and the so-called *wire drawing* caused by high-velocity water leaking through narrow passages. Oxygen, in addition, causes corrosion. If steam expansion causes higher moisture content than 12 percent, moisture extraction at certain stages in the turbine is resorted to keep the moisture content within this limit. This is the practice in boiling-water reactor turbines, for example. The moisture extracted represents a mass-flow, and hence work, loss to the turbine, though this effect can be minimized by combining it with bled steam for feedwater heating. Moisture extraction can be accomplished by constructing the moving blades with grooves on the back side, where the drops are known to collect (Fig. 5-21). The drops are then thrown radially by the centrifugal force of the rotating blades into a collecting chamber in the casing where they may be bled to a feedwater heater or the condenser [39].

From an operational point of view, contaminants in the steam besides oxygen, such as particulate matter and chemicals such as sodium and chlorine from water treatment operations, can cause stress-corrosion cracking (caused by otherwise tolerable stressing, but in a corrosive atmosphere) and erosion. This calls for better water-chemistry control, monitoring, and maintenance [40].



Figure 5-21 A grooved moisture-extracting turbine blade [39].

### Leaving Loss

We have noted a velocity residual in individual turbine stages, both impulse and reaction. The corresponding kinetic energy is usually recovered in subsequent stages, except for that due to the last row in the turbine. The velocity leaving this row, as a result of low-pressure steam of maximum specific volume, and the corresponding kinetic energy represent a loss to the turbine. This velocity is approximately normal to the plane of rotation near rated load but has a large forward component at lighter loads. The magnitude of this velocity can be changed by the designer by the proper combination of last-blade height, speeds, and area of the exhaust ducts to the condenser. (We already noted that low-pressure turbine sections are double-flow and have two

exhaust ducts each.) Whereas high leaving velocities result in energy loss, velocities that are too low result in inordinately high blades, large exhaust ducts, and increased capital costs. In modern large turbines, leaving velocities around 900 to 1000 ft/s (270 to 300 m/s) are typical. They result in a 2 to 3 percent loss to the turbine.

Exhaust hoods to the condenser that gradually increase in area like a diffuser further decrease the exhaust-steam velocity and increase its pressure as it enters the condenser. Such hoods allow the turbine to operate down to a slightly lower pressure than that required by the condenser (which is dictated by the available cooling-water temperature), thus increasing the turbine work. This practice is more common with 3000- and 3600-r/min than 1500- and 1800-r/min turbines because the latter have larger blades and exhaust ducts to begin with.

### Heat-Transfer Losses

Heat-transfer losses from turbines, as usual, are caused by conduction, convection, and radiation. Conduction occurs internally through metal between stages and is aided by convection, which is largely the result of the high steam velocities. Conduction also takes place between the turbine casing and the foundation. Convection and radiation losses occur from the turbine casings to the surroundings in the turbine hall and are more pronounced for the high-pressure section, where steam temperatures are the highest. That section, however, is smallest in diameter and is usually well insulated. The larger low-pressure sections operate with steam not much above room temperature, and are usually uninsulated.

Although a turbine hall usually feels warm, the total heat losses per unit mass flow of steam of large turbines are so small that they are negligible. This is not the case, however, with small turbines, such as those used for mechanical drives, for which the heat-transfer losses usually amount to several percent of the turbine energy.

### Mechanical and Electrical Losses

Now that the turbine has extracted work from the system, it must deliver it to the electric generator. In so doing, it encounters frictional losses in bearings, governor mechanism, and reduction gearing, if present. It must also supply mechanical work to accessories such as oil pumps, etc.

Mechanical losses are practically constant and independent of load and thus increase in percentage as load decreases. On the other hand, the percentage is also smaller the larger the turbine. In general, mechanical losses are fairly small, amounting to 1 percent or less of the turbine energy.

As turbines are usually rated by the electric generator output, a knowledge of the extent of generator losses is essential. Modern large electric generators are hydro-cooled, well designed, and very efficient. Efficiencies around 98 to 99 percent are common, increasing slightly with load, and are somewhat higher for 1500- and 1800-r/min than 3000- and 3600-r/min generators.

## 5-7 TURBINE EFFICIENCIES

We have already seen that, because constant pressure lines diverge on a Mollier chart (true also for gases), the isentropic enthalpy drops charged to a turbine stage are greater than those for multiple stages and for the entire turbine. It follows that the efficiency of a stage is less than that of a turbine section, etc. This can be seen with the help of Fig. 5-15 for a reaction turbine, though it applies to all turbines

$$\text{Efficiency of 2 stages} = \frac{h_0 - h_4}{h_0 - h_{4s}} > \text{efficiency of 1 stage} \frac{h_2 - h_4}{h_2 - h_{4s}}$$

The ratio of the total individual isentropic enthalpy drops to the enthalpy drop of a turbine section or whole turbine is called the *reheat factor*  $R_h$ .  $R_h$  is obviously greater than 1.0, with values ranging between just above 1.0 to perhaps 1.065, depending upon the pressure range. For the two stages of Fig. 5-15

$$R_h = \frac{(h_0 - h_{2s}) + (h_2 - h_{4s})}{h_0 - h_{4s}} \quad (5-42)$$

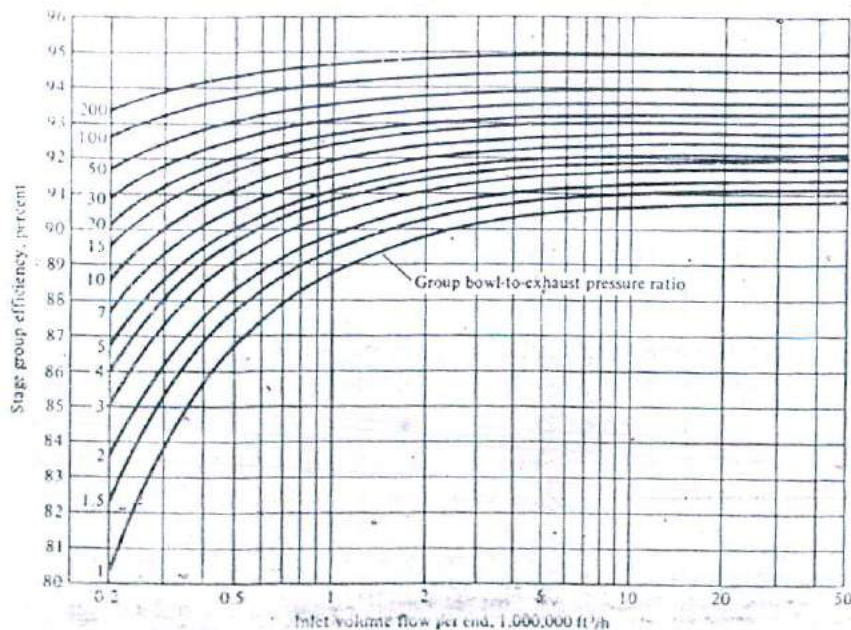


Figure 5-22 Typical stage group efficiencies for turbine section operation in superheat region as a function of steam inlet volume flow and ratio of bowl (inlet) pressure to group exhaust pressure. Leaving loss not included [41].



If the designer wishes to have equal work from the stages, dividing the isentropic enthalpy drop for the whole turbine in equal parts will not, because of the divergence of the pressure lines, result in equal actual work in each stage; that is, if  $h_0 - h_{2s} = h_{2s} - h_{4s}$ , it does not follow that  $h_0 - h_2 = h_2 - h_4$ . To get the same actual work, the designer must take into account this divergence.

We have also seen that turbine stages operating in superheated steam are more efficient than those operating in the two-phase region. The performance and efficiency of stages or of a whole steam turbine are undoubtedly a complex function of many variables. Accurate knowledge of the condition curve of a turbine, which is affected by the individual stage rather than the whole turbine efficiency, is necessary, for example, to do the cycle analysis in reheat and moisture-extraction turbines.

Methods for predicting the performances and efficiencies of various steam turbines are often manufacturer's proprietary information, but some may be found in the literature [41, 42]. One such method [41] predicts the performance of large turbines used in modern nuclear powerplants operating with low-superheat or saturated steam in Figs. 5-22 and 5-23 for the superheat and two-phase regions, respectively. These figures give base efficiencies for a volumetric flow ( $10^6$  ft<sup>3</sup>/h, 7.867 m<sup>3</sup>/s) and other data. Corrections for the departure from these data are available in the original paper.

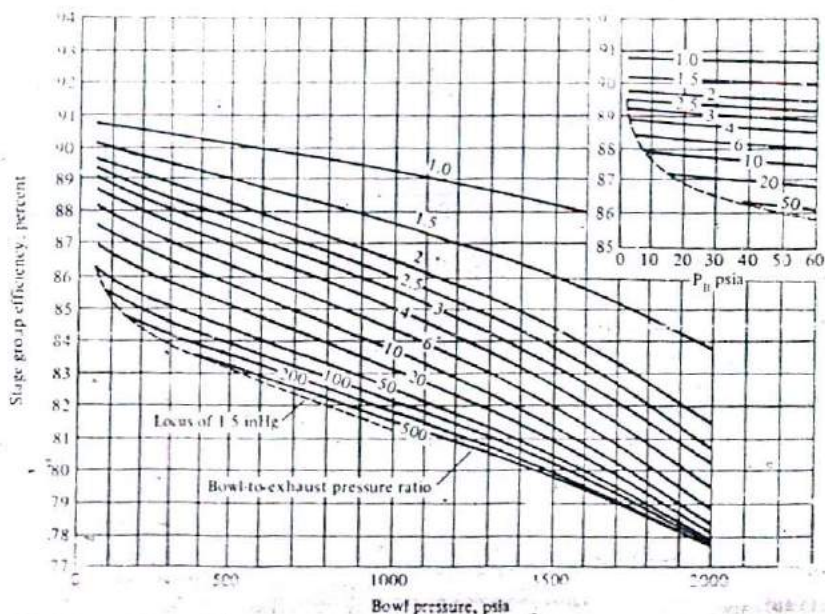


Figure 5-23 Typical stage group efficiencies for turbine section operating in two-phase region as a function of bowl (inlet) pressure and ratio of bowl pressure to group exhaust pressure. Leaving loss not included [41].

## 5-8 TURBINE ARRANGEMENTS

### Combination Turbines

In earlier times, turbines used to be built as pure impulse, of one type or another, or pure reaction. With the expiration of patents, manufacturers were free to use combinations, especially in medium and large sizes. One popular arrangement used to be a Curtis stage (two-row velocity-compounded impulse) followed by a series of Rateau (pressure-compounded impulse) stages. Another was a de Laval (single-stage impulse) followed by a Rateau or reaction turbine.

A more common arrangement is a combination of a Curtis stage followed by a large number of reaction stages. There are certain advantages of this arrangement. The impulse stage is more suited to the high pressure of admission than the reaction stage because there is virtually no pressure drop in the moving blades. Recall that for the same enthalpy drop, a much larger pressure drop occurs at high pressure. Also the clearance between the blade tip and the casing is greater for the shorter high-pressure blades, which aggravates the leakage problem should there be a pressure drop across the moving blades. After the impulse stage, the pressure is sufficiently low that the more efficient reaction stages can now be used. They become progressively longer, the clearance proportionately less, and the pressure drop across their moving blades progressively less.

Partial admission to the Curtis stage, because of the limited number of nozzles around the periphery, is conveniently used for governing. The nozzles are arranged in groups, each receiving steam through a valve that is actuated by the governor. The valves open in succession as demanded by the turbine load. Such a stage is called a *governing stage* or a *control stage*.








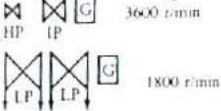
A pressure drop naturally occurs in the governing stage, depending upon total steam flow (load) and number of nozzles in effect. Usually the pressure drop is larger the lighter the load.

The governing stage has an additional peripheral advantage in that large pressure and temperature drops occur in the fixed nozzles, thus subjecting the turbine proper to greatly reduced pressures and temperatures, an important factor in modern turbines that use high-pressure and high-temperature steam.

### Turbine Configurations

We have noted the necessity of double-flow turbine sections to cancel out the axial thrust (Sec. 5-5). In addition, modern large turbines, dictated by practical design and manufacturing considerations, are made of multiple *sections*, also called *cylinders*, in both *tandem* (on one axis) or *cross-compound* (on two parallel axes) arrangements (Table 5-2). The sections may be one high-pressure (HP), one intermediate-pressure (IP), and two low-pressure (LP) sections, all in tandem, but with the two LP sections operating in parallel as far as steam flow is concerned. They may be one HP, three

Table 5-2 Turbine-generator configurations\*

Fossil	Fossil	Nuclear
TC-2F LSB 26, 30 and 33.5 in Two casings 3600 r/min  125-400 MW	TC-6F LSB 26, 30 and 33.5 in Five casings 3600 r/min  550-1000 MW	TC-4F LSB 38 and 43 in Three casings 1800 r/min  450-1000 MW
TC-4F LSB 26, 30 and 33.5 in Three casings 3600 r/min  250-650 MW	TC-6F LSB 30 and 33.5 in Five casings 3600 r/min (double reheat)  450-725 MW	TC-6F LSB 38 and 43 in Four casings 1800 r/min  600-1100 MW
TC-4F LSB 26, 30 and 33.5 in Four casings 3600 r/min  550-850 MW LP LP G	CC-4F LSB 38 and 43 in Four casings 3600/1800 r/min  600-1250 MW	

\* Data provided by the General Electric Company. TC = tandem compound, CC = cross compound, F = number of flow ducts to condenser, LSB = last-stage blade.

LP, etc. The multiplicity of the LP sections further reduces the blade lengths, giving for example, *last-stage-blade* or *-bucket* (LSB) lengths of 43 in for a 1000-MW, 1800-r/min (water-cooled nuclear reactor) turbine; 33.5 in for a 1000-MW, 3600-r/min (fossil and high-temperature nuclear) turbine; etc.

Configurations are also affected by admission requirements. Figure 5-24a shows a number of *straight-through* turbine sections (for simplicity). Figure 5-24b shows a turbine with *single reheat* (steam expanding part way, reheated in the steam generator, and readmitted to the turbine). Figure 5-24c shows an *extraction* turbine in which steam is bled for feedwater, for process steam uses (cogeneration, Sec. 2-15), or both. Figure 5-24d shows an *induction* turbine, the reverse of an extraction turbine; in which low-pressure steam is injected at a low-pressure stage. This low-pressure steam comes from a process, in special-design utility boilers as Dresden nuclear powerplant or early British gas-cooled reactor systems [3], or in some combined gas-turbine-steam-turbine cycles (Sec. 8-11).

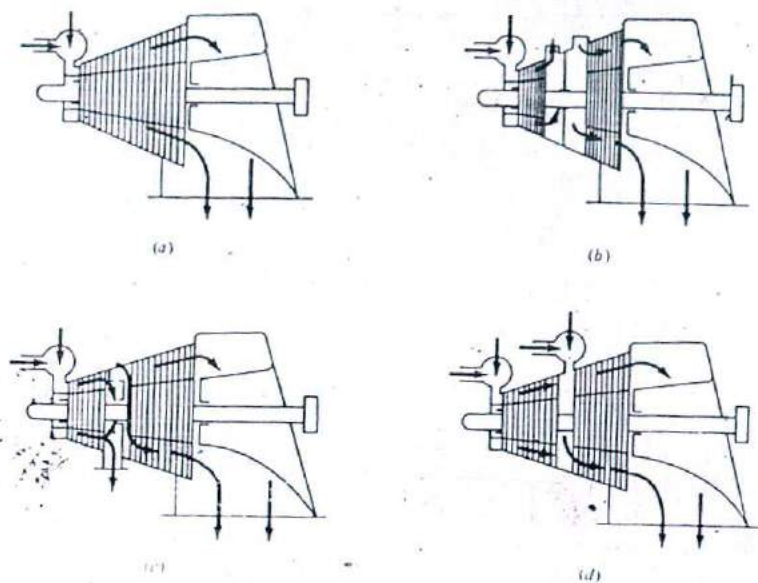


Figure 5-24 Turbine arrangements as affected by different steam paths: (a) straight through; (b) single reheat; (c) extraction; (d) induction.

Figures 5-25 and 5-26 show cross sections for a 3600-r/min fossil-fueled turbine and a 1800-r/min nuclear-fueled turbine, respectively.

### Turbine Rotors

The rotor is the heart of the turbine. Current designs are shown in Fig. 5-27. Figure 5-27a and b shows two versions of a rotor produced from a *single forging*. Figure 5-27c shows a *composite construction* produced by shrinking rotor discs on a central shaft. Figure 5-27d shows a *drum-type rotor* composed of separate rotor discs that are welded together. This last design is receiving acceptance for the very large units being built today, 500 to 1000 MW and larger, which would otherwise be extremely heavy and uneconomical and would pose severe mechanical problems.

Materials for such rotors are carefully chosen to yield lasting resistance to softening and creep, receive uniform heat treatment, and have lasting ductility and good resistance to scale. Besides materials, attention must be paid to manufacturing methods and operating success [42].

Water-cooled nuclear-reactor turbines pose fewer problems than fossil-fueled turbines because they operate with lower steam temperatures, around 540°F versus 1000°F (285°C versus 540°C).

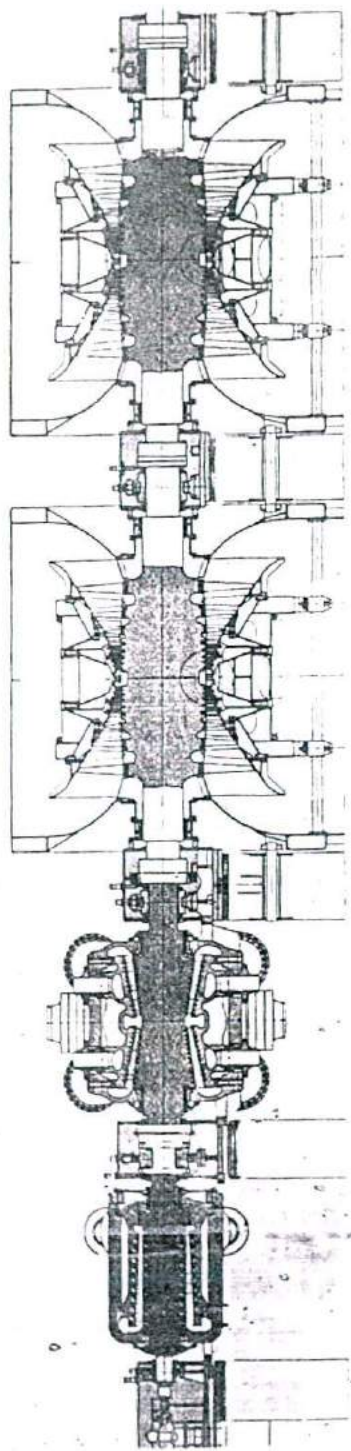


Figure 5-25. A 3600-r/min tandem compound steam turbine with one high-pressure, one intermediate-pressure, and two low-pressure sections. (Courtesy of Alfa Chalmers and Kraftwerk Union KWU.)

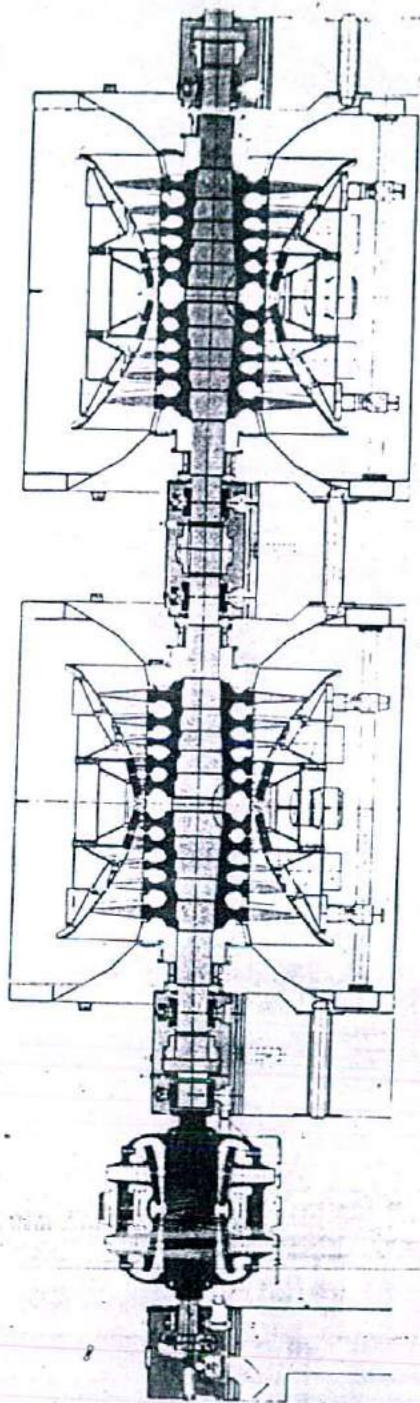


Figure S-26 A 1800-r/min tandem compound steam turbine with one high-pressure and two low-pressure sections. (Courtesy of Allis Chalmers and Kraftwerk Union, K/WU.)

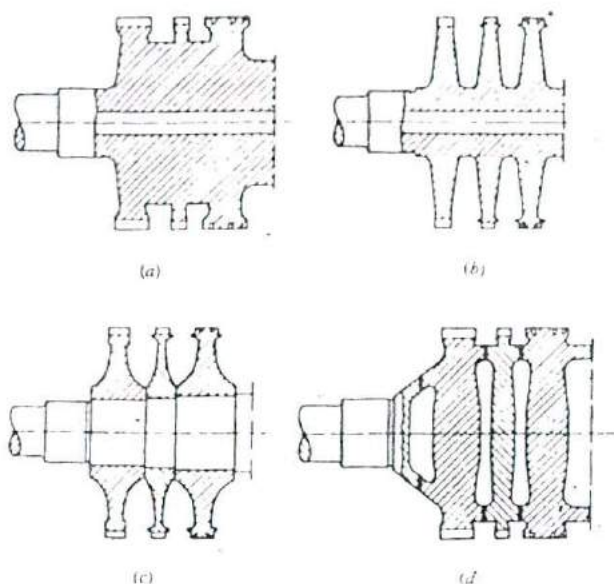


Figure 5-27 Different turbine rotor designs.

## 5-9 GAS TURBINES

Gas turbines for utility service are normally used for peak power production but sometimes also for intermediate and base-load duties when called upon during a major plant outage. Gas-turbine cycles will be covered in Chap. 8.

There are two basic types of gas turbines: radial-flow and axial-flow. The *radial-flow gas turbine* is similar in appearance to a centrifugal compressor, with the exception, of course, that gas flow is radially inward instead of radially outward. Radial-flow turbines are widely used in small sizes. They form a compact rigid rotor when combined with centrifugal compressors. A common use of such a combination is for *turbochargers* on stationary and marine diesel engines and, more recently, on both diesel and gasoline motor vehicle engines. Radial gas turbines, however, are not as suitable to the high-temperature gases necessary for good thermal efficiency (Chap. 8), and except for small sizes, are not as efficient as axial gas turbines. *Axial-flow gas turbines* resemble the steam turbines discussed in this chapter. Because we are concerned with larger sizes, the discussion that follows pertains to axial-flow gas turbines.

Gas-turbine stages are similar to those of steam turbines, except that the fluid is either a pure gas, such as helium, which is proposed for use with high-temperature gas cooled nuclear reactors, or air-and-combustion products in a fossil-fueled gas turbine. There are, obviously, no steam-condensation problems to worry about.

The inlet pressures to gas turbines are much lower than those for steam turbines.

being about 6 to 10 atm in fossil-fueled gas turbines and about 2 to 3 atm in helium turbines. The number of stages in fossil-fueled turbines is small, usually one to three, but the number is much larger in helium turbines. This can be shown by recalling that blade velocity  $V_B$  is a direct function of gas velocity  $V_s$ :  $V_{B,opt} = V_s \cos \theta$  [Eq. (5-35)]. The gas velocity can be obtained, ignoring inlet velocity to the fixed blades  $V_o$ , from

$$\frac{V_s^2}{2g_c J} = h_o - h_s = c_p (T_o - T_s) \quad (5-43)$$

where the subscripts  $o$  and  $s$  indicate entrance and exit of the fixed blades or nozzles. For a gas in ideal expansion

$$\frac{T_s}{T_o} = \left( \frac{P_s}{P_o} \right)^{(k-1)/k} = r_{pf}^{1-k} \quad (5-44)$$

where  $r_{pf} = P_o/P_s$ , the pressure ratio across the fixed blades. Combining Eqs. (5-43) and (5-44)

$$r_{pf} = \left( 1 - \frac{V_s^2}{2g_c J c_p T_o} \right)^{k/(1-k)} \quad (5-45)$$

For helium  $k$  and, particularly,  $c_p$  are greater than for air (approximating combustion gases). Equation (5-45) shows then that the pressure ratio across a single stage (related to that across the fixed blades by the degree of reaction) is much lower for helium than for air. Thus while the overall pressure ratio of a helium turbine is less than that of a combustion turbine, the pressure ratio per stage is far less and the number of stages is greater. Note that the overall pressure ratio is equal to the pressure ratio per stage to a power equal to the number of stages. A cross section of a 36-MW air-combustion turbine with a 16-stage compressor and a 3-stage turbine is shown in Fig.

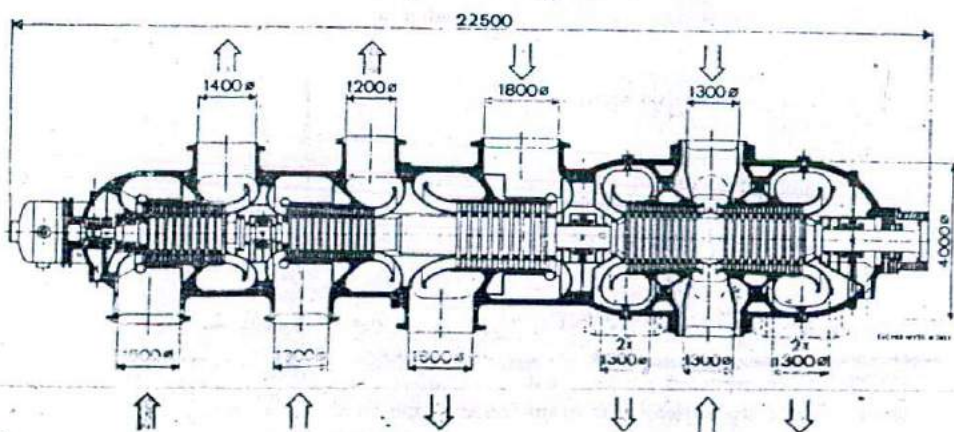


Figure 5-28: A proposed design for a helium-driver gas turbine, dimensions in millimeters [44].



8-12. Figure 5-28 shows a cross section of a proposed design for a single-shaft, 600-MW helium turbine showing, from left to right, 9-stage low-pressure, 10-stage medium-pressure, and 12-stage high-pressure axial compressors, and a double-flow turbine with a total of 20 stages [44].

### Gas-Turbine Blading

In steam-turbine practice, relatively inexpensive straight blading, i.e., untwisted, is used and designed on conditions at mean diameter, except in the long-bladed low-pressure stages where the large change in blade velocity with radius necessitates the use of twisted or vortex blading. The gas-turbine (Brayton) cycle is not as efficient as the Rankine cycle, and the gas-turbine designer, striving to squeeze improvements in efficiency from every stage, has used twisted blading throughout. Gas-turbine blading is invariably of the reaction type, meaning, as in steam-turbine blading, part reaction and part impulse, but the degree of reaction increases from blade root to tip. Hence it has not been the practice of the gas-turbine designer to designate a degree of reaction, or even impulse and reaction blading, but rather to use the so-called vortex theory [45, 46].

A detailed discussion of vortex theory is beyond the scope of this book. We shall assume for simplicity that the degree of reaction is constant along the blade and hence draw the velocity diagrams for gas-turbine blades in the same manner\* as steam-turbine reaction blades (Sec. 5-5). The velocities, however, are calculated from gas relationships. Helium, being a monatomic gas, has constant specific heats and is relatively easy to do. Combustion-gas properties can either be approximated by variable specific heat air (the air-to-fuel ratios are usually high) or obtained by the use of gas tables that take into account variable specific heats, the fuel-air mixture, and dissociation, App. I [48].

For the case of helium, or other gas with assumed constant specific heats, the enthalpy drop across the turbine  $\Delta h_T$  per unit mass-flow is given with reference to Fig. 5-29 by

$$\Delta h_T = c_p(T_o - T_e) \quad (5-46)$$

$$\frac{T_{e,s}}{T_o} = r_p r^{(k-1)/k} \quad (5-47)$$

$$\text{and} \quad \frac{T_o - T_e}{T_o - T_{e,s}} =: \eta_T \quad (5-48)$$

where  $T_o$  and  $T_e$  = the inlet and exit temperatures, °R or K, respectively

$T_{e,s}$  = exit temperature if turbine were adiabatic reversible, °R or K

\* We may add here that, in gas-turbine practice, blade and velocity angles are measured from the axial direction instead of the tangential direction as in steam practice and as we have done throughout this chapter. This practice we will ignore here and continue the same procedure as for steam blading.  $\beta$

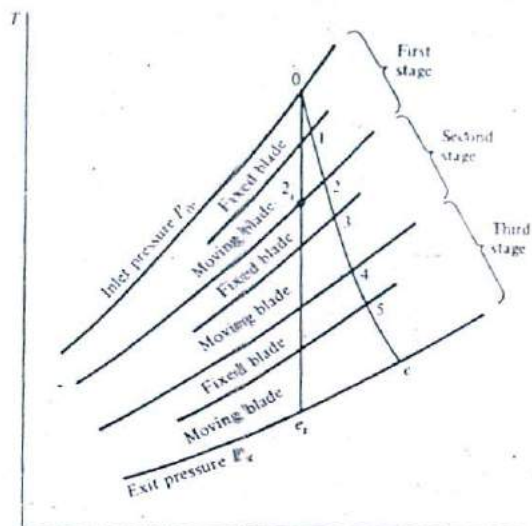


Figure 5-29  $T$ - $s$  diagram for gas turbine expansion.

$c_p$  = specific heat at constant pressure = 1.250 Btu/(lb<sub>m</sub> · °R)  
or 5.233 kJ/(kg · K) for helium and 0.240 Btu/(lb<sub>m</sub> · °R)  
or 1.005 kJ/(kg · K) for air at low temperatures

$k$  = ratio of specific heats = 1.659 for helium and 1.40 for air  
at low temperatures

$r_{p,T}$  = pressure ratio across turbine = ratio of inlet pressure  $P_0$   
to exit pressure  $P_e$

$\eta_T$  = turbine polytropic (adiabatic, or isentropic) turbine efficiency

For equal work by the stages, the total temperature difference  $T_0 - T_e$  is divided equally (for constant specific heat), and the stage exit temperatures, and pressures, are found. For example,  $T_2$  and  $T_4$  are the exit temperatures of the first and second stages in a three-stage turbine (Fig. 5-29). The stage is now divided according to the degree of reaction. For a 60 percent reaction in the second stage for example,  $T_3$ , the fixed-blade exit temperature, is found from  $(T_2 - T_3)/(T_2 - T_4) = 0.40$ . The fixed-blade exit velocity, and the moving blade inlet velocity  $V_{23}$ , is obtained from the nozzle equation for gases

$$V_{23}^2 - V_{12}^2 = 2g_c J c_p (T_2 - T_3) \quad (5-42)$$

where  $V_{12}$ , the inlet velocity to the fixed blades, is obtained from the velocity diagram of the previous stage, and  $J = 778.16 \text{ ft} \cdot \text{lb/Btu}$ , if English units are used.  $V_{e,0}$  may be negligible, however.

The velocity diagrams are now constructed in the manner of Figure 5-14, using Eqs. (5-31) and (5-32) where here  $\Delta h_f = c_p(T_2 - T_3)$  and  $\Delta h_m = c_p(T_3 - T_4)$ .

For the case of combustion gases with variable specific heats, products of combustion and dissociation, the gas tables [8] (see App. I) are used. This is best illustrated by an example.

**Example 5-3** A gas turbine using 200 percent theoretical air receives combustion gases at 2460°R. The first stage has a pressure ratio of 2.0, an efficiency of 0.9, and a 60 percent reaction (assumed constant along the blades). Referring to Figs. 5-14 and 5-29, take  $\theta = 20^\circ$ ,  $V_R$  corresponding to optimum, and calculate (1) the stage exit temperature  $T_2$ , (2) the fixed-blade exit temperature  $T_1$  and velocity  $V_{s1}$ , (3) the moving-blade inlet and exit angles, and (4) the exit velocity for zero exit whirl. The molecular weight of the gases is 28.88.

**SOLUTION** Using the gas tables for 200 percent theoretical air, App. I:

$$T_o = 2460^\circ\text{R}, h_o = \frac{19168.6}{28.88} = 663.7 \text{ Btu/lb}_m, \text{ and } P_{r_o} = 521.1.$$

$$P_{r_2} = \frac{521.1}{2} = 260.55$$

Thus

$$T_{2s} = 2099.7^\circ\text{R} \quad h_{2s} = 555.4 \text{ Btu/lb}_m$$

$$\eta_{\text{stage}} = 0.9 = \frac{h_o - h_2}{h_o - h_{2s}}$$

Therefore

$$h_2 = 566.2 \text{ Btu/lb}_m$$

Thus

$$T_2 = 2135.8^\circ\text{R}$$

For the stage  $\Delta h = h_o - h_2 = 97.5 \text{ Btu/lb}_m$ . For 60 percent reaction  $\Delta h_f = 0.4 \times 97.5 = 39.00 \text{ Btu/lb}_m$ ,  $h_1 = h_o - 39.00 = 624.7 \text{ Btu/lb}_m$ . Thus

$$T_1 = 2331.3^\circ\text{R}$$

Therefore

$$V_{s1} = \sqrt{2 \times 32.2 \times 778.16 \times 39.00} = 1398.0 \text{ ft/s}$$

$$V_R = V_{R,\text{opt}} = V_{s1} \cos \theta = 1398.0 \cos 20 = 1313.7 \text{ ft/s}$$

$$\phi_b = 90^\circ$$

$$V_{r1} = V_{t1} \sin \theta = 478.1 \text{ ft/s}$$

$$\Delta h_m = 0.6 \times 97.5 = 58.50 \text{ Btu/lb}_m$$

$$\frac{V_{r2}^2 - V_{r1}^2}{2g_s} \doteq \Delta h_m = 58.50 \times 778.16 = 45524.0 \text{ ft}\cdot\text{lb}_f$$

Therefore

$$V_{r2} = \sqrt{2 \times 32.2 \times 45524.0 + 478.1^2} = 1777.7 \text{ ft/s}$$

For zero exit whirl  $\delta = 90^\circ$ . Thus

$$\gamma = \cos^{-1} \frac{V_u}{V_{r2}} = \cos^{-1} \frac{1313.7}{1777.7} = 42.3^\circ$$

$$V_{z2} = V_{r2} \sin \gamma = 1777.7 \sin 42.3 = 1197.7 \text{ ft/s}$$

## PROBLEMS

- 5-1 A flat plate mounted on wheels, Fig. 5-2a, receives a perpendicular jet of water from a 5-cm<sup>2</sup> nozzle at a velocity of 20 m/s. Calculate the maximum power, in watts, imparted to the plate and the velocity of the plate, in meters per second, corresponding to that maximum power. Take water density as 1000 kg/m<sup>3</sup>.
- 5-2 A large movable cylindrical blade, Fig. 5-2b, receives a jet of air of 1-in<sup>2</sup> cross-sectional area. The air is at 2-atm pressure and 1000°F. Find the necessary air velocity, in feet per second, to produce a maximum power to the blade of 45 kW.
- 5-3 Steam enters a single-stage impulse (DeLaval) turbine at 900 psia and 900°F and leaves at 300 psia. Flow is adiabatic and reversible. The nozzle angle is 20°. The blade speed corresponds to maximum blade efficiency. The moving blade is symmetric. Determine the velocity diagram and find (a) the velocity of the steam leaving the nozzle, in feet per second, (b) the blade entrance angle, (c) the horsepower developed for a steam flow of 1 lb<sub>m</sub>/s, and (d) the blade efficiency.
- 5-4 A single-stage impulse turbine is required to develop 50 MW of power. Steam enters the nozzles saturated at 70 bars and leaves at 50 bars. The blades are symmetrical and have a velocity coefficient of 0.96. Calculate (a) the minimum steam flow, in kilograms per second, that would result in the required power, (b) the blade efficiency, and (c) the stage efficiency.
- 5-5 Steam expands ideally in a turbine from 2500 psia and 1000°F to 1 psia. Compare the maximum steam velocities and the number of stages required by (a) a velocity-compounded impulse turbine, (b) a pressure-compounded impulse turbine, and (c) a 50 percent reaction turbine if the optimum blade velocity may not exceed 885 ft/s in any of them. Take all nozzle angles to be 25°.
- 5-6  $1.08 \times 10^6$  lb<sub>m</sub>/h of steam enter a Curtis stage with an absolute velocity of 4000 ft/s. The nozzle angle and discharge angle of stationary blades are both 20°. The moving blades are symmetric and rotate at 600 ft/s. Assuming ideal steam flow in the nozzle and blades, determine the velocity diagram and find (a) the power, in horsepower and megawatts, developed in the stage, and (b) the blade efficiency.
- 5-7 A Curtis stage receives  $3.6 \times 10^6$  lb<sub>m</sub>/h of steam at 2380 ft/s and 20° angle. The blade speed is 550 ft/s. The velocity coefficients in moving and stationary blades are 0.905 and 0.932, respectively. Determine the velocity diagram and find (a) the total stage power in feet-pound force per second, horsepower, and kilowatts and (b) the blade efficiency of the stage.
- 5-8 Steam enters a Curtis impulse stage at 1000 psia and 1000°F, and exits at 1 atm. The nozzle angle is 20° and its efficiency is 87 percent. The fixed blade exit angle is 23°. The moving blades are symmetrical.

All velocity coefficients are 0.97. For optimum work, calculate (a) the blade velocity, in feet per second, (b) the work done by each stage, in Btus per pound mass of steam, (c) the stage efficiency.

5-9 A Rateau turbine operating between 1000 psia and 1000°F and 1 atm has symmetrical blades, nozzle angles of 20°, nozzle efficiencies of 97 percent, and velocity coefficients of 0.97. (The same data as that for the Curtis stage in Prob. 5-8.) Calculate (a) the number of stages necessary to limit the optimum blade velocity to that of the Curtis stage (1009.6 ft/s), (b) the work of each stage, in Btus per pound mass, (c) the turbine efficiency, and (d) the percent error in steam inlet velocity to the second stage due to ignoring the absolute steam velocity leaving the first stage.

5-10 A 50 percent reaction turbine operates between 1000 psia and 1000°F and 1 psia (the same conditions as for the velocity-compound and pressure-compound impulse turbines of Probs. 5-8 and 5-9). All steam expansion efficiencies in fixed and moving blades are 87 percent. All steam absolute angles ( $\theta$  and  $\gamma$ ) are 20°. The turbine has the same optimum blade speed as the impulse turbines of Probs. 5-8 and 5-9 (1009.6 ft/s), assumed constant for all stages for simplicity. (a) Find the number of stages, (b) determine the steam velocity diagram, (c) calculate the work done by each stage, in Btus per pound mass, and (d) calculate the first stage efficiency.

5-11 A two-nozzle acolpile similar to that of Hero of Alexandria contains saturated steam at 6 bars and exhausts to 1 atm. The nozzles are 60 percent efficient, have exit areas of 20 cm<sup>2</sup> each and their areas are 2 m apart. Calculate the torque, in joules, on the turbine shaft.

5-12 Consider one stage in a 50 percent reaction turbine. 1 lb<sub>m</sub>/s steam enters the stage at 100 psia and 400°F and leaves at 40 psia. The adiabatic efficiency of the stage is 0.90. The blades have exit angles of 20°. The blade-speed ratio (blade velocity to incoming steam velocity) is 0.8. Determine the velocity diagram and find (a) the pressure at the exit of the fixed blades, in psia, (b) the blade speed, in feet per second, and (c) the horsepower developed in the stage.

5-13 A 50 percent reaction stage in a steam turbine undergoes a total of 20 Btu/lb<sub>m</sub> enthalpy drop. The nozzle efficiency and angle are 88 percent and 25°, respectively. The blades move at 420 ft/s and have  $V_{12} = 332$  ft/s,  $V_{21} = 386$  ft/s, and  $\gamma = 22^\circ$ . The steam flow is  $1.08 \times 10^6$  lb<sub>m</sub>/h. Find (a) the work done by the stage in horsepower and megawatts, (b) the blade efficiency, (c) the stage (nozzle and blade) efficiency, and (d) the blade velocity corresponding to maximum efficiency, in feet per second.

5-14 A reaction turbine has 33-in-long blades that receive a constant steam velocity 800 ft/s along their entire lengths. The blades are designed for optimum conditions at midlength. They are attached to a 60-in-diameter rotor. Assuming ideal frictionless flow, calculate the blade entrance and exit angles ( $\beta$  and  $\gamma$ ) at the base, midpoint, and tip of the blades, respectively. Assume a constant exit whirl along the length of the blades.

5-15 A steam turbine having  $N$  stages develops 20,000 hp when receiving 110,000 lb<sub>m</sub>/h, 800 psia, 900°F steam, and exhausting at 1 psia. All stages have equal enthalpy drops and equal efficiencies. For a reheat factor  $r_h = 1.07$ , find (a) the individual stage efficiency and (b) the turbine efficiency.

5-16 10<sup>6</sup> lb<sub>m</sub>/h of steam enters an ideal steam turbine stage at 100 psia and 350°F and leaves it at the Wilson line, assumed in this case to occur at 50 psia. Calculate the stage exit temperature, in degrees Fahrenheit, and the power produced in the stage, in megawatts, in the cases of (a) supersaturation, assuming that supersaturated steam expansion may be represented by perfect gas laws with a polytropic exponent  $n = 1.32$ , and (b) thermodynamic equilibrium.

5-17 Consider a simple combination turbine with one Delaval impulse stage and one 60 percent reaction stage. The nozzle of impulse stage receives steam at 900 psia and 900°F and leaves it at 300 psia. The nozzle efficiency is 97 percent and its angle is 20°. The blade speed is optimum and its velocity coefficient is 0.95. The impulse stage is followed on the same shaft by the reaction stage which exhausts to 100 psia. The steam entrance angles for that stage are also 20°. The efficiency of the fixed blades (nozzles) is 90 percent. Because of different diameters of the impulse and reaction moving blades, the velocity of the reaction blade is 1.5 that of the impulse blade. (a) Determine all steam velocities and draw the velocity diagram of the combined turbine, (b) calculate the work of each stage, in Btus per pound mass, and (c) calculate the individual stage and the turbine efficiencies.

5-18 It is required to compare the design of an ideal helium to an ideal air gas turbine. Both have the same inlet gas temperature of 2000°R and maximum gas velocity of 1250 ft/s. Find the number of stages of each

if the overall pressure ratios are 2 for the helium turbine and 6 for the air turbine. Take  $c_p = 1.25 \text{ Btu/lb}_m \cdot ^\circ\text{R}$  for helium and  $0.243 \text{ Btu/lb}_m \cdot ^\circ\text{R}$  for air.

5-19 A gas turbine composed of two reaction stages receives  $1 \text{ lb}_m/\text{s}$  of combustion gases (assumed to be pure air) at  $80 \text{ psia}$  and  $1800^\circ\text{F}$ . It exhausts at  $15 \text{ psia}$ . All stages are 50 percent reaction. Flow is considered adiabatic and reversible. The blade exit angles are  $20^\circ$ . The blade speeds correspond to maximum efficiency. Both stages produce equal power. Determine the velocity diagram and find the turbine power in horsepower and megawatts. For simplicity, assume  $V_n = \text{constant}$ , and  $c_p = 0.24 \text{ Btu/lb}_m \cdot ^\circ\text{R}$  and  $k = 1.4$ .

5-20 An ideal helium gas turbine has six rows of 50 percent reaction blades and an overall pressure ratio of 2.5. All stages have the same enthalpy drop. The maximum helium temperature is  $1000^\circ\text{F}$ . The blade speed corresponds to optimum work. All blade entrance angles are  $20^\circ$ . Considering the high-pressure stage, determine the velocity diagram, and calculate (a) the helium exit temperature and (b) the horsepower and megawatts developed in the stage for a helium flow of  $1 \text{ lb}_m/\text{s}$ .

5-21 An ideal gas turbine receives combustion gases at  $6 \text{ atm}$  and  $2000^\circ\text{F}$ , and exhausts to  $1 \text{ atm}$ . It has two stages of 50 percent reaction blading producing equal work per stage.  $\gamma = \theta = 20^\circ$ ,  $V_2 = V_1$ . Consider the turbine to be adiabatic and reversible. For the high-pressure stage (a) draw the velocity diagram, assuming optimum blade speed, (b) find the horsepower for  $1 \text{ lb}_m/\text{s}$  air flow, and (c) the blade efficiency. For simplicity assume the gases to have a constant  $c_p = 0.24 \text{ Btu/lb}_m \cdot ^\circ\text{R}$   $k = 1.4$ .

5-22 An ideal-gas turbine composed of two reaction stages receives  $1 \text{ lb}_m/\text{s}$  of combustion gases with 200 percent theoretical air at  $80 \text{ psia}$  and  $1800^\circ\text{F}$ . It exhausts at  $15 \text{ psia}$ . All stages are 50 percent reaction. The blade exit angles are  $20^\circ$ . The blade speeds correspond to maximum efficiency. Both stages produce equal power. Determine the velocity diagram and find the turbine power in kilowatts. For simplicity, assume  $V_n = \text{constant}$ . The molecular weight of the gases is 28.88. Use the gas tables, App. I.

5-23 A reaction gas turbine stage with 59.16 percent degree of reaction (based on an isentropic enthalpy drop) receives  $10^6 \text{ lb}_m/\text{s}$  of combustion gases with 200 percent theoretical air at  $2560^\circ\text{R}$ . The pressure ratio across the stage is 1.987. The fixed blades (nozzles) exit angle is  $22^\circ$  and their efficiency is 86.72 percent. The stage efficiency is 83.94 percent. The moving blade speeds are optimum. The molecular weight of the gases is 28.88. Using the gas tables determine the velocity diagram and calculate (a) the gas velocity, in feet per second, and temperature, in degrees Rankine, entering the moving blades, (b) the gas velocity, in feet per second, and temperature, in degrees Rankine, leaving the stage, and the stage power, in megawatts.

5-24 A reaction gas turbine stage with 59.16 percent degree of reaction receives combustion gases with 200 percent theoretical air at  $2560^\circ\text{R}$ . The pressure ratio across the stage is 1.987. The fixed blade (nozzle) efficiency is 86.72 percent. The stage efficiency is 83.94 percent. Calculate (a) the gas velocity entering the moving blades, in feet per second, (b) the stage efficiency, and (c) the power developed, in megawatts. The molecular weight of the gases is 28.88.

## THE CONDENSATE-FEEDWATER SYSTEM

## 6-1 INTRODUCTION

We will now continue following the working fluid around the powerplant cycle. We started with steam generation and combustion in Chaps. 3 and 4 and then continued on with turbines in Chap. 5. In this chapter we will cover the major components that make up the condensate-feedwater system, which takes us back to the steam generator. These are primarily heat-transfer equipment, such as the condenser and feedwater heaters, but they also include some important items that are necessary for the efficient operation of the cycle, such as boiler water makeup and treatment.

The plant heat-rejection system, which deals with the circulating cooling water of the condenser, requires separate and special attention and will be covered in the next chapter.

The primary purpose of the condenser is to condense the exhaust steam from the turbine and thus recover the high-quality feedwater for reuse in the cycle. In so doing, it actually performs an even more useful function. If the circulating cooling-water temperature is low enough, as is usually the case, it creates a low back pressure (vacuum) for the turbine to exhaust to. This pressure is equal to the saturation pressure that corresponds to the condensing steam temperature, which in turn is a function of the cooling-water temperature. As is now known, the enthalpy drop, and hence turbine work, per unit pressure drop is much greater at the low-pressure than the high-pressure end of a turbine. A condenser, by lowering the back pressure by only a few psi, increases the work of the turbine, increases the plant efficiency, and reduces the steam flow for a given plant output. The lower the pressure, the greater the effects; hence, thermodynamically, it is important to use cooling-water temperatures that are the lowest

available. Condensing powerplants are therefore much more efficient than noncondensing ones. All modern powerplants are of the condensing type. A condenser is a major and very important piece of equipment in a powerplant.

There are primarily two types of condensers: *direct-contact* and *surface condensers*. The latter are used in the majority of powerplants.

The main purpose of feedwater heaters (Chap. 2) is to improve cycle efficiency by heating the condensate and feedwater before returning it to the steam generator. The heating could be as high as 400 to 500°F (200 to 260°C) in a fossil-fueled powerplant but is lower in a water-cooled nuclear-reactor powerplant. There are also two basic types of feedwater heaters: the closed, *surface* or shell-and-tube type, and the *open*, *direct-contact* or *deaerating* type.

## 6-2 DIRECT-CONTACT CONDENSERS

*Direct-contact*, or *open*, *condensers* are used in special cases, such as when dry-cooling towers are used (Sec. 7-6), in geothermal powerplants (Chap. 12), and in powerplants that use temperature differences in ocean waters (OTEC) (Chap. 15). Modern direct-contact condensers are of the spray type. Early designs were of the barometric or jet types.

### The Spray Condenser

Direct-contact condensers, as the name implies, condense the steam by mixing it directly with the cooling water. In the *spray condenser* this is done by spraying the water into the steam. Thus turbine exhaust steam at point 2, Figs. 6-1 and 6-2, mixes

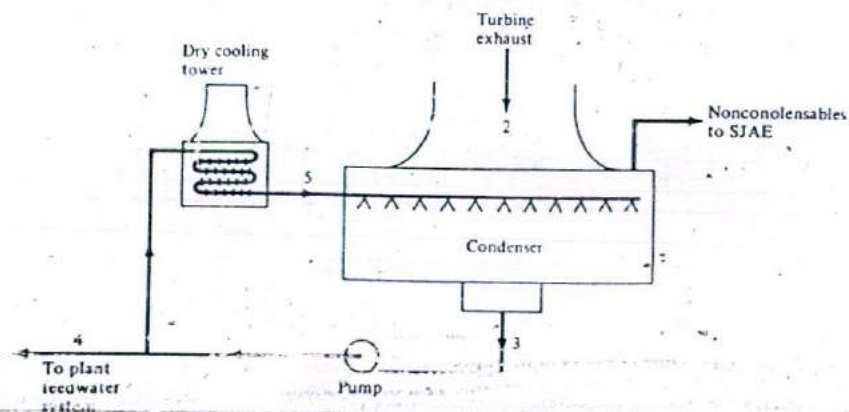


Figure 6-1 Schematic flow diagram of a direct-contact condenser of the spray type. SJAE = steam-jet air ejector.



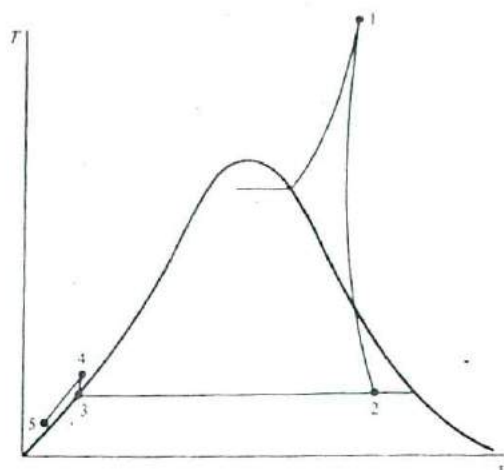


Figure 6-2  $T$ - $s$  diagram of condensate and cooling water in a direct-contact condenser system. (Difference between line 4-5 and saturated-liquid line is exaggerated).

with cooling water at 5 to produce nearly saturated condensate at 3, which is pumped to 4. Part of the condensate, equal to the turbine exhaust flow, is sent back to the plant as feedwater. The rest is cooled, usually in a dry- (closed-) cooling tower to point 5. The cooled water at 5 is sprayed into the turbine exhaust, and the process is repeated. Thus cooling water continually circulates. Its purity must be maintained because it mixes with the steam, hence its use with closed-type dry-cooling tower. Otherwise the mixture at 4 is discarded, as in geothermal or OTEC plants.

A mass balance on the system, where  $\dot{m}$  denotes mass-flow rates, gives

$$\dot{m}_2 = \dot{m}_4 \quad (6-1)$$

and

$$\dot{m}_3 = \dot{m}_2 + \dot{m}_5$$

An energy balance, where  $h$  denotes specific enthalpies, gives

$$\dot{m}_2 h_2 + \dot{m}_5 h_5 = \dot{m}_3 h_3 \quad (6-2)$$

and the ratio of circulating cooling water to steam flow is given by

$$\frac{\dot{m}_5}{\dot{m}_2} = \frac{h_2 - h_3}{h_3 - h_5} \quad (6-3)$$

Thus circulating-water flow is much greater than steam flow because  $h_2 - h_3$  represents a large fraction of the large latent heat of vaporization at the reduced pressure, whereas  $h_3 - h_5$  represents the much smaller sensible heat of the liquid.

**Example 6-1** Find the ratio of circulating water to steam flows if the condenser pressure is 1 psia and the cooling tower cools the water to 60°F. Assume turbine exhaust at 90 percent quality.

SOLUTION From the steam tables

$$h_2 = 69.73 + 0.9 \times 1036.1 = 1002.22 \text{ Btu/lb}_m$$

$$h_3 = 69.73 \text{ Btu/lb}_m$$

$$h_5 \approx h_f \text{ at } 60^\circ\text{F} = 28.06 \text{ Btu/lb}_m$$

$$\frac{\dot{m}_5}{\dot{m}_2} = \frac{1002.22 - 69.73}{69.73 - 28.06} = 22.38$$

In Fig. 6-1, two pumps, one in the feedwater line and the other in the circulating-water line, may be used instead of the single pump shown. The effect of this arrangement on mass and energy balances is minimal.

### Barometric and Jet Condensers

These early type condensers operate on the same principle as the spray condenser, except that no pump is required. The vacuum in the condenser is obtained by virtue of a static head, as in the barometric condenser (Fig. 6-3a), or a diffuser, as in the jet condenser (Fig. 6-3b).

In the *barometric condenser*, the cooling water is made to cascade down a series of baffles in the form of water curtains or sheets of high surface-to-volume ratio to

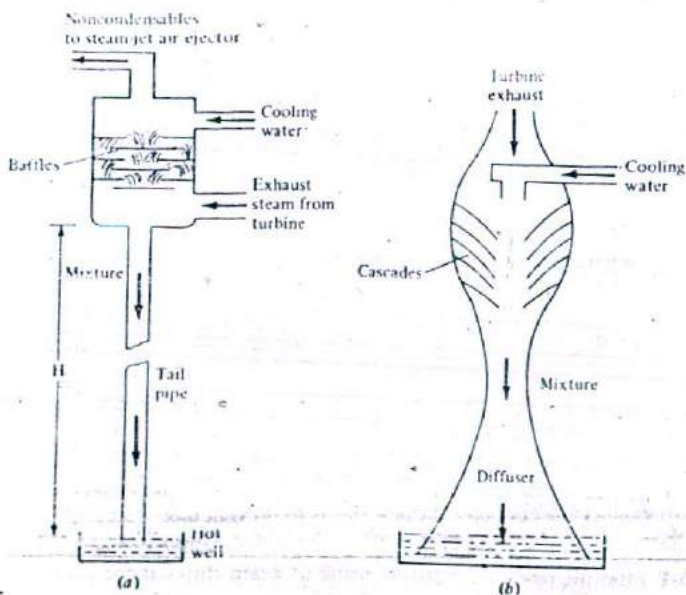


Figure 6-3 Schematics of early direct-contact condensers: (a) barometric, (b) diffuser or jet.

mix thoroughly with the turbine exhaust that is trying to rise from a lower inlet. The steam condenses and the mixture goes down a *tail pipe* to the hot well.

The tail pipe compresses the mixture to atmospheric pressure at the hot well by virtue of its static head and thus replaces the pump used in the spray-type condenser. The pressure differential created by the tail pipe must overcome the pressure difference between the atmosphere  $P_{atm}$  and the condenser proper  $P_{cond}$ , plus the friction pressure drop caused by the mixture flow  $\Delta P_f$  in the tail pipe itself. Thus

$$\rho H \frac{g}{g_c} = P_{atm} - P_{cond} + \Delta P_f \quad (6-4)$$

where  $\rho$  = density of mixture,  $\text{lb}_m/\text{ft}^3$  or  $\text{kg}/\text{m}^3$

$H$  = height of tail pipe, ft or m

$g$  = gravitational acceleration,  $\text{ft}/\text{s}^2$  or  $\text{m}/\text{s}^2$

$g_c$  = conversion factor,  $32.2 \text{ lb}_m \cdot \text{ft}/(\text{lb}_f \cdot \text{s}^2)$  or  $1 \text{ kg} \cdot \text{m}/(\text{N} \cdot \text{s}^2)$

It can be seen that for low values of the friction pressure drop the tail pipe height  $H$  is around 32 ft (9.6 m) and is higher the larger the friction. Friction is reduced by increasing tail-pipe diameter, which results in a tall, heavy system.

In the *jet-type condenser* (Fig. 6-3b), the height of the tail pipe is reduced by replacing it with a diffuser. The diffuser acts on the same principle as the diverging section of a convergent-divergent nozzle in subsonic flow. It thus helps raise the pressure in a shorter distance than the tail pipe. Even though the height is reduced, the mass and cost of the system are probably increased, however.

In both barometric and diffuser-type condensers, the mixture is split and cooled in the same manner as in the spray-type condenser. In all direct-contact condensers, as in surface-type condensers (below), noncondensable gases must be removed, usually with a steam-jet air ejector (SJAE).

### 6-3 SURFACE CONDENSERS: GENERAL

Surface condensers are the most common type used in powerplants. They are essentially shell-and-tube heat exchangers, in which the primary heat-transfer mechanisms are the condensing of the saturated steam on the outside of the tubes and the forced-convection heating of the circulating water inside the tubes. Figure 6-4 is a schematic of a surface condenser with two passes on the water side. It is composed of a steel shell with water boxes on each side, the right one divided to allow for the two water passes. The water tubes are rolled at each end into tube sheets, and there are steel support plates at intermediate points between the tube sheets to prevent tube vibration. The hot well that receives the condensate acts as a reservoir, with a capacity equal to the total condensate flow during a prescribed time, e.g., 1 min.

Surface condensers have grown in size since late in the last century to present-day sizes that exceed 1 million  $\text{ft}^2$  ( $\sim 93,000 \text{ m}^2$ ) of heat-transfer surface area. A

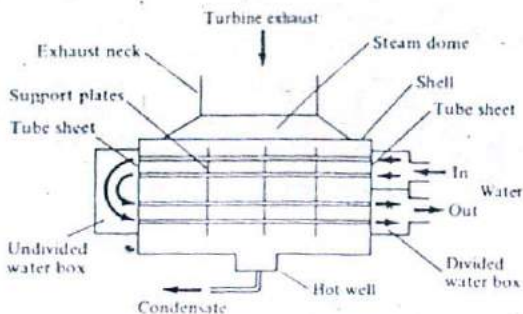


Figure 6-4 Schematic of a two-pass surface condenser.

landmark of development was two 80,000 ft<sup>2</sup> (7432 m<sup>2</sup>) units built in 1929 by the Foster Wheeler Corporation for the predecessor of the Commonwealth Edison Co. of Chicago, Illinois. These were and remained through the late 1940s the largest units built. They were constructed of sections of cast-iron shells that were bolted together and were single-pass with full reverse backwashing provided by valving built integrally with the water boxes.

Besides size, philosophies of design have also changed over the years. The early surface condensers used simple circular tube sheets that supported as many tubes that could be tightly packed between them. They were 3 or 4 ft in diameter, and the tubes were no more than 10 or 12 ft in length. As powerplants and their condensers grew in size, this simple design resulted in heat-transfer problems because the upper tubes shielded the steam from effective condensing and in high-steam-pressure drop problems because of the long tortuous path of the steam through the bundle. (We would like to see the minimum pressure at turbine exhaust, if possible.) The heat-transfer problem was solved by using larger spacings between tubes (called ligaments) and placing them in rows that provided lanes or steam paths to allow the steam to penetrate deeply into the lower tubes.

The next improvement tackled the high-pressure drops by cutting the bundle in half, thus in effect forming two smaller bundles side by side. This gave the condenser a kidney cross-sectional shape that was popular with most manufacturers through the 1940s. Even this solution was not sufficient for the larger units that were coming on line because the bundles were still too deep for effective steam penetration. Four tube bundles were then used. This also helped reduce condenser height, an increasingly frequent requirement because of the low available head room in the plant.

The current design philosophy is to have a tube layout in the shape of a funnel with most tubes, and the largest tube passage area, where the steam enters the condenser from the turbine. As the steam condenses and its volume decreases, there are fewer tubes and smaller passage areas. Steam is made to enter the tube bundle, or bundles, from all sides toward a central air cooler for deaeration (below). In effect a low and balanced (to avoid cross-flow) steam-pressure drop should be ensured.

The tubes are rolled into the tube sheets at both ends to prevent leakage of the

circulating water into the steam. An *expansion joint* allows for the different rates of expansion between the tubes and the shell. The tube sheets are usually made of Muntz metal, which is similar to brass.

A problem of steam distribution, other than vertical penetration, is end-to-end or horizontal distribution that arises with present-day long-tube units. Tube lengths of 30 to 50 ft (~9 to 15 m) are commonplace. Multipressure condensers (below) may have 70- to 90-ft (~21- to 27-m) tubes. Long tubes result in larger changes in water temperature inside them and hence greater changes in condensing ability. Thus, the tubes would be too close at the cold end, where condensing is good, and too open at the hot end. A design compromise is, of course, necessary. This results in some short-circuiting that may be counteracted by cross baffles.

Another distribution problem is the result of the unavoidably unequal steam flow from the turbine exhaust duct to the condenser tubes. Thus special attention must be paid to the design of the connection between turbine and condenser (called the *exhaust neck*), such as adding a well-tapered *steam dome* above the tube bundle to minimize this problem. An expansion joint is usually provided between the turbine exhaust and the condenser steam inlet. This permits the condenser to be rigidly mounted on the floor. Another, less common, arrangement is to bolt the condenser directly to the turbine exhaust duct and support it on springs that allow a certain vertical movement and reduce the strain on the turbine casing.

### Number of Passes and Divisions

Condensers are designed with one, two, or four cooling-water passes. The number of passes determines the size and effectiveness of a condenser. Four passes are seldom used in utility installations. A *single-pass condenser* is one in which the cooling water flows through all the condenser tubes once, from one end to the other. In a *two-pass condenser* the water enters half the tubes at one end of a divided inlet water box, passes through these tubes to an undivided water box at the other end, reverses direction, and passes through the other half of the tubes back to the other side of the divided water box. A single-pass condenser with the same total number and size of tubes, i.e., the same heat-transfer area, and with the same water velocity, requires twice as much water flow but results in half the water temperature rise and thus lower condenser pressure. Thus such a single-pass condenser is good for plant thermal efficiency and reduces thermal pollution, but requires more than twice the water and hence four times the pumping power.

Water boxes are often divided beyond the divisions required by the number of passes. A divided water box single-pass condenser, for example, may have a partition in both the inlet and outlet water boxes at opposite ends of the condenser. This allows half the condenser to operate while the other half is being cleaned or repaired. In the case of a divided two-pass condenser, the water boxes are divided into four quarters. Divided water boxes have duplicate inlet and outlet connections, each with its own circulating-water circuit. Valves in the division plates permit backwashing by reversing water flow for cleaning purposes.

## Single- and Multipressure Condensers

As is now known, large powerplants usually have two or more low-pressure turbine sections in tandem. The condenser may be divided into corresponding sections or shells, situated below the low-pressure turbine sections.

If the turbine exhaust pressure in all sections is the same, i.e., when the exhaust ducts are not isolated from each other, we would have a *single-pressure condenser*. If the exhaust ducts are isolated from each other, these individual condenser shell pressures will increase because the circulating-water temperature will increase as it flows from shell to shell. We would then have a *multipressure condenser*.

A multipressure condenser results in efficiency improvement because the average turbine back pressure is less compared with that of a single-pressure condenser (which is determined by the highest circulating-water temperature). Multipressure condensers are more commonly used in nuclear powerplants. They are usually single-pass units

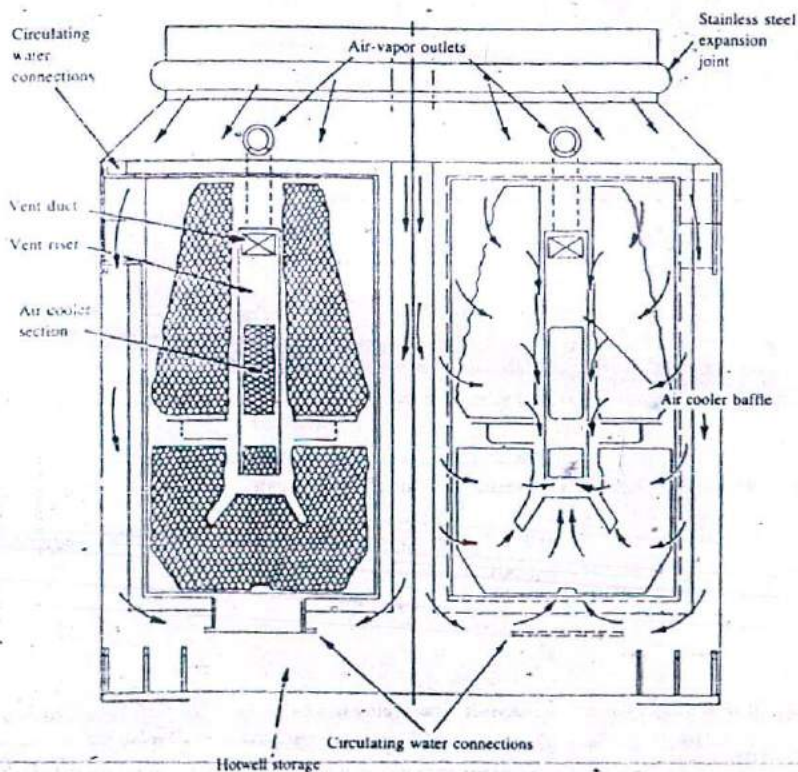


Figure 6-5 cross section of a single-pass, divided-box surface condenser. Note the radial pattern of steam flow.

arranged with their tubes parallel to the turbine shaft. They are roughly as long as the low-pressure turbine sections combined, often 70 to 90 ft (~21.3 to 27.4 m). Single-pressure condensers, on the other hand are usually 30 to 50 ft (~9.1 to 15.2 m) long and are often arranged with their tubes perpendicular to the turbine shaft.

In essence, condensers are almost custom-designed to suit individual requirements of steam flow, available cooling-water flow and temperature, available space, and other variables.

Figure 6-5 shows a cross section of a typical modern large condenser. It is a single-pass, single-pressure, radial-flow type condenser in which the steam enters the bundles from top, sides, and bottom and flows toward the center of the tube nest. At that point most of it has condensed, leaving only air and other noncondensable gases that are cooled before being removed by the deaeration system (below). Figure 6-6 shows a two-pass divided-box surface condenser.

Table 6-1 lists typical condenser dimensions for plants up to 500-MW capacity.

### Tube Sizes and Materials

Tube sizes and gauges (Birmingham Wire Gauge, BWG) are listed for condenser and feedwater heater tubes in App. K. Note that the higher the gauge number, the thinner

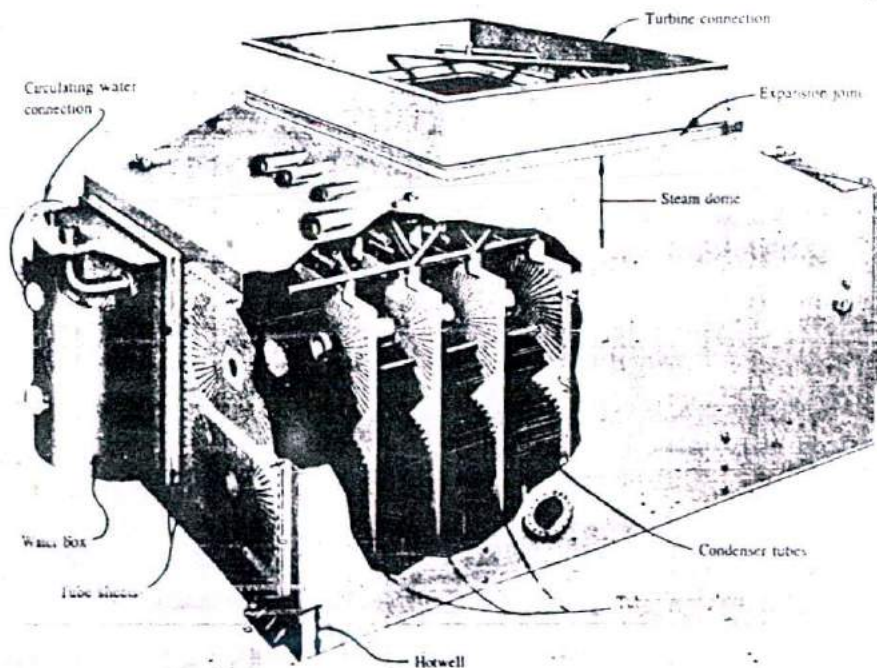
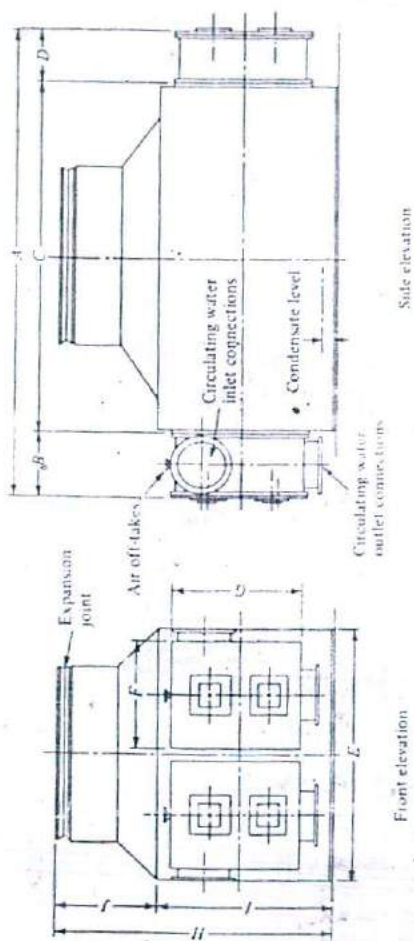


Figure 6-6 A two-pass divided-box surface condenser.

Table (1-1) Condenser dimension sheet\*



Capacity MW	Steam flow, lb./hr	Surface area, ft <sup>2</sup>	Number of passes	Circulating water inlet temp., °F	Vacuum, in Hg	Hotwell storage, min	Condenser tubes			Connections		
							Length in.	OD in.	Inlet, in.	Circulating water Outlet, in.	Turbine exhaust Width	Length
50	320,000	42,500	2	80	2	5	26	7/8	30	30	9'-5"	12'-5"
75	376,000	55,000	2	80	2	5	26	7/8	36	36	9'-5"	12'-5"
100	486,000	75,000	2	80	2	5	28	7/8	42	42	14'-0"	14'-0"
125	600,000	90,000	2	80	2	5	28	7/8	48	48	14'-0"	14'-0"
150 <sup>c</sup>	710,000	110,000	2	80	2	5	28	7/8	54	54	14'-0"	14'-0"



200	915,000	150,000	2	80	2	5	30	$\frac{7}{8}$	60	60	17'-4"	19'-4"
250	1,030,000	180,000	2	80	2	5	30	$\frac{7}{8}$	66	66	18'-0"	20'-0"
300	1,110,000	210,000	2	80	2	5	30	$\frac{7}{8}$	72	72	18'-0"	20'-0"
400	1,740,000	280,000	2	80	2	5	30	$\frac{7}{8}$	78	78	18'-0"	20'-0"
500	2,110,000	340,000	2	80	2	5	30	$\frac{7}{8}$	84	84	18'-0"	20'-0"

Table 6: Condenser dimension : heef (continued)

Dimensions												
Capacity MW	A	B	C	D	E	F	G	H	I	J		
50	31'-6"	3'-6"	26'-0"	2'-0"	19'-3"	7'-1"	9'-0"	19'-4"	12'-4"	7'-0"		
75	32'-8"	4'-0"	26'-0"	2'-6"	21'-2"	8'-0"	10'-1"	20'-5"	13'-5"	7'-0"		
100	35'-4"	4'-6"	28'-0"	3'-0"	22'-10"	8'-10"	11'-3"	22'-7"	14'-7"	8'-0"		
125	36'-6"	5'-0"	28'-0"	3'-6"	24'-4"	9'-7"	12'-3"	23'-7"	15'-7"	8'-0"		
150	37'-6"	5'-6"	28'-0"	4'-0"	26'-2"	10'-6"	13'-5"	25'-9"	16'-9"	9'-0"		
200	40'-6"	6'-0"	30'-0"	4'-6"	29'-0"	11'-9"	15'-0"	28'-0"	19'-0"	9'-0"		
250	41'-8"	7'-6"	30'-0"	5'-0"	31'-0"	12'-9"	16'-4"	30'-4"	20'-4"	10'-0"		
300	42'-6"	7'-0"	30'-0"	5'-6"	34'-0"	13'-9"	17'-7"	31'-7"	21'-7"	10'-0"		
400	43'-6"	7'-6"	30'-0"	6'-0"	38'-0"	15'-9"	20'-3"	34'-3"	24'-3"	10'-0"		
500	44'-6"	8'-0"	30'-0"	6'-6"	41'-0"	17'-3"	22'-1"	36'-1"	26'-1"	10'-0"		

\* Courtesy Westinghouse Electric Corporation.

Note: Based on using admiralty tubes.

and lighter the tubes. 5/8-in. tubes (all sizes refer to OD) are easily clogged and are used only for small and special applications. Modern condensers commonly use 7/8 or 1.0 in. of 18 gauge, which is adequate for the water pressures encountered in condensers.

Tube materials in common use are listed in Table 6-2. Admiralty metal,\* the popular choice for a long time, although still occasionally specified, is being supplanted by type 304 stainless steel. Type 304 stainless, now readily available at reasonable cost, has excellent erosion and corrosion resistance in fresh water and immunity to ammonia and sulfide attack. It also eliminates the risk of introducing copper ions into the feedwater, a potential possibility with other materials. Its disadvantages are a low thermal conductivity and low resistance to chloride attack and biofouling. 90-10 copper-nickel is another choice for fresh water.

In the case of seawater and brackish water, 90-10 copper-nickel is the primary choice whether these waters are clean or polluted. 70-30 copper-nickel is preferred in the case of clean waters where shell-side ammonia is a problem. Copper-nickel has excellent corrosion resistance in salt and brackish water and good immunity to stress-corrosion cracking. Aluminum-brass is another tube material, though at present a remote possibility with polluted water.

\* Other materials that have seen use are arsenical copper and aluminum-bronze. It is expected that, for the foreseeable future, stainless steel and copper-nickel will dominate the market for condenser tubes. Other materials of promise include titanium and AL6X, which are expected to see increasing service under severe conditions. In any case no one material can function perfectly without periodic cleaning, and there is a growing interest in devising methods of on-line cleaning.

## Deaeration

In steam and other vapor cycles, it is important to remove the noncondensable gases that otherwise accumulate in the system. The noncondensables are mostly air that leaks from the atmosphere into those portions of the cycle that operate below atmospheric pressure, such as the condenser, but also include other gases caused by the decomposition of water into oxygen and hydrogen by thermal or radiolytic (under the influence of nuclear radiation) action and by chemical reactions between water and materials of construction. The presence of noncondensable gases in large quantities has undesirable effects on equipment operation for several reasons.

1. They raise the total pressure of the system because that total pressure is the sum of the partial pressures of the constituents. Thus in a condenser the pressure will be the sum of the saturation pressure of the steam, determined by its temperature, and the partial pressure of the noncondensables. An increase in condenser pressure lowers plant efficiency.

\* Admiralty metal: 70 to 73 percent copper (Cu), 0.9 to 1.2 percent tin (Sn), 0.07 percent maximum iron (Fe), the rest zinc (Zn).

2. They blanket the heat-transfer surfaces such as the outside surface of the condenser tubes, thus resulting in a severe decrease in the condensing heat-transfer coefficient and hence in condenser effectiveness.
3. The presence of some noncondensables results in various chemical activities. Oxygen causes corrosion, most severely in the steam generator. Hydrogen, which is capable of diffusing through some solids, causes hydriding (e.g., uranium hydride, which swells and ruptures nuclear-fuel elements). Hydrogen, methane, and ammonia are also combustible.

The process of removing noncondensables is called *deaeration*. Most fossil powerplants have a deaerating feedwater heater (Sec. 6-6), but whether or not a plant has such a heater, or other separate deaerator, it is essential that the condenser itself be the place of good deaeration. Manufacturers usually guarantee a maximum oxygen concentration in the condensate leaving the condenser. For some time, this maximum was set at 0.03 cm<sup>3</sup>/L (0.003 percent by volume), but this has been reduced recently to 0.01 cm<sup>3</sup>/L, required, and 0.005 cm<sup>3</sup>/L frequently guaranteed.

Good deaeration within a condenser requires time, turbulence, and good venting equipment. The cold condensate falling from the lower tubes must have sufficient falling height and scrubbing steam for reheat and deaeration. The scrubbing steam is provided by allowing some of the incoming steam to pass through an open flow area directly to the bottom tubes to reheat the condensate. The reason is that noncondensables are more easily released from a hotter than a colder liquid.

Once the noncondensables are released, they are cooled to reduce their volume before being pumped out of the condenser. For this a number of water tubes, about 6 to 8 percent in the center of the tube bundle, are set aside for this function (Figs. 6-5 and 6-7). This, called an *air cooler section*, is baffled to separate the noncondensables from the main steam flow. The noncondensables flow toward the cold end of the condenser, where they connect to a vent duct that leads to the venting equipment.

The venting equipment, as other components, went through several stages of development, including reciprocating compressors, called *dry-vacuum pumps*, which were used for some time. These were, however, superseded by *jet pumps*, which have now found almost universal acceptance because of their simplicity and lack of moving parts and, hence, low maintenance and good reliability.

The jet pumps used on condensers have come to be known as *steam-jet air ejectors* (SJAЕ) because they use a steam jet as their motive or driving flow. They are usually multistage units, usually two or three. Figure 6-8 shows a two-stage SJAЕ. It uses main steam at a reduced pressure that enters a driving-flow nozzle in the first-stage ejector, from which it exits with high velocity and momentum and reduced pressure. This reduced pressure draws in the noncondensables from the condenser. By a process of momentum exchange, the gases are entrained by the steam jet. The combined flow of steam and gas is now compressed in the diffuser of the first-stage ejector and discharged into a small intercondenser, where the steam is condensed by passing across cooling pipes in much the same manner as the main condenser. Cooling here, however, is accomplished by the main condenser condensate and is part of the feedwater heating system, resulting in improvement in efficiency of the plant.

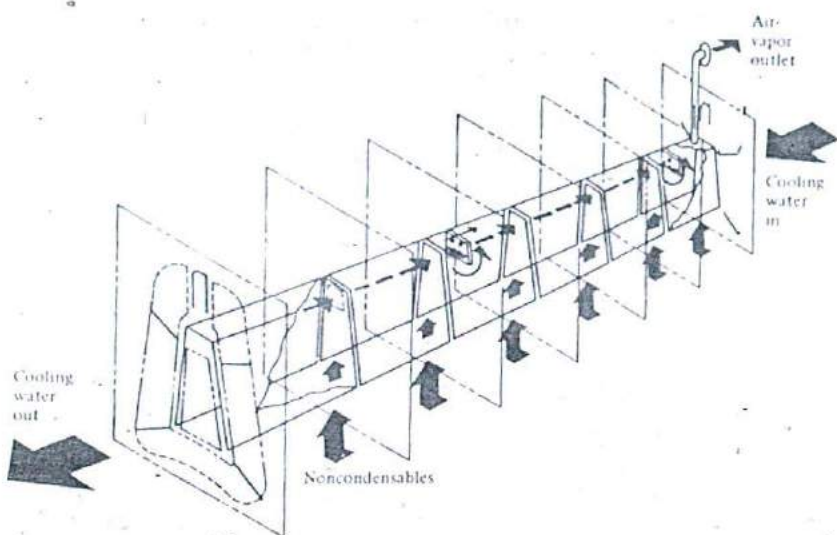


Figure 6-7 Condenser air-removal system. (Courtesy Foster Wheeler Energy Corporation.)

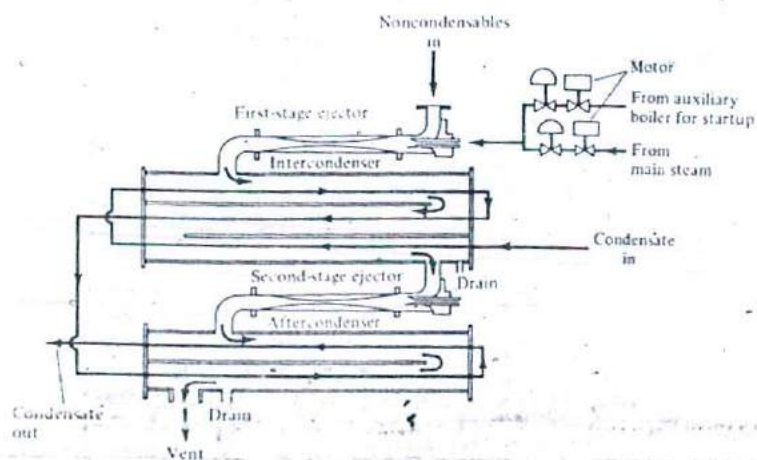


Figure 6-8 A two-stage steam-jet air ejector (SJAE).

The condensed steam is drained and returned to a low-pressure part of the cycle. The noncondensables and any remaining steam are then passed to the second-stage ejector, where they are compressed further and passed to an aftercondenser. A third-stage ejector may or may not be necessary to bring the system to the discharge pressure or, in nuclear powerplants, to the off-gas system.

## 6-4 SURFACE-CONDENSER CALCULATIONS

### Heat-Transfer Surface Area

The heat-transfer calculations for determining the number of tubes and total surface area required by a surface condenser are rather complex. They require a knowledge of the total heat load on the condenser, i.e., the heat removed by the turbine exhaust steam, low-pressure feedwater heater drains, steam-jet air ejector (SJAЕ) drains, small drive turbine exhausts, etc. They also require a knowledge of the heat-transfer mechanisms and coefficients in various parts of the condenser. The heat-transfer mechanisms are condensation of the steam over the colder but varying-temperature tube surfaces, conduction through the tube walls, forced convection of the circulating water inside the tubes, and forced convection of the noncondensables in the air-removal section.

The outer tube surfaces are usually clean when the condenser is new but quickly develop an oily film that changes condensation from dropwise to filmwise condensation [2,47]. This is expected in most condensing equipment, and heat-transfer coefficients are conservatively based on the lower filmwise condensation mechanism. The heat-transfer coefficient here depends upon the difference between the steam-saturation temperature and tube-wall temperature (being inversely proportional to that difference to the power 0.25), on the relative positions of tubes, steam velocity and turbulence, the extent of noncondensables, and the existence of superheated steam, if any. The circulating-water heat-transfer coefficient depends upon its velocity and, hence, temperature and the cleanliness of the inside surface. Because this circulating water may be obtained from a natural body of water, algae and other deposits accumulate on that surface, thus affecting heat transfer and necessitating frequent cleaning.

Because all the above are variables with many uncertainties, manufacturers have usually based their designs in general accordance with a method proposed by the Heat Exchange Institute Standards for Steam Surface Condensers [48]. The method is based on the usual heat transfer equation

$$Q = UA \bar{\Delta T}_m \quad (6-5)$$

where  $Q$  = heat load on condenser, Btu/h or J/s

$\bar{U}$  = overall condenser heat-transfer coefficient, based on outside tube area, Btu/(h · ft<sup>2</sup> · °F) or J/(s · m<sup>2</sup> · K) or W/(m<sup>2</sup> · K)

$A$  = total outside tube surface area, ft<sup>2</sup> or m<sup>2</sup>

$\bar{\Delta T}_m$  = log mean temperature difference in the condenser, °F or °C, given by

Table 6-2 Constants in Eq. (6-7)

Tube outer diameter, in	3/4	7/8	1.0							
$C_1$ [V in ft/s, U in Btu/(h · ft <sup>2</sup> · °F)]	270	263	251							
$C_1$ [V in m/s, U in W/(m <sup>2</sup> · K)]	2777	2705	2582							
Water temperature, °F	35	40	45	50	55	60	70	80	90	100
$C_2$	0.57	0.64	0.72	0.79	0.86	0.92	1.00	1.04	1.08	1.10
Tube material	304 stainless steel	Admiralty arsenic-copper	Aluminum-brass	Muntz metal	Aluminum-bronze	90-10 Cu-Ni	70-30 Cu-Ni			
$C_3$	18 gauge	0.58	1.00	0.96	0.90	0.83				
	17 gauge	0.56	0.98	0.94	0.87	0.80				
	16 gauge	0.54	0.96	0.91	0.84	0.76				
$C_4$	0.85 for clean tubes, less for algae covered or sludged tubes									

$$\Delta T_m = \frac{\Delta T_i - \Delta T_o}{\ln(\Delta T_i / \Delta T_o)} \quad (6-6)$$

$\Delta T_i$  = difference between saturation-steam temperature and inlet circulating water temperature (Fig. 6-9), °F or °C

$\Delta T_o$  = difference between saturation-steam temperature and outlet circulating-water temperature (Fig. 6-9), °F or °C, also called *terminal temperature difference*, TTD

The overall heat-transfer coefficient  $U$  is given empirically by

$$U = C_1 C_2 C_3 C_4 \sqrt{V} \quad (6-7)$$

where  $V$  = circulating-water velocity in the tubes at inlet (cold) conditions, ft/s or m/s

$C_1$  = dimensional factor depending upon tube outer diameter

$C_2$  = dimensionless correction factor for circulating-water inlet temperature

$C_3$  = dimensionless correction factor for tube material and gauge

$C_4$  = dimensionless cleanliness factor

Refer to Table 6-2 for the factors in Eq. (6-7).

In using Eqs. (6-5) to (6-7), it is necessary to know the steam-saturation temperature and the circulating-water inlet temperature, hence  $\Delta T_i$ , and to select a value for the *terminal temperature difference* (TTD) of the condenser, which in this case is  $\Delta T_o$ . For a given  $\Delta T_i$ , calculated  $U$ , and selected  $\Delta T_o$ , the tube surface area is calculated and the condenser design is fixed. For a given  $\Delta T_i$ , a large TTD results in a large  $\Delta T_m$  and small condenser (small  $A$ ) but an increased water flow because the water-temperature rise ( $T_2 - T_1$ , Fig. 6-9) is reduced. A small TTD results in a larger condenser,

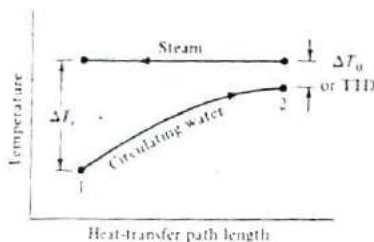


Figure 6-9 Condenser temperature distributions.

reduced water flow, and higher exit-water temperature. An oversized condenser, bigger than design, will increase capital cost but reduce operating costs because it would decrease  $\Delta T_m$  and lower condenser pressure. Proper design, therefore, depends upon many factors, such as capital costs, operating costs, water availability, and environmental concerns.

The circulating-water inlet temperature should be sufficiently lower than the steam-saturation temperature to result in reasonable values of  $\Delta T_m$ . It is usually recommended that  $\Delta T_1$  should be between about 20 and 30°F (11 to 17°C) and that  $\Delta T_2$ , the TTD, should not be less than 5°F (2.8°C).

### Circulating-Water Flow and Pressure Drop

It is important to determine the necessary circulating-water flow and the pressure drop through the condenser because this, along with other parts of the circulating-water system (Chap. 7), determine the pump horsepower necessary.

The water mass-flow rate  $\dot{m}_w$  is simply given by

$$\dot{m}_w = \frac{Q}{c_p(T_2 - T_1)} \quad (6-8)$$

where  $c_p$  is the specific heat of the water and  $T_1$  and  $T_2$  are the inlet and exit temperatures, respectively.

The pressure drop in the condenser is composed of (1) the pressure drop in the water boxes and (2) the friction pressure drop in the tubes. Again these depend upon many factors, such as the flow pattern in and the size of the water boxes, the inlet and exit of the tubes at the tube sheets, the size and length of the tubes, and the water temperatures and velocities. The Heat Exchange Institute recommends the values given in Figs. 6-10 and 6-11. The pressure drops are given in terms of head  $H$ , which is related to the pressure loss  $\Delta P$  by

$$\Delta P = \rho H \frac{g}{g_c} \quad (6-9)$$

where  $\rho$  is the density,  $g$  the gravitational acceleration, and  $g_c$  the conversion factor 32.2 lb<sub>m</sub> · ft/(lb<sub>f</sub> · s<sup>2</sup>) or 1.0 N · m/(kg · s<sup>2</sup>)

Water inlet velocities in condenser tubes are usually limited to a maximum 8

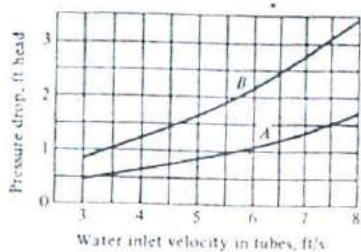


Figure 6-10 Pressure drop in condenser water boxes, expressed as head in feet: (a) one-pass, (b) two-pass

ft/s ( $\sim 2.5$  m/s) to minimize erosion, and a minimum of 5 or 6 ft/s (1.5 to 1.8 m/s) for good heat transfer. Values between 7 and 8 ft/s ( $\sim 2.1$  to 2.5 m/s) are most common.

**Example 6-2** Design a condenser that would handle  $3 \times 10^6$  lb<sub>m</sub>/h of 90 percent quality steam at 1 psia, as well as 360,000 lb<sub>m</sub>/h of 112°F drain water from the low-pressure feedwater heater, and 1875 lb<sub>m</sub>/h of 440°F drains from the steam-jet air ejector. Fresh cooling water is available at 70°F.

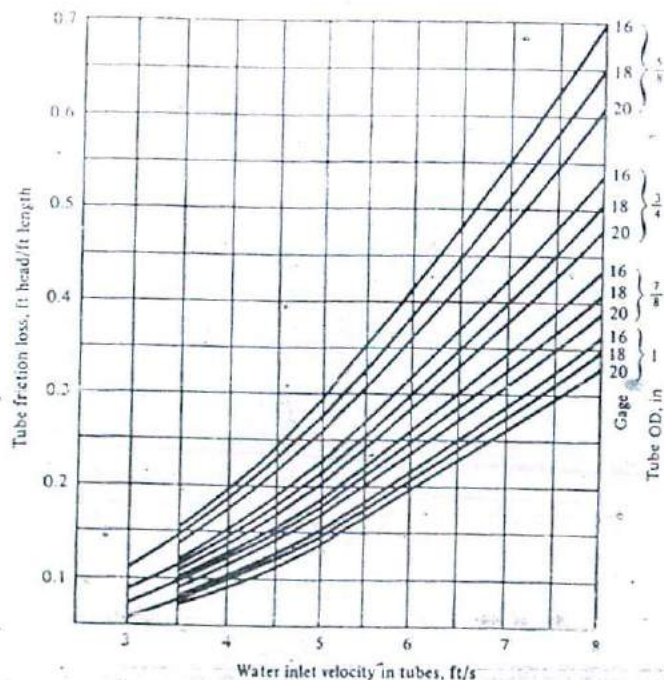


Figure 6-11 Pressure drop in condenser tubes, expressed as head in feet per foot length of tubes.



## SOLUTION

Heat-transfer calculations:

Select:

1. A two-pass condenser
2. Type 304 stainless steel tubing
3. Tubes: 50 ft in length, 7/8 in OD, 18 BWG
4. TTD = 6°F
5. Inlet water velocity = 7 ft/s

$$\begin{aligned}
 \text{Heat load } Q &= \text{turbine exhaust} + \text{low-pressure drain} + \text{SJAE drain} \\
 &= 2 \times 10^6 \times x h_{fg} + 240,000(h_{112^\circ\text{F}} - h_f) + 1250(h_{440^\circ\text{F}} - h_f) \\
 &= 3 \times 10^6 \times 0.9 \times 1036.1 + 360,000(79.98 - 69.7) \\
 &= 2.798 \times 10^9 + 3.701 \times 10^6 + 0.656 \times 10^6 \\
 &= 2.802 \times 10^9 \text{ Btu/h}
 \end{aligned}$$

$$\Delta T_l = t_{\text{sat}} - 75 = 101.74 - 70 = 31.74^\circ\text{F}$$

$$\Delta T_o = 6^\circ\text{F}$$

$$\Delta T_m = \frac{31.74 - 6}{\ln(31.74/6)} = 15.45^\circ\text{F}$$

$$\begin{aligned}
 U &= 263 \times 1.00 \times 0.58 \times 0.85 \sqrt{7} \\
 &= 343.0 \text{ Btu/(h} \cdot \text{ft}^2 \cdot ^\circ\text{F)}
 \end{aligned}$$

Thus

$$\text{Total tube surface area} = \frac{2.802 \times 10^9}{343.0 \times 15.45} = 528,675 \text{ ft}^2$$

For 7/8-in tubes, surface area per foot is 0.2291/ft<sup>2</sup> (see App. A). Therefore

$$\text{Total length of tubes} = \frac{528,675}{0.2291} = 2,307,615 \text{ ft}$$

and

$$\text{Number of tubes} = \frac{2,307,615}{50} = 46,150$$

Water calculations:

$$T_2 - T_1 = \Delta T_l - \Delta T_o = 31.74 - 6 = 25.74^\circ\text{F}$$

$$\text{For } c_p = 0.99 \text{ Btu/(lb}_m \cdot ^\circ\text{F)}$$

$$\dot{m}_w = \frac{2.802 \times 10^9}{0.99 \times 25.74} = 1.0996 \times 10^8 \text{ lb}_m/\text{h}$$

Note: A check on  $\dot{m}_w$ , obtained above from Eq. 6-8, and that obtained by multiplying the water velocity by the density by the total cross-sectional area of flow (in this case of half the tubes) should be made at this point. If not equal, a correction for the TTD and/or the tube length would have to be made.

$$\begin{aligned} \text{Volumetric flow rate} &= \dot{m}_{w, \text{TOT}} = \frac{1.0996 \times 10^8 \times 0.01605}{60} \\ &= 29,414 \text{ ft}^3/\text{min} = 29,414 \times 7.481 = 220,043 \text{ gal/min} \end{aligned}$$

$$\begin{aligned} \text{Pressure drop in water boxes} &= 2.7 \text{ ft head (Fig. 6-10)} \\ &= 62.3 \times 2.7 \times \frac{32.2}{32.2} = 168.3 \text{ lb}_f/\text{ft}^2 = 1.17 \text{ psi} \end{aligned}$$

$$\begin{aligned} \text{Pressure drop in tubes} &= 0.32 \text{ ft head/ft (Fig. 6-11)} \\ &= 62.3 \times 0.32 \times \frac{32.2}{32.2} = 19.936 \text{ lb}_f/\text{ft}^2 \text{ per ft} = 0.1384 \text{ psi/ft} \end{aligned}$$

Allow for 1.2 in thick tube sheets, and thus each pass would have a length of  $50 + 2 \times 1.2/12 = 50.2 \text{ ft}$ .

$$\text{Total pressure drop in tubes} = 0.1384 \times 2 \times 50.2 = 13.90 \text{ psi}$$

$$\text{Total pressure drop in condenser} = 1.17 + 13.90 = 15.07 \text{ psi}$$

The power attributed to the water flow in the condenser only would be

$$\frac{\dot{m} \Delta P}{\rho} = \dot{m} v \Delta p = 3.7916 \times 10^9 \text{ ft} \cdot \text{lb}_f/\text{h} = 1915 \text{ hp}$$

## 6-5 CLOSED FEEDWATER HEATERS: GENERAL

It has been demonstrated (Chap. 2) that regenerative feedwater heaters are indispensable in Rankine-cycle type powerplants if improved cycle performance is to be expected. They raise the temperature of the feedwater before it enters the economizer or steam drum. Both open- and closed-type feedwater heaters are used. In small industrial systems, only one open-type feedwater heater may be used. Utility and large industrial plants use a multiple of feedwater heaters, typically five to seven closed and one open, which doubles up as a deaerator. Nuclear powerplants of the pressurized- or boiling-water reactor types do not use open-type feedwater heaters, but gas-cooled and fast-breeder reactor powerplants do. Open-type feedwater heaters will be described in the next section.

Closed-type feedwater heaters are shell-and-tube heat exchangers. In essence they are small condensers that operate at higher pressures than the main condenser because bled steam is condensed on the shell side, whereas the feedwater, acting like circulating condenser water, is heated on the tube side.

Closed feedwater heaters are placed within the cycle to receive bled steam from

the turbines at pressures determined roughly by equal temperature increments from the condenser to the boiler saturation temperatures (Sec. 2-13). They are therefore classified as low-pressure (LP) and high-pressure (HP) heaters, depending upon their location in the cycle. The LP heaters are usually located between the condensate pump and the open heater, which is followed by the main boiler-feed pump. The HP heaters are located between that pump and the economizer. Occasionally a boiler-feed booster pump is located up-stream of the main boiler feed pump, in which case the feedwater heaters are classified as LP, IP (intermediate pressure), and HP. The shell-side (bled-steam) pressure extends from vacuum to several hundred psia in LP heaters and may exceed 1200 psia in HP heaters. Tube-side (feedwater) pressures after the boiler feed pump are higher than the maximum steam pressure because of the pressure drop through the feedwater system and may exceed 5000 psia in supercritical-pressure cycles (Sec. 2-14).

When bled steam entering a feedwater heater is superheated, as is often the case in fossil-fueled high-pressure and some low-pressure heaters, the heater includes a *desuperheating zone* where the steam is cooled to its saturation temperature (Fig. 6-12). This is followed in all closed feedwater heaters by a *condensing zone* where the latent heat of vaporization is removed and the steam is condensed to a saturated liquid. This liquid, now called the *heater drain*, is, in all heaters, except sometimes the one or two lowest-pressure heaters, cooled below its saturation temperature in a *subcooling zone* or a *drain-cooling zone* before the drain is cascaded backwards or pumped forward (Chap. 2).

The above is a *three-zone* closed-type feedwater heater (Fig. 6-12). There are, however, *two-zone* heaters that include a desuperheating and a condensing zone or a condensing and a subcooling zone. And there are also *single-zone* heaters that include only a condensing zone. A drain-cooling zone, instead of being integral with the shell, may be located external to it. Details of construction and standards of feedwater heaters are given in Ref. 49.

Closed feedwater heaters could be either horizontal or vertical, depending upon space availability. Vertical heaters are designed with their head (water box) down or

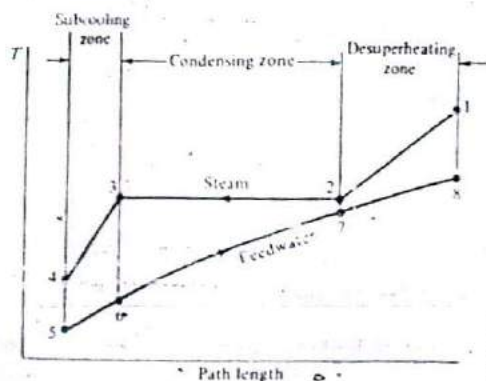


Figure 6-12 Temperature-path length diagram for a three-zone closed feedwater heater.

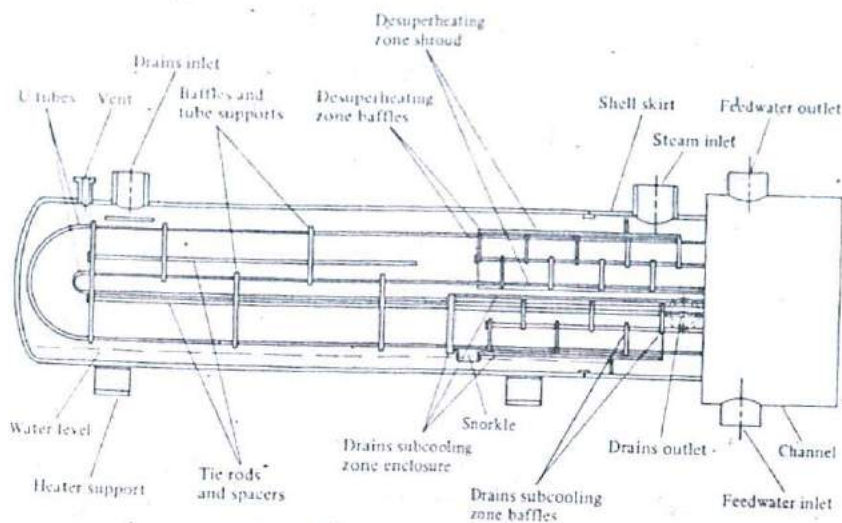


Figure 6-13 A three-zone horizontal closed-type feedwater heater [49].

up, the latter only in special circumstances. Figure 6-13 shows a typical horizontal three-zone closed feedwater heater. The feedwater tubes are usually in the form of U-tube bundles, although occasionally they are straight, like those of a condenser. The feedwater enters via a divided water box through the subcooling zone, flows through the U tubes in a generally parallel but opposite direction to the steam flow, and leaves to the water box through the desuperheating zone.

The bled steam flows first through the desuperheating zone, which is usually separated from the rest of the heater by a shroud and which is fitted with a series of vertically cut baffles that provide both a good heat-transfer path and proper tube support. The condensing zone is the major portion of the heater and also provides a baffled steam-flow path. The subcooling zone is separated from the rest of the heater by an end plate and an enclosure but connects to the main water level through a "snorkle" entrance. While the main water level is low, the subcooling zone is completely submerged with liquid by the differential pressure between it and the condensing zone. The liquid flows through properly spaced baffles and exits from the heater through a nozzle next to the tube sheet to cascade to the next lower-pressure heater.

Cascaded drain from the higher-pressure heater or from a moisture-separator-reheater are throttled upon entrance to the shell and flash into high-velocity steam. The tubes are protected from erosion by this steam by the use of stainless steel impingement plates. The drain inlet is usually at or beyond the tubes U bend, in horizontal heaters, in order to keep the flashing steam from the tubes and provide sufficient volume for it.

Figure 6-14 shows a vertical closed-type feedwater heater with head down, the usual arrangement.

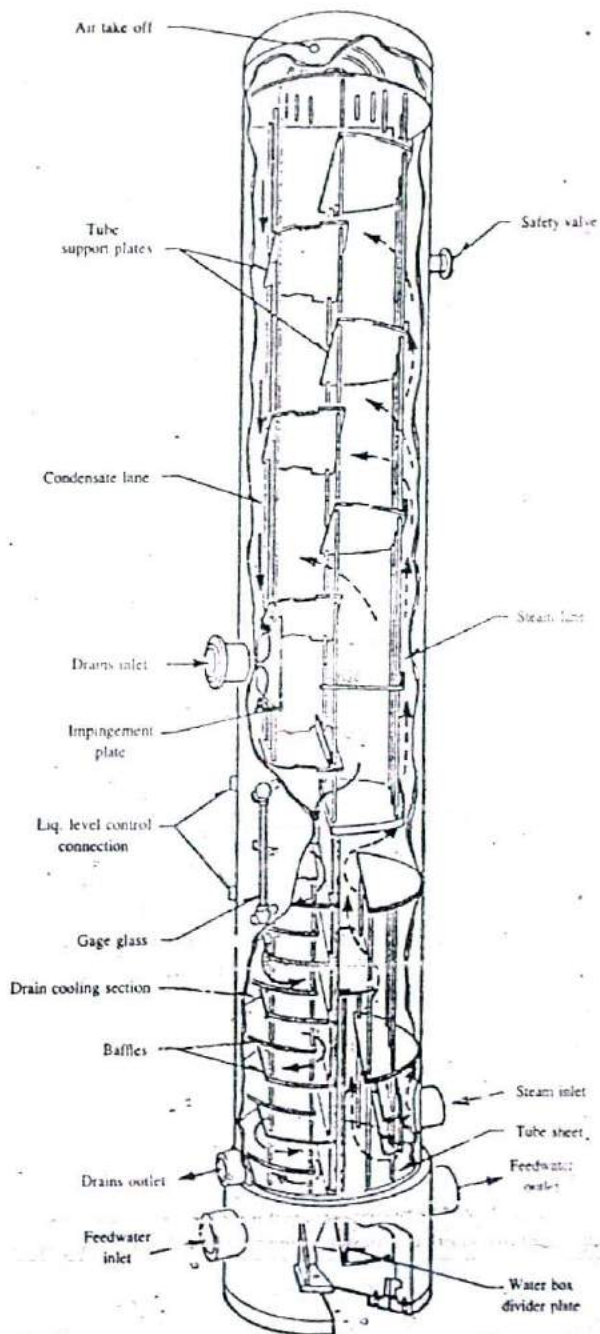


Figure 6-14 A three-zone vertical closed-type feedwater heater [49].

## Tubes and Materials

The tube sheet is an integral part of the head (water box). In high-pressure heaters the tubes are welded then rolled or explosively expanded into the tube sheet. Sometimes a stainless steel insert is provided with carbon-steel tubing to prevent inlet end erosion. In low-pressure heaters, the tubes are usually rolled into the tube sheets. Tube sizes vary from 5/8 to 1 in OD with gauges (BWG) varying from 10 to 20 (App. K). Because closed feedwater heaters operate at much higher water (and steam) pressures than condensers and are usually bent, a minimum tube thickness (and hence maximum gauge) must be selected that would be adequate for such service. The minimum tube thickness  $t$  is given by

$$t = \frac{Pd_o}{2S + 0.8P} \left( 1 + \frac{d_o}{4R_u} \right) \quad (6-10)$$

where  $P$  = tube design pressure, psi

$d_o$  = tube outside diameter, in

$S$  = allowable design stress, psi

$R_u$  = inside radius of U-tube bend, taken as  $1.5 d_o$ , in

Tube materials evolved over the years. Admiralty metal and copper-nickel alloys were extensively used before the age of the high-pressure systems. As steam pressures and temperatures increased, new materials were required. For fossil-fueled powerplants with subcritical steam, the preferred materials for low-pressure heaters are now type 304 stainless steel (which is becoming less costly) and 90-10 copper-nickel. For high-pressure heaters, type 304 stainless steel and tempered Monel 30-70 copper-nickel are the preferred materials, with stress-relieved 70-30 copper-nickel and carbon steel also specified. For supercritical steam (once-through boilers), type 304 stainless steel and carbon steel are specified for low-pressure heaters and carbon steel for high-pressure heaters. Copper-base alloys are not specified.

For nuclear-reactor powerplants of the pressurized- or boiling-water types, type 304 stainless steel is specified for all heaters.

One problem with heater tubes is corrosion caused by the presence of noncondensable gases, especially in heaters operating below atmospheric pressure. These gases also reduce the overall heat transfer of the heaters by blanketing the tube outer surfaces, much as they do in the main condenser. The gases are released by a proper vent mechanism.

## 6-6 CLOSED-FEEDWATER-HEATER CALCULATIONS

### Heat Transfer

A closed-type feedwater heater will have as many overall heat-transfer coefficients as there are zones. For example, a three-zone heater will have one coefficient each for the desuperheating, condensing, and subcooling zones. These may be combined into

one overall heat-transfer coefficient, if desired, but they must be evaluated independently. Once they are calculated, the total number of tubes for the heater and the zone lengths are calculated.

The overall heat-transfer coefficient for any zone is given by the usual relationship

$$U = \frac{1}{(1/h_o) + (tA_o/RA_m) + (A_o/h_iA_i)} \quad (6-11)$$

where  $U$  = overall heat-transfer coefficient of the zone in question, based on the outside area of the tubes, Btu/(h · ft<sup>2</sup> · °F) or W/(m<sup>2</sup> · s)

$h_o$  = heat-transfer coefficient of fluid outside tubes, Btu/(h · ft<sup>2</sup> · °F) or W/(m<sup>2</sup> · K)

$k$  = thermal conductivity of tube material, Btu/(h · ft · °F) or W/(m · K)

$h_i$  = heat-transfer coefficient of water inside tubes, Btu/(h · ft<sup>2</sup> · °F) or W/(m<sup>2</sup> · K)

$A_o$  = outside surface area of tubes per unit length, ft<sup>2</sup>/ft or m<sup>2</sup>/m

$A_i$  = inside surface area of tubes ft<sup>2</sup> per unit length, ft<sup>2</sup>/ft or m<sup>2</sup>/m

$A_m$  = log mean area of tubes per unit length

$$= (A_o - A_i) / \ln \frac{A_o}{A_i} = \frac{A_o + A_i}{2} \text{ for thin tubes, ft}^2/\text{ft or m}^2/\text{m}$$

$t$  = thickness of tubes, ft or m

In the *desuperheating zone*,  $h_o$  is evaluated for forced convection of the superheated steam, between points 1 and 2 in Fig. 6-12, and  $h_i$  is evaluated for forced convection of feedwater inside the tubes between points 7 and 8.

In the *condensing zone*,  $h_o$  is the result of steam condensation between points 2 and 3 and  $h_i$  of feedwater forced convection between 6 and 7.

In the *subcooling zone*,  $h_o$  and  $h_i$  are due to forced convection of water outside the tubes between 3 and 4 and inside the tubes between 5 and 6, respectively.

For single- or two-zone heaters, the unapplicable zones are simply deleted.

The outer tube surface area  $A_o$ , and hence the zone lengths, is then obtained from

$$A_o = \frac{Q}{U \Delta T_m} \quad (6-12)$$

where  $Q$  is the heat load and  $\Delta T_m$  the logarithmic mean temperature difference for the zone in question. (Note that an overall  $\Delta T_m$  for the heater based on temperatures at 1, 4, 5, and 8 cannot be obtained because of the discontinuities in the steam temperature line 1-2-3-4.)

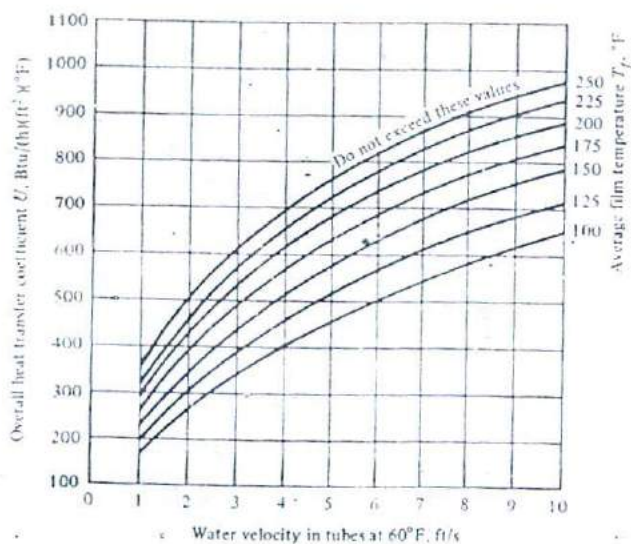
The values of  $h_o$  for each zone can be obtained from standard heat-transfer calculations.

As in the main condenser, there are many flow and other variables and uncertainties. Condensation heat-transfer coefficients are usually high, a few thousand

Btu/(h · ft<sup>2</sup> · °F), and the tube thicknesses are small, so the main heat-transfer resistance is due to the boundary layer of the feedwater inside the tubes. An empirical calculation for  $U$  in the *condensing zone*, shown in the form of a graph (Fig. 6-15), thus uses the average film (boundary-layer) temperature as well as water velocity as parameters. The average film temperature is defined arbitrarily as

$$T_f = T_s - 0.8 \Delta T_m \quad (6-13)$$

where  $T_f$  = average film temperature, °F



Gauge	Adms.	90'10 Copper- nickle	80'20 Copper- nickle	70'30 Copper- nickle	Monel	302,304 Stainless steel
18	1.00	0.97	0.95	0.92	0.89	0.85
17	1.06	0.94	0.91	0.87	0.85	0.80
16	1.00	0.91	0.88	0.84	0.82	0.77
15	0.99	0.89	0.86	0.82	0.79	0.74
14	0.96	0.85	0.82	0.77	0.75	0.70
13	0.93	0.81	0.78	0.73	0.70	0.65
12	0.90	0.77	0.73	0.68	0.65	0.60
11	0.87	0.74	0.70	0.65	0.62	0.57
10	0.83	0.69	0.66	0.60	0.58	0.52
9	0.80	0.65	0.62	0.56	0.54	0.48

Multipliers of base heat-transfer rates for various tube materials and gauges  
(for tube OD  $\frac{1}{2}$  to 1 in. inclusive)

Figure 6-15 Overall heat-transfer coefficient for condensing zone only as a function of average film temperature as defined by Eq. (6-13) [49].



$$T_s = \text{saturated-steam temperature} = T_{2,3}, \text{ } ^\circ\text{F}$$

$$\Delta T_m = \text{log mean temperature difference in condensing zone, } ^\circ\text{F}$$

$$\Delta T_m = \frac{(T_3 - T_6) - (T_2 - T_7)}{\ln[(T_3 - T_6)/(T_2 - T_7)]} \quad (6-14)$$

There is an upper limit for  $U$  for values of  $\Delta T_m$  250°F or higher. The variation of water velocity with temperature is taken care of in Fig. 6-15 by specifying a velocity based on water density at 60°F, 62.4 lb<sub>m</sub>/ft<sup>3</sup>. Correction factors for various tube materials and gauges are included in Fig. 6-15.

### Pressure Drop

Pressure drops of the feedwater in feedwater heaters are usually large because of the flow friction in long small-diameter tubes in several heaters. Calculations for such pressure drops are necessary for the design of condensate and boiler feed pumps.

An empirical correlation for the pressure drop in closed feedwater heaters, also applicable for external drain coolers, is given by the following equation [49]

$$\Delta P = \frac{F_1 F_2 (L + 5.5d_i) N}{d_i^{1.24}} \quad (6-15)$$

where  $\Delta P$  = total tube-side pressure drop, psi

$F_1$  = factor depending upon water velocity, also corrected for density at 60°F (Fig. 6-16)

$F_2$  = factor depending upon average water temperature  $T_{av}$  (Fig. 6-16), given by  $T_{av} = T_s - \Delta T_m$ , °F

$d_i$  = inside tube diameter, in (App. K)

$N$  = number of tube passes

$L$  = length of tubes in one pass

The usual water velocities in closed feedwater heaters, corrected to 60°F, are 6 to 8 ft/s.

**Example 6-3** Find the number and length of tubes for a three-zone feedwater heater that is used after the reheater (no. 2 high-pressure heater) in a subcritical fossil-fueled powerplant, for the following data:

Feedwater:  $3.0 \times 10^6$  lb<sub>m</sub>/h, 3000 psia, 370°F in, 398°F out

Bled steam: 140,000 lb<sub>m</sub>/h, 240 psia, 800°F

Drain in from no. 1 HP heater: 300,000 lb<sub>m</sub>/h, 570 psia, 410°F

Drain out, total: 440,000 lb<sub>m</sub>/h, 350°F

Overall heat-transfer coefficients: desuperheating zone =

125 Btu/(h · ft<sup>2</sup> · °F), drain-cooling zone = 300 Btu/(h · ft<sup>2</sup> · °F)

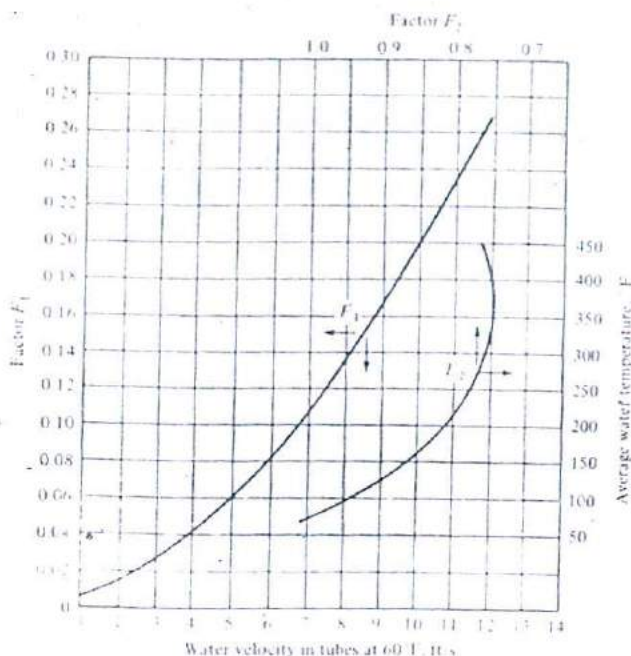


Figure 6.16 Factors in Eq. (6-15) for pressure drop in tubes of closed feedwater heaters and drain coolers [16].

#### SOLUTION

##### Tubes:

Choose a U-tube design, tubes 3/4 in OD, type 304 stainless steel. To find gauge, use maximum allowable stress = 20,000 psi. Eq. (6-10) gives minimum tube wall thickness

$$t = \frac{3000 \times 0.75}{2 \times 20,000 + 0.8 \times 3000} \left( 1 + \frac{0.75}{4 \times 1.5 \times 0.75} \right) = 0.062 \text{ in}$$

From App. K, 16 BWG with 0.065 in thickness is selected.

##### Number of tubes:

Volümetric water flow corrected to 60°F =  $3 \times 10^6 \cdot v_{60^\circ\text{F}} = 3 \times 10^6 \times 0.016033$  (from steam tables) = 48,099 ft<sup>3</sup>/h. Cross-sectional area of 16 BWG, 3/4-in tubes = 0.302 in<sup>2</sup> (App. K). Choose water velocity at 60°F = 8 ft/s. Therefore

$$\text{Number of tubes} = \frac{48,099}{3600} \times \frac{144}{0.302 \times 8} = 796 \text{ tubes}$$

which will be rounded to 800 tubes, (meaning 1600 tubes in a cross section of the U-tube bundle).

*Desuperheating zone:*

Referring to Fig. 6-12:  $h_1 = 1423.8$  Btu/lb<sub>m</sub>,  $h_2 = 1200.6$  Btu/lb<sub>m</sub>, and heat load  $Q_s = 140,000(h_1 - h_2) = 31,248,000$  Btu/h. But  $Q_s = 3 \times 10^6(h_8 - h_7)$ .  $h_8$  at 398°F and 3000 psia (assuming pressure drop relatively small) = 376.37 Btu/lb<sub>m</sub>. Thus  $h_7 = 365.95$  Btu/lb<sub>m</sub>, corresponding to  $T_7 = 388.1^\circ\text{F}$ . The log mean temperature difference in desuperheating zone is

$$\Delta T_{m,s} = \frac{(800 - 398) - (397.39 - 388.1)}{\ln[(800 - 398)/(397.39 - 388.1)]} = \frac{392.71}{3.7675} = 104.24^\circ\text{F}$$

Outside tube area in desuperheating zone  $A_{o,s}$  is

$$A_{o,s} = \frac{Q_s}{U_s \Delta T_{m,s}} = \frac{31,248,000}{125 \times 104.24} = 2398.16 \text{ ft}^2$$

From App. K, outside tube surface area per foot length = 0.1963 ft<sup>2</sup>. Therefore the length of desuperheating zone tubes  $L_s$  is

$$L_s = \frac{2398.16}{0.1963 \times 800} = 15.27 \text{ ft} = 4.655 \text{ m}$$

*Drain-cooler zone:*

$h_3 = 372.27$  Btu/lb<sub>m</sub>,  $h_4$  (at 380°F and 240 psia) = 353.63 Btu/lb<sub>m</sub>,  $h_5$  (at 370°F and 3000 psia) = 347.06 Btu/lb<sub>m</sub>. Heat load  $Q_{dc} = (140,000 + 300,000)(h_3 - h_4) = 8,201,600$  Btu/h. But  $Q_{dc} = 3 \times 10^6(h_6 - h_c)$ . Therefore,  $h_c = 349.79$  Btu/lb<sub>m</sub>, corresponding to  $T_6 = 372.6^\circ\text{F}$ . Log mean temperature difference in drain-cooler zone

$$T_{m,dc} = \frac{(397.39 - 372.6) - (380 - 370)}{\ln[(397.39 - 372.6)/(380 - 370)]} = \frac{14.79}{0.9079} = 16.29^\circ\text{F}$$

Outside tube area in drain-cooler zone is

$$A_{o,dc} = \frac{8,201,600}{300 \times 16.29} = 1678.25 \text{ ft}^2$$

Therefore length of drain-cooler zone tubes  $L_{dc}$  is

$$L_{dc} = \frac{1678.25}{0.1963 \times 800} = 10.69 \text{ ft} = 3.26 \text{ m}$$

*Condenser zone:*

$h_2$  (at 410°F and 520 psia) = 326.21 Btu/lb<sub>m</sub>. Heat load in condenser zone  $Q_c$  is due to both bled steam and drain from the higher-pressure heater, called 2'.  $Q_c = 140,000(h_2 - h_3) + 300,000(h_2 - h_3) = 120.149 \times 10^6$  Btu/h. Log mean temperature difference in condensing zone is

$$\begin{aligned}\Delta T_{m,c} &= \frac{(397.39 - 372.6) - (397.39 - 388.1)}{\ln[(397.39 - 372.6)/(397.39 - 388.1)]} \\ &= \frac{15.5}{0.9815} = 15.79^\circ\text{F}\end{aligned}$$

Average film temperature =  $397.39 - 0.8 \times 15.79 > 250^\circ\text{F}$ . Therefore  $U$  from Fig. 6-15, at 8 ft/s = 910 Btu/(h · ft<sup>2</sup> · °F). Correction factor for 16 gauge stainless steel = 0.770. Therefore overall heat-transfer coefficient in condensing zone is

$$U_c = 910 \times 0.770 = 700.7 \text{ Btu/(h} \cdot \text{ft}^2 \cdot ^\circ\text{F)}$$

Outside tube area in condensing zone  $A_{o,c}$  is

$$A_{o,c} = \frac{120.149 \times 10^6}{700.7 \times 15.79} = 10,857.94 \text{ ft}^2$$

Length of condenser zone tubes  $L_c$

$$L_c = \frac{10,857.94}{0.1963 \times 800} = 69.14 \text{ ft} = 21.07 \text{ m}$$

Total tube length:

Allowing for a 3-in-thick tube sheet, total heater tube length  $L_{tot}$  is

$$\begin{aligned}L_{tot} &= 15.27 + 10.69 + 69.14 + 2 \times \frac{3}{12} \\ &= 95.6 \text{ ft} = 29.14 \text{ m}\end{aligned}$$

Thus the average length of the U-tube bundle is 47.8 ft, which may be rounded to 50 ft, or 15 m.

Pressure drop in tubes:

From Eq. (6-15)

$$\text{Average water temperature in heater} = \frac{370 + 398}{2} = 384^\circ\text{F}$$

The average water temperature, obtained for the condenser zone (the largest zone), is  $397.39 - 15.79 = 381.6^\circ\text{F}$ , which is adequate for Fig. 6-16. Thus  $F_1 = 0.1275$ ,  $F_2 = 0.75$ ,  $d_i$  (App. K) = 0.620 in.

$$\Delta P = \frac{0.1375 \times 0.75(100 + 5.5 \times 0.620)}{0.620^{1.24}} = 19.29 \text{ psi} \approx 1.330 \text{ bar}$$

## 6-7 OPEN FEEDWATER HEATERS

An open feedwater heater, also called direct-contact and deaerating (DA) heater, is one that heats the feedwater by directly mixing it with bled steam from the turbine (Sec. 2-8). Usually only one such heater is used in fossil- and high-temperature nuclear-

Tray detail A



Spray nozzle detail B

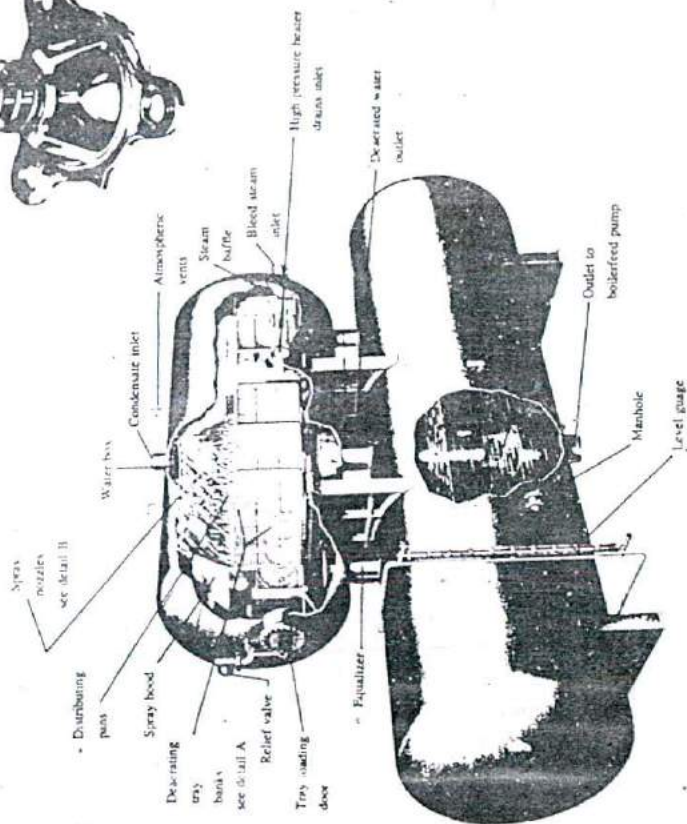
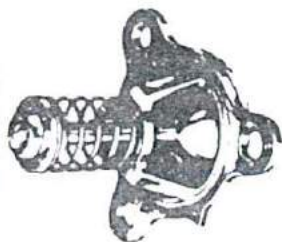


Figure 6-17 A typical combination open-type deaerating feedwater heater

reactor powerplants. None are used in water-cooled nuclear-reactor powerplants, which rely on a more elaborate condenser deaeration system. Because the pressure in such a heater cannot exceed the turbine pressure at the point of extraction, a pump, usually the main boiler feed pump, must follow the heater. The confluence of steam and water flows makes possible the efficient removal of noncondensables as well as the heating of the feedwater. Hence the various names for this type of heater.

The DA heater is usually positioned in the feedwater line at a pressure to prevent air leakage and at a temperature at which oxygen retention is least likely. Most DA heaters are designed for oxygen concentrations in the outlet feedwater below 0.005 cm<sup>3</sup>/L.

The DA outlet feedwater is at or near saturation. Pumping saturated water results in cavitation because of the pressure drop below saturated pressure, thus causing flashing on the back side of pump vanes. The DA heater is therefore usually positioned in the powerplant steam-generator house high above its pump by perhaps 60 ft. This provides sufficient pump inlet pressure to render the saturated water compressed (or subcooled) and prevents cavitation.

There are three types of DA heaters for industrial and utility use.

1. *Spray-type deaerators* In this type the feedwater enters the heater through nozzles that spray it into the extraction-steam-filled heater space. The water is heated and scrubbed to release the noncondensable gases. A second agitation of the now-heated feedwater by another steam flow is provided by an internal baffling system.
2. *Tray-type deaerators* Here the feedwater is directed onto a series of cascading horizontal trays. It falls in sheets or tubes from tray to tray and comes into contact with rising extraction steam admitted from the bottom of the tray system. As scrubbing occurs and noncondensable gases and some steam rise, they come into contact with colder water, resulting in a reduced volume of high concentration of noncondensables to vent into the atmosphere.
3. *Combination spray-tray deaerators* In these the feedwater is first sprayed into a steam-filled space, then made to cascade down trays. This combination type with horizontal stainless steel trays is currently preferred by the utilities. Spray types are more common in industrial service.

Figure 6-17 shows a typical combination-type deaerating heater. Shown also, just below the heater, is a relatively large feedwater tank, a hotwell, which allows sufficient water for rapid load variations.

## 6-8 BOILER MAKEUP AND TREATMENT

Steam powerplants lose a fraction of their water-steam circuit because of leakage from fittings and bearings, escape with noncondensable gases in deaeration processes, boiler blowdown, and other causes. The fraction is 0.5 to 1.5 percent of the flow rate, depending upon design and age of the plant, with nuclear powerplants in the low end of the range. This fraction should be made up. The water added must be well treated

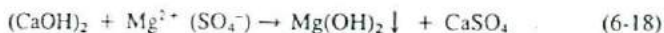
to maintain water and steam purity in order to prevent deposition of suspended solids and scale on boiler surfaces and also silica deposition and corrosion damage to turbine blades and the condensate-feedwater system.

A water makeup system begins by *pretreating* the raw water. This is followed by a *demineralizing system*, which is essential to all powerplants. For plants with stringent water-quality requirements, such as those using once-through boilers and boiling-water nuclear reactors, a *condensate-polishing system* is used to further "polish" the water. Raw water usually has different concentrations of a variety of impurities present in it. They may include suspended solids and turbidity, organics, hardness (calcium and magnesium), alkalinity (bicarbonates, carbonates, hydrates), other dissolved ions (sodium, sulfate, chloride, etc.), silica, and dissolved gases ( $O_2$ ,  $CO_2$ ).

### Pretreatment

The extent of pretreatment depends upon the source of the raw water used. Well water usually requires simple filtration. Raw water from a surface source, such as a river or lake, on the other hand, requires more elaborate pretreatment. The first step is *clarification*, in which the water is chlorinated to prevent biofouling of the equipment. The suspended solids and turbidity are then made to coagulate by special chemicals and by being brought together by a slow agitation in the middle of the clarifier vessel (chlorination that oxidizes organic matter also helps them coagulate). The coagulated matter then settles by gravity in the clarifier and is removed.

In the next step, the clarified water, depending upon its hardness and alkalinity, undergoes *softening*. Hardness, the chief source of scale in heat exchangers, boilers, and pipelines, is caused by the presence of calcium and magnesium salts containing  $Ca^{2+}$  and  $Mg^{2+}$ . Alkalinity is mostly bicarbonate  $HCO_3^-$  but is also carbonate and hydrate. Softening is usually done in a cold process using lime/soda ash. Lime, calcium hydroxide  $Ca(OH)_2$ , precipitates calcium bicarbonate as calcium carbonate  $CaCO_3$ , and magnesium salts as magnesium hydroxide  $Mg(OH)_2$  according to



The soda ash, sodium carbonate  $Na_2CO_3$ , is added to react with calcium chloride and calcium sulfate to form calcium carbonate



The products, calcium carbonate and magnesium hydroxide, are insoluble in water and settle to the bottom of the vessel. In softening, calcium, magnesium, and carbonate alkalinity are reduced to a few 10 ppm each. A problem of sludge removal, however, arises. Environmental regulations do not permit the sludge to be discharged. Instead, it is "dewatered," either in a settling basin or by thickeners and centrifuges. The water is then discharged to its source or recycled. Other softening processes use hot-process phosphate and zeolite softening.

The next step in pretreatment is *filtration*, which further removes residual suspended solids and turbidity. Filtration can be done under gravity or pressure, although the latter is preferred. Various filter media are used, sand being the most common. The pressure difference across the filtering medium is an indication of solid accumulation. When it reaches a given limit, the solids are removed from the bed by backwashing and are discharged to waste. Further filtration by activated charcoal may be necessary to absorb organics and remove residual chlorine from the chlorination process.

## Demineralization

*Demineralization* is the process of removing dissolved solids by *ion exchange*. Two types of resins are used: cation and anion resins. *Cation resin* has a positively charged hydrogen ion attached to a negatively charged polymer. The hydrogen ion is exchanged for the cations calcium, magnesium, and sodium. *Anion resin* is similar to the cation except that it has a negatively charged hydroxide ion ( $\text{OH}^-$ ), attached to a positively charged polymer structure. The hydroxide ion is exchanged for the anions sulfates, chlorides, and bicarbonates (alkalinity). Both ion-exchange processes are reversible, and the resins are restored to their original form by regeneration. Regeneration is called for when the resins are about to be exhausted and traces of dissolved solids begin showing up in the demineralizer exit. It is accomplished by passing a concentrated acid through the cation resin and caustic or sodium hydroxide through the anion resin.

A typical demineralizing "train" (Fig. 6-18) consists of a series of demineralizers that contains weak-acid cation, strong-acid cation, weak-base anion, strong-base anion, and mixed-bed units, which contain both cation and anion resins used for polishing to produce very high-quality water. Sometimes a decarbonator is added to the train to help the anion resin in reducing alkalinity. This reduces the amount of strong-base anion used. This is a mechanical dealkalizer that operates by blowing air up through downward-flowing water to drive  $\text{CO}_2$  from the water, thus removing the alkalinity.

The demineralizing and regeneration equipment, including tanks, pumps, etc., is programmed to operate automatically. The result is high-quality water, at least equal to the best from evaporators (below), that can be used directly in the steam plant without scale formation or corrosion.

A method of demineralization that is gaining acceptance for boiler makeup is *reverse osmosis*. Osmosis is the diffusion of a solvent, in this case water, through a semipermeable membrane from a region of no or low solid concentration to a region of high solid concentration. The membrane blocks the passage of the solutes, in this case the dissolved solids. The motion is in the direction of the high partial pressure of the purer water to the low partial pressure of the less pure water. It is a response to an osmotic pressure, which can be relatively large even for dilute solutions. Osmosis plays a vital role in many biological processes such as the passage of nutrients and waste material through the cell wall of animal tissue. The diffusion can be prevented by applying to the region of high concentrations an external pressure equal to the osmotic pressure. If a greater pressure is applied, the flow is reversed. In our case,



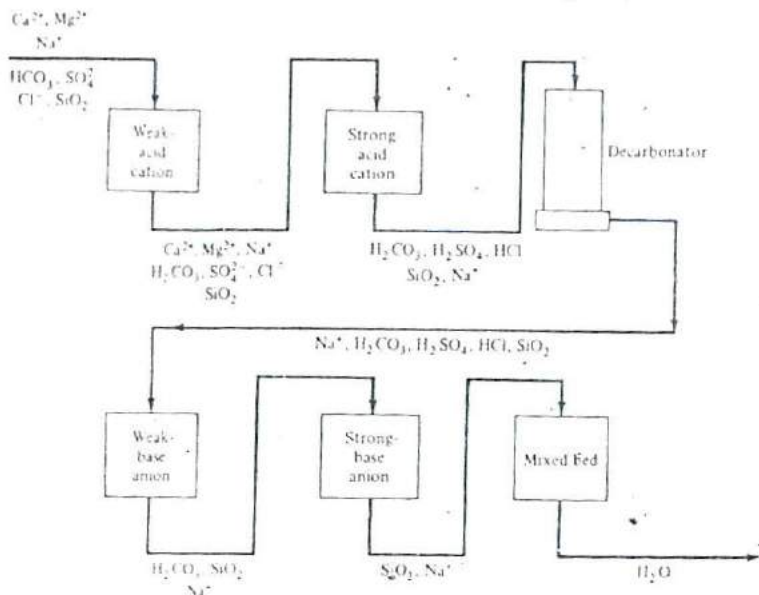


Figure 6-18 A typical demineralizing train.

pure water flows from the region of high concentrations to the region of pure water. This is reverse osmosis. The membranes used are expensive, and coagulation, settling, and filtration are used first to protect them.

### Condensate Polishing

Although the above systems produce high-quality makeup water for the plant, the water in its journey through the cycle can pick up metallic ions, such as iron and copper, from pipelines, etc., as well as impurities due to condenser leakage from the circulating water. As mentioned above, powerplants such as those using once-through boilers and boiling-water nuclear reactors (Sec. 10-7) require continual high-quality water and use a condensate polishing system. *Condensate polishing* is accomplished by passing the condensate through large demineralizing vessels that contain both cation and anion resins. The resins remove dissolved solids in the above manner as well as act as filters for impurities or suspended solids.

Condensate-polishing systems are similar for once-through boilers and boiling-water reactors, except that they are shielded in the latter case because the water goes through the reactor and the solids become radioactive. Some pressurized-water reactor systems (Sec. 10-2) require polishing to meet changing water-quality standards.

## Boiler Blowdown

Condensate polishing is not a requirement for drum-type boilers because they can utilize blowdown to control water purity. *Blowdown lines* periodically remove a portion of the water from the drum where concentrations increase because of steam flashing. This water is replaced by pure feedwater. The blowdown is then cooled and treated for reuse. A common treatment uses cartridge filters to remove suspended solids, notably iron and copper oxides, through the use of demineralizers. Condensate polishers may be indicated in some cases.

Nuclear boilers also feature blowdown. In pressurized-water-reactor steam generators (Sec. 10-3), the general practice is to use throwaway filter cartridges followed by demineralizers. In boiling-water reactors (Sec. 10-7), where the steam generator is also the reactor core, blowdown is radioactive and is treated and returned back to the reactor in a closed loop, called the *reactor-water cleanup system*.

## 6-9. EVAPORATORS

One form of boiler makeup, used in older plants and still used in ships (to produce both powerplant makeup and potable water from seawater), uses *flash-type distilling units*, or *evaporators*. Evaporators could be of the *one-stage*, or *single-effect*, type or the *multistage*, or *multieffect*, type. Usually two and sometimes three effects are used.

Older units had water sprayed on a bank of tubes heated by steam from the plant. This design has been largely replaced by the submerged type, which consists of a shell containing the steam tubes, which in turn are completely submerged by the water.

Figure 6-19 is a schematic of a single-effect evaporator. *Raw water*, pretreated (but not demineralized) as above, is introduced at point *w*. Steam from the plant, called *motive steam*, extracted at a relatively low pressure, is introduced at *m*, goes into a steam chest, flows through the tubes, and is discharged as condensate at *c*. The condensate is returned to the plant. The tubes slope slightly toward discharge to allow proper drainage. The pretreated water boils and pure saturated vapor is extracted at *v* to go to the plant as makeup. Care must be taken to avoid carryover of raw water with the vapor because that would defeat the purpose of the evaporator. This is done by proper separation and baffling for the receiving tube (much as in a boiler steam

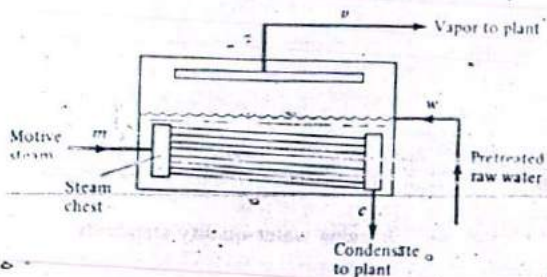


Figure 6-19 Schematic of a single-effect submerged evaporator.

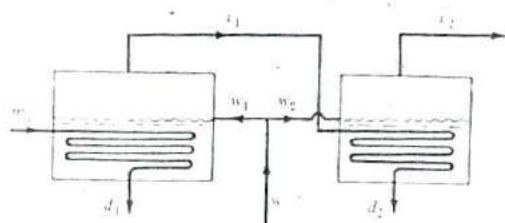


Figure 6-20 Schematic of a double-effect evaporator.

drum) and by keeping the rate of vapor formation per unit water surface area at a low enough level to reduce violent boiling at that surface. The raw-water surface is kept at approximately the centerline of the shell, where it would have maximum area. The level is maintained by a float-controlled valve on the raw-water line.

Scale that collects on the outside tube surfaces should be periodically cleaned to maintain heat-transfer rates. This is done during shutdown either manually or by subjecting the tubes to alternate high and low temperatures. Periodical blowdown is necessary to remove the raw-water sediment that accumulates in the shell.

Figure 6-20 shows a double-effect evaporator. Here pretreated raw water is introduced into two shells at  $w_1$  and  $w_2$ , respectively. The motive steam  $m_1$  condenses to  $d_1$  and is returned to the plant. The vapor produced in the first-effect evaporator  $v_1$  becomes the motive steam for the second-effect evaporator. Its condensate  $d_2$  is returned to the plant. Both the vapor  $v_2$  produced in the second effect and the condensate  $d_2$  constitute the boiler makeup.

A temperature-enthalpy (or heat-transfer length) diagram is shown in Fig. 6-21. It is now necessary to define *heat head* as the difference between the saturation temperature of the motive steam and the saturation temperature of the vapor.

The overall heat-transfer coefficient  $U$  of an evaporator is a function of both motive-steam saturation temperature and the heat head and is given empirically by the curves in Fig. 6-22. Heat heads below 20°F are not effective. Those above 100°F result in film boiling and a reduction in heat transfer. The most effective heat heads are in the range 35 to 55°F.

Single-effect evaporators, which can be built in parallel multiples, average approximately 0.8 lb<sub>m</sub> of vapor produced per lb<sub>m</sub> of motive steam. Double-effect evaporators produce almost double, 1.5 lb<sub>m</sub>/lb<sub>m</sub>, while triple-effect evaporators improve

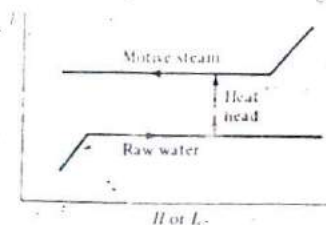


Figure 6-21 Temperature vs. enthalpy (or path-length) diagram of a single-effect evaporator.

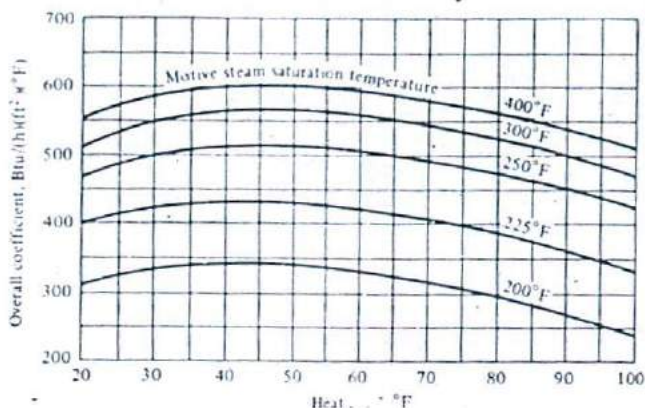


Figure 6-22 Overall heat-transfer coefficient for evaporators.

this further to about 2.0 lb<sub>m</sub>/lb<sub>m</sub>, but at the cost of increased complexity and capital cost.

Heat heads are usually divided up equally among the effects used. If the heat head and the overall heat-transfer coefficient for each heat head are known, the heat-transfer areas can then be easily obtained.

**Example 6-5** Calculate the mass-flow rate of motive steam required and the heat-transfer areas of a double-effect evaporator to produce 100,000 lb<sub>m</sub>/h of vapor. Pretreated water is available at 60°F. Motive steam is available at 70 psia, saturated. The vapor leaves the evaporator to a feedwater heater at 15 psia.

**SOLUTION** Referring to Fig. 6-20 and the steam tables:  $T_{s1} = 302.93^\circ\text{F}$ ,  $h_{s1} = 1180.6$  Btu/lb<sub>m</sub>, and  $h_{d1} = 272.7$  Btu/lb<sub>m</sub>.  $T_{s2} = 213.03^\circ\text{F}$ ,  $h_{s2} = 1150.9$  Btu/lb<sub>m</sub>.  $T_{v1} = \frac{1}{2}(302.93 + 213.03) = 258^\circ\text{F}$ ,  $P_{v1} = 34.24$  psia,  $h_{v1} = 1166.7$  Btu/lb<sub>m</sub>,  $h_{d2} = 226.72$  Btu/lb<sub>m</sub>,  $h_w = 28.06$  Btu/lb<sub>m</sub>.

Assume raw water flows to the first and second effects to be  $w_1$  and  $w_2$  lb<sub>m</sub>/lb<sub>m</sub> motive steam at  $m_1$ , respectively.

Energy balance on the first effect:

$$w_1(h_{v1} - h_w) = h_{m1} - h_{d1}$$

Therefore

$$w_1 = \frac{1180.6 - 272.7}{1166.7 - 28.06} = 0.797 \text{ lb}_m/\text{lb}_m$$

Second effect:

$$w_2(h_{s2} - h_w) = w_1(h_{v1} - h_{d2})$$

Therefore

$$w_2 = 0.797 \left( \frac{1166.7 - 226.72}{1150.9 - 28.06} \right) = 0.797 \times 0.837$$

$$= 0.667 \text{ lb}_m/\text{lb}_m$$

$$\text{Total purified water} = w_1 + w_2 = 0.797 + 0.667 = 1.464 \text{ lb}_m/\text{lb}_m$$

$$\text{Motive steam required} = \frac{100,000}{1.464} = 68,306 \text{ lb}_m/\text{h}$$

First-effect heat-transfer area:

$$Q = \dot{m}_{w,1}(h_{v,1} - h_w) = \frac{0.797}{1.464} \times 100,000(1166.7 - 28.06)$$

$$= 62 \times 10^6 \text{ Btu/h}$$

$$\text{Heat head} = T_{m,1} - T_{v,1} = 302.93 - 258 = 45^\circ\text{F}$$

From Fig. 6-22 at  $T_{m,1}$  and heat head,  $U = 565 \text{ Btu}/(\text{h} \cdot \text{ft}^2 \cdot ^\circ\text{F})$

$$\text{Area} = \frac{Q}{U \times \text{heat head}} = \frac{62 \times 10^6}{565 \times 45} = 2438 \text{ ft}^2$$

Second-effect heat-transfer area:

$$Q = \dot{m}_{w,2}(h_{v,2} - h_w) = \frac{0.667}{1.464} \times 100,000(1150.9 - 28.06)$$

$$= 51.16 \times 10^6 \text{ Btu/h}$$

$$\text{Heat head} = T_{v,2} - T_{v,1} = 45^\circ\text{F}$$

At  $T_{v,1}$  and heat head,  $U = 520 \text{ Btu}/(\text{h} \cdot \text{ft}^2 \cdot ^\circ\text{F})$

$$\text{Area} = \frac{51.16 \times 10^6}{520 \times 45} = 2186 \text{ ft}^2$$

## PROBLEMS

6-1 A direct-contact condenser of the spray type receives  $60 \text{ kg/s}$  of 92% quality steam at 0.06 bar. A dry cooling tower system cools the feedwater to  $15^\circ\text{C}$ . Calculate the condensate pump volume flow rate, in cubic meters per second, and the pump power input, in kilowatts, if the pressure losses in the dry cooling tower system are 2 bar and the pump efficiency is 0.7.

6-2 A barometric condenser is used to condense  $100,000 \text{ lb}_m/\text{h}$  of 90 percent quality steam at 1 psia using cooling water at  $60^\circ\text{F}$ . The tail pipe inside diameter is 1 ft. The friction factor in it is 0.020. Find the necessary height of the tail pipe, in feet.

6-4 It is required to compare the cooling water requirements and pumping powers of single-pass and two-pass surface condensers having the same total heat-transfer surface area and inlet water conditions. Assume

at 15°C. Calculate the height of the tail pipe, in meters, if the frictional losses in bar are given by  $40V^2$ , where  $V$  is the water velocity, in meters per second.

6-4 It is required to compare the cooling water requirements and pumping powers of single-pass and two-pass surface condensers having the same total heat-transfer surface area and inlet water conditions. Assume that both have 20,000 40-ft-long 7/8-in-OD 18-BWG tubes. Cooling water enters the tubes at 64°F and 6.5 ft/s. The pressure drops are 0.4 psf/ft in the tubes, 0.6 psi in each water box and  $5 \times 10^{-11} \dot{m}^2$  in the intake, ducting, and discharge system, where  $\dot{m}$  is the mass flow rate, in pound mass per hour. Calculate for each (a) the cooling water requirements, in pound mass per hour and cubic feet per minute, and (b) the pumping power, in kilowatts, if the pumps are 70 percent efficient.

6-5 It is required to compare the effects of single-pass and two-pass surface condensers on the powerplant for the same total heat-transfer surface area and inlet water conditions. Both condensers have 20,000 40-ft-long 7/8-in-OD, 18-BWG tubes. Cooling water enters the tubes at 64°F and 6.5 ft/s (the same conditions as Prob. 6-4). Assume for simplicity that both condensers have the same overall heat-transfer coefficient, the same steam inlet of  $2 \times 10^6$  lb<sub>m</sub>/h and 92.6 percent quality, but that the single-pass condenser operates at 100°F. Calculate for each (a) the condenser operating temperature, in degrees Fahrenheit, and pressure, in pound per square inch absolute, (b) the cooling water exit temperature, in degrees Fahrenheit, and (c) the heat removed, in Btus per hour and megawatts.

6-6 Consider a powerplant operating on an ideal Rankine cycle without feedwater heating. Steam enters the turbine saturated at 1000°F at the rate of  $5 \times 10^6$  lb<sub>m</sub>/h. The turbine exhausts to a surface condenser at 1 psia. The condenser has an overall heat-transfer coefficient of 435 Btu/h-ft<sup>2</sup>-°F, a heat-transfer surface area of 402,467 ft<sup>2</sup> and cooling water inlet temperature of 60°F. Calculate (a) the plant net power, in megawatts, (b) the plant efficiency, in percent, (c) the cooling water exit temperature, in degrees Fahrenheit, and (d) the water flow rate, in pound mass per hour and in cubic feet per minute.

6-7 It is required to evaluate the effects of changing surface condenser size on powerplant performance. Consider for simplicity an ideal Rankine cycle without feedwater heaters. The turbine inlet steam is saturated at 1000 psia and has a mass flow rate of  $5 \times 10^6$  lb<sub>m</sub>/h. Condenser cooling water is available at 60°F. For a condenser heat-transfer area of 402,467 ft<sup>2</sup> and overall heat transfer coefficient of 435 Btu/h-ft<sup>2</sup>-°F, the condenser operates at 1 psia (the same conditions as Prob. 6-6). Now consider that the same plant operates with a condenser that has 15 percent more tubes (and surface area) and 15 percent more cooling water flow. Calculate (a) the new exit water temperature, in degrees Fahrenheit, (b) the new condenser pressure, in pounds per square inch absolute, and (c) the new plant power, in megawatts, and efficiency. Assume that the overall heat-transfer coefficient is unchanged.

6-8 A two-pass surface condenser contains 20,000 10-m-long 3/4-in 18-BWG 90-10 Cu-Ni Tubes. Cooling water enters the tubes at 10°C and 2 meters per second. The condensing temperature is 38°C. Calculate (a) the capacity of the condenser (heat rejected) in megawatts, and (b) the exit water temperature, in degrees centigrade. Take for water  $c_p = 4184$  J/kg · K and density = 1000 kg/m<sup>3</sup>.

6-9 Consider for simplicity an ideal Rankine cycle with turbine inlet and exit steam at 2500 psia and 1000°F, and 1 psia, respectively, and no feedwater heating. The steam mass flow rate is  $2 \times 10^6$  lb<sub>m</sub>/h. The plant has a two-pass surface condenser with 45-ft-long 7/8-in 18-BWG-type 304 stainless steel tubes. Cooling water enters the tubes at 70°F and 7 ft/s. With no flows into the condenser other than turbine steam, find (a) the plant power, in megawatts, and efficiency and (b) the total number of tubes if the condenser terminal temperature difference is 8°F.

6-10 It is required to evaluate the effects of changing surface condenser inlet water temperature on powerplant performance. Consider the ideal Rankine cycle and condenser of Prob. 6-9 (with 25,696 tubes) but the cooling water inlet temperature is changed from 70° to 60°F. Calculate (a) the new exit cooling water temperature, in degrees Fahrenheit, (b) the new condenser pressure, in pounds per square inch absolute, and (c) the new plant power, in megawatts.

6-11 A 1100-MW two-pass surface condenser has 50-ft-long 18-BWG tubes. It uses seawater with tube inlet at 7 feet per second and 80°F, and 100°F exit. The condenser is situated 18 ft above sea level. The pressure drops in the circulating water system, expressed in head are: 4 ft in the inlet tunnel, 6 ft in the inlet pipe, 3 ft in the outlet pipe, and 2 ft in the outlet tunnel. Calculate (a) the water flow rate in pound

mass per hour and gallons per minute, and (b) the pumping in horsepower and megawatts required if the pumps efficiency is 80 percent. Use for seawater  $c_p = 0.962 \text{ Btu lb}_m^{-1} \text{ } ^\circ\text{R}$ , and density =  $64 \text{ lb}_m/\text{ft}^3$ .

6-12 A condensing only feedwater heater uses 7.8-in-OD 90-10 copper-nickel tubes. It receives  $84,000 \text{ lb}_m/\text{h}$  of 95 percent quality bled steam at 20 psia, and  $160,000 \text{ lb}_m/\text{h}$  of drain from the next higher pressure heater at  $240^\circ\text{F}$ .  $3.9 \times 10^6 \text{ lb}_m/\text{h}$  of feedwater goes through the heater at 7 ft/s, 2000 psia, and  $195^\circ\text{F}$ . The terminal temperature difference is  $5^\circ\text{F}$ . Determine the size, length, and number of tubes based on a U-tube design. Take a maximum allowable stress in the tubes of  $15,000 \text{ psi}$ .

6-13 A closed type two-pass feedwater heater receives  $100,000 \text{ lb}_m/\text{h}$  steam at 300 psia and  $450^\circ\text{F}$  and feedwater at  $380^\circ\text{F}$ . The terminal temperature difference is  $-2.65^\circ\text{F}$ . No drain cooler is used. Find (a) the mass flow rate of feedwater heated, and (b) the water pressure drop, in pounds per square inch, if the adjusted cold water velocity is 8 ft/s, the tube length is 20 ft, and the tube inside diameter is 0.652 in.

6-14 A one-pass condensing only closed feedwater heater receives saturated extraction steam at 80 psia and  $10^6 \text{ lb}_m/\text{h}$  of feedwater at  $240^\circ\text{F}$ . The terminal temperature difference is  $4^\circ\text{F}$ . Calculate (a) the total tube heat-transfer area if they are made of 16 gage admiralty metal and the velocity adjusted to  $62.4 \text{ lb}_m/\text{ft}^2$ , is 8 ft/s, (b) the amount of extraction steam required, in pound mass per hour, and (c) the new log mean temperature difference and the new bled steam temperature and pressure if the water velocity was changed to 6 ft/s at the same inlet temperature.

6-15 A condensing only closed type feedwater heater receives saturated bled steam at 80 psia.  $0.9 \times 10^6 \text{ lb}_m/\text{h}$  of feedwater enter the tubes at  $260^\circ\text{F}$  and 6 ft/s. The tubes are 45.5-ft-long U-shaped 3.4-in-OD 18-BWG admiralty metal. The terminal temperature difference is  $5^\circ\text{F}$ . Calculate (a) the mass flow rate of the bled steam, in pound mass per hour, (b) the number of tubes, and (c) the pressure drop in the heater, in pounds per square inch.

6-16 A closed-type two-pass feedwater heater with desuperheating zone but no drain cooler uses 20.7 long 3.4-in 18-BWG admiralty tubes.  $10^6 \text{ lb}_m/\text{h}$  of feedwater enter the tube at  $260^\circ\text{F}$  and  $8.527 \text{ ft/s}$ . Bled steam is at 80 psia and  $350^\circ\text{F}$ . The terminal temperature difference is  $4^\circ\text{F}$ . The overall heat-transfer coefficient in the desuperheating zone is  $120 \text{ Btu h}^{-1} \text{ ft}^2 \text{ } ^\circ\text{F}$ . Calculate (a) the mass flow rate of bled steam, in pound mass per hour, (b) the number of tubes, (c) the pressure drop in the heater, in pounds per square inch.

6-17 A sample of water upon analysis showed that each liter contained  $0.0018 \text{ g} \cdot \text{mol}$  calcium bicarbonate,  $0.0005 \text{ g} \cdot \text{mol}$  magnesium bicarbonate,  $0.0008 \text{ g} \cdot \text{mol}$  magnesium sulfate, and  $0.0006 \text{ g} \cdot \text{mol}$  sodium sulfate. Calculate (a) the total hardness in parts per million, (b) the masses of lime and soda ash, kilogram per day needed to soften  $100,000 \text{ L}$  of the water per day and (c) the mass of sludge, in kilograms, that must be disposed of per day. Take the density of water as  $1000 \text{ kg/m}^3$ .

6-18 A single-effect evaporator receives motive steam at 7 bars and  $180^\circ\text{C}$  and pretreated raw water at 9 bars and  $16^\circ\text{C}$ . It has  $123 \text{ m}^2$  of heat-transfer area. Calculate the mass flow rates of motive steam and vapor produced in kilograms per second. Ignore the pressure drop in the evaporator.

6-19 A  $35,000 \text{ lb}_m/\text{h}$  double-effect evaporator receives motive steam at 40 psia and  $300^\circ\text{F}$ . Pretreated raw water enters at  $60^\circ\text{F}$ . The pressure in the second effect is 5 psia. Calculate, for equal heat heads, (a) the amount of motive steam required, in pound mass per hour, and (b) the surface areas for each evaporator, in square feet.

6-20 A double-effect evaporator is to evaporate  $15,000 \text{ lb}_m/\text{h}$  of  $60^\circ\text{F}$  raw water using 25 psia motive steam. The vapor from the second effect is at 3.0 psia. Find (a) the heat head for each effect, (b) the mass flow rate of motive steam, in pound mass per hour, (c) surface area of each effect, in square feet, and (d) total purified water, in pound mass per hour, if the pressure of the motive steam was changed to 17 psia during part load operation.

## THE CIRCULATING-WATER SYSTEM

## 7-1 INTRODUCTION

The circulating-water system supplies cooling water to the turbine condensers and thus acts as the vehicle by which heat is rejected from the steam cycle to the environment. The system also supplies lesser amounts of auxiliary cooling water for turbine and steam-generator buildings, for the fire protection system, and for general station yard use. In the case of nuclear powerplants, it supplies, in addition, auxiliary cooling water to the reactor building (for cooling a closed-loop cooling-water circuit to limit radioactivity release back to the environment), water for dilution and dispersion of radioactive wastes released from the plant, and water for decay heat removal when necessary. The total auxiliary requirements are usually about 5 percent of condenser flow requirements.

The circulating-water system is called upon to reject heat to the environment in an efficient manner but one that also conforms to thermal-discharge regulations. Its performance is vital to the efficiency of the powerplant itself because a condenser operating at the lowest temperature possible results in maximum turbine work and cycle efficiency and in minimum heat rejection. Hence, a good heat-rejection system makes its own job easier; i.e., it is called upon to reject less heat and is smaller and requires less cooling water.

The heat rejected by the circulating-water system is greater than that converted to useful work by the steam cycle. In currently operating powerplants, new and old, the heat rejected varies from 1.5 to 3.0 times the useful work output of these plants. This is given by the equation

$$\dot{Q}_R = \left( \frac{1}{\eta} - 1 \right) \dot{W} \quad (7-1)$$



Table 7-1 Effect of cycle efficiency on heat rejection by 1000-MW powerplants

$W$	$\eta$	$\dot{Q}_A$	$\dot{Q}_R$	$\dot{Q}_R/W$
1000	0.20	5000	4000	4.0
1000	0.25	4000	3000	3.0
1000	0.33	3000	2000	2.0
1000	0.40	2500	1500	1.5
1000	0.50	2000	1000	1.0

where  $\dot{Q}_R$  is the heat rejection rate,  $W$  the power, and  $\eta$  the cycle efficiency. To evaluate the effect of  $\eta$  on  $\dot{Q}_R$  one should compare plants with the same  $W$ , say 1000 MW (Table 7-1). The first and last efficiencies roughly represent old small industrial units and hoped-for advanced future units.  $\eta = 0.25$  is for older but still-operating powerplants.  $\eta = 0.33$  represents current nuclear powerplants of the pressurized- and boiling-water-reactor type.  $\eta = 0.40$  represents modern high-temperature fossil-fueled and gas-cooled and fast-breeder nuclear-reactor powerplants. It can be seen that an improvement of 7 percent in efficiency, from 25 to 33 percent, results in 33 percent savings in heat rejection (not 8 percent as one is inclined to guess), whereas an efficiency improvement of 7 percent from 33 to 40 percent, results in 25 percent savings.

## 7-2 SYSTEM CLASSIFICATION

Circulating-water systems are broadly classified as (1) once-through, (2) closed-loop, and (3) combination systems.

**Once-through systems** In once-through systems, water is taken from a natural body of water such as a lake, river, or ocean and pumped through the condenser, where it is heated and then discharged back to the source (Fig. 7-1). There are generally three methods of discharge:

1. *Surface discharge*, by which the condenser water is released in a relatively thin layer on the surface of the original body of water. The resulting plume is cooled by evaporation of some of the water to the atmosphere and by mixing with the cooler water below.
2. *Submerged discharge*, by which the water is released as a buoyant jet below the surface of the body. The jet mixes with the cooler water, and heat is eventually dissipated by evaporation from the mixture.
3. *Diffuser discharge*, by which the water is let out through a number of nozzles from a long pipe submerged across the flowing system, such as across a river. The jets may point upstream to promote more rapid mixing. Again heat rejection is accomplished by evaporation from the mixture.

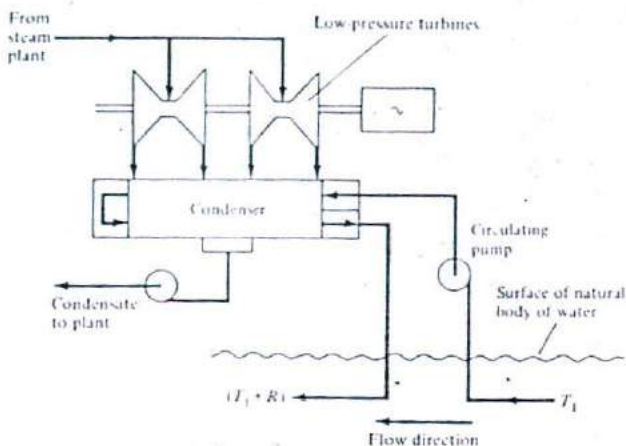


Figure 7-1 Schematic of a once-through circulating-water system.

Once-through cooling is, thermodynamically, the most efficient means of heat rejection. It uses the lowest-temperature heat sink available to the powerplant. There are, however, instances when water is scarce or when environmental regulations limit the utilization of surface waters or the amount of heating they may be subjected to. In such cases, the less efficient closed-loop systems are used.

**Closed-loop systems** In closed-loop systems, water is taken from the condenser, passed through a cooling device, and returned to the condenser. Often a reservoir is placed between the cooling device and the condenser. A nearby natural body of water is still necessary to supply makeup water to replace that lost by evaporation during the cooling process and to receive blowdown from it. There are several types of cooling devices available for closed-loop systems. These are:

1. *Cooling towers* may be of the wet type, (Sec. 7-4), dry type (Sec. 7-6), or combination wet-dry type (Sec. 7-8). The dry-type cooling tower is the least efficient of all heat rejection methods but requires no makeup water and hence is suited for desert installations or where the use of natural waters is absolutely prohibited. Cooling towers are also classified as *natural draft* or *mechanical draft*. A cooling tower operating in a closed loop is said to be operating in the *closed mode* (Fig. 7-2).
2. *Spray ponds* rely upon winds that blow across the ponds and cool fine sprays of water by evaporation.
3. *Spray canals* are like spray ponds except the water is sprayed into large droplets so that drift loss (water carryover with the wind) is reduced, but at a lower mass-transfer rate and hence lower cooling efficiency.

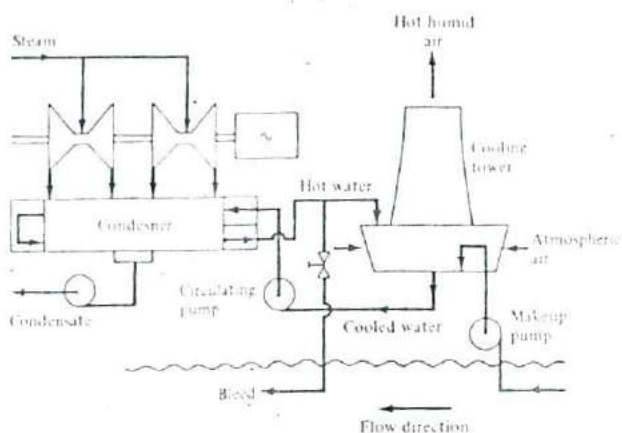


Figure 7-2 Schematic of a wet-cooling tower operating in the closed mode

4. *Cooling lakes* are areas in which the water is cooled naturally by evaporation and radiation. They are the least efficient of the three artificial bodies of water and therefore require the greatest acreage, but also the least mechanical equipment.

**Combination systems** Combination systems combine once-through systems with a cooling device, usually a cooling tower, that cools the water before returning it to the natural body of water. A cooling tower operating this way is said to be operative in the *open mode* (Fig. 7-3), also called the *terminal-difference mode*. A cooling tower

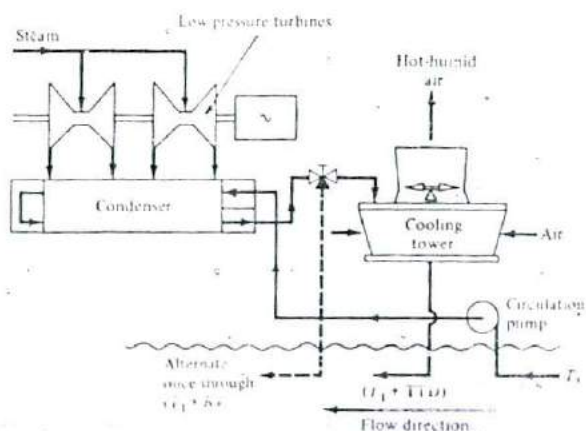


Figure 7-3 A wet-cooling tower operating in the open mode. An alternate once-through system is shown by the dashed line.

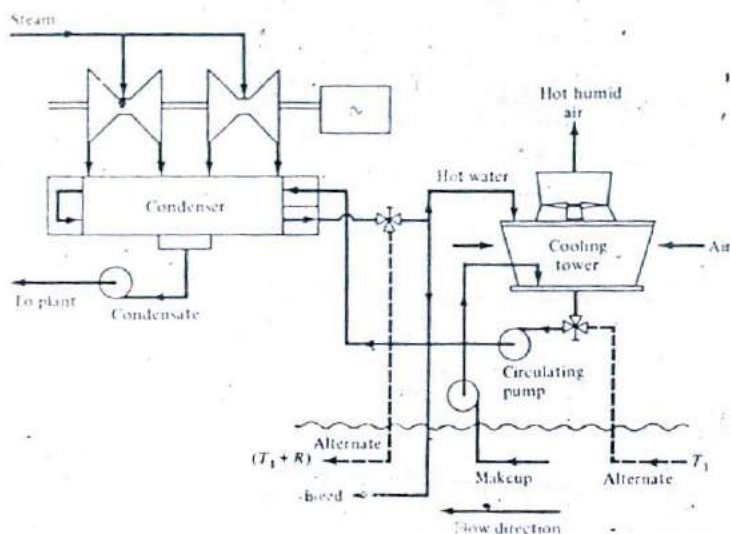


Figure 7-4 A wet-cooling tower operating in the helper mode.

may also operate in the *helper mode* (Fig. 7-4), in which both once-through and cooling-tower closed mode share cooling duties. This is the case when water supplies may be unreliable, as during drought periods, upstream intermittent use, or river temperature limitations during certain periods. The cooling tower may carry anywhere from 0 to 100 percent of the cooling load. A cooling-tower installation may also be operated in the closed, open, or helper modes by the proper use of a variety of gates and valves.

In Figs. 7-1 through 7-4

$R$  = range = temperature rise across condenser

TTD = terminal temperature difference = exit cooling  
tower temperature - source temperature

### 7-3 THE CIRCULATION SYSTEM

The system is composed of a number of components. Besides the condenser and the cooling device, they are:

1. An intake structure from a natural body of water in an open system or from cooling towers, spray ponds, etc., in a closed or helper mode
2. A circulating-water pumping station

3. Circulating-water conduits
4. Flow gates
5. Vacuum breaking system
6. Cold- and warm-water channels

The *intake system* begins with a *skimmer wall* that assists in obtaining cooler bottom water from the natural source. The intake structure, located at the land end of an intake channel, is usually constructed of reinforced concrete. It houses the necessary equipment for screening debris from the water (Fig. 7-5). The water passes through *bar racks* that are mounted across each inlet bay to intercept large debris. The bar-rack grill sections extend from the inlet-bay floor to the top of the intake structure with an incline, usually  $15^\circ$  from vertical.

The debris is removed from the upstream face of the bar racks by a *traversing trash rake*, usually operator actuated, that travels across the top of the intake structure on two parallel rails. Its main component is a *rake basket*, typically 10 ft wide, equipped with teeth. As the basket is lowered, it is opened and the teeth are turned away from the bar rack to clear the debris from the rack. As the basket is raised, it is closed so that the teeth penetrate between the rack bars to clean out the embedded debris. When it reaches the discharge position at the top, it is opened to dump the trash into the trash cart. When full, the latter can be removed from the end of the trash-rake frame and towed to a disposal area.

The main circulating-water pumps are further protected by *traveling screens* at their intakes (Fig. 7-6). These screens are composed of a series of screen panels, which typically have  $3/8$ -in<sup>2</sup> openings and are connected in a continuous loop across rotating drive sprockets. As water flows through the initially stationary screens, debris is deposited on them and held by the force of the moving water. When sufficient debris accumulates, the pressure drop across the screens reaches a point at which the screen drive is automatically actuated. The screen panels rotate at top and are washed by a spray, and the debris collects in a large tray. Manual operation of the screens is also provided from the control room. There are typically six such traveling screens per circulating pump.

The cooling water now enters a number of large *circulating-water pumps* operating in parallel. The number of pumps depends upon the plant and pump sizes, but a usual arrangement is three pumps per pumping station or unit. In nuclear powerplants, the size of the circulating pumps is such that any one is sufficient to dissipate reactor-shutdown decay heat. In emergency conditions that pump can be started by the two standby diesel generators that are part of these powerplants. Each pump discharge to the condensers is equipped with a motor-operated butterfly valve, which is interlocked with its pump motor so that both will start together to minimize surges in the condenser.

The combined flow goes through a tunnel to the condenser inlet conduit. The conduit, which could be 6.5 ft (2 m) in diameter, has a motor-operated butterfly valve in a vertical run of it. It directs the water to each side of the condenser divided inlet water box. A similar arrangement on the condenser discharge side, also with a motor-operated butterfly valve, permits throttling for testing or equalization of flows in case there is more than one condenser. The discharge from the condensers now goes through

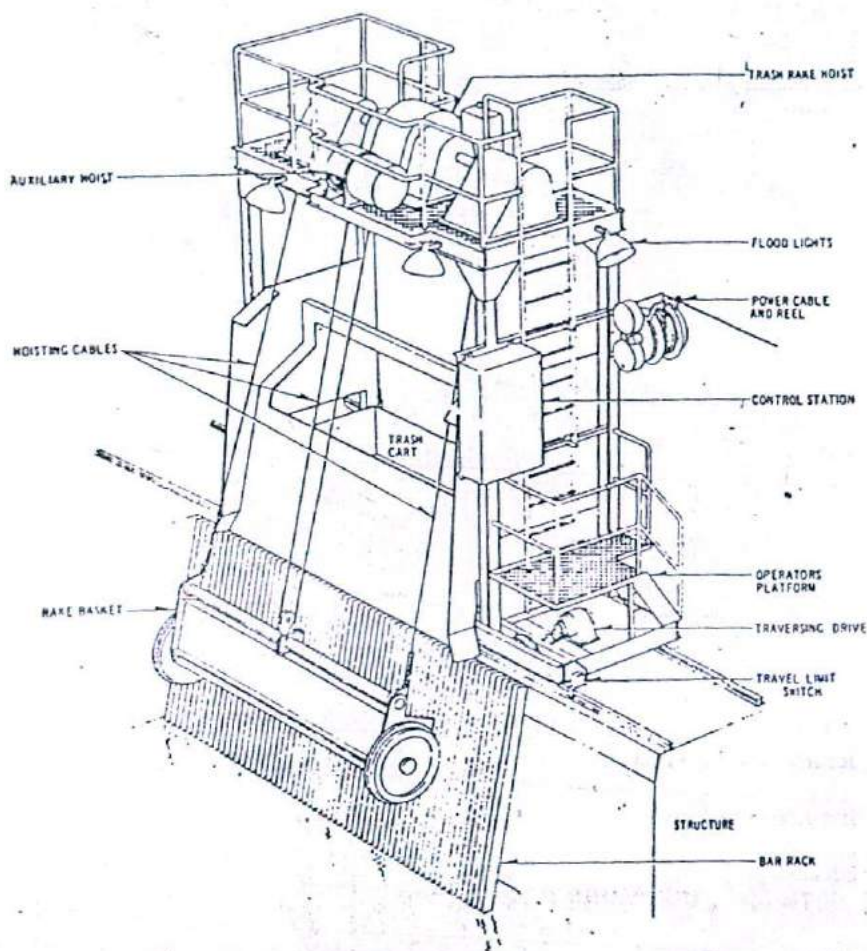


Figure 7-5 A typical intake system bar rack and traversing trash rake.

a discharge tunnel to a warm-water channel that feeds the cooling tower. Alternatively, when conditions permit, the warm water is returned to the pump reservoir by means of diffuser pipes. These are partially perforated, corrugated, galvanized steel pipes laid side by side across the bottom of the reservoir. They provide thermal mixing with the reservoir water.

When the circulating-water system is operated in the closed or helper modes, the warm-water from the condenser is directed to the cooling tower pumping stations, one per tower, typically composed of two pumps and located in separate reinforced

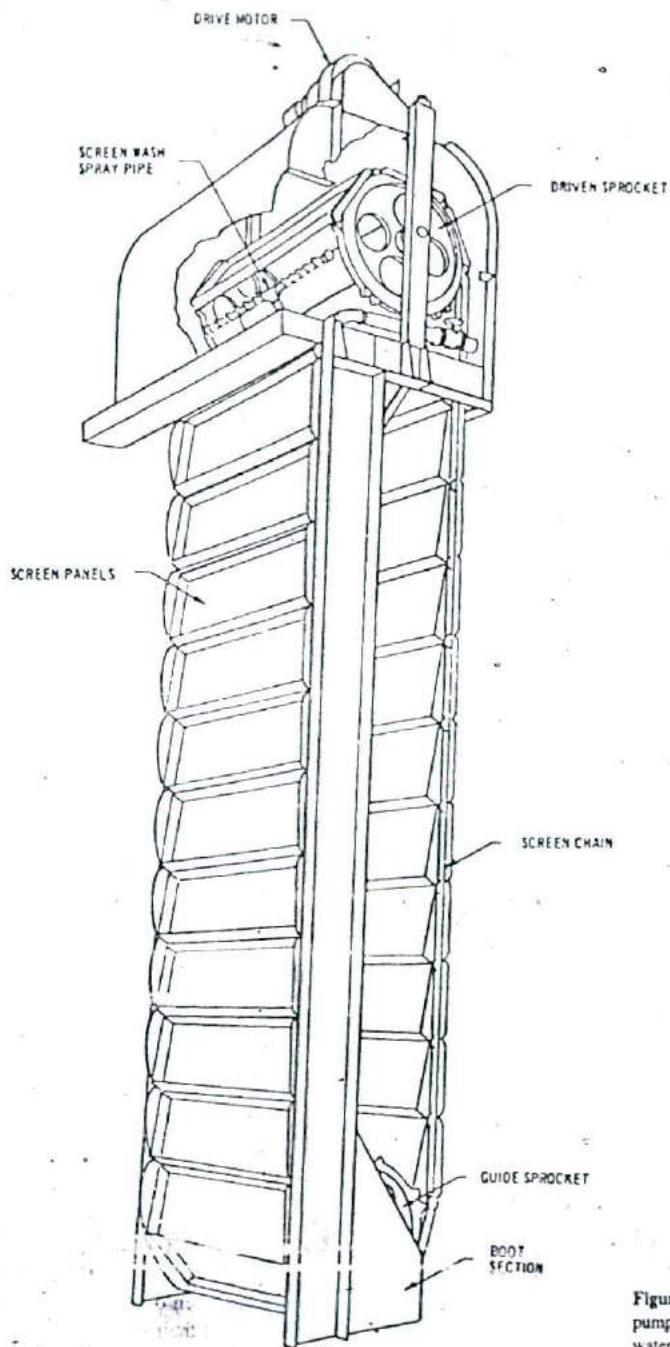


Figure 7-6 A typical pump intake traveling water screen.

concrete pits. The discharges from the cooling towers flow into a number of common open cold-water channels, over a weir, through a gate into a reservoir connecting to the circulating pump intake structure. The weir adjusts for the difference in water level between the higher cooling towers and the lower reservoir.

*Vacuum systems* are provided at the high points in tunnels, usually in the warm-water channel, that are at a pressure below atmospheric at normal design flows (the syphon effect). The vacuum is normally maintained by a vacuum priming system but must be broken by the control-room operator in the case of unusual happenings downstream that may cause backflow through the pump and intake structure.

## 7-4 WET-COOLING TOWERS

Wet-cooling towers dissipate heat rejected by the plant to the environment by these mechanisms: (1) addition of sensible heat to the air and (2) evaporation of a portion of the recirculation water itself. When operated in the open mode, there is a third mechanism: (3) addition of sensible heat to the natural body of water as a result of the terminal temperature difference (TTD).

Wet cooling towers have a hot-water distribution system (Fig. 7-7) that showers or sprays the water evenly over a latticework of closely set horizontal slats or bars called *fill*, or *packing*. The fill thoroughly mixes the falling water with air moving through the fill as the water splashes down from one fill level to the next by gravity. Outside air enters the tower via louvers in the form of horizontal slats on the side of the tower. The slats usually slope downward to keep the water in. The intimate mix between water and air enhances heat and mass transfer (evaporation), which cools the water. Cold water is then collected in a concrete basin at the bottom of the tower where it is pumped back to the condenser (closed or helper mode) or returned to the natural body of water (open mode). The now hot, moist air leaves the tower at the top.

In Table 7-1 it was shown that a modern 1000-MW fossil-fueled plant with  $\eta = 0.40$  would reject about 1500 MW at full load. This is roughly equivalent to  $512 \times 10^6$  Btu/h and uses about 760,000 gal/min ( $48 \text{ m}^3/\text{s}$ ) of circulating water, based on an  $18^\circ\text{F}$  ( $10^\circ\text{C}$ ) range. A water-reactor nuclear plant, with  $\eta = 0.33$ , would reject  $683 \times 10^6$  Btu/h. Depending upon climatic conditions, the portion carried by evaporative mechanism is about 75 percent in hot weather and 60 percent in cold weather. It would result in the evaporation, and hence the need for makeup, of about 7500 gal/min ( $\sim 0.47 \text{ m}^3/\text{s}$ ) for the fossil plant and 10,000 gal/min ( $\sim 0.63 \text{ m}^3/\text{s}$ ) for the nuclear plant in hot weather. In cold times the figures would perhaps be reduced by 20 percent (Table 7-2). Additional makeup is required for blowdown and cooling-tower drift (below). The balance of heat rejected is mostly due to heating the air, and is greater in cold than in hot weather. Blowdown is normally 20 percent and drift is 2 to 2.5 percent of the evaporation losses [53].

Although cooling towers show the obvious advantage of reducing water demand for available water by at least 75 times, they do this at the expense of large capital, land, and operational costs, as well as some water pollution of their own, noise and,



it is often said, sight pollution. Nevertheless, environmental regulations and thermal pollution of once-through systems, and the increasing scarcity of dependable natural water supplies in many parts of the world, are forcing utilities into building more and more cooling towers (and some other systems such as cooling ponds). Once-through systems, it should be recalled, are the most efficient cooling systems and should be preferred if there is an abundance of natural water.

Wet-cooling towers are classified as either (1) *mechanical-draft* or (2) *natural-draft* cooling towers. Each of these types is further classified as (1) *counterflow* or (2) *cross-flow* cooling towers (Fig. 7-7).

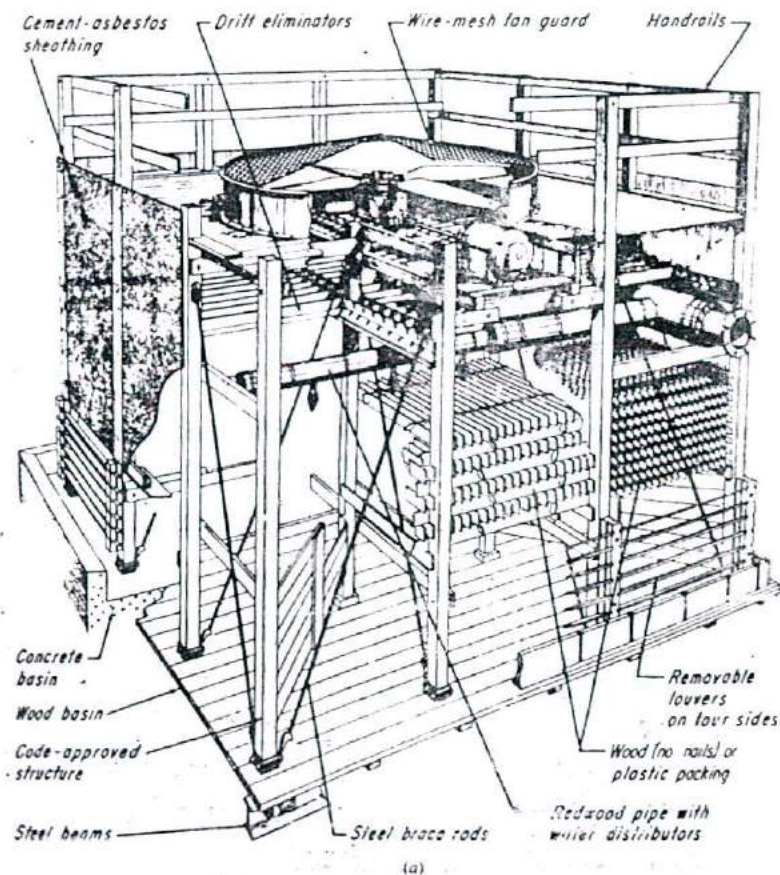
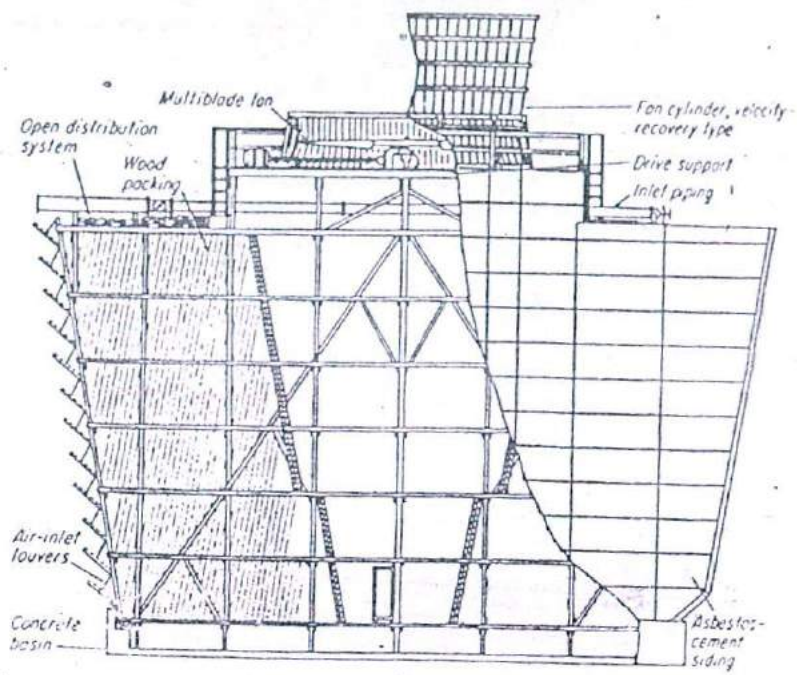
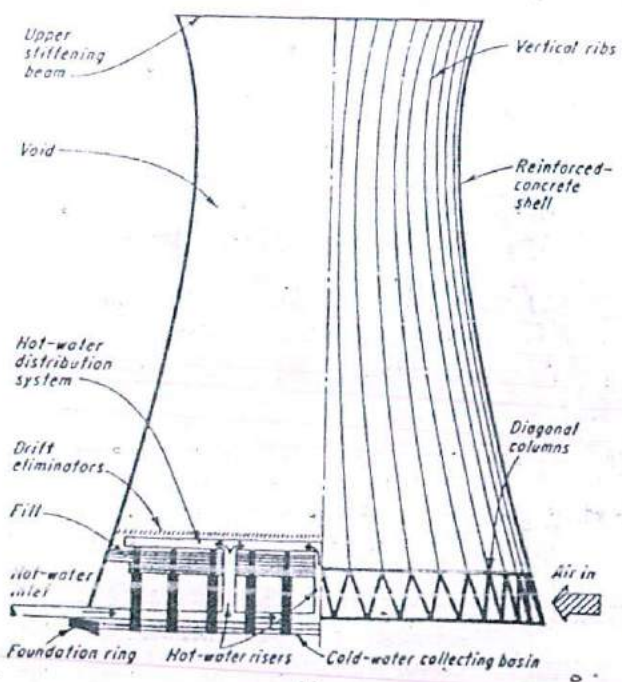


Figure 7-7 The four types of wet-cooling towers: (a) mechanical-draft counterflow, (b) mechanical-draft cross-flow, (c) natural-draft counterflow, (d) natural-draft cross-flow [51,52]. (Not drawn to same scale.)

(Continued on next two pages.)



(b)



(c)

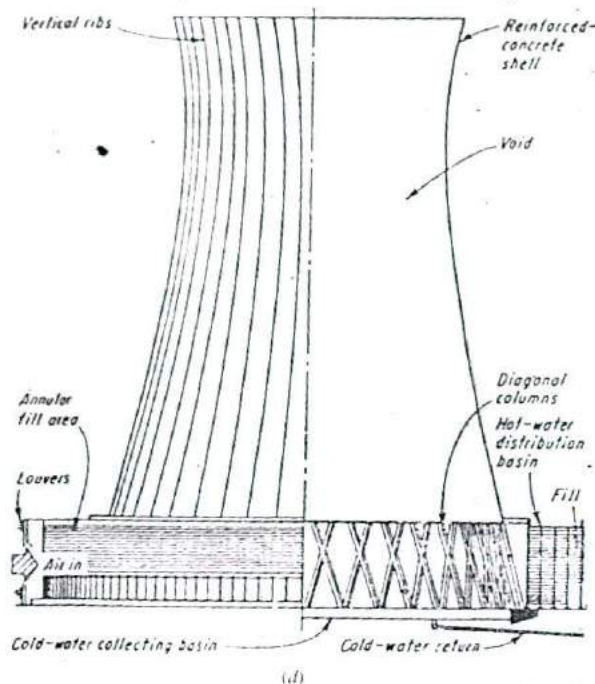
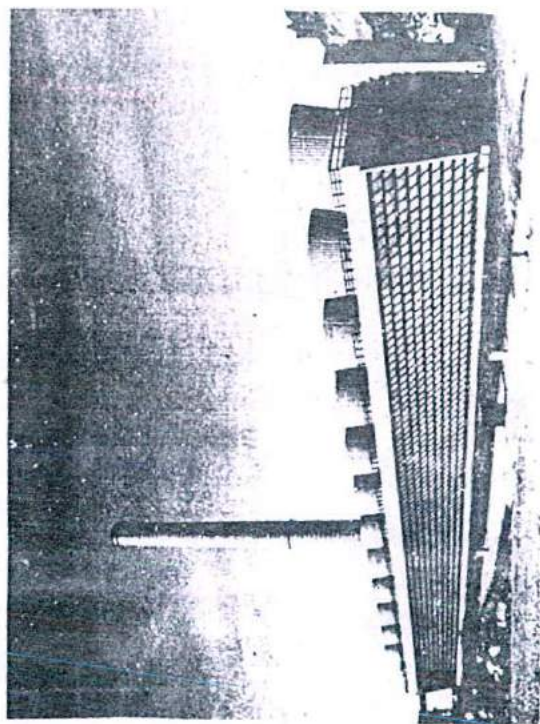


Figure 7-7 (continued)

Table 7-2 Typical evaporation from wet-cooling towers serving a 1000-MW plant

$\eta$	$Q_w$ , MW	Circulating-water flow, $T_R = 18^\circ\text{F} = 10^\circ\text{C}$		Climate	Evaporation		
		gal/min	$\text{m}^3/\text{s}$		gal/min	$\text{m}^3/\text{s}$	%
0.23	2000	735,000	47.8	Hot	10,000	0.63	1.3
				Cold	8000	0.50	1.0
0.40	1500	568,000	35.8	Hot	7500	0.47	1.3
				Cold	6000	0.38	1.0



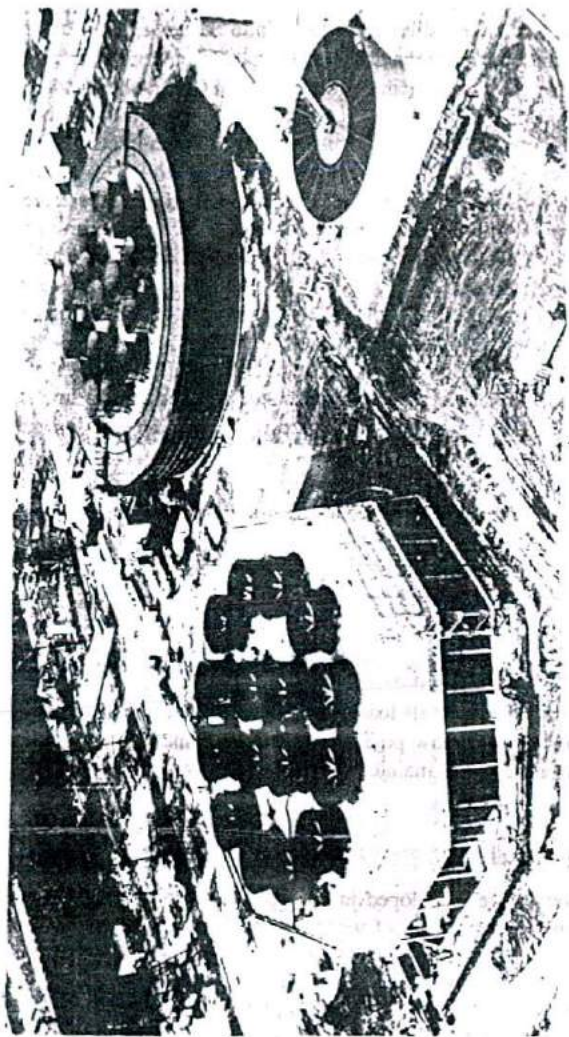


Figure 7-8 Multicell induced-draft cooling towers showing cross-flow in-line, cross-flow round, and counterflow octagonal arrangements. (Courtesy the Marley Cooling Tower Company, Mississauga, Ontario.)

## Mechanical-Draft Cooling Towers

In *mechanical-draft* cooling towers, the air is moved by one or more mechanically driven fans. As in steam generators, the fans could be of the *forced-draft*<sub>1</sub> (FD) type, which would be mounted on the lower sides to force air into the tower. This type would theoretically be preferred because the fans would operate on cooler air and hence consume less power. However, experience with this type of fan has shown some disadvantages because of air distribution problems, leakage, recirculation of the hot and moist exit air back to the tower, and frost accumulation at the fan inlets during winter operation.

The majority of mechanical-draft cooling towers for utility application are therefore of the *induced-draft* (ID) type. With this type, air enters the sides of the tower through large openings at low velocity and passes through the fill. The fan is located at the top of the tower, where it exhausts the hot, humid air to the atmosphere. Induced-draft cooling towers are usually multicell with a number of fan stacks on top and come in various arrangements: rectangular, octagonal, circular, etc. (Fig. 7-8).

The fans are usually multibladed and large, ranging from 2 to 33 ft (0.6 to 10 m) in diameter (Fig. 7-9). They are driven by electric motors, as large as 250 hp, at relatively low speeds through reduction gearing. They are of the propeller type, which move large volumetric flow rates at relatively low static pressures. They have adjustable-pitch blades for minimum power consumption, depending upon load and climatic conditions. The fans and their drives are designed to function satisfactorily in the hot, humid atmosphere they are in. The blades are usually made of cast aluminum, stainless steel, or fiberglass, although plastic and laminated wood have been used.

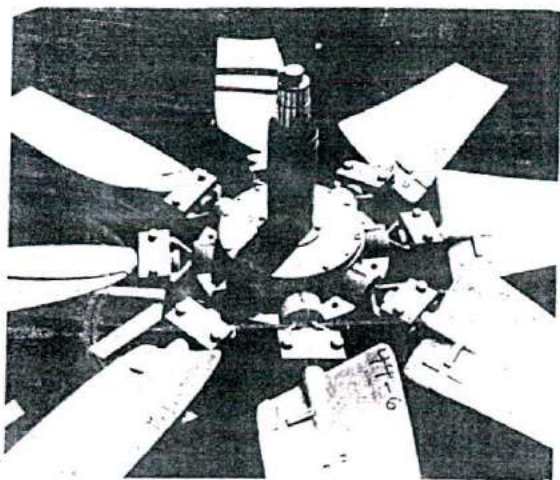
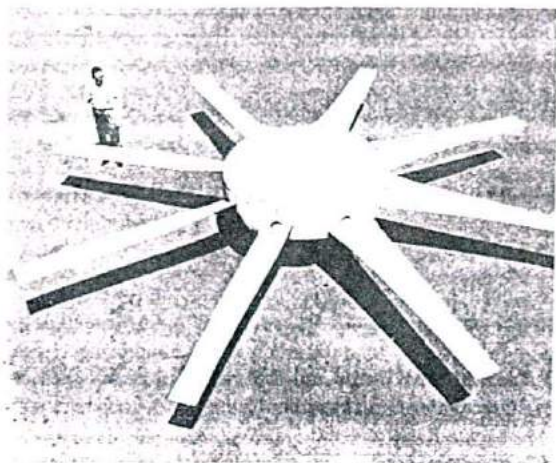
The airflow into the tower is roughly horizontal. The flow in the fill however is either horizontal, in which case it is a *cross-flow* cooling tower, or vertical, in which case it is a *counterflow* cooling tower (Fig. 7-7a and 7-7b).

The main advantages of mechanical-draft cooling towers are the assurance of moving the required quantity of air at all loads and climatic conditions, low initial capital and construction costs, and a low physical profile. Their main disadvantages are power consumption, operating and maintenance costs, and greater noise [54].

## Natural-Draft Cooling Towers

*Natural-draft* cooling towers were developed in Europe. The first ones, erected in Holland early in this century, were made of wood. They evolved to wood on steel and finally to the reinforced concrete used today. The early shapes were nearly cylindrical, followed by an inverted truncated cone on top of another, and finally the hyperbolic shape of today. Their most extensive use has been in England. In the United States, the first unit was built in 1972, and the number being built has risen dramatically since. One hundred units were expected to be constructed by 1980 [51].

Natural-draft cooling towers use no fans. They depend for airflow upon the natural driving pressure caused by the difference in density between the cool outside air and the hot, humid air inside. The driving pressure  $\Delta P_d$  is given by



**Figure 7-9** Typical fans used in induced-draft cooling towers. On the bottom is one with a large diameter. On the top is one with automatic variable-pitch control. (Courtesy the Marley Cooling Tower Company, Mission, Kansas.)

$$\Delta P_d = (\rho_o - \rho_i) H \frac{g}{g_c} \quad (7-2)$$

- where
- $\rho_o$  = density of outside air,  $\text{lb}_m/\text{ft}^3$  or  $\text{kg}/\text{m}^3$
  - $\rho_i$  = density of inside air, taken at exit of the fill,  $\text{lb}_m/\text{ft}^3$  or  $\text{kg}/\text{m}^3$
  - $H$  = height of tower above the fill, ft or m
  - $g$  = gravitational acceleration,  $\text{ft}/\text{s}^2$  or  $\text{m}/\text{s}^2$
  - $g_c$  = conversion factor =  $32.2 \text{ lb}_m \cdot \text{ft}/(\text{lb}_f \cdot \text{s}^2)$  or  $1.0 \text{ kg} \cdot \text{m}/(\text{N} \cdot \text{s}^2)$

This driving pressure must balance the air-pressure losses through the tower.

Because  $\rho_o - \rho_i$  is relatively small,  $H$  must be large to result in the desired  $\Delta P_d$ . Natural-draft cooling towers are therefore very tall, often a few hundred feet. The tower body, above the water distribution system and the fill, is an empty shell of circular cross section but with a hyperbolic vertical profile. Natural-draft cooling towers are therefore often referred to as *hyperbolic towers*. The hyperbolic profile has been found to offer superior strength and the greatest resistance to outside wind loading (pressure due to strong winds) compared with other forms, so that substantially less material is needed and thicknesses can be as low as 6 or 7 in at the waist. It has little to do with inside airflow. Natural-draft cooling towers are made of reinforced concrete, very large volumes of concrete, and sit on "stilts" or diagonal support columns in a shallow basin of water. They are an imposing sight from afar, dwarfing the powerplant itself (Fig. 7-10).

Natural-draft cooling towers are also of the counterflow or cross-flow types (Figs. 7-7c and 7-7d). In counterflow, the fill is inside (above the stilts), spread over a large area, and is therefore shallower. In cross-flow, the fill sits in a ring outside the tower outside the stilts.

The choice between different types of cooling towers depends upon many factors, the most important of which are climatic and economic. Mechanical-draft towers are the choice when the approach (the difference between the temperature of the cold water leaving the tower and the wet-bulb temperature of the outside air) is low and when a broad range of water flow is expected. The latter factor is made possible because they are usually built as multicell units with a variable-airflow fan, a design which offers versatility and good response to changes in cooling parameters and demands.

Natural-draft towers are selected most often: (1) in cool, humid climates (low wet-bulb temperatures and high relative humidity); (2) when there is a combination of low wet-bulb temperatures and high condenser-water inlet and outlet temperature, i.e., a broad range and long approach; or (3) in cases of heavy winter loads. Economic factors favor them when, because of their large capital costs, a long amortization period can be arranged. In general, they are favored for very large powerplants where fewer



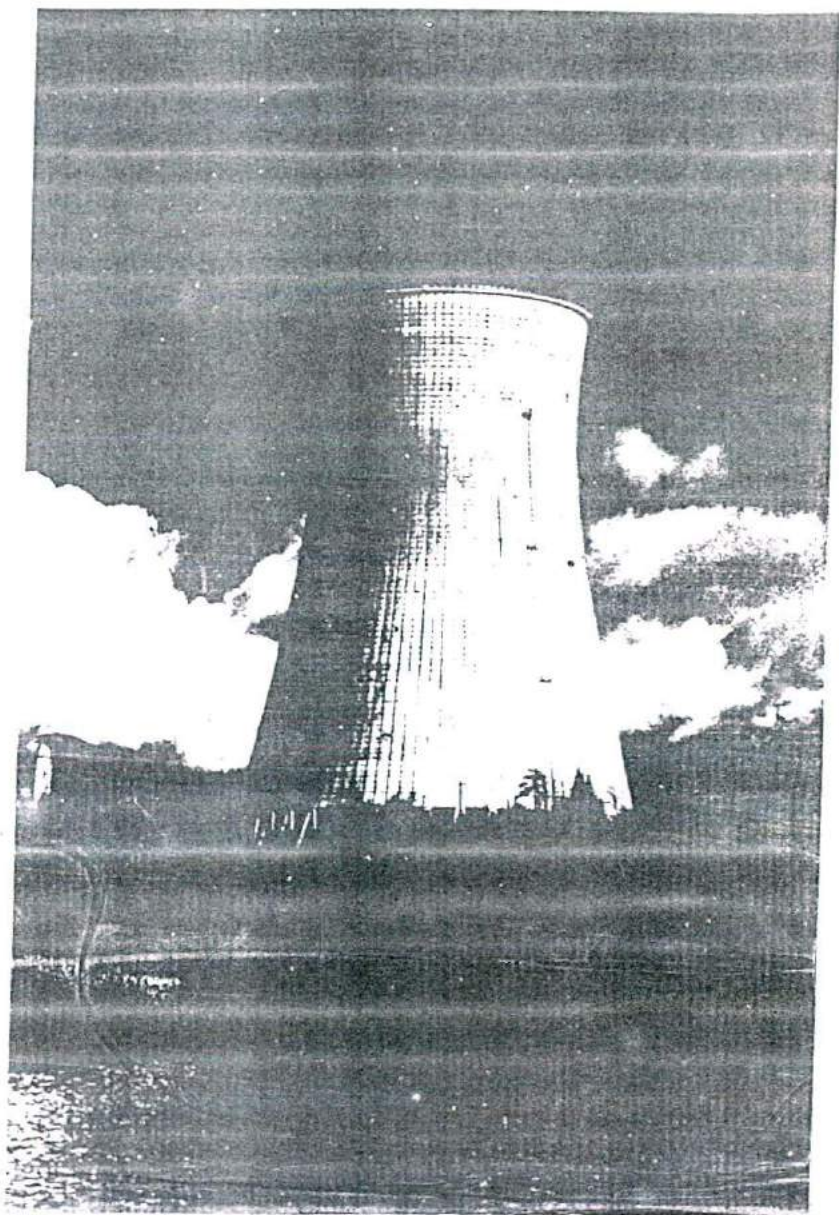


Figure 7-10 A natural-draft cooling tower next to a nuclear-reactor containment building. (Courtesy Research Cottrell, Bound Brook, New Jersey.)

and larger towers can be built. In the early 1980s mechanical-draft towers still commanded the lion's share in utility and large industrial installations, although natural-draft towers are expected to gradually increase their share in the future.

The choice between cross-flow and counterflow of either type is less clear. Cross-flow towers offer less resistance to airflow, thus allowing higher air velocities than counterflow towers. They are, however, less efficient. Both designs, therefore, have counterbalancing advantages and limitations, and the choice depends upon the particular application. Natural-draft towers, however, recently ordered have been in the counterflow variety only.

### The Water-Distribution System

The *water-distribution system* dispenses hot condenser water evenly over the fill. There are several types, among them are: (1) *Gravity distribution*, used mainly on cross-flow towers, consists of vertical hot-water risers that feed into an open concrete basin, from which the water flows by gravity through orifices to the fill below (Fig. 7-11a). (2) *Spray distribution*, used mainly on counterflow towers, has cross piping with spray-downward nozzles (Fig. 7-11b). (3) *Rotary distribution* consists of two slotted distributor arms that rotate about a central hub through which water comes in under pressure. The slots are aimed downward but slightly to one side, resulting in a curtain of water at an angle and a reaction force that rotates the arms at 25 to 30 r/min. The speed of rotation can be varied by adjusting the slot angle (Fig. 7-11c).

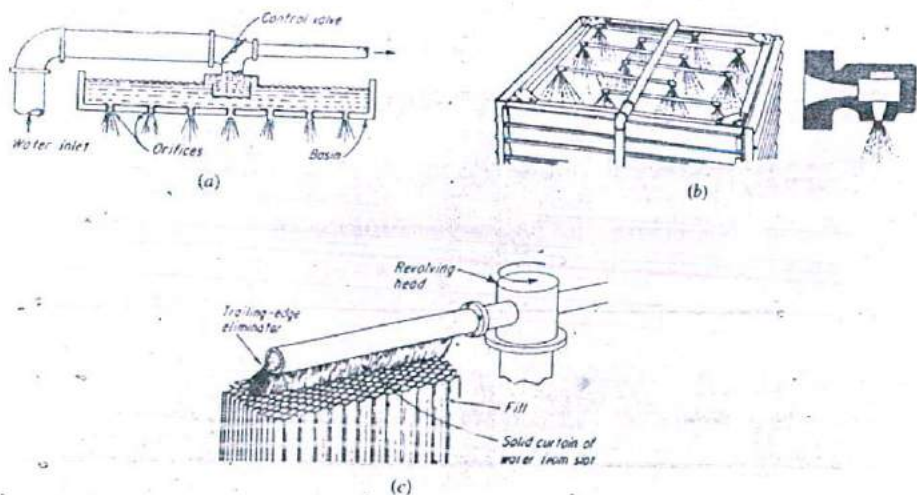


Figure 7-11 Water-distribution systems: (a) gravity, (b) spray, (c) rotary [51].

## The Fill

The *fill*, or *packing*, is the heart of the cooling tower. It should provide both good water-air contact for high rates of heat transfer and mass transfer and low resistance to airflow. It should also be strong, light, and deterioration-resistant. There are basically two types of fill: (1) *splash type* and (2) *film*, or *nonsplash*, type.

*Splash packing* is made of bars stacked in decks (Fig. 7-12*a*) that break the water into drops as it falls from deck to deck. The bars come in different shapes [52]—narrow, square, or grid—are smooth or rough, and are made of different materials—redwood, high-impact polystyrene, or polyethylene. Splash fill provides excellent heat and mass transfer between water and air.

*Film fill* is usually made of vertical sheets that have a rough absorbent surface that wets well and allows the water to fall as film that adheres to the vertical surfaces (Fig. 7-12*b*). This exposes the maximum water surface to the air without breaking it into drops or small rivulets. Film fill also comes in different shapes and materials: redwood battens, cellulose corrugated sheets, asbestos-cement sheets, and waveform

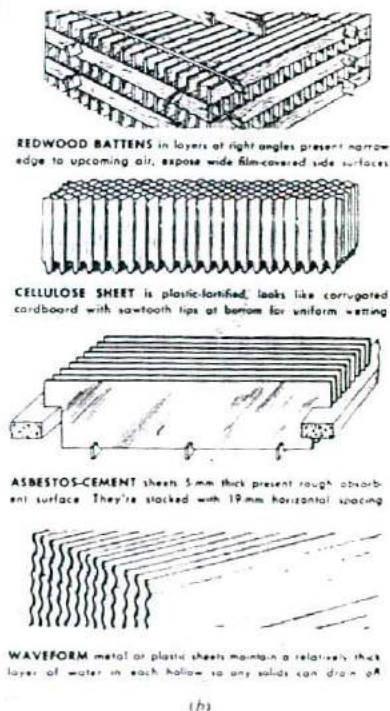
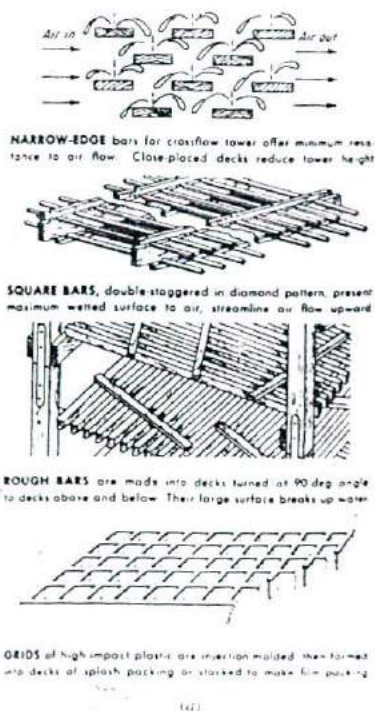


Figure 7-12 Types of fill: (a) splash (b) film [52]

metal or plastic. Film fill presents less resistance to airflow and requires less total height than splash fill.

The present trend in materials for wet-cooling towers favors concrete structures with plastic fill, drift eliminators (below), fan stacks, fan blades, and manifolds, valves, and nozzles. The concrete-plastic combination results in longer life and less maintenance.

### Drift and Drift Eliminators

*Drift* is water entrained by and carried with the air as unevaporated drizzle or fine droplets. This water is thus lost to the circulating-water system and does not contribute to heat removal by evaporation. (The problem is somewhat similar to the carryover of droplets by the steam in a boiler drum.) Drift is minimized by *drift eliminators* (Fig. 7-13), which are baffles that come in one, two, or three rows. The baffles force the air to make a sudden change in direction. The momentum of the heavier drops separates them from the air and impinges them against the baffles, thus forming a thin film of liquid that falls back into the tower. The baffles are made of wood, metal, or plastic. 100 percent drift elimination is not possible, but a well-designed system results in water loss less than 0.2 percent of the circulating water. This, of course, should be compensated for by the makeup system. The drift eliminators are situated at air exit from the fill, above it in counterflow towers, and to the side in cross-flow towers.

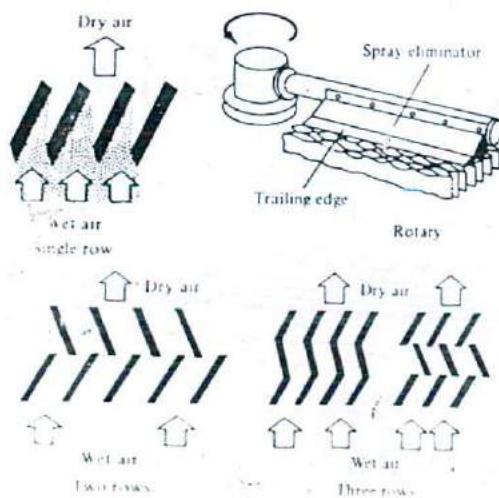


Figure 7-13 Types of drift eliminators [52]

## The Basin

The *cold-water basin*, situated beneath the tower, collects and strains the water before it is pumped back to the condenser (in the closed mode). It also receives the circulating-water makeup. It has makeup inlet and outlet, quickfill, overflow, drain, and bleedoff connections. Large utility tower basins are usually made of concrete. They are sized to permit tower operation for several hours without adding makeup. The drain is used to remove silt deposits and control water level in case of flow surges. Water leaves the basin via a sloped canal at the bottom and through screens that prevent debris from entering the pumps.

## Makeup

The total makeup required by a cooling tower is the sum of that which would compensate for evaporation, drift, and bleeding or blowdown. The latter is water intentionally discharged from the circulating-water system and replaced with fresh water. This water, in addition to makeup for evaporation and drift, keeps the concentration of salts and other impurities down. Otherwise these concentrations would continuously build up as the water continues to evaporate. As indicated earlier (Table 7-2), the evaporation loss rate is 1 to 1.5 percent of the total circulating-water flow rate. The drift loss is much less, perhaps 0.03 percent. Large quantities of drift cannot be tolerated because, in addition to the plume [55], they can cause water and ice deposition problems at and near the plant site. Bleeding accounts for an amount comparable to the evaporation loss if the solids concentrations are to be kept low but may be reduced if higher concentrations can be tolerated. Table 7-3 gives a breakdown of water makeup requirements for typical 1000-MW fossil-fired and water-reactor nuclear powerplants for different cooling ranges [53]. It shows that the total makeup is independent of range but that the percentage of total flow is not.

## Circulating-Water Quality and Blowdown Pollution

The circulating water is warm and fully aerated, contains suspended solids, is relatively high in conductivity, and is a good biological nutrient.

It is almost always corrosive, requiring a corrosion inhibitor such as chromates. To prevent scale and deposits that foul heat-transfer surfaces, it often needs scale inhibitors. Silt washed off the air by the cooling tower usually is in the form of small colloidal matter and is difficult to remove, but can be treated by a family of chemicals called *polyelectrolytes*. These keep the particles suspended in flowing water but allow them to precipitate in basins where they can be removed as mud. Microbiological growth (algae, slime, bacteria), besides fouling, contributes to corrosion by shielding metal surfaces and thus producing oxygen-concentration cells. In addition, the decomposition of the organisms produces  $H_2S$ ,  $CO_2$ , and other products, themselves corrosive. Chlorination, alternated with biocides, is used (organisms can build up tolerance to chlorine, if used alone).

Table 7-3 Typical makeup demand for 1000-MW powerplants

Range, °F	Tower water flow, gal/min	Drift, gal/min	Evap., gal/min	Bleed required to maintain concentration,* gal/min			
				2	4	6	8
Fossil-fueled plant							
15	600,000	180	6750	6,570	2070	1170	784
25	360,000	108	6750	6,642	3142	1242	856
35	257,153	77.2	6750	6,673	2173	1273	887
45	200,000	60	6750	6,690	2190	1290	904
Total makeup required, gal/min				13,500	9100	8100	7714
Nuclear-fueled plant							
15	900,000	270	10,125	9,855	3,105	1,755	1,176
25	540,000	162	10,125	9,963	3,213	1,863	1,284
35	385,715	115.7	10,125	10,009	3,259	1,909	1,331
45	300,000	90	10,125	10,035	4,285	1,935	1,356
Total makeup required, gal/min				20,250	13,500	12,450	11,571

\* Concentration =  $(\text{evap.} + \text{drift} + \text{bleed}) / (\text{drift} + \text{bleed})$ .

Note: Based on heat-rejection rates of 4500 and 6750 Btu/kWh, respectively. Data based on (1) evaporation 0.075 percent of recirculated gal/min per °F range and (2) 0.03 percent drift loss. Data from Ref. 53.

Because of all the above additives, cooling-tower bleed or blowdown can be an unacceptable source of pollution to the natural body of water. (Boiler blowdown is another source of pollution. It is mainly thermal but also contains small quantities of phosphates and organics.) Bleed may contain chemicals and various minerals contained in or added to the circulating water, including chromate inhibitors, various phosphates, organic and inorganic compounds, combined with some heavy metals.

Bleed, therefore, has to be handled with care. Depending upon the size of plant and the extent of contaminants, it may be discharged to the body of water, treated before being returned, or allowed to mix with other plant wastes, such as boiler blowdown, etc., and treated all in one installation.

An example of treatment is the removal of chromates by reducing them from hexavalent form to trivalent chrome with  $\text{FeSO}_4$ , then precipitated as  $\text{Cr}(\text{OH})_3$  by elevating the pH with lime (or an alkaline stream from somewhere else in the plant). The resulting sludge can be disposed of in various ways or reused. Another alternative is to use nonpolluting inhibitors, but these are, at least for now, of questionable ability and economics [56].

### A Hybrid Wet Tower

Natural-draft cooling towers are huge in material, height, and land requirements but consume little power for operation. Mechanical-draft cooling towers are smaller and

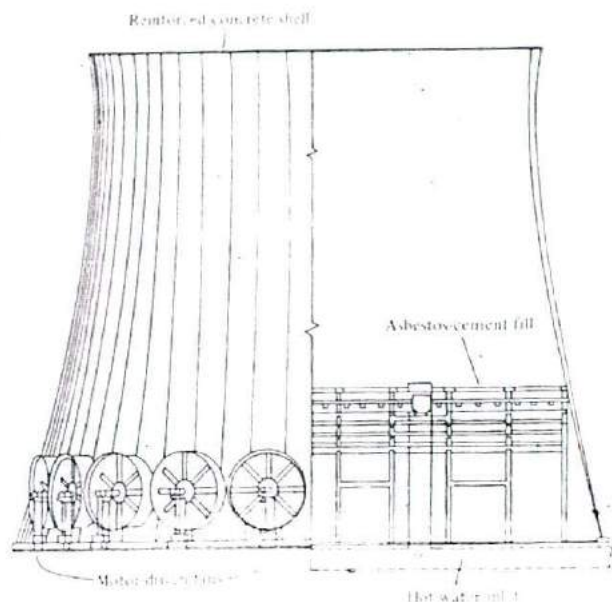


Figure 7-14 A hybrid or fan-assisted hyperbolic tower [51]

cheaper but consume power and suffer from air recirculation. As often happens, someone has come up with a compromise. This is the *hybrid or fan-assisted hyperbolic tower*, which combines the best features of natural- and mechanical-draft towers.

The hybrid tower (Fig. 7-14) has a reinforced concrete hyperbolic shell, similar but smaller than that of the natural-draft tower. In addition, it has a number of large electrically-driven forced-draft fans situated around the periphery of the base. The hybrid tower will have roughly two-thirds the base diameter (45 percent of the land area) and half the height of a natural-draft tower designed for the same performance, and hence will have less of a visual impact on the landscape. The fans will give better airflow control than natural-draft and will consume less power than mechanical draft. The high velocity and height of the exit air will eliminate the hot-air recirculation problems associated with mechanical-draft towers. Hybrid towers can also be operated during the cold part of the year without fans as natural-draft units. Construction costs will be intermediate between natural- and mechanical-draft towers.

## 7-5 WET-COOLING TOWER CALCULATIONS

Wet-cooling tower calculations involve energy and mass balances. The energy balances here will be based on the first-law steady-state steady-flow (SSSF) equation. There are, however, three fluids entering and leaving the system: the cooling water, the dry

air, and the water vapor associated with it. The mass balance should also take into account these three fluids.

Because air humidity is an important factor in wet-tower calculations, a short review of tower and psychrometric terminology is appropriate at this time.

**Approach** This is the difference between the cold-water temperature and the wet-bulb temperature of the outside air.

**Range (or cooling range)** The range is the difference between the hot-water temperature and the cold-water temperature.

**Saturated air** This is air that can accept no more water vapor at its given temperature. A drop in that temperature would result in condensation and the new cooler air would also be saturated. An increase in that temperature would make it unsaturated so that it could accept more water vapor. The partial pressure of water vapor in saturated air equals the saturation pressure  $P_{sat}$  (obtained from the steam tables) at the air temperature. For example, saturated air at 60°F and 14.696 psia, would have

$$\text{Partial pressure of water vapor } P_{v_{sat}} = 0.256 \text{ psia}$$

$$\text{Partial pressure of dry air } P_d = 14.440 \text{ psia}$$

$$\text{Total pressure } P = 14.696 \text{ psia}$$

Recall from thermodynamics of gas mixtures that the partial pressure ratios, the volume ratios, and the mole fractions of constituents are all equal. Water vapor in air is at such low pressure (its partial pressure) that it is treated as a gas with little error.

**Relative humidity** This is equal to the partial pressure of water vapor in air  $P_v$ , divided by the partial pressure of water vapor that would saturate the air at its temperature  $P_{sat}$ . Relative humidity is given the symbol  $\phi$ .

$$\phi = \frac{P_v}{P_{sat}} \quad (7-3)$$

Thus, for air at 60°F, 14.696 psia, and 50 percent relative humidity

$$P_v = \phi P_{sat} = 0.5 \times 0.256 = 0.128 \text{ psia}$$

$$P_d = P - P_v = 14.696 - 0.128 = 14.568 \text{ psia}$$

$$P = 14.696 \text{ psia}$$

and  $\phi = 100$  percent refers to saturated air.

**Absolute humidity (also called humidity ratio)** This is the air per unit mass of dry air (da). Absolute humidity is given the symbol  $\omega$ . Using  $PV = mRT$  for both water vapor and dry air



$$\omega = \frac{m_v}{m_d} = \frac{53.3P_v}{85.7P_d} = \frac{0.622P_v}{P - P_v} \quad (7-4)$$

where 53.3 and 85.7 are the gas constants for dry air and water, respectively. The absolute humidity of saturated air is then given by

$$\omega_{\text{sat}} = \frac{0.622P_{\text{sat}}}{P - P_{\text{sat}}} \quad (7-5)$$

In the above example, air at 60°F, 14.696 psia, and 50 percent  $\phi$  would have  $\omega = 0.005465$  lb<sub>m</sub> water vapor/lb<sub>m</sub> da and  $\omega_{\text{sat}} = 0.01103$ .

Because saturation pressure increases rapidly with temperature (as all vapor pressures do), it can be deduced that warm air can hold much more moisture than cool air.

**Dry-bulb temperature** This is the temperature of the air as commonly measured and used. In psychrometric work, it is called dry-bulb to distinguish it from the wet-bulb temperature (below). It is the temperature as measured by a thermometer with a dry mercury bulb, a thermocouple, etc., and is given the symbol  $T$  or  $T_{\text{db}}$ .

**Wet-bulb temperature** This is the temperature of the air as measured by a psychrometer, in effect a thermometer with a wet gauze on its bulb, hence the name. Air is made to flow past the gauze. If the air is relatively dry, water would evaporate from the gauze at a rapid rate, cooling the bulb and resulting in a much lower reading than if the bulb were dry. If the air is humid, the evaporation rate is slow and the wet-bulb temperature approaches the dry-bulb temperature. If the air is saturated, i.e.,  $\phi = 100$  percent, the wet-bulb temperature equals the dry-bulb temperature. Thus, for a given  $T$ , the wet-bulb temperature is lower the drier the air. The wet-bulb temperature is given the symbol  $T_{\text{wb}}$ .

**Dew point** The temperature below which water vapor in a given sample of air begins to condense is called the dew point. It is equal to the saturation temperature corresponding to the partial pressure of the water vapor in the sample. Thus for the above air at 60°F and  $\phi = 50$  percent, the dew point equals the saturation temperature at 0.128 psia, which is 41.3°F. For saturated air  $T$ ,  $T_{\text{wb}}$ , and the dew point are all equal.

**Psychrometric chart** This is a chart that relates  $\phi$ ,  $\omega$ ,  $T_{\text{wb}}$ , and  $T$  but which may also contain additional information such as enthalpy and specific volume (App. M). Psychrometric charts are calculated for 1 standard atmosphere pressure and are based on a unit mass of dry air plus associated water vapor, that is, on  $1 + \omega$ . Thus all data in App. M are for a fixed 1.0 lb<sub>m</sub> of dry air (da) plus a variable  $\omega$  lb<sub>m</sub> water vapor/lb<sub>m</sub> da. Check the above examples on the chart.

**Energy balance** The first-law SSSF equation with three fluids will now be written for the tower fill as a system (Fig. 7-15). It applies to all types of wet towers. Changes

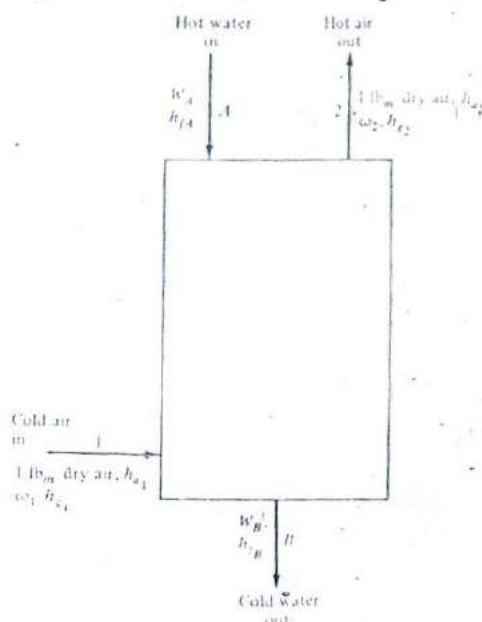


Figure 7-15 The tower fill as a steady-state steady-flow system.

in potential and kinetic energies and heat transfer are all negligible. No mechanical work is done. Thus only enthalpies of the three fluids appear. Following psychrometric practice, the equation is written for a unit mass of dry air

$$h_{a1} + \omega_1 h_{v1} + W_A h_{wA} = h_{a2} + \omega_2 h_{v2} + W_B h_{wB} \quad (7-6)$$

where

$h_a$  = enthalpy of dry air, Btu/lb<sub>m</sub> or J/kg

$\omega$  = mass of water vapor per unit mass of dry air  
= absolute humidity, dimensionless

$h_v$  = enthalpy of water vapor, Btu/lb<sub>m</sub> or J/kg

$W$  = mass of circulating water per unit mass of dry air, dimensionless

$h_w$  = enthalpy of circulating water, Btu/lb<sub>m</sub> or J/kg

The subscripts 1 and 2 refer to air inlet and exit, and the subscripts A and B refer to circulating-water inlet and exit, respectively.

Because of the low pressures and temperatures commonly encountered in towers, the above equation can be simplified with little error by the following approximations.

$$h_{a2} - h_{a1} = c_p (T_2 - T_1) \quad c_p = 0.24 \text{ Btu/(lb}_m \cdot ^\circ\text{F)}$$

$$h_i = h_e \text{ from the steam tables}$$

$$h_w = h_f \text{ from the steam tables}$$

The air leaving the system at 2 is often saturated.

**Mass balance** The dry air goes through the tower unchanged. The circulating water loses mass by evaporation. The water vapor in the air gains mass due to the evaporated water. Thus, based on a unit mass of dry air

$$\omega_2 - \omega_1 = W_A - W_B \quad (7-7)$$

Equation (7-6) can now be written in the form

$$\omega_1 h_{e1} + W_A h_{f,A} = c_p (T_2 - T_1) + \omega_2 h_{e2} + [W_A - (\omega_2 - \omega_1)] h_{f,B} \quad (7-8)$$

At pressures  $P$  other than 1 standard atmosphere, where the psychrometric chart would not apply, and when  $T$  and  $T_{wb}$  are known, the value of  $P_{v,wb}$  and hence  $\omega_1$  from Eq. (7-4) is obtained from the empirical Carrier equation.

$$P_{v,wb} \text{ (psia)} = P_{v,wb} - \frac{(P - P_{v,wb})(T - T_{wb})}{2800 - 1.3T_{wb}} \quad (7-9)$$

where  $P_{v,wb}$  is the vapor pressure corresponding to  $T_{wb}$ , psia, and  $T$  and  $T_{wb}$  are in  $^{\circ}\text{F}$ .

**Air densities** We will now evaluate  $\rho_o$  and  $\rho_i$  in Eq. (7-2), repeated below.

$$\Delta P_d = (\rho_o - \rho_i) H \frac{g}{g_c} \quad (7-2)$$

The driving pressure  $\Delta P_d$ , which should equal the air-pressure losses in the tower, is used to calculate  $H$  in natural-draft cooling towers. Here  $\rho_o$  is the outside air density and  $\rho_i$  the inside air density at the air exit of the fill, and  $H$  the height of the tower above the fill. The density of any gas mixture is equal to the sum of the densities of its constituents as they all occupy the same volume. Thus, using  $\rho = m/V = P/RT$ ,

$$\rho_o = \frac{P - P_{v1}}{R_a T_1} + \frac{P_{v1}}{R_v T_1} \quad (7-10)$$

and

$$\rho_i = \frac{P - P_{v2}}{R_a T_2} + \frac{P_{v2}}{R_v T_2} \quad (7-11)$$

where the subscripts 1 and 2 again refer to air inlet and outlet,  $R_a$  and  $R_v$  are the gas constants of dry air and water, respectively, and the temperatures are in degrees absolute.

The densities can also be obtained from the specific volume  $v$  lines of the psychrometric chart if  $P = 1$  standard atmosphere. Note, however that these are given in  $\text{ft}^3/\text{lb}_m \text{ da}$ , so the densities of the moist-air mixture would be  $1 + \omega$  divided by  $v$  as given in the chart. Note also that the  $v$  lines are rather widely spaced, which leads to less accurate evaluations. Small inaccuracies in  $\rho_o$  and  $\rho_i$  could lead to large errors in the difference between them.

**Example 7-1** A natural-draft cooling tower with a range of  $20^\circ\text{F}$  receives 360,000 gal/min of  $90^\circ\text{F}$  circulating water. The outside air is at  $60^\circ\text{F}$ , 14.696 psia, and 50 percent relative humidity. The exit air is at  $80^\circ\text{F}$  saturated. Calculate (1) the amount of makeup water to compensate for evaporation, (2) the outside air required in  $\text{ft}^3/\text{min}$ , and (3) the height of the cooling tower if the total pressure losses are 0.0105 psi.

**SOLUTION** Referring to Fig. 7-15,

$$\omega_1 = 0.005465 \text{ (calculated earlier)}$$

$$\omega_2 = \frac{0.622 \times 0.50683}{14.696 - 0.50683} = 0.022217$$

$$h_{e1} = 1087.7 \text{ Btu/lb}_m \quad h_{e2} = 1096.4 \text{ Btu/lb}_m$$

$$T_A = 90^\circ\text{F} \quad T_R = 90 - 20 = 70^\circ\text{F} \quad v_{r,A} = 0.016050 \text{ ft}^3/\text{lb}_m$$

$$\dot{W}_A = \text{mass flow rate of water entering tower} = \frac{360,000 \times 0.1337}{0.01605}$$

$$= 3 \times 10^6 \text{ lb}_m/\text{min}$$

$$h_{f,A} = 58.018 \text{ Btu/lb}_m \quad h_{f,B} = 38.052 \text{ Btu/lb}_m$$

Referring to Eq. (7-8)

$$0.005465 \times 1087.7 + \dot{W}_A \times 58.018 = 0.24(80 - 60) + 0.022217 \\ \times 1096.4 + [\dot{W}_A - (0.022217 - 0.005465)] \times 38.052$$

Therefore

$$\dot{W}_A = 1.1308 \text{ lb}_m \text{ water/lb}_m \text{ da}$$

$$\text{Dry air required} = \frac{\dot{W}_A}{\dot{W}_A} = \frac{3 \times 10^6}{1.308} = 2.653 \times 10^6 \text{ lb}_m/\text{min}$$

$$\text{Makeup due to evaporation} = 2.653 \times 10^6 (\omega_2 - \omega_1)$$

$$= 0.0444 \times 10^6 \text{ lb}_m/\text{min}$$

$$= \frac{0.0444 \times 10^6 \times 0.01605}{0.1337} = 5335 \text{ gal/min}$$

Referring to Eqs. (7-10) and (7-11)

$$\begin{aligned}\rho_o &= \frac{(14.696 - 0.128) \times 144}{53.34(60 + 460)} + \frac{0.128 \times 144}{85.76(60 + 460)} \\ &= 0.07563 + 0.00041 \\ &= 0.07604 \text{ lb}_m \text{ ft}^{-3}\end{aligned}$$

$$\begin{aligned}\rho_i &= \frac{(14.696 - 0.50683) \times 144}{53.34(80 + 460)} + \frac{0.50683 \times 144}{85.76(80 + 460)} \\ &= 0.07094 + 0.00158 \\ &= 0.07251 \text{ lb}_m \text{ ft}^{-3}\end{aligned}$$

$$\begin{aligned}\text{Total outside air required} &= 2.653 \times 10^6 (1 + \omega_1) \\ &= 2.653 \times 10^6 (1 + 0.005465) \\ &= 2.667 \times 10^6 \text{ lb}_m \text{ /min}\end{aligned}$$

$$\begin{aligned}\text{Actual volume flow rate of outside air} &= \frac{2.667 \times 10^6}{0.07604} \\ &= 35.072 \times 10^6 \text{ ft}^3 \text{ /min}\end{aligned}$$

Referring to Eq. (7-2)

$$\begin{aligned}\text{Height of tower above fill} &= \frac{\Delta P_d}{(\rho_o - \rho_i)g/g} \\ &= \frac{0.0105 \times 144}{0.07604 - 0.07251} \\ &= 428.33 \text{ ft}\end{aligned}$$

## 7-6 DRY-COOLING TOWERS

A *dry-cooling tower* is one in which the circulating water is passed through finned tubes over which the cooling air is passed. All the heat rejected from the circulating water is thus in the form of sensible heat to the cooling air. A dry-cooling tower can be either mechanical-draft or natural-draft.

Dry-cooling towers have attracted much attention in recent years. They permit plant siting without regard for large supplies of cooling water. Typical sites are at or near sources of abundant fuel, which cuts down fuel transportation costs; at or near the utility load-distribution center, which cuts down transmission costs; and at existing plants that need to be expanded but do not have sufficient water for the addition. Other advantages of dry-cooling towers are that they are less expensive to maintain than wet

towers and do not require large amounts of chemical additives and periodic cleaning as do wet towers. Their main disadvantage is that they are not as efficient as evaporative cooling, and the result is higher turbine back pressure, lower plant cycle efficiency, and increased heat rejection. (The situation worsens at high atmospheric air temperatures.) Small dry-cooling towers have seen extensive service in such installations as industrial-process cooling, air conditioning, and atmospheric-air-cooled heat exchangers. Large utility dry-cooling towers have seen more usage in Europe where they have been developed, with a number of installations in successful operation. The recent attraction in the United States is certain to grow as powerplants get bigger and available water supplies dwindle so that even the makeup water needed by a wet tower will be burdensome, not to speak of once-through cooling.

Another important plus for dry-cooling towers is the increasingly restrictive environmental legislation on thermal pollution of once-through systems, blowdown pollution, and fogging and icing of wet towers, which are a real menace in certain localities.

Because of the above-mentioned advantages, dry-cooling towers are intended to operate only in the closed mode. There are two basic dry-cooling tower types: *direct* and *indirect*.

### Direct Dry-Cooling Towers

This system combines the condenser with the tower (Fig. 7-16). Turbine exhaust steam is admitted to a steam header through large ducts to minimize pressure drop and is condensed as it flows downward through a large number of finned tubes or coils in

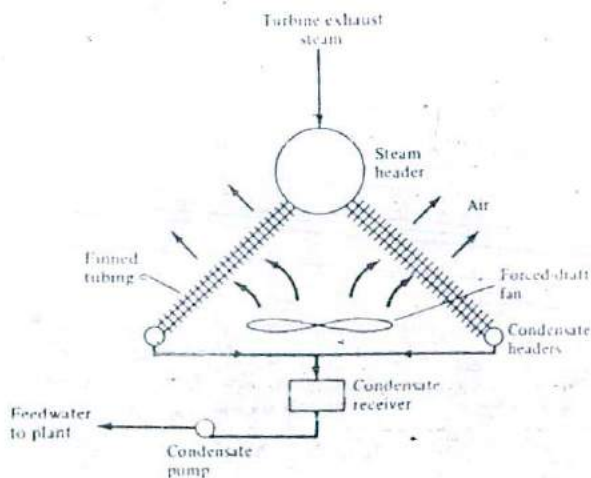


Figure 7-16 Schematic cross section of a direct dry-cooling tower.

parallel (only two are shown). The latter are cooled by atmospheric air flowing in a natural-draft cooling-tower setup or, as shown, by a forced-draft fan. As with surface condensers (Sec. 6-3), there is a system for removing noncondensables and air. There also is a system for the prevention of freezing in cold weather (below). The condensate flows by gravity to condensate receivers and is pumped back to the plant feedwater system by the condensate pump.

Direct systems operate at the disadvantage of high vacuum in the cooling-coils and the need for large steam ducts. They are limited to small-size powerplants. The largest direct installation in the United States is the 330-MW minemouth Wyodak powerplant near Gillette, Wyoming, built by Pacific Power and Light Co. and the Black Hills Power and Light Co. Turbine exhaust steam is admitted to the coils via two 13-ft diameter ducts.

### Indirect Dry-Cooling Towers

These are of three general designs. The first uses a conventional surface condenser (Fig. 7-17). The circulating water leaving it goes through finned tubing cooled by atmospheric air in the tower. The latter could be natural-draft or, as is shown, induced-draft. In this design there are two heat exchangers in series and two temperature drops, one between steam and water and one between water and air. This double irreversibility imposes a severe penalty on turbine back pressure, thus necessitating operating at condenser pressures of about 2.5 to 4.0 psia (0.17 to 0.27 bar) compared with 0.5 to

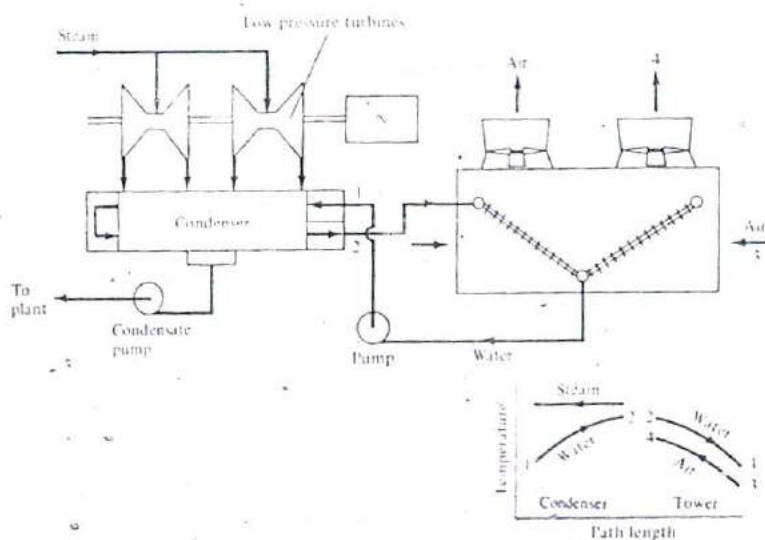


Figure 7-17 Schematic of an indirect-dry cooling tower with a conventional surface condenser.

1.0 psia (0.034 to 0.069 bar) for once-through systems. The results are loss in cycle efficiency and increased heat rejection.

The second design of indirect dry-cooling towers eliminates the intermediate water loop and uses an open- or direct-contact condenser (also called a jet or spray condenser, Sec. 6-2). As operation (of all dry-cooling towers) is in the closed mode and no atmospheric or surface water impurities enter the system through makeup, the circulating water can be mixed with the steam from the plant, hence the open-type condenser. The turbine exhaust steam enters the open condenser where the cold circulating water is sprayed into the steam for intimate mixing (Fig. 7-18). The condensate falls to the bottom of the condenser, from which most of it is pumped by a recirculation pump under positive pressure to finned tubing or coils in the tower. This part, cooled, returns to the condenser sprays. The balance of the condensate, equal to the steam mass flow, is pumped to the plant feedwater system by the condensate pump. Again the tower may be natural-draft or forced-draft. The ratio of circulation to feedwater is large (Sec. 6-2). Alternately only one pump may be used on the condensate from the condenser and flows adjusted by proper valving. Condensate polishers (Sec. 6-8) may be used to maintain the circulation water at condensate quality. Another optional component is a water-recovery turbine, between tower exit and condenser inlet, that is connected to the drive shaft of the circulating-water pump to recover some of the work of that pump. This indirect system is expected to be more efficient, more economical, and more feasible for large plants.

The third indirect dry-cooling tower design uses a circulating vaporizing coolant

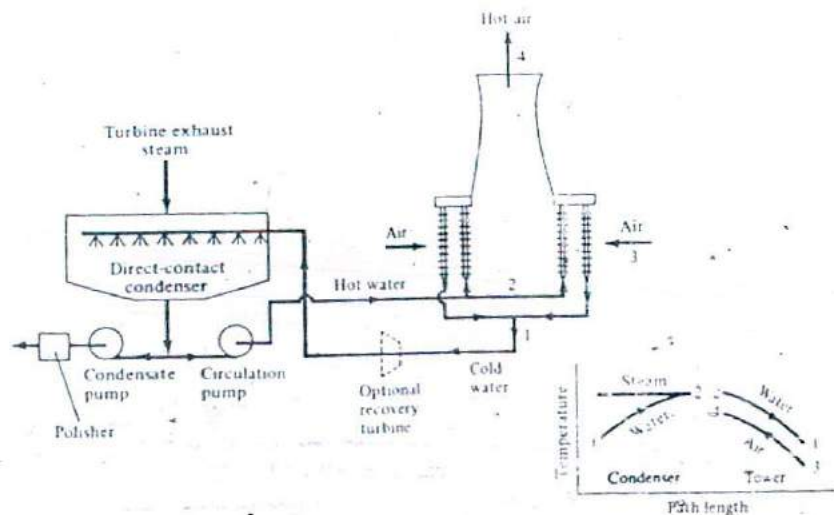


Figure 7-18 Schematic of an indirect dry-cooling tower with an open-type condenser.



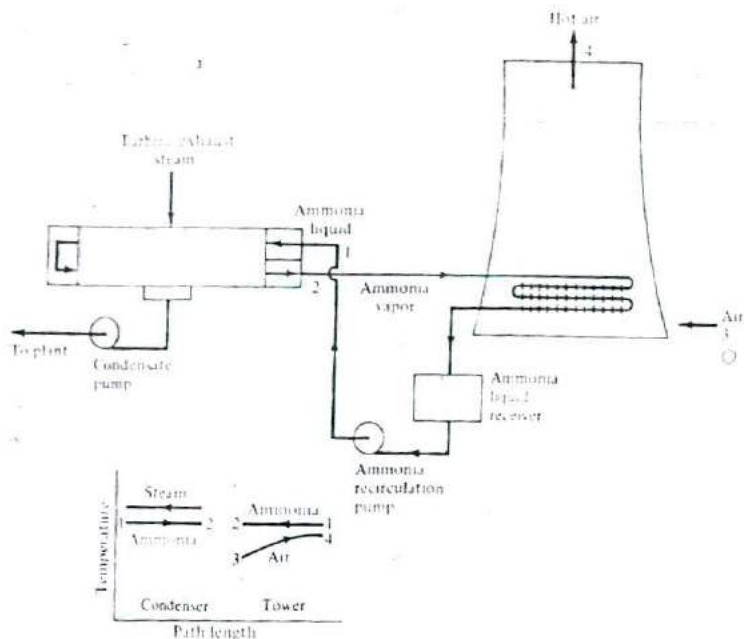


Figure 7-19 Schematic of an indirect dry-cooling tower with a surface condenser and a two-phase recirculating coolant (ammonia).

instead of water. The one that has been developed uses ammonia as the heat-transfer medium between the steam and air (Fig. 7-19). The use of ammonia enables phase-change heat-transfer boiling in the condenser tubes and condensation in the tower tubes. Nearly saturated liquid ammonia enters the surface condenser and is vaporized to saturated vapor. The vapor flows to the lower finned coils and is condensed to saturated liquid. The latter is pumped back to the condenser. The boiling and condensation modes have much higher heat-transfer coefficients, on the tube side, than forced convection of a single-phase fluid (as water in Fig. 7-17). This results in (1) a lower temperature difference between steam and ammonia, and between ammonia and air, and (2) reduced size and power requirements of the equipment. An optional addition is a compressor on the ammonia vapor to raise its temperature sufficiently above that of the air during particularly hot days, which would result in enhanced heat transfer in the tower. This makes the system resemble that of a vapor-compression refrigeration system. The work of the compressor can be partly recovered by the placement of an expander (turbine) in the liquid line.

A 6-MW demonstration plant using an ammonia system is undergoing tests near Bakersfield, California. The plant is part of the 150-MW Kern powerplant of the

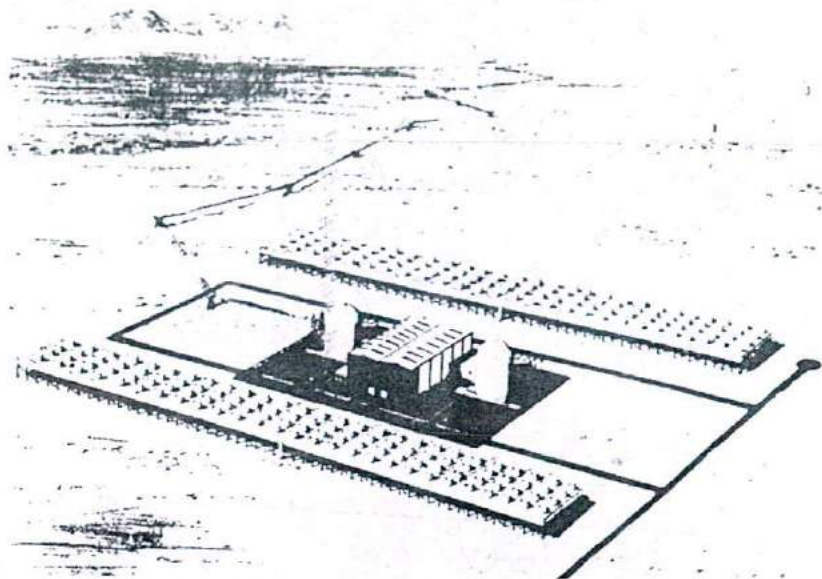


Figure 7-20 An artist's conception of a dry-cooling-tower system serving a twin-reactor nuclear powerplant in an arid area. (Courtesy the Marley Cooling Tower Company, Mission, Kansas.)

Pacific Gas and Electric Co. The tests are sponsored by the Electric Power Research Institute, the Department of Energy, and a consortium of utilities [57].

Thermodynamic data of ammonia may be found in App. C.

Because of their lower heat-transfer capabilities, dry-cooling towers in general are larger and require more land area than wet towers. Figure 7-20 is an artist's conception of the dry-cooling tower system needed for a twin-reactor nuclear powerplant.

### 7-7 DRY-COOLING TOWERS AND PLANT EFFICIENCY AND ECONOMICS

A parameter of importance to dry cooling towers is the *initial temperature difference* (ITD), given by

$$\text{ITD} = \text{temperature of hot water or other fluid entering the tower} - \text{temperature of outside cooling air}$$

The temperature of the outside air here is the dry-bulb temperature. Wet-bulb temperatures do not apply to dry-cooling towers. The most economical ITD range is 50 to 60°F (10 to 16°C).

The heat dissipated by a dry-cooling tower is proportional to the product of the size of cooling surface in the tower and the ITD, other things being equal. Thus for a given tower, an increase in load causes an increase in ITD, and hence an increase in the temperature of the circulating water entering the condenser and the back pressure on the turbine. For example, if the outside air is at 74°F, ITD = 60°F, the tower inlet circulating water temperature is 134°F. With a 6°F condenser terminal temperature difference, the steam condensing temperature would be 140°F, corresponding to 2.89 psia (0.2 bar).

If the plant heat rejection increases by 10 percent, ITD becomes 66°F and the condensing temperature and pressure would climb to 146°F and 3.37 psia (0.23 bar).

On the other hand, if the heat rejection and ITD remain the same, but the outside air temperature increases from 74°F to 90°F, the condensing temperature and pressure would be 156°F and 4.31 psia (0.3 bar).

This dependency of tower performance on load and outside temperature is much more pronounced for dry towers than for wet ones because the latter depend upon evaporation for much of their heat-rejection mechanism. For a wet tower operating with the same air at 90°F dry-bulb, and 76°F wet-bulb, and with 18°F approach, 24°F range, and 6°F TTD, the corresponding values would be 124°F and 1.890 psia (0.13 bar).

In many parts of the United States, 90°F air is exceeded during a good part of the summer and condensing temperatures of dry-cooling towers would range from 150°F to 160°F, corresponding to 4.31 and 4.74 psia (0.3 to 0.33 bar). During extremely hot weather condensing pressures may reach 6 or 7 psia (0.4 to 0.48 bar).

These turbine back pressures, which compare with 0.5 to 1.0 psia for once-through cooling systems, result in the loss of turbine work and cycle efficiency and an increase in heat rejection, thus necessitating a bigger tower yet. So, although dry-cooling towers save water, thermal pollution, fogging, etc., they are not as effective as wet towers, a natural consequence of heat transfer to air being lower than evaporative heat transfer. Figure 7-21 shows the operating turbine back pressures when the ambient temperature is changed from a base of 100°F. For example, if the tower is designed to yield a turbine back pressure of 6 inHg absolute (2.95 psia, 0.2 bar) at 100°F, an ambient temperature of 60°F would reduce the turbine back pressure to 2 inHg abs (1 psia, 0.068 bar).

The turbine work losses for the 90°F air example above would be around 6.5 percent, compared with 0.4 percent for a wet tower at the same conditions. Recall (Chap. 2) that a small change in pressure at the low-pressure end of turbine expansion results in a much larger change in work than a corresponding change at the high-pressure end.

The effect of using dry-cooling towers on electricity unit production costs versus using once-through and wet-cooling towers is given in Table 7-4 for three nuclear plants under construction (1, 2, and 3) and a hypothetical nuclear plant (4) in various parts of the United States. The study, conducted by R. W. Beck and Associates, was based on 1975 completion date prices and the figures should now be used only in a relative sense. Unit power costs are in mill/kWh (1 mill = 1/1000 of a U.S. dollar = 0.1¢). They are the sum of fixed charges on the capital costs, the fuel cycle

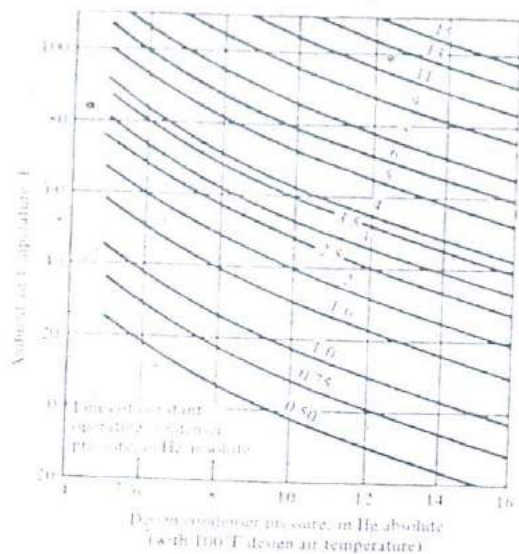


Figure 7-21 Effect of change in ambient air temperature on condenser pressure for various design pressures at 100°F air temperature [51].

Table 7-4 Increase in busbar cost as a result of using dry-cooling rather than wet-cooling towers, mill kWh\*

Plant cooling system <sup>†</sup>	Fixed charges								
	12%			15%			18%		
	Fuel costs, $\epsilon 10^6$ Btu								
	15	18	21	15	18	21	15	18	21
Mechanical-draft-dry-cooling system									
1	0.99	1.02	1.05	1.18	1.21	1.24	1.36	1.39	1.42
2	0.81	0.82	0.83	0.94	0.95	0.97	1.07	1.09	1.10
3	0.71	0.73	0.74	0.85	0.87	0.87	0.98	0.99	1.01
4	0.72	0.73	0.74	0.86	0.87	0.89	0.99	1.01	1.03
Natural-draft dry-cooling system									
1	1.04	1.07	1.10	1.25	1.27	1.30	1.44	1.47	1.50
2	0.88	0.89	0.89	1.03	1.30	1.05	1.17	1.18	1.19
3	0.81	0.82	0.82	0.96	0.97	0.98	1.11	1.11	1.13
4	0.76	0.77	0.72	0.91	0.91	0.92	1.05	1.06	1.07

\* Data taken from Ref. 51.

- † 1 = Once-through, northeastern plant, 906.6 MW  
 2 = Mechanical-draft wet tower, southeastern, 860.6 MW  
 3 = Natural-draft wet tower, western, 928.5 MW  
 4 = Mechanical-draft wet tower, eastern, 860.6 MW

costs, and operation and maintenance costs and hence depend on the initial plant costs and plant efficiency.

The above dry-cooling tower "effects" must be coped with. Large turbines capable of operating at high back pressures need to be used and optimized with dry cooling. Units capable of back pressures up to 15 inHg abs (7.4 psia, 0.5 bar) can be obtained by strengthening or eliminating the last row of blades of existing turbines or by designing a new line of turbines.

The loss of effectiveness during periods of excessively high ambient temperatures and/or high electric demand can be countered by the use of water. Several schemes are considered:

1. The deluge or spraying with water of the outside tube surfaces. (The tower may be designed to have the tubes surrounded by a wet-tower-type fill for that purpose.)
2. Cooling the inlet air by presaturation (by water evaporation) or by sensible-heat removal [58].
3. Using an additional standby wet-cooling tower.
4. Using an additional standby circulating-water system, a scheme considered with ammonia towers (above).
5. Using wet-dry cooling towers (below).

## 7-8 WET-DRY-COOLING TOWERS

We have seen that wet-cooling towers consume some water by evaporation, drift, and bleed and that they suffer from plume problems. We have also seen that dry-cooling towers impose a penalty on powerplant operation, especially during periods of hot weather. As often happens in such cases, a compromise wet-dry cooling tower has been developed that reduces these disadvantages.

As the name implies, a *wet-dry-cooling tower* operates by a combination of wet and dry cooling. It has two air paths in parallel and two water paths in series. Figure 7-22 shows a mechanical- (induced-) draft wet-dry cooling tower. The top part of the tower, below the fan, is the dry section that contains finned tubing. The lower, wider part is the wet section that contains the fill. The hot circulating water is admitted through a header at midsection. It first flows up and down through the dry section finned tubing. It then leaves the dry section and gravitates through the fill of the wet section towards the cold-water basin.

Ambient air is drawn in two streams through the dry and wet sections. The two streams converge and mix inside the tower before leaving it. Because the first stream is dry heated and comes out even drier (lower relative humidity) than ambient air, whereas the second stream normally is saturated, the mixture leaving the tower is subsaturated (Fig. 7-23).

There are, therefore, two primary advantages of the wet-dry-cooling tower: (1) The subsaturated exit air provides a less visible plume than a completely wet tower and, in favorable weather conditions, completely eliminates it. (2) Because the water is precooled in the dry section, evaporative losses and hence makeup are substantially reduced.

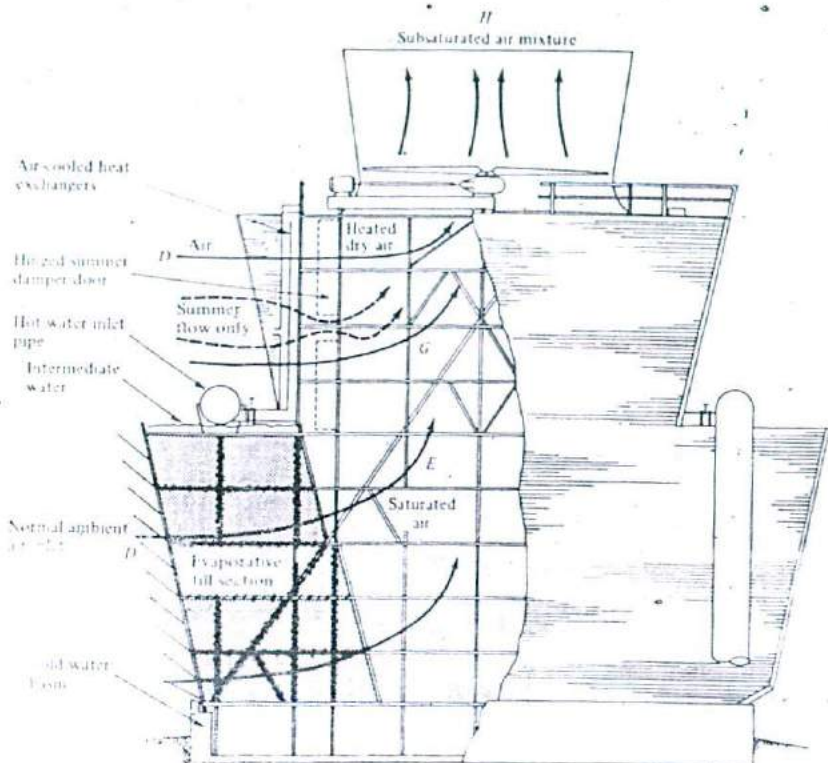


Figure 7-22 A wet-dry cooling tower with an induced-draft fan [51].

The ratio of heat removed in the dry and wet sections is adjusted both by design and operation. For example, if water consumption is the main problem, the tower is built with a larger dry section than wet section. In addition, evaporation can be varied by a control device that would regulate airflow through the wet section. In cold winter weather, the tower can operate nearly dry by blocking the air through the wet section. On the other hand, a doorlike damper, located in the heated air stream between dry heat exchanger and fan, reduces airflow through the dry section, thus allowing airflow to increase in the wet section. This damper is used in hot weather where the dry section (like a completely dry-cooling tower) would pose a penalty on powerplant performance. The damper is not intended to be completely closed, however, because of the necessity for plume control.

Wet-dry cooling towers are seeing increasing service in those in-between cases of moderate water availability and the need for good though not complete plume reduction.

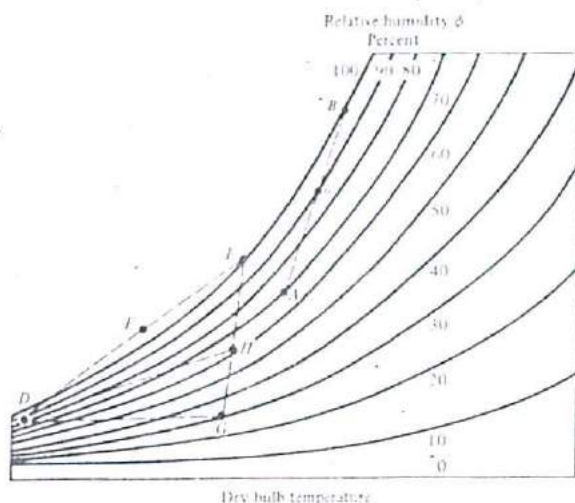


Figure 7-23 Psychrometric chart representation of wet- and wet-dry cooling towers. A-B = wet-cooling tower in summer. Exit air at B mixes with outside air at A outside tower resulting in C and vanishing plume visibility. D-E wet-cooling-tower operation in winter. Exit at E mixes with outside air at D resulting in condensation ( $\phi > 100$  percent) and foggy plume at F. With dry portion of wet-dry cooling tower DG, exit air would be subsaturated at H, resulting in no visible plume.

## 7-9 COOLING-TOWER ICING

Icing is a problem in both wet and dry towers in cold weather. In wet towers, ice may form where the cold air entering the tower first comes into contact with the water. It usually forms on air-intake louvers and on fill nearest to them. If allowed to build up, it may restrict airflow and/or cause structural damage. In natural-draft wet towers this condition is controlled by increasing warm-water flow to the outer periphery near the air intake, thus melting the ice and preventing new ice formation. In mechanical-draft wet towers, where the amount of ice formed is directly proportional to airflow, icing is controlled by reducing fan speed or shutting it down completely or by using fully adjustable air-intake towers. This reduces cooling and allows the warmer water to melt the ice. In extreme cases, such as extended periods of extremely cold weather, the fan may be reversed so that both warm air and water help in melting the ice. In multicell mechanical-draft towers, fans are usually shut off alternately for 12-h periods during ice-forming periods.

In dry-cooling towers, the problem is that of freezing of condenser cooling water inside the heat-exchange tubes during times of extremely cold outside air. Water has a minimum specific volume (or maximum density) at about  $4^{\circ}\text{C}$ , or  $39^{\circ}\text{F}$ . When it freezes to ice at  $0^{\circ}\text{C}$ , its specific volume increases about 10 percent. If the expansion is unhindered, no problems arise, as for example when a crust of ice forms on the

inner surface of a tube with water flowing through it. However, if plugs of ice form or the flow is stopped by valves, the increase in volume of the ice and trapped water can cause severe stresses in the tube walls.

Normal full-load (full water-flow) operation usually poses no problems even in freezing weather. The problem arises at very low ambient temperatures, at reduced load, and/or if the tower or a section of it is shutdown and not properly drained of water.

Theoretical analyses of freezing inside tubes in the static case (water at rest), in steady flow, and in transient conditions are fairly complex and will not be attempted here. A review and analysis of the problem, as well as recommendations for preventing ice formation inside dry tower tubes or keeping it within tolerable limits, may be found in Ref. 58.

## 7-10 COOLING LAKES OR PONDS

*Cooling lakes*, also called *ponds*, are the oldest and simplest type of artificially made heat-rejection systems. Hot circulating water from the condenser is simply dumped into an artificially made lake (or a modified natural lake, regulations permitting) and left to cool. Cool water from the lake is returned to the circulating-water system. Cooling is accomplished naturally by evaporation, by thermal radiation to the sky, especially during cloudless nights, and by convection to the wind. The cooling rates, unaided by any mechanical means such as sprays (below), are slow, and very large land areas are required for such lakes. The water residence time has to be long, thus requiring a large separation distance between intake and outlet. The effectiveness of a cooling lake may be enhanced by making the hot water circulate around a series of baffle dikes or natural barriers so that most of the lake area is utilized for cooling. Some grill work, partitions, and troughs may also be added.

Cooling lakes may be formed by enclosing a relatively flat area with a dike and filling it with water. The result is a *perched lake*. Another method is damming a natural watershed, which results in a *natural contour lake*.

The main disadvantages of a cooling lake, as mentioned above, are the very low cooling effectiveness and therefore the very large acreage required. Others are the cost of added structures and the relative lack of freedom in choosing its shape. Its advantages are simplicity, low maintenance, the ability to operate for extended periods without makeup water, and the low power requirements, as the only mechanical equipment needed are pumps for occasional addition of makeup water. Circulating-water pumps are of course needed by cooling lakes, as by all other systems. Another advantage is that the appearance of cooling lakes is less objectionable than cooling towers and that they can be turned into recreational areas.

The heat transfer to and from a large body of water such as a cooling lake is a complex combination of many processes [59]. The processes by which heat is added are:

- Heat addition to the lake from the powerplant
- Absorption of short-wave radiation from the sky



Absorption of long-wave radiation from the atmosphere  
 Convection through the bottom from the earth  
 Transformation of kinetic energy to sensible energy  
 Heat addition due to chemical processes  
 Condensation of water vapor onto the lake

The processes by which heat is *rejected* are:

Reflection of short-wave solar radiation by the water  
 Reflection of long-wave atmospheric radiation  
 Long-wave radiation emitted by the water  
 Conduction of heat to the atmosphere  
 Evaporation from the lake into the atmosphere.

The net effect, cooling of the lake, is not constant over the total lake area because it is a function of the local water temperature as well as climatic conditions, such as dry- and wet-bulb temperatures of the air above the water, wind conditions, solar radiation, clouds, day and night variations, and others.

The lower limit of cooling is the *equilibrium temperature*. This is the temperature that the water asymptotically approaches if all parameters are held constant. The equilibrium temperature is given by [60]

$$\frac{T_C - T_E}{T_H - T_E} = e^{-\frac{UA}{\dot{m}}} \quad (7-12)$$

where  $T_E$  = equilibrium temperature, °F or °C  
 $T_C$  = cold-water temperature, °F or °C  
 $T_H$  = hot-water temperature, °F or °C  
 $U$  = overall heat-transfer coefficient, Btu/(h · ft<sup>2</sup> · °F)  
 or W/(m<sup>2</sup> · °C)  
 $A$  = lake surface area, ft<sup>2</sup> or m<sup>2</sup>  
 $\dot{m}$  = water mass-flow rate, lb<sub>m</sub>/h or kg/s  
 $c$  = water specific heat, Btu/(lb<sub>m</sub> · °F) or J/(kg · K)

and the heat dissipation rate  $\dot{Q}_R$ , Btu/h or W, is given by

$$\dot{Q}_R = \dot{m}c(T_H - T_C) \quad (7-13)$$

Values of  $T_E$  and  $U$  depend upon the weather conditions, including solar and sky radiation, dry- and wet-bulb temperatures, and wind speed. They can be evaluated by procedures outlined in Refs. 61 and 62. The quantity  $UA/\dot{m}c$  is then obtained and used to size the lake for design conditions of  $U$ ,  $T_E$ ,  $T_H$ , and  $T_C$ . The same quantity can also be used to analyze off-design performance. In a numerical example [59], the quantity  $UA/\dot{m}c$  was 1.173 and  $U$  was 11.0 Btu/(h · ft<sup>2</sup> · °F) [62.4 W/(m<sup>2</sup> · °C)].

The foregoing is a simplified model that neglects stratification; i.e., it assumes the entire surface area is equally effective and that there are constant and uniform weather conditions. Further uncertainties include such effects as buoyancy, turbulence, and the effects of makeup water and extraneous streams. A rigorous treatment of the problem requires a computerized hydrodynamic model, which is beyond the scope of this book.

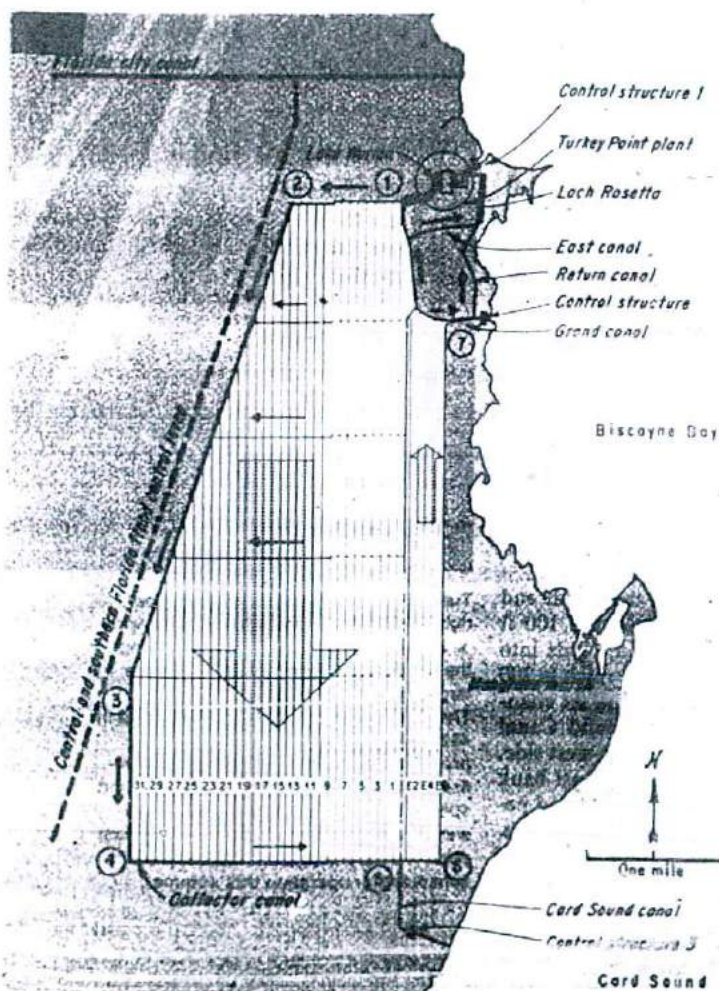


Figure 7-24 The cooling-canal system of the Turkey Point generating station at Biscayne Bay, Florida.

Long-term tests on actual cooling lakes [63] have shown that the average heat dissipation from the surface was about  $3.5 \text{ Btu/dth} \cdot \text{ft}^2 \cdot ^\circ\text{F}$ , or  $20 \text{ W}/(\text{m}^2 \cdot ^\circ\text{C})$ , and that an area between 1 and 2 acres ( $4000$  to  $8000 \text{ m}^2$ ) is required per megawatt of plant output.

Figure 7-24 shows a plan for a closed cooling-canal system at the Turkey Point generating station of the Florida Power and Light Company at Biscayne Bay which has two 432-MW fossil-fuel plants and two 666-MW nuclear plants. The system is composed of 38 channels, with a total length of 168 mi. Water enters a feeder canal at 1 and branches into 32 channels traveling south at  $0.25 \text{ ft/s}$  ( $0.076 \text{ m/s}$ ) to a collector canal at 4, then north through 6 channels back to the plant. Control structures around the circuit adjust flow, blowdown, and makeup. Regulations restrict the salinity, temperature, and flow of purge water into Card Sound at 5.

## 7-11 SPRAY PONDS AND CANALS

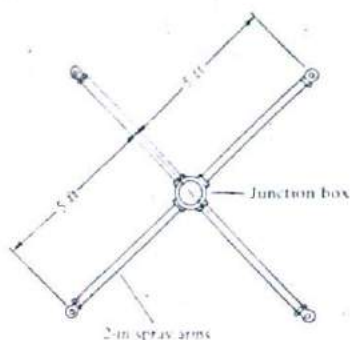
Spray ponds and canals, in a sense, operate like wet-cooling towers in that they depend primarily upon evaporation for cooling the circulating water. A *spray pond* is similar in water-flow pattern to a cooling lake or pond, only much smaller. Like a cooling lake, a spray pond can be turned into a recreational area. A *spray canal* usually consists of a long open canal or series of canals. In both, water is sprayed into the air above the surface. The spray in the canal is usually coarser than in the pond in order to reduce the drift loss (carryover with the air outside the canal boundaries) at the expense of lower heat-transfer rates because of the coarser drops.

The water is sprayed by modules that are self-contained units consisting of electrically driven propeller-type pumps that distribute the water through a diffuser system to spray nozzles, usually four per module. The spray pattern from a single diffuser can range up to 50 ft ( $\sim 15 \text{ m}$ ) in diameter and between 10 and 20 ft ( $\sim 3$  to  $6 \text{ m}$ ) high (Fig. 7-25). The modules are properly spaced within the pond (Fig. 7-26). They may be fixed or floating. In the latter, floatation is provided by polyurethane-filled fiberglass or stainless steel floats, which can easily be moored into place and attached to anchors.

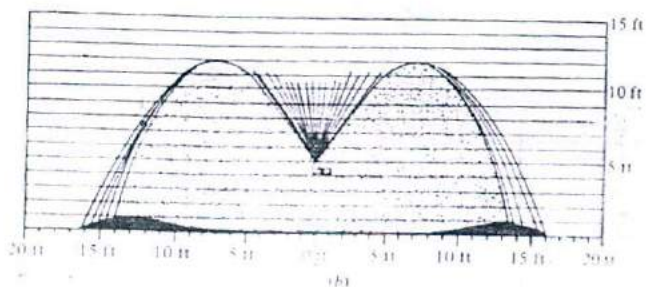
The spray, consisting of a very large number of small drops, greatly increases the total water surface area in contact with the air. Cooling occurs as the spray is propelled upwards and then falls down to the surface. Additional cooling is to be expected from the surface as is the case of a cooling lake. Heat transfer is by evaporation, conduction to the air, and some radiation. In warm weather evaporation is the predominant mode of heat transfer, whereas conduction is predominant in cold weather. Evaporation, as usual, is affected by weather conditions: dry- and wet-bulb temperatures and wind speed. The water temperature after spraying approaches the lower wet-bulb rather than the dry-bulb temperature of the air, an advantage of spray cooling.

A simplified governing equation for a spray canal is [60]

$$\frac{T_c - T_{wb}}{T_H - T_{wb}} = \exp\left(-\frac{N(1-f) r n t u b}{c}\right) \quad (7-14)$$



(a)



(b)

Figure 7-25 A typical spray module and pattern from a diffuser system consisting of four nozzles [63]. (a) Plan view of spray module. (b) Spray pattern. Spraco #1751 nozzle; pressure, 7 lb/in<sup>2</sup> gage; flow rate, 53 gal/min.

where  $T_{wb}$  = wet-bulb temperature of atmospheric air, °F or °C

$N$  = number of nozzles

$f$  = interference allowance to correct for local wet-bulb temperature elevation

$r$  = ratio of nozzle flow rate to recirculation water flow rate

$b$  = rate of change of enthalpy with temperature  $dh/dT$ ,

Btu/(lb<sub>m</sub> · °F) or J/(kg · K),

evaluated at a film temperature

$T_f = 0.5 (T_{wb} + T_n)$ , given in the table below

$ntu$  = a characteristic number of the spray system

$T_f$ , °F	32	40	60	80	100
$b$ , Btu/(lb <sub>m</sub> · °F)	0.38	0.48	0.64	0.99	1.6

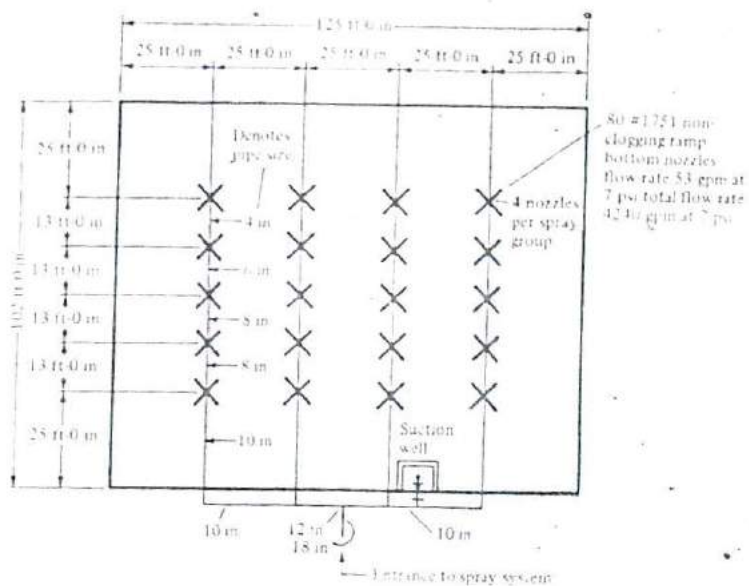


Figure 7-26 A typical layout of a spray pond [63].

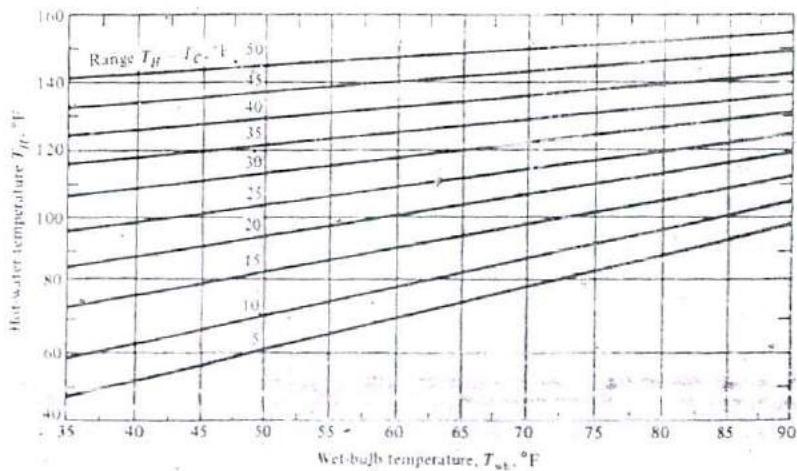


Figure 7-27 Spray-pond cooling range [63].

In a numerical example [60], the quantity  $N(1 - fr)$  was taken as 3.45 and  $ntu$  was taken as 0.15, both dimensionless.

The many variables in a spray-cooling system, such as climatic conditions, winds, spray nozzle design, and pond layout, make the use of theoretical analyses useful for comparative evaluations only and make empirical and test results more useful for specific cases. Figure 7-27 shows a chart prepared by Spray Engineering Company of Burlington, Massachusetts [63], based on numerous tests over several years under many climatic conditions and in several locales in the United States and abroad. The chart gives the range  $T_H - T_C$  for given values of  $T_H$  and  $T_{amb}$ .

The same tests have shown that heat dissipation by a spray pond averaged 127

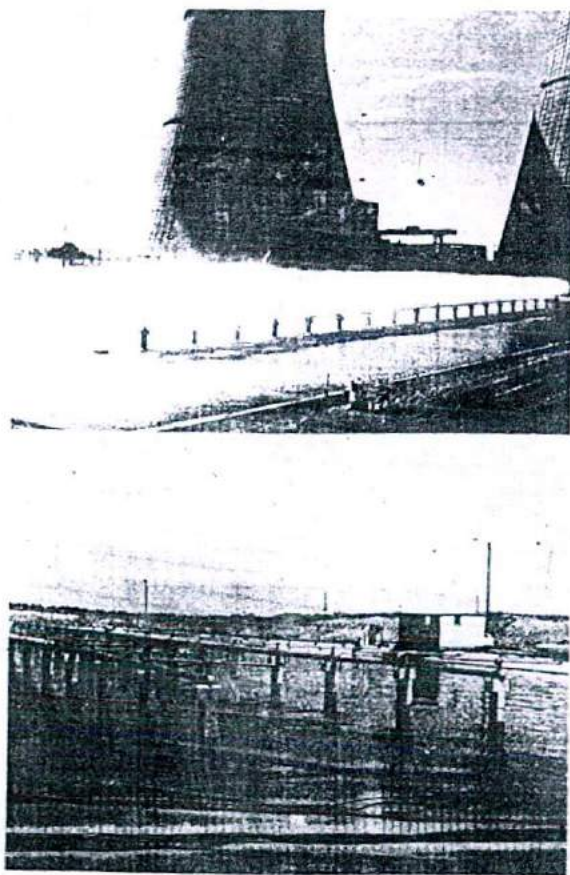


Figure 7-28 Spray pond at Rancho Seco nuclear powerplant.

Btu/(h · ft<sup>2</sup> · °F), or 720 W/(m<sup>2</sup> · °C). Comparing this with 3.5 Btu/(h · ft<sup>2</sup> · °F) for a cooling lake shows that a spray pond would be, on the average, 4 percent as large in area as a cooling lake. Others estimate the ratio to be closer to 10 percent. The difference is, nonetheless, impressive. The areas are designed from known nozzle-module flow rate and the diameter of the spray pattern obtained. For example [63] a four-nozzle module under 7 psig pressure delivers 212 gal/min and sprays it over a 32-ft diameter area (Fig. 7-25). It is important to provide a sufficiently free airspace between sprays so that they will not interfere with one another and thus reduce the efficiency of cooling. The number of modules is easily obtained from the total water flow. (The recommended spacing is as shown in Fig. 7-26.) Figure 7-28 is a photograph of a typical spray-pond installation at Rancho Seco nuclear powerplant, near Sacramento, California.

Finally, cooling lakes and spray ponds and canals can be combined with cooling towers, once-through or other circulating-water cooling systems, both open and closed, to supplement cooling requirements both for new plant construction and existing installations.

## PROBLEMS

- 7-1 A 900-MW powerplant of the pressurized-water nuclear-reactor type uses once-through cooling from a river. Regulations do not permit cooling water discharge back to the river hotter than 5°C above river ambient. Estimate (a) the necessary water flow, in kilograms per second, and (b) the reduction, in percent, in this water flow if the plant efficiency is improved by 1 percentage point. Take  $c_p$  for water = 4.184 kJ/kg · K.
- 7-2 A 900-MW powerplant of the pressurized water nuclear-reactor type uses a wet cooling tower in the closed mode. The condenser range is 10°C. Estimate, for hot-weather conditions, (a) the amount of makeup water flow in kilograms per second, (b) the percent makeup flow of the total condenser flow, and (c) the reduction, in percent, in the makeup if the plant efficiency is improved by 1 percentage point.
- 7-3 A natural-draft cooling tower is 450 ft high. Air enters the tower at 14.696 psia, 50°F, and 50 percent relative humidity and leaves in a saturated condition. The pressure drop in the tower is 0.015 psi. Calculate (a) the air exit temperature, in degrees Fahrenheit, and (b) the makeup due to evaporation, in pound mass per pound mass of dry air.
- 7-4 A natural draft cooling tower receives 250,000 ft<sup>3</sup>/min of air at standard atmospheric pressure, 70°F, and 45 percent relative humidity. The air leaves saturated at 100°F. 3500 gallons per minute of water at 104°F is cooled. Calculate (a) the temperature of the water at tower exit, and (b) the necessary height of the tower if the total pressure losses are 2.00 lb<sub>f</sub>/ft<sup>2</sup>.
- 7-5 An induced-draft cooling tower cools 90,000 gallons per minute of water from 84 to 68°F. Air at 29.75 inHg absolute pressure, 70°F dry bulb, and 60°F wet bulb, enters the tower and leaves saturated at 80°F. Find (a) the volume flow rate of air, in cubic feet per minute, and (b) the makeup water required, in pound mass per hour.
- 7-6 A wet cooling tower receives  $1.5 \times 10^6$  lb<sub>m</sub>/min of condenser water at 96°F, and  $1.25 \times 10^6$  lb<sub>m</sub>/min of air at 1 standard atmosphere, 62°F, and 50 percent relative humidity. The air leaves saturated at 82°F. Calculate (a) the exit water temperature, in degrees Fahrenheit, and (b) the percent condenser cooling water makeup due to evaporation.
- 7-7 A cooling tower is situated above sea level where the pressure is 14.5 psia. Air at 50°F and 50 percent relative humidity enters the tower at the rate of  $2 \times 10^6$  lb<sub>m</sub>/min and leaves saturated at 80°F. The condenser cooling water enters at 96°F. The condenser range is 18°F. Calculate (a) the mass flow rate of the condenser cooling water and (b) the makeup due to evaporation, in pound mass per minute.

7-8 A mechanical-draft cooling tower receives  $3.3 \times 10^6 \text{ lb}_w/\text{min}$  of condenser water at  $92^\circ\text{F}$ . The condenser range is  $20^\circ\text{F}$ . The outside air is at  $60^\circ\text{F}$  dry bulb,  $46^\circ\text{F}$  wet bulb, and  $14.696 \text{ psia}$ . The exit air is saturated at  $82^\circ\text{F}$ . The pressure drop in the tower is  $0.0125 \text{ psi}$ . Find the fan horsepower requirements in the case of (a) an induced-draft fan, and (b) a forced-draft fan. Assume that both fans have an efficiency of 65 percent.

7-9 A cooling tower receives  $3.3 \times 10^6 \text{ lb}_w/\text{min}$  of condenser cooling water at  $92^\circ\text{F}$ . The condenser range is  $20^\circ\text{F}$ . The outside air is at  $60^\circ\text{F}$  dry bulb,  $46^\circ\text{F}$  wet bulb, and  $14.696 \text{ psia}$ . The exit air is saturated at  $82^\circ\text{F}$ . The pressure drop in the tower is  $0.0125 \text{ psi}$ . (The conditions are the same as those in Prob. 7-8.) Calculate (a) the height of the tower if it is of the natural-draft type, and (b) the forced-draft horsepower requirements if a hybrid wet tower half the height of the natural draft tower is used. Because the pressure drop is mainly in the fill, assume that both have the same pressure drop. The fan efficiencies are 65 percent.

7-10 A hybrid tower is designed to cool  $2 \times 10^5 \text{ lb}_w/\text{h}$  of condenser water from  $94$  to  $72^\circ\text{F}$ . The outside air is at one standard atmosphere,  $66^\circ\text{F}$  dry bulb, and  $60^\circ\text{F}$  wet bulb. It leaves the tower saturated at  $86^\circ\text{F}$ . The pressure drop in the tower is given by  $5.75 \times 10^{-11} \dot{m}_a^2 \text{ psia}$ , where  $\dot{m}_a$  is the mass flow rate of air in pound mass per hour. Calculate the height of the hybrid tower if the total fan power should not exceed  $3000 \text{ kW}$ . The fan efficiency is 0.65.

7-11 An induced-draft wet cooling tower situated on a natural body of water at  $60^\circ\text{F}$  operates in the helper mode. The total condenser water flow is  $3 \times 10^6 \text{ lb}_w/\text{min}$ . The condenser exit water is at  $96^\circ\text{F}$ . The tower receives half the condenser water, and  $1 \times 10^6 \text{ lb}_w/\text{min}$  of air at 1 standard atmosphere, at  $62^\circ\text{F}$ , and 50 percent relative humidity. The air leaves the tower saturated at  $82^\circ\text{F}$ . Calculate (a) the water supply from the lake in pound mass per minute, assuming losses due to evaporation only, (b) the tower water exit temperature, and (c) the condenser inlet temperature, in degrees Fahrenheit.

7-12 It is desired to compare the effect of two types of dry cooling tower systems on powerplant performance. The towers are of the indirect cooling type. One operates with a surface condenser with an  $8^\circ\text{F}$  terminal temperature difference, and the other with a direct-contact condenser with  $0^\circ\text{F}$  terminal temperature difference. Consider for simplicity a simple ideal Rankine cycle with inlet saturated steam at  $1000 \text{ psia}$ . Further consider that both have the same condenser cooling water mass flow rate of  $7.21 \times 10^7 \text{ lb}_w/\text{h}$ , the same inlet temperature of  $70^\circ\text{F}$ , the same dry tower air temperature range of  $60^\circ\text{F}$  in and  $90^\circ\text{F}$  out, and the same air mass flow rate of  $5 \times 10^4 \text{ lb}_w/\text{h}$ . Calculate for each case (a) the condenser temperature, in degrees Fahrenheit, and pressure, in psia, (b) the steam mass flow rate, in pound mass per hour, (c) the cycle efficiency, and (d) the cycle work, in megawatts, ignoring the pump work.

7-13 A wet-dry cooling tower receives  $20 \times 10^6 \text{ lb}_w/\text{h}$  of condenser cooling water at  $110^\circ\text{F}$ . The water is cooled in the dry section to  $90^\circ\text{F}$  and in the wet section to  $70^\circ\text{F}$ . The outside air is at 1 standard atmosphere,  $60^\circ\text{F}$ , and 40 percent relative humidity. The air leaves both dry and wet sections at  $81^\circ\text{F}$ . Calculate (a) for the dry section the outside cooling air required, in pound mass per hour, and the relative humidity leaving it, (b) for the wet section the outside cooling air required, in pound mass per hour, (c) the condition (temperature and relative humidity) of the air leaving the tower, (d) the required makeup of condenser cooling water due to evaporation, in pound mass per hour, and (e) the percentage savings in that makeup because of the use of a wet-dry instead of an all-wet tower.

7-14 A cooling lake is used to cool a 200-MW powerplant that has a 39 percent efficiency. The condenser cooling water inlet and exit temperatures are  $75^\circ\text{F}$  and  $95^\circ\text{F}$ , respectively. The lake equilibrium temperature and overall heat-transfer coefficient based on the available climatic conditions are  $65^\circ\text{F}$  and  $3.5 \text{ Btu/h} \cdot \text{ft}^2 \cdot ^\circ\text{F}$ . Determine the surface area of the lake, in acres.

7-15 A spray pond is used to cool a 200-MW powerplant that has a 39 percent efficiency. The condenser cooling water outlet temperature is  $90^\circ\text{F}$ . The atmosphere is at  $70^\circ\text{F}$  and 60 percent relative humidity. The spray nozzles have  $nu = 0.15$ ,  $r = 0.015$  and  $f = 0.25$ . Determine (a) the number of spray modules required, (b) the flow per module, in gallons per minute, and (c) the approximate pond area, in acres.



## GAS-TURBINE AND COMBINED CYCLES

### 8-1 INTRODUCTION

Gas turbines are used by themselves in a very wide range of services, most notably for powering aircraft of all types but also in industrial plants for driving mechanical equipment such as pumps, compressors, and small electric generators in electrical utilities and for producing electric power for peak loads as well as for intermediate and some base-load duties.

There is also growing interest in using gas turbines in combined-cycle plants. These plants use combinations of gas and steam turbines in a variety of configurations of turbines, heat-recovery boilers, and regenerators.

Gas turbines for industrial and utility applications have many advantages. Compared with steam plants they, and their total systems, are small in size, mass, and initial cost per unit output. They are available with relatively short delivery times and are quick to install and put to use. They are quick-starting, often by remote control, and are smooth-running. They offer flexibility in supplying process needs, such as compressed air, in addition to electric power and in using a range of liquid and gaseous fuels, including the new synthetic fuels like low-Btu gas (Sec. 4-11). They are also subject to fewer environmental restrictions than other prime movers.

Gas turbines have one major disadvantage that prevents utilities from using them as major base-load prime movers: their present low cycle efficiency. Another disadvantage is their incompatibility with solid fuel. The combinations of low capital cost and low efficiency have determined their use primarily as power-peaking units where they are not expected to be on line for more than 1000 or 2000 h/year and where a large steam plant designed to meet peak loads would operate at an uneconomical load factor during most of the year.

Improvement in gas-turbine cycle efficiencies can be effected by a boost in the inlet combustion gas temperatures to the turbine from the present 2000 to 2300°F (1100 to 1260°C). Manufacturers are engaged in expensive research and development work to raise this to close to 2800°F (1540°C), with an eye on 3000°F (1650°C) for the future.

The use of gas turbines in combined cycles is one scheme to overcome their present low cycle efficiency for utility base-load use, while at the same time offering the utilities the gas-turbine advantages of quick starting and flexible operation over a wide range of loads.

Gas turbines are available in one- or two-shaft models (Fig. 8-1). The latter has two shafts that rotate at different speeds. One shaft has the compressor and a turbine that drives it, the other has the power turbine connected to the external load. Or one shaft might have high-pressure sections of the compressor and the turbine, while the other has the low-pressure compressor, turbine, and external load. In either case, the portion of the system containing the compressor, combustion chamber, and high-pressure turbine is sometimes called the *gas generator*. The two-shaft configuration allows the load to be driven at variable speed, which is well suited to many industrial applications. Gas turbines designed for aircraft propulsion are sometimes modified and used for industrial service [64]. Single-shaft turbines have the compressor, turbine, and load on one shaft running at constant speed. This configuration is used to drive small generators as well as large generators for utility use.

## Gas-Turbine Cycles

The hot gas emerging from a combustor or a gas-cooled reactor can be used directly as the primary working fluid, i.e., by expanding through a gas turbine, or indirectly, by heating a secondary fluid acting as the working fluid. For each of these two cases, i.e., the direct or the indirect cycle, we may also have an open or a closed cycle. Following are the possible combinations.

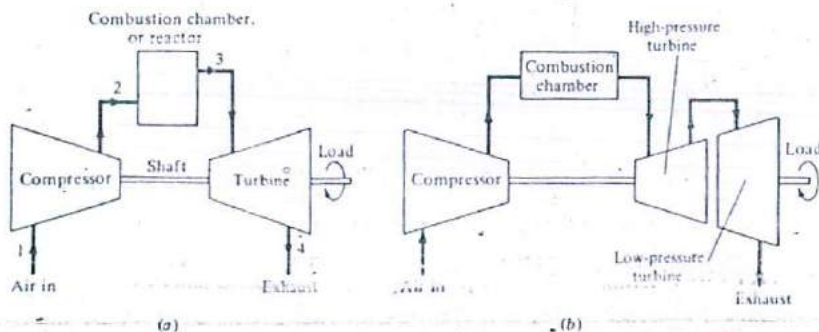


Figure 8-1. Schematic of a direct open gas-turbine cycle: (a) single shaft and (b) two shaft.

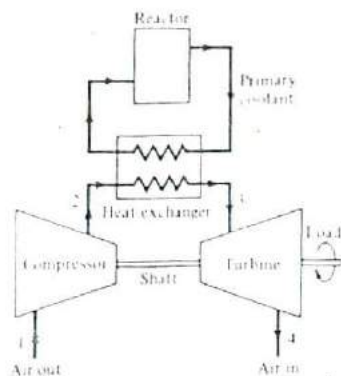


Figure 8-2 Schematic of an indirect open gas-turbine cycle.

**Direct open cycle** The direct open cycle is shown schematically in Fig. 8-1. The gas enters a compressor at point 1, where it is compressed to point 2. The gas then enters the combustion chamber or reactor, where it receives heat at constant pressure (ideally) and emerges hot at point 3. From there it expands through the turbine to point 4. The hot exhaust mixes with the atmosphere outside the cycle, and a fresh cool supply is taken in at point 1. The turbine supplies the compressor power. Useful power may be supplied by the turbine (or by the gas expanding further in a nozzle that supplies propulsion to the vehicle carrying the power plant, such as a jet aircraft). Because this is an open cycle, air is the only feasible working fluid (on earth).

**Indirect open cycle** The elements of the indirect open cycle (Fig. 8-2) are similar to those in the direct open cycle except that here the air is a secondary fluid that receives its heat from a primary coolant in a heat exchanger. This cycle is suitable for uses where environmental concerns prevent the air from receiving heat directly, such as from a nuclear reactor where radioactivity releases may spread to the atmosphere. Nuclear-reactor use, however, is best served by a closed cycle (see below).

**Direct closed cycle** In the direct closed cycle (Fig. 8-3) the gas coolant is heated in the reactor, expanded through the turbine, cooled in a heat exchanger, and compressed back to the reactor. In this cycle a gas other than air may be used. No effluent of radioactive gases passes into the atmosphere under normal operating conditions. Closed cycles permit pressurization of the working fluid with consequent reduction in the size of rotating machinery. The most suitable working fluid in this case is helium.

**Indirect closed cycle** The indirect closed cycle combines the indirect open cycle and the direct closed cycle in that the reactor is separated from the working fluid by a heat exchanger, whereas the working gas rejects heat to the atmosphere via a heat exchanger (Fig. 8-4). The primary coolant may be water, a liquid metal, or a gas such as helium.

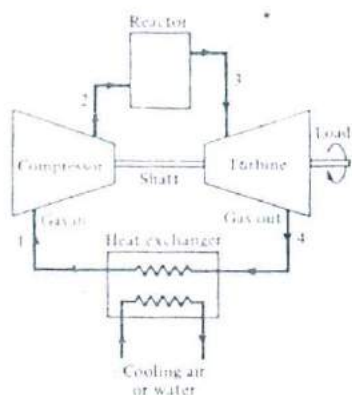


Figure 8-3 Schematic of a direct closed gas-turbine cycle.

## 8-2 THE IDEAL BRAYTON CYCLE

The ideal cycle for gas turbine work is the *Brayton cycle*. It is composed of two adiabatic-reversible (and hence isentropic) and two constant-pressure processes (Fig. 8-5). The gas is compressed isentropically from point 1 to 2, heated at constant pressure from 2 to 3, and then expanded isentropically through the turbine from point 3 to 4. Cooling occurs from point 4 to point 1, either in a heat exchanger (closed cycle) or in the open atmosphere (open cycle).

The work done in the turbine (a steady-flow machine) per unit time (power), with

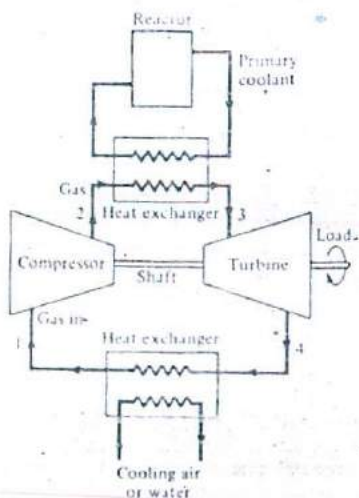
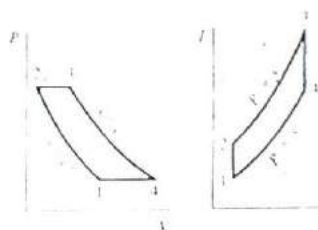


Figure 8-4 Schematic of an indirect closed gas-turbine cycle.

Figure 8-5  $P$ - $V$  and  $T$ - $s$  diagrams of an ideal Brayton cycle

relatively negligible change in the kinetic energy of the gas,  $\dot{W}_T$  in Btu/h or W, is equal to the rate of change in its enthalpy. Thus

$$\dot{W}_T = \dot{H}_3 - \dot{H}_4 = \dot{m}(h_3 - h_4) \quad (8-1)$$

where  $\dot{H}$  = total enthalpy of flowing gas, Btu/h or W  
 $h$  = specific enthalpy, Btu/lb<sub>m</sub> or J/kg  
 $\dot{m}$  = mass rate of flow of gas, lb<sub>m</sub>/h or kg/s

For a gas, Eq. (8-1) may be rewritten in the form

$$\dot{W}_T = \dot{m} \int_{T_4}^{T_3} c_p(T) dT \quad (8-2)$$

where  $c_p(T)$  is the specific heat at constant pressure of the gas, which is a function of temperature  $T$ .

We will now assume constant specific heats for simplicity, a procedure sometimes referred to as analysis for the air-standard cycle (when  $c_p$  is a constant for air). However, it should be noted that specific heats for monatomic gases such as helium and argon are essentially constant and independent of temperature (except when highly compressed, at very low temperatures and high pressures). Specific heats increase with temperature for diatomic gases such as air and  $N_2$  and increase even faster with temperature for triatomic gases such as  $CO_2$  (Fig. 8-6 and Table 8-1). The following analysis, therefore, is *exact* for monatomic gases and only *approximate* for others. For a constant  $c_p$ , Eq. (8-2) becomes

$$\dot{W}_T = \dot{m} c_p (T_3 - T_4) \quad (8-3)$$

Using the perfect-gas laws (Table 1-2), we can write Eq. (8-3) in terms of the pressure ratio across the turbine  $r_{pr}$ , given by

$$r_{pr} = \frac{P_3}{P_4}$$

which is related to the absolute temperature ratio across the turbine by

$$\frac{T_3}{T_4} = r_{pr}^{(\gamma-1)/\gamma} \quad (8-4)$$

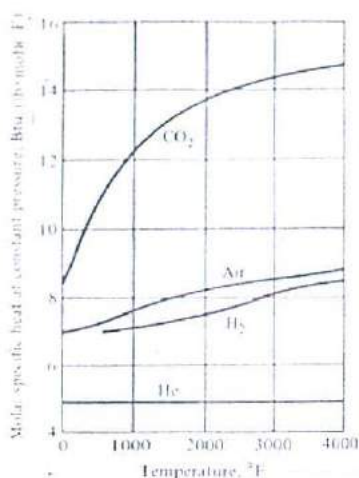


Figure 8-6 Variation of molar  $c_p$  with temperature for various gases.

where  $k$  is the ratio of specific heats at constant pressure and constant volume

$$k = \frac{c_p}{c_v}$$

and since

$$c_p - c_v = R \quad (1-14)$$

where  $R$  is the gas constant, a constant  $c_p$  means a constant  $c_v$  and a constant  $k$ . Equations (8-3) and (8-4) can now be combined to give

$$W_T = \dot{m}c_p T_3 \left( 1 - \frac{1}{r^{(k-1)/k}} \right) \quad (8-5)$$

Table 8-1  $c_p$  and  $k$  for gases at low pressure\*

Gas	M	$c_p$ , Btu/(lbm · °F)†			$k$ , dimensionless		
		Low	1000°F	2000°F	Low	1000°F	2000°F
H <sub>2</sub>	2.016	3.421			1.405		
He	4.003	1.250	1.250	1.250	1.659	1.659	1.659
Air	28.97	0.240	0.264	0.289	1.400	1.353	1.314
N <sub>2</sub>	28.02	0.249	0.269	0.293	1.401	1.357	1.321
A	39.95	0.125	0.125	0.125	1.668	1.668	1.668
CO <sub>2</sub>	44.01	0.202	0.280	0.313	1.293	1.192	1.169

\* Data from Ref. 65.

† To convert to kJ/(kg · °C), multiply by 4.1868.

Using a pressure ratio across the compressor  $r_p$ , where

$$r_p = \frac{P_2}{P_1}$$

and

$$\frac{T_2}{T_1} = r_p^{k-1/k} \quad (8-6)$$

The absolute magnitude of the rate of work of the compressor would also be given by

$$\begin{aligned} |\dot{W}_c| &= \dot{m}(h_2 - h_1) \\ &= \dot{m}c_p T_2 \left( 1 - \frac{1}{r_p^{k-1/k}} \right) \end{aligned} \quad (8-7)$$

Assuming  $r_{pr} = r_{pc} = r_p$ , that is, no pressure losses in the cycle, a common assumption in the ideal case, the net work rate of the cycle  $\dot{W}_n$  is given by

$$\dot{W}_n = \dot{W}_T - |\dot{W}_c| = [\dot{m}c_p(T_3 - T_2)] \left( 1 - \frac{1}{r_p^{k-1/k}} \right) \quad (8-8)$$

The expression within the brackets on the right-hand side of this equation is obviously the heat added  $\dot{Q}_A$  in Btu/h or W

$$\dot{Q}_A = \dot{m}c_p(T_3 - T_2) \quad (8-9)$$

The second expression must then be the cycle thermal efficiency  $\eta_{th}$ , a function of both  $r_p$  and  $k$

$$\eta_{th} = 1 - \frac{1}{r_p^{k-1/k}} \quad (8-10)$$

Although the above equations pertain to constant specific-heat gases, the trends they predict apply to all gases. The thermal efficiency of the cycle for any one gas (same  $k$ ) is a sole function of  $r_p$ , increases asymptotically with it, and is independent of initial or maximum cycle temperatures  $T_1$  and  $T_3$ . (As we shall see later, this is not true for nonideal cycles.) However, while  $\eta_{th}$  increases indefinitely with  $r_p$ , the specific power, the power per unit mass-flow rate (and the specific work or work per unit mass of working fluid) does not and reaches a maximum at an optimum  $r_p$ . This can be seen by rewriting Eq. (8-8) in terms of  $T_1$  and  $T_3$ , using Eq. (8-6). Again for  $r_{pr} = r_{pc} = r_p$

$$\frac{\dot{W}_n}{\dot{m}} = c_p (T_3 - T_1 r_p^{k-1/k}) \left( 1 - \frac{1}{r_p^{k-1/k}} \right) \quad (8-11a)$$

or

$$\frac{\dot{W}_n}{\dot{m}} = c_p \left[ T_1 (1 - r_p^{k-1/k}) + T_3 \left( 1 - \frac{1}{r_p^{k-1/k}} \right) \right] \quad (8-11b)$$

Examination of Eqs (8-8) and (8-11) shows the following:

1. Other things being equal, that is, for the same  $T_1$ ,  $T_3$ ,  $r_p$ , and  $k$ , the work per unit mass of gas is a direct function of  $c_p$ . Hence, helium can produce more than five times  $W_p/\dot{m}$  than air (at low temperatures).
2. Other things being equal, gases with higher values of  $k$ , that is, higher  $(k-1)k$ , produce more work per unit mass of gas than gas with lower values of  $k$ . Again, this shows an advantage for He over air ( $k$  for air decreases with temperature).
3. For any one gas, an increase in  $r_p$  from its lowest value of 1.0 (where the work is zero) decreases one part of Eq. (8-11) and increases the other. The net work thus goes through a maximum at an optimum value of  $r_p$ . This state of affairs can be shown graphically by the three ideal cycles of Fig. 8-7. These operate between the same temperatures  $T_1$  and  $T_3$  and have the same inlet and exhaust pressures but different values of  $r_p$ . The net work in each case is represented by the enclosed area of the cycle.

The optimum pressure ratio can be evaluated for ideal cycles by differentiating the net work in Eq. (8-11) with respect to  $r_p$  and equating the derivative to zero. This gives a value of  $T_2$  expressed by

$$T_2 = (T_1 T_3)^{1/2} \quad (8-12)$$

and since  $T_2/T_1 = T_3/T_4 = r_p^{k-1}$  (for same pressure ratio), then

$$(T_2 = T_4)_{\text{opt}} \quad (8-13)$$

and

$$r_{p,\text{opt}} = \left(\frac{T_2}{T_1}\right)^{k/(k-1)} = \left(\frac{T_3}{T_1}\right)^{k/2(k-1)} \quad (8-14)$$

Note that the quantity  $k/2(k-1)$  decreases as  $k$  increases. Thus, for fixed initial and maximum cycle temperatures, the optimum pressure ratio for monatomic gases (He) is, in general, lower than for diatomic gases (air,  $N_2$ ). These in turn have lower ratios than the triatomic gases ( $CO_2$ ). It follows that a monatomic gas, for example, may

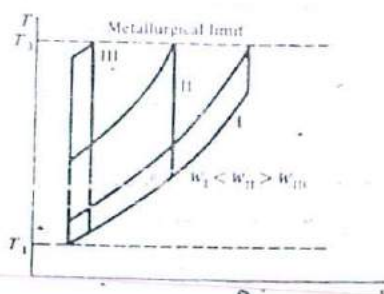


Figure 8-7 Effect of pressure ratio on ideal Brayton cycle work given by enclosed areas on  $T$ - $s$  diagram.  $T_1$  and  $T_3$  are fixed for all cycles.



operate at lower maximum pressures or, if the pressure in the low-pressure section of the cycle is increased (in closed cycle), may operate with a larger average density. This is accompanied by a reduction in plant size and mass.

**Example 8-1** Find the pressure ratio required by an ideal Brayton cycle to produce a net work of 600 Btu/lb<sub>m</sub> of (1) helium and (2) air (with  $c_p$  at low temperatures). The cycle has initial and maximum temperatures of 500°R and 2500°R, respectively. Also calculate the optimum pressure ratio for both gases.

**SOLUTION**

(1) *Helium*:

$$c_p = 1.250 \quad k = 1.659 \quad (k - 1)/k = 0.3972$$

From Eq. (8-11):

$$600 = 1.25(2500 - 500r_p^{0.3972}) \left( 1 - \frac{1}{r_p^{0.3972}} \right)$$

$$\text{or} \quad (r_p^{0.3972})^2 - 5.04(r_p^{0.3972}) + 5 = 0$$

which yields two values of  $r_p = 2.16$  and 26.62

$$r_{p,\text{opt}} = \left( \frac{2500}{500} \right)^{1/(1.659 - 1)} = 7.58$$

From Eq. (8-11), this optimum pressure ratio yields a maximum work of 954.8 Btu/lb<sub>m</sub>. Note that  $r_p = 1.0$  results in zero work. There is also a maximum value of  $r_p$  that results in zero work and beyond which the work becomes negative. This is the  $r_p$  that makes  $T_2 = T_3$ . For He it is given by

$$r_p^{0.3972} = \frac{T_2}{T_1} = \frac{T_3}{T_1} = \frac{2500}{500} = 5$$

which yields a maximum  $r_p$  of 57.5.

(2) *Air*:

$$c_p = 0.24 \quad k = 1.4 \quad (k - 1)/k = 0.2857$$

$$600 = 0.24(2500 - 500r_p^{0.2857}) \left( 1 - \frac{1}{r_p^{0.2857}} \right)$$

$$r_p^{0.2857} - r_p^{0.2857} + 5 = 0$$

which yields imaginary values of  $r_p$ , indicating that air is incapable of producing 600 Btu/lb<sub>m</sub>.

$$r_{p,\text{opt}} = \left( \frac{2500}{500} \right)^{1/(1.4 - 1)} = 16.72$$

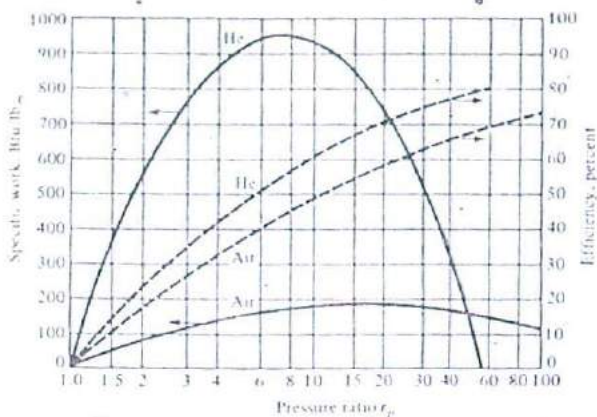


Figure 8-8 Specific power and efficiency versus pressure ratio for ideal Brayton cycles operating with helium and air.

Compared with 7.58 for He, the maximum work at  $r_p = 16.72$  from Eq. (8-11) is 183.3 Btu/lb<sub>m</sub>, less than the 600 Btu/lb<sub>m</sub> asked for and the 954.8 Btu/lb<sub>m</sub> He is capable of. The maximum  $r_p$  for air, obtained as for He, is 279.6.

Figure 8-8 shows results of calculations for  $W/\dot{m}$  and  $\eta_{th}$  for ideal Brayton cycles using He and air as working fluids, where the initial and maximum temperatures  $T_1$  and  $T_3$  are the same as in Example 8-1, i.e., 500°R and 2500°R, respectively. Note that the specific work Btu/lb<sub>m</sub> of He is generally much higher than that of air, and in the practical range of pressure ratios, occurs at much lower pressure ratios. Recall, however, that while helium turbines operate with lower overall pressure ratios than air, they need many more stages (Sec. 5-9). To obtain the specific work based on a unit mole (or volume at same  $P$  and  $T$ ), multiply the ordinates of Fig. 8-8 by the molecular mass of each gas.

### 8-3 THE NONIDEAL BRAYTON CYCLE

The Brayton cycle with fluid friction is represented on the  $P$ - $V$  and  $T$ - $s$  diagrams of Fig. 8-9 by 1-2-3-4. Both the compression process with fluid friction 1-2 and the expansion process with fluid friction 3-4 show an increase in entropy as compared with the corresponding ideal processes 1-2, and 3-4. Drops in pressure during heat addition (process 2-3) and heat rejection (process 4-1) are neglected in this analysis, so the turbine pressure ratio equals the compressor pressure ratio as before.

The compression and expansion processes with fluid friction can be assigned polytropic, also called adiabatic or isentropic efficiencies (Sec. 1-8), as follows.

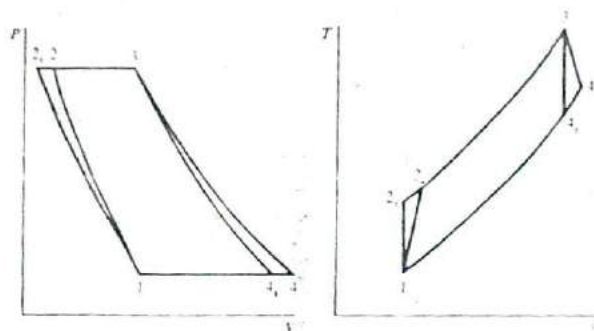


Figure 8-9  $P$ - $V$  and  $T$ - $s$  diagrams of ideal and nonideal Brayton cycle.

$$\begin{aligned} \eta_c = \text{compressor polytropic efficiency} &= \frac{\text{ideal work}}{\text{actual work}} \\ &= \frac{h_{2s} - h_1}{h_2 - h_1} \end{aligned} \quad (8-15)$$

If we assume constant specific heats

$$\eta_c = \frac{T_{2s} - T_1}{T_2 - T_1} \quad (8-16)$$

and

$$\begin{aligned} \eta_T = \text{turbine polytropic efficiency} &= \frac{\text{actual work}}{\text{ideal work}} \\ &= \frac{h_3 - h_4}{h_3 - h_{4s}} \end{aligned} \quad (8-17)$$

and for constant specific heats

$$\eta_T = \frac{T_3 - T_4}{T_3 - T_{4s}} \quad (8-18)$$

where in each case the smaller work is always in the numerator.

The net power of the cycle is  $\dot{W}_n = \text{power of turbine} - [\text{power of compressor}]$ .

For constant specific heats

$$\dot{W}_n = mc_p [(T_3 - T_4) - (T_2 - T_1)] \quad (8-19a)$$

$$\text{or} \quad \dot{W}_n = mc_p \left[ (T_3 - T_{4s}) \eta_T - \frac{T_2 - T_1}{\eta_c} \right] \quad (8-19b)$$

This equation can be written in terms of the initial temperature  $T_1$ , a chosen metallurgical limit  $T_3$ , and the compressor and turbine efficiencies (above) to give

$$\dot{W}_a = \dot{m}c_p T_1 \left[ \left( \eta_r \frac{T_3}{T_1} - \frac{r_p^{k-1/k}}{\eta_c} \right) \left( 1 - \frac{1}{r_p^{k-1/k}} \right) \right] \quad (8-19c)$$

The second quantity in parentheses can be recognized as the efficiency of the corresponding ideal cycle, i.e., one having the same pressure ratio and using the same fluid. As in the case of the ideal cycle, the specific power of the nonideal cycle,  $\dot{W}_a/\dot{m}$ , attains a maximum value at some optimum pressure ratio and is a direct function of the specific heat of the gas used.

The heat added in the cycle,  $\dot{Q}_A$ , is given by

$$\dot{Q}_A = \dot{m}c_p(T_3 - T_2) = \dot{m}c_p \left[ (T_3 - T_1) - \left( T_1 \frac{r_p^{k-1/k}}{\eta_c} - 1 \right) \right] \quad (8-20)$$

The efficiency of the nonideal cycle can then be obtained by dividing Eq. (8-19c) by Eq. (8-20). Although the efficiency of the ideal cycle is independent of cycle temperatures, except as they may affect  $k$ , and increases asymptotically with  $r_p$ , the efficiency of the nonideal cycle is very much a function of the cycle temperatures. It also assumes a maximum value at an optimum pressure ratio for each set of temperatures  $T_1$  and  $T_3$ . The two optimum pressure ratios, for specific power and for efficiency, are not the same, and this necessitates a compromise in design.

Another effect of nonideality is fluid friction in heat exchangers, piping, etc. This results in a pressure drop between 2 and 3 (Fig. 8-9) and a pressure at 4 greater than at 1. In other words the pressure ratio across the compressor  $r_{p_c}$  would be greater than the pressure ratio across the turbine  $r_{p_t}$ . General equations that would take these and other effects on the Brayton cycle will be presented next. Further nonidealities result from mechanical losses in bearings friction and auxiliaries, heat losses from combustion chambers, and air bypass to cool the turbine blades (Sec. 8-7).

Figures 8-10 and 8-11 show results of calculations [66] for  $\eta$  and  $\dot{W}/\dot{m}$  of a simple air-combustion Brayton cycle (solid lines) and of one with a regenerator (dashed lines). Regeneration is explained below. For the simple cycle, the following data were assumed.

$$T_1 = 15^\circ\text{C} = 59^\circ\text{F} = \text{constant}$$

$$P_1 = 1.013 \text{ bar} = 1 \text{ atm} = \text{constant}$$

$$\eta_c = 90\%; \eta_r = 87\%$$

$$\text{Mechanical losses} = 1\%$$

$$\text{Combustion chamber losses} = 2\%$$

$$\text{Air bypass} = 3\%$$

$$\text{Pressure losses: at inlet} = 1\%$$

$$\text{in combustion chamber} = 3\%$$

$$\text{at outlet} = 2\%$$

$$\text{in regeneration} = 4\%$$

Actual variable properties of air and combustion gases were used.

It can be seen that both  $\eta$  and  $\dot{W}/\dot{m}$  are strongly dependent on  $T_3$ , which necessitates operating at as high a  $T_3$  as metallurgically possible. They are also strong functions

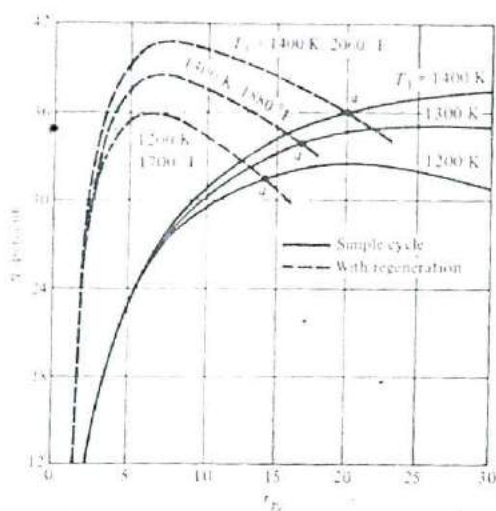


Figure 8-10 Efficiency versus compressor pressure ratio of a nonideal Brayton cycle, showing effects of maximum temperature and regeneration [66].

of  $r_p$ , with optimum  $r_p$  increasing with  $T_3$  for both efficiency and specific power. It can also be seen that the optimum  $r_p$  is greater for  $\eta$  than for power.

Figure 8-12 is a photograph of a single-shaft, direct-cycle, open air combustion gas-turbine package. It shows a 16-stage axial compressor, one of ten combustion chambers, and a three-stage turbine. A diesel engine for starting is shown on the left.

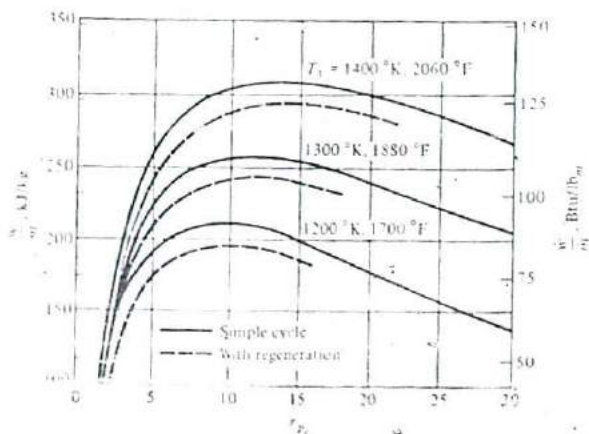


Figure 8-11 Specific power versus compressor pressure ratio of a nonideal Brayton cycle, showing effects of maximum temperature and regeneration [66].

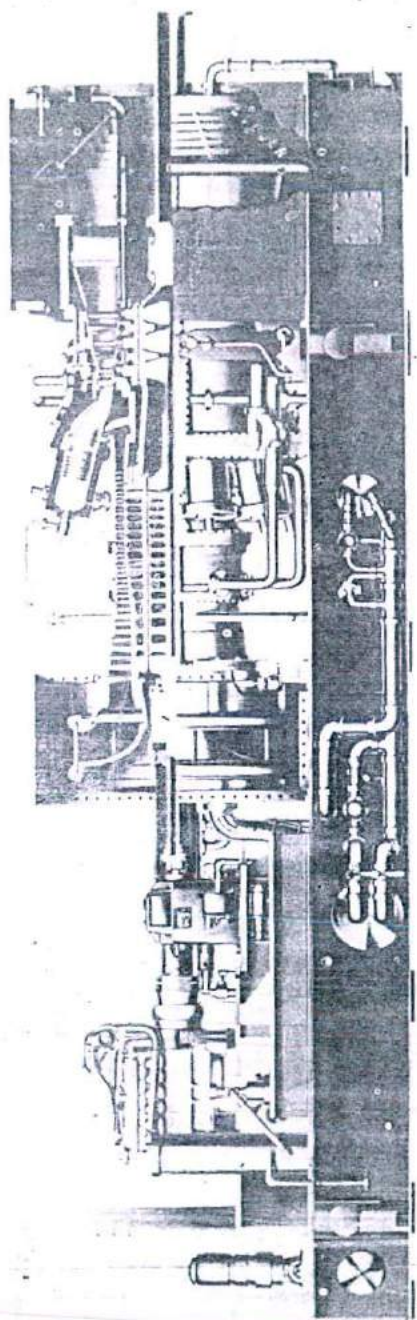


Figure 8-12 35.75 MW direct-cycle gas-turbine powerplant. (Courtesy: Gas Turbine Division, General Electric Company, Schenectady, New York.)

The powerplant, General Electric model MS6001, produces 35.75 MW, is 30.50 percent efficient, runs at 5100 r/min, and has overall dimensions, including electric generator (not shown), 38 m (122 ft) long, 11 m (36 ft) high, and 8 m (26 ft) wide.

## 8-4 MODIFICATIONS OF THE BRAYTON CYCLE

Although the above calculations show reasonable efficiencies, they nonetheless do not take into account some of the complications of a real powerplant and are hence on the optimistic side. While a simple gas-turbine cycle is economically adequate for many purposes, such as peaking units and jet transports, cyclic and base-loaded units require modifications to improve the output and efficiency (and hence the heat rate). Besides increasing  $T_3$ , the modifications are:

1. Regeneration
2. Compressor intercooling
3. Turbine reheat
4. Water injection

### Regeneration

Regeneration, as in steam cycles, is the internal exchange of heat within the cycle. In the Brayton cycle,  $T_4$  is often higher than  $T_2$  and heat addition is from 2 to 3 (Fig. 8-9). Regeneration, therefore, is used to preheat the compressed gas at 2 by the exhaust gases at 4 in a surface-type heat exchanger called the *regenerator* or, sometimes, the *recuperator*. Figure 8-13 shows such an arrangement for a closed cycle, suitable for He, but also used equally effectively for open cycles with air.

If the regenerator were 100 percent effective, the temperature of the gas entering the combustion chamber or nuclear reactor would be raised from  $T_2$  to  $T_2'$ . The net work of the cycle would be maintained, except for the effect of the added pressure loss in the regenerator, but the heat added would be materially reduced from  $H_3 - H_2$  to  $H_3 - H_2'$ , with corresponding increase in cycle efficiency. Actually, the regenerator effectiveness is never 100 percent, and the compressed gases are heated instead to a lower temperature such as  $T_2'$ . Regenerator *effectiveness*,  $\epsilon_R$ , is defined as the ratio of the actual to maximum possible temperature change. In other words

$$\epsilon_R = \frac{T_2' - T_2}{T_4 - T_2} \quad (8-21a)$$

and since point 4' is at the same temperature as point 2

$$\epsilon_R = \frac{T_2' - T_2}{T_4 - T_2'} \quad (8-21b)$$

Figures 8-10 and 8-11 include the effects of adding a regenerator with  $\epsilon_R = 0.75$ , shown by the dashed lines. It can be seen that the effect of adding a regenerator on efficiency is remarkable and shifts the optimum pressure ratio for efficiency to lower

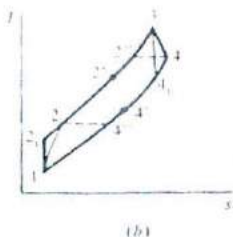
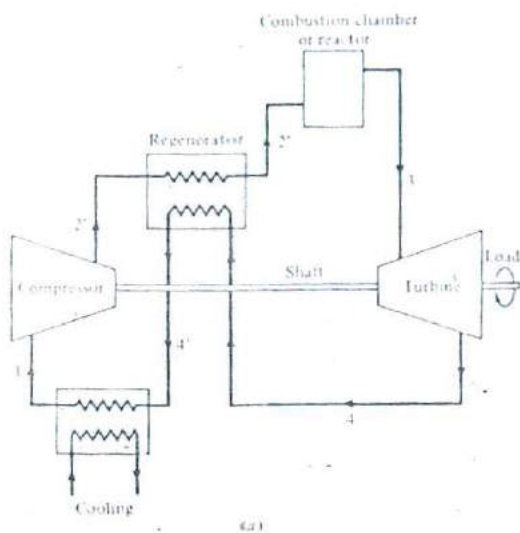


Figure 8-13 Flow and  $T$ - $s$  diagrams of a closed nonideal Brayton cycle with regeneration.

values. This is because the lower the pressure ratio, the greater the difference between  $T_4$  and  $T_2$  and the greater the reduction in cycle heat input. At very low value of  $r_p$ , the effect of reduced cycle work predominates and the curves drop, though still higher than those for the simple cycle. The efficiency curves for a cycle with regenerator cross those for the simple cycle at points such as  $a$ , beyond which the effect of a regenerator on efficiency is negative. These points represent pressure ratios at which the exhaust gases are cooler than those after compression.

The effect of the regenerator on the specific power curves is only to reduce them somewhat because of the added pressure losses in the regenerator.

Because regenerative gas-turbine cycles are more efficient than simple gas-turbine cycles, thus reducing fuel consumption by 30 percent or more, they are now used by utilities for meeting cycling duty as well as base-load assistance in driving pumps, compressors, and the like.



### Compressor Intercooling

The work in a flow system, such as a compressor or turbine, is given by Eq. (1-9), here repeated

$$W = - \int_1^2 V dP \quad (1-9)$$

For a perfect gas where  $PV = mRT$ , this equation can be written as

$$W = - \int_1^2 mRT \frac{dP}{P} \quad (8-22)$$

For a given  $dP/P$ , therefore, the work is directly proportional to temperature. A compressor working between points 1 and 2 (Fig. 8-13), therefore, would expend more and more work as the gas approaches point 2. Since compressor work is negative and a drain on the net cycle work, it is advantageous to keep  $T$  low while reaching the desired pressure  $P_2$ . This can theoretically be done by continuous cooling of the compressed gas to keep it at  $T_1$ , as shown by the lower horizontal dashed line of Fig. 8-14. However, this is not physically possible, and cooling, instead, is done in stages. Figure 8-13, drawn for simplicity for ideal (isentropic) compression and expansion, shows two stages of intercooling where gas is partially compressed from 1 to 2', cooled back to 1' at constant pressure (ideally), compressed again to 2'', intercooled to 1'', then finally compressed to 2''. Ideally  $T_1 = T_1' = T_1''$  and  $T_2 = T_2' = T_2''$ . In that case we have three compressor sections operating in tandem with equal work because for any one compressor section (from Table 1-2)

$$W = m \frac{nR(T_2 - T_1)}{1 - n}$$

where  $n$  is the polytropic exponent for compression (equal to  $k$  for ideal compression). When the temperature rises are equal, the pressure ratios are equal because

$$r_p = \left( \frac{T_2}{T_1} \right)^{n/(n-1)}$$

and the pressure ratio per stage is given by

$$r_{p, \text{stage}, c} = \sqrt[N_c]{r_{p, \text{tot}, c}} \quad (8-23)$$

where  $N_c$  is the number of compressor sections. Thus for an overall compressor pressure ratio of 10 and 3 sections, the pressure ratio per stage is  $\sqrt[3]{10} = 2.154$  (not  $10/3 = 3.33$ ). The improvement in the cycle is in increased work and efficiency. The increase in work is the result of the reduction in total compressor work since

$$(H_2 - H_1) + (H_2' - H_1') + (H_2'' - H_1'') < H_2 - H_1$$

because of operation at lower temperatures. This can also be easily seen from the  $T$ - $s$  diagram where the work has increased by area  $2-1'-2'-1''-2''-1''$  and the heat added has also increased by  $H_1' - H_2'$ . However, the work increase of the cycle more than offsets the increase in heat addition, resulting in an improvement in efficiency.

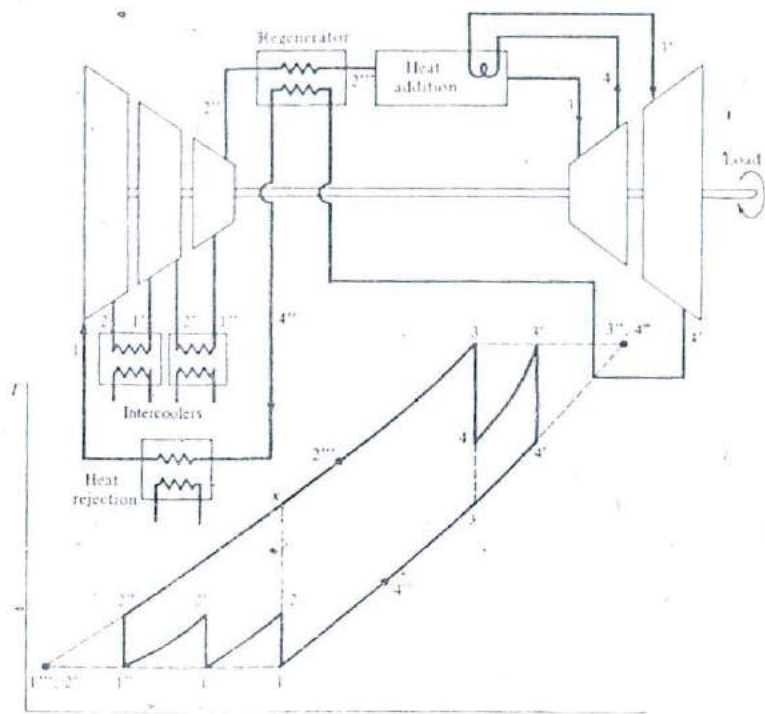


Figure 8-14 Flow and  $T$ - $s$  diagrams of a closed ideal Brayton cycle with two stages of intercooling, one stage of reheat, and regeneration.

Intercoolers can be air-cooled heat exchangers but are more commonly water-cooled.

### Turbine Reheat

Equation (8-22) has shown that compressor work can be decreased by keeping the gas temperatures in the compressor low. It also shows that turbine work can be increased by keeping the gas temperatures in the turbine high. This can also be done theoretically by continuous heating of the gas as it expands through the turbine, as shown by the upper horizontal dashed line of Fig. 8-14. Note that if cooling and heating were at constant temperatures, and if the rest of the cycle were ideal, we would have an ideal Ericsson cycle, which has the same efficiency as a Carnot cycle operating between the same temperature limits  $T_1$  and  $T_3$ .

Again, continuous heating is not practical and reheat is done in steps or stages. Figure 8-14 shows two turbine sections and one stage of reheat. The gas expands in the high-pressure section of the turbine from 3 to 4, is then reheated at constant pressure (ideally) to 3', and finally expands in the low-pressure section of the turbine to 4'. For  $T_3 = T_3'$  and  $T_4 = T_4'$ , the pressure ratio per turbine stage is

$$r_{p, \text{stage}, T} = \sqrt[n_T]{r_{p, \text{tot}, T}} \quad (8-24)$$

The increase in cycle work is shown by the area 4-3'-4'-y, whereas the heat added is increased by  $H_{3'} - H_4$ . The net effect is an increase in both work and efficiency.

Intercooling, reheat, and regeneration can all be combined in one cycle as shown in Fig. 8-14.

General equations for the specific power and heat added for a composite cycle as the one discussed above, for the case of constant specific heat, but with nonidealities taken into account, are

$$\frac{\dot{W}_n}{\dot{m}c_p} = T_3 \eta_T (n_T + 1) \left( 1 - \frac{1}{r_{p,T}^{(k-1)/k}} \right) - T_1 \frac{n_c + 1}{\eta_c} (r_{p,c}^{(k-1)/k} - 1) \quad (8-25)$$

$$\begin{aligned} \frac{\dot{Q}_A}{\dot{m}c_p} = T_3 \left\{ (n_T + 1) - (n_T + \epsilon_R) \left[ 1 - \eta_c \left( 1 - \frac{1}{r_{p,c}^{(k-1)/k}} \right) \right] \right\} \\ - T_1 (1 - \epsilon_R) \left[ 1 + \frac{1}{\eta_c} (r_{p,c}^{(k-1)/k} - 1) \right] \end{aligned} \quad (8-26)$$

where  $\dot{W}_n$  = net power =  $\dot{W}_T - |\dot{W}_c|$

$\eta_T$  = turbine adiabatic efficiency, assumed same for all turbine sections

$\eta_c$  = compressor adiabatic efficiency, assumed same for all compressor sections

$r_{p,T}$  = overall turbine pressure ratio

$r_{p,c}$  = overall compressor pressure ratio

$\epsilon_R$  = regenerator effectiveness

$n_T$  = number of reheat stages (e.g., 1 in Fig. 8-14)

$n_c$  = number of intercooling stages (e.g., 2 in Fig. 8-14)

The efficiency of the cycle may now be obtained by dividing Eq. (8-25) by Eq. (8-26). The greater the number of reheat and intercooling stages there are, the higher the efficiency. However, this is attained at the cost of the capital investment and size of the plant. The design of the plant should be optimized, with consideration given to capital versus operating (fuel, etc.) expenses and to size.

## Water Injection

Water injection is a method by which the power output of a gas-turbine cycle is materially increased and the efficiency is only marginally increased. In some aircraft-propulsion units and some stationary units, water is injected into the compressor and evaporates as the air temperature rises through the compression process. The heat of vaporization thus reduces the compressed air temperature, reducing the compressor work, an effect similar to that of intercooling (above).

In gas-turbine cycles that have regenerators, water injection is more beneficial if it is injected between the compressor and regenerator [67, 68]. The method can be used on both single- and two-shaft units. Figure 8-15 shows a schematic of a two-shaft unit with water injection between compressor and regenerator. On the  $T$ - $s$  diagram, 1-2-4-5-7-9'-1 represents the cycle without water injection, in which 4 and 9' are the compressed air and exhaust exits of the regenerator, respectively. With water injection the compressed air at 2 is cooled at nearly constant pressure by the evaporating water to 3. (A small increase in pressure does take place from 2 to 3.) The cooled compressed air at 3 is then preheated in the regenerator to a temperature almost the

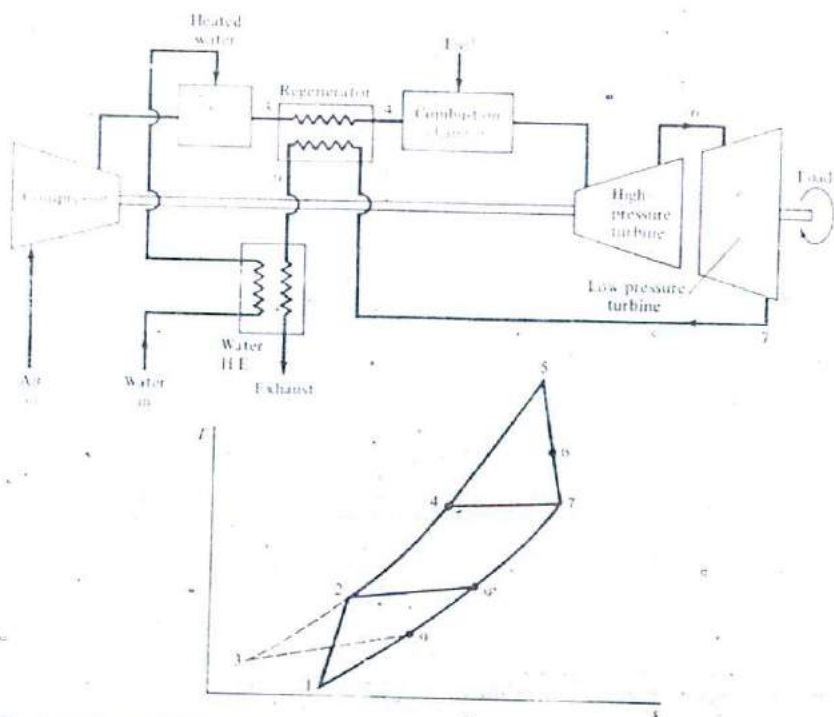


Figure 8-15 Flow and  $T$ - $s$  diagrams of a two-shaft gas-turbine cycle with water injection and regeneration.

same as (actually very slightly below) 4. The added heat required to heat the moist air back from 3 to 2 is obtained from the exhaust gases by heat between 9' and 9, which would have been lost to the cycle in any case. 9, then represents the new exhaust temperature. The inlet water may (as shown) or may not be preheated by the gases at 9 before injection.

The quantity of water vapor to be injected is that which would saturate the compressed air at  $T_3$ . A greater amount of water results in liquid carrythrough which, although it results in somewhat increased work, also results in reduced efficiency compared with that of saturated air and in fouling of the regenerator, local severe temperature differences, and associated thermal stresses.

The increase in work of a turbine plant with water injection is, in part, a result of increased turbine work due to the increased mass-flow rate of air and water vapor without a corresponding increase in compressor work. The increased mass stems from the saturated vapor at point 3 (Fig. 8-15) minus the water vapor originally in the air at point 1. Using Eq. (7-4), this is given by

$$\omega_3 - \omega_1 = 0.622 \left( \frac{P_{v,3}}{P_3 - P_{v,3}} - \frac{P_{v,1}}{P_1 - P_{v,1}} \right) \quad (8-27)$$

where  $\omega_3$  and  $\omega_1$  = mass of water vapor per unit mass of dry air at points 3 and 1, respectively

$P_{v,3}$  and  $P_{v,1}$  = partial pressure of water vapor, saturated at point 3, and function of relative humidity (Sec. 7-5) at point 1

$P_3$  and  $P_1$  = pressure of the air-vapor mixtures at points 3 and 1, respectively;  $P_3$  is very nearly the same as the compressor exit pressure  $P_2$

The temperature at point 3 can be obtained by an energy balance on the dry air and water vapor

$$h_{a,3} - h_{a,2} = (\omega_3 - \omega_1)(h_w - h_{v,3}) \quad (8-28)$$

where  $h_{a,3} - h_{a,2}$  = enthalpy change of dry air

$h_{v,3}$  = enthalpy of saturated vapor of  $T_3$

$h_w$  = enthalpy of injected water

**Example 8-2** Air at 60°F, 14.696 psia, and 60 percent relative humidity is compressed by a compressor with a pressure ratio of 10 and 89.63 percent polytropic efficiency. The air is then saturated by water at 60°F. Find the mass of added water per unit mass of original air and the temperature of the saturated compressed air. For simplicity use  $c_p = 0.24$  Btu/(lb<sub>m</sub> · °F) and  $k = 1.40$  for air.

**SOLUTION** Refer to Fig. 8-14 and use the steam tables (App. A). For  $T_1 = 60$  °F,  $P_{a,1} = 0.25611$  psia, and  $P_{v,1} = 0.6 \times 0.25611 = 0.1537$  psia.

$$\begin{aligned} \text{Thus } \omega_1 &= \frac{0.622 \times 0.1537}{14.696 - 0.1537} = 0.00657 \\ \omega_2 &= \omega_1 = 0.00657 \\ P_2 &= 14.696 \times 10 = 146.96 \text{ psia} \end{aligned}$$

$$\begin{aligned} T_{2,1} \text{ (isentropic compression)} &= (60 + 460)(10)^{1.4 - 1.014} = 1004^\circ\text{R} \\ h_w &= \text{enthalpy of injected water at } 60^\circ\text{F} = 28.06 \text{ Btu/lb}_m \end{aligned}$$

From Eq. (8-16)

$$\frac{1004 - 520}{T_2 - 520} = 0.8963$$

Therefore

$$\begin{aligned} T_2 &= 1060^\circ\text{R} = 600^\circ\text{F} \\ h_{a,3} - h_{a,2} &= c_p(T_3 - T_2) = 0.24(T_3 - 600) \end{aligned}$$

The problem requires a trial-and-error solution. Assume values of  $T_3$  that would satisfy Eq. (8-28):

$T_3, ^\circ\text{F}$	$P_{r,3}$	$\omega_3$ (Eq. 7-4)	$\omega_3 - \omega_1$	$h_{a,3}$	$(\omega_3 - \omega_1)(h_w - h_{a,3})$	$h_{a,3} - h_{a,2}$
220	17.186	0.08237	0.0758	1153.4	-85.30	-91.20
222	17.860	0.08605	0.0795	1154.2	-89.50	-90.72
224	18.556	0.08989	0.0833	1154.9	-93.87	-90.24

By interpolation

$$T_3 = 222.5^\circ\text{F} \quad \omega_3 - \omega_1 = 0.0804$$

Thus the mass increases by 8.04 percent of dry air, or  $0.0804/(1 + \omega_1) = 0.08$ , or 8 percent of original air.

Another reason for the increase in work of a cycle with water injection is that the optimum pressure ratio for work increases. The cycle efficiency, too, is shown to increase, and its optimum pressure ratio also increases, though to a lesser degree than the work [67]. It would thus be advantageous to select a higher pressure ratio to increase the work, provided the cycle efficiency is not disadvantaged.

Another advantage for water injection is that partial load operation could be affected by reduction of the water injection rate while the turbine inlet temperature  $T_3$  is kept constant, which would maintain high efficiency during that portion of the load. When the load drops below that requiring water injection, the turbine inlet temperature is reduced.

The exhaust emissions are also favorably affected by water injection. Emissions of CO and unburned hydrocarbons in gas-turbine powerplants are not significant because of the high air-to-fuel ratios used in them. They become of concern only at very high loads when the air-to-fuel ratios are reduced. The oxides of nitrogen,  $\text{NO}_x$ , however, are becoming a problem in gas-turbine combustion because of the steadily increasing combustion temperatures in modern units. It has been found that water injection reduces  $\text{NO}_x$  by at least half [69].

## 8-5 CYCLE ANALYSIS WITH VARIABLE PROPERTIES

As indicated above, cycle analysis with constant properties—in effect  $c_p$  and  $k$ , which are needed to calculate enthalpies and  $P$ ,  $V$ , and  $T$  relationships—are accurate (except at extremely low temperatures and high pressure) for monatomic gases such as helium. For diatomic gases (air,  $\text{N}_2$ , CO), and more so for triatomic gases ( $\text{CO}_2$ ,  $\text{H}_2\text{O}$  in gas form), and larger molecules ( $\text{NH}_3$ ), the use of constant  $c_p$  and  $k$  yields results that are useful only to predict trends of variables for the particular gas considered. For such gases, a knowledge of the variation of  $c_p$  with temperature is necessary. For air, for example,  $c_p$  in Btu/lb $_m$  $^\circ\text{R}$  is given by [70]

$$c_p = 0.2317 + 9.0083 \times 10^{-6}T + 2.1998 \times 10^{-9}T^2 - 9.0067 \times 10^{-12}T^3 \quad (8-29)$$

The value of the specific heat at constant volume  $c_v$  is obtained by subtracting the gas constant for air, i.e.,  $53.34/778.16 = 0.0685$  from Eq. (8-29). The value of  $k$  as a function of  $T$  is then obtained as  $c_p(T)/c_v(T)$ . The change in enthalpy is obtained by

$$\Delta h = \int_{T_1}^{T_2} c_p(T) dT \quad (8-30)$$

$$\text{or by} \quad \Delta h = \bar{c}_p(T_2 - T_1) \quad (8-31)$$

where  $\bar{c}_p$  is an average specific heat given by

$$\bar{c}_p = \frac{\int_{T_1}^{T_2} c_p(T) dT}{T_2 - T_1} \quad (8-32)$$

To obtain  $P$ ,  $V$ , and  $T$  relationships for polytropic reversible processes an average value of  $k$  should also be found.

Such procedure suffers from two drawbacks: (1) It is complicated, especially when the final temperature of a given process is unknown, and (2) it does not take into account the effects of fuel and combustion products composition and dissociation. In analyzing gas-turbine cycles, it is more convenient to rely on tabulated properties of air and products of combustion and component gases as given in the gas tables by Keenan and Kaye [8]. It is probably best to illustrate the procedure by an example.

**Example 8-3** A single-shaft gas-turbine 25-MW plant has one stage of intercooling, no reheat, and a regenerator. Air enters the compressor at 1 atm and 520°R. The compressor has an overall pressure ratio of 10, and each of its two sections has a polytropic efficiency of 90 percent. The intercooler cools the air back to 520°R. The regenerator has an effectiveness of 75 percent. The air-fuel ratio corresponds to 200 percent of theoretical air. The fuel may be represented by  $\text{CH}_2$ . Because of pressure losses through regenerator and combustion chamber and also at exit, the turbine pressure ratio is 9.2. The turbine inlet temperature is 2500°R. It has a polytropic efficiency of 87 percent. The mechanical efficiency of the system is 95 percent. The electric-generator efficiency is 98 percent. Calculate the various pressures and temperatures around the cycle, the plant efficiency, and the necessary airflow. Estimate the plant efficiency if no regenerator were used.

**SOLUTION** Refer to Fig. 8-16 and the gas tables or App. 1.

(1) *Compressor:*

$$r_p \text{ per section} = \sqrt{10} = 3.1623$$

$$T_1 = 520^\circ\text{R}, P_{r,1} = 1.2147, h_1 = 124.27$$

$$P_{r,2} = 1.2147 \times 3.1623 = 3.8412$$

Therefore

$$T_{2,s} = 722^\circ\text{R} \quad h_{2,s} = 172.88$$

$$\eta_c = 0.9 = \frac{h_{2,s} - h_1}{h_2 - h_1} = \frac{172.88 - 124.27}{h_2 - 124.27}$$

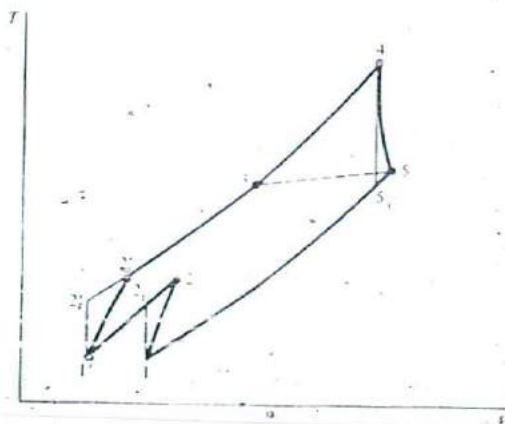


Figure 8-16  $T$ - $s$  diagram of gas-turbine powerplant of Example 8-3.



Therefore

$$h_2 = 178.28 \quad \text{and} \quad T_2 = 744^\circ\text{R} = 284^\circ\text{F}$$

For  $T_1 = 520^\circ\text{R}$ , calculations for the high-pressure section of the compressor 1'-2' are identical to those of the low pressure section 1-2. Thus

$$T_{2'} = 744^\circ\text{R} \quad h_{2'} = 178.28$$

The total work of the compressor is

$$[2(h_2 - h_1)] = 2(178.28 - 124.27) = 2 \times 54.01 = 108.02 \text{ Btu}/(\text{lb}_m \text{ air})$$

(2) *Turbine:*

$$T_4 = 2500^\circ\text{R} \quad p_{r,4} = 559.8 \quad \bar{h}_4 = 19520.7$$

$$p_{r,5} = \frac{559.8}{9.2} = 60.97$$

Therefore

$$T_{5,s} = 1482^\circ\text{R} \quad \bar{h}_{5,s} = 10905.5$$

$$\eta_T = 0.87 = \frac{h_4 - h_5}{h_4 - h_{5,s}} = \frac{19520.7 - \bar{h}_5}{19520.7 - 10905.5}$$

Therefore

$$\bar{h}_5 = 12025.5 \quad \text{and} \quad T_5 = 1620^\circ\text{R}$$

Turbine work is

$$\bar{h}_4 - \bar{h}_5 = 19520.7 - 12025.5 = 7495.2 \text{ Btu}/(\text{lb} \cdot \text{mol})$$

(3) *Regenerator:*

$$\text{Effectiveness } \epsilon_R = \frac{T_3 - T_2}{T_5 - T_2} = 0.75 = \frac{T_3 - 744}{1620 - 744}$$

Therefore

$$T_3 = 1401^\circ\text{R}$$

From the air tables (App. 1)

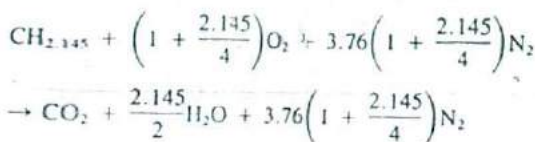
$$h_3 = 343.16 \text{ Btu}/(\text{lb}_m \text{ air})$$

It is now important to base all calculations on the same basis, say 1 lb<sub>m</sub> of air. The enthalpies of the combustion gases are based on 1 lb · mol of components. At 200 percent theoretical air, the molecular mass of the products = 28.880,

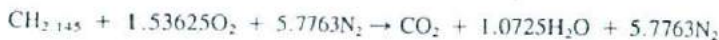
$$\text{therefore} \quad h_4 = \frac{14520.7}{28.88} = 499.7 \text{ Btu}/\text{lb}_m \text{ products}$$

$$\text{and} \quad \text{Turbine work} = \frac{7495.2}{28.88} = 259.5 \text{ Btu}/\text{lb}_m \text{ products}$$

The air-fuel ratio for 100 percent theoretical air is obtained by writing the chemical equation



or



The air-fuel ratio is

$$\frac{1.53625 \times 32 + 5.7763 \times 28}{12 + 2.145} = 14.91$$

For 200 percent theoretical air, air-fuel ratio = 29.82. Thus there are  $1 + 1.29.82 = 1.0335 \text{ lb}_m$  products of combustion per  $\text{lb}_m$  air. Therefore

$$\text{Heat added} = h_4 - h_3 = 675.9 \times 1.0335 - 343.16 = 355.38 \text{ Btu/lb}_m \text{ air}$$

$$\begin{aligned} \text{Net cycle work} &= \text{turbine work} - |\text{compressor work}| \\ &= 259.5 \times 1.0335 - 108.02 = 160.17 \text{ Btu/lb}_m \text{ air} \end{aligned}$$

$$\text{Net plant work} = 160.17 \times 0.95 \times 0.98 = 149.12 \text{ Btu/lb}_m \text{ air}$$

$$\text{Plant efficiency} = \frac{149.12}{355.38} = 0.42 = 42\%$$

Since  $1 \text{ MW} = 3.412 \times 10^6 \text{ Btu/h}$

$$\text{Airflow necessary} = \frac{25 \times 3.412 \times 10^6}{149.12 \times 3600} = 158.9 \text{ lb}_m/\text{s}$$

Without a regenerator the plant efficiency would be approximately  $W_{net}/(h_4 - h_2')$  or

$$\frac{149.12}{675.9 \times 1.0335 - 178.28} \times 100 = 28.65\%$$

The approximation is because, without a regenerator, the turbine pressure ratio would be slightly higher than 9.2 and the plant work and efficiency slightly higher. However, the difference between the thermal efficiencies as calculated is indicative of the large effect of regeneration.

## 8-6 DESIGN FOR HIGH TEMPERATURE

It should be evident by now that it is becoming more necessary to operate gas-turbine plants with higher and higher turbine inlet temperatures to achieve higher efficiencies

and outputs. This also means higher pressure ratios because optimum pressures increase with increasing turbine inlet temperatures for both efficiency and power. High-pressure ratio units have higher capital costs than lower-pressure ones, but the decrease in fuel consumption rapidly pays back for this capital cost differential. Another concern that goes with higher temperatures is increased potential for corrosion, which has to be dealt with. As indicated earlier, research and development is underway to raise turbine inlet temperatures from the present 2000 to 2300°F (1090 to 1260°C) to near 2800°F (1540°C). Such temperatures are well above those that modern steam turbines have to cope with, which are around 1000 to 1200°F (540 to 650°C). The present range is suitable for peaking service, and with regeneration, for cyclic and some base-load service. It is also competitive with steam plants when used in a combined cycle (Sec. 8-7). Future ranges would make them competitive on their own.

There are several approaches to the problems associated with high gas temperatures. In general they can be categorized as developing suitable (1) materials, (2) cooling, and (3) fuels.

### Materials

The components that suffer most from a combination of high temperatures, high stresses, and chemical attack are those of the turbine first-stage fixed blades (nozzles) and moving blades. They must be weldable and castable and must resist corrosion, oxidation, and thermal fatigue. Heat resistant materials and precision casting are two recent advances, largely attributable to aircraft engine developments. Cobalt-based alloys have been used for the first-stage fixed blades (which are subjected to the highest temperatures but not the high stress of the moving blades). These alloys are now being supplemented by vacuum-cast nickel-base alloys that are strengthened through solution- and precipitation-hardened heat treatment. For the moving blades, cobalt-based alloys with high chromium content are now used.

Ceramic materials are also being developed, especially for the turbine inlet fixed blades. Developmental problems here are inherent brittleness, which causes fabrication problems and raises uncertainties about the mechanical properties of ceramic materials.

### Cooling

Early turbines operated uncooled, as do many present-day ones. The increases in temperatures we are witnessing require cooling, however.

The thermal stresses in high-temperature turbine moving blades are caused by the high rotational speeds, uneven temperature distributions in the different blade cross sections, and static and pulsating gas forces that may give rise to dangerous vibrational stresses. Other thermal stresses occur during start-up, shutdown, and load changes. Thermal stresses are thus caused by steady-state as well as transient operation. The latter give rise to low-cycle fatigue, which reduces blade life. In addition there are problems of creep rupture, high-temperature corrosion, and oxidation. It is generally agreed that blade surfaces should be kept below about 1650°F (900°C) to reduce corrosion to a tolerable degree.

A blade is cooled by being made hollow so that a coolant can circulate through

it. A hollow blade is lighter than a solid blade and has a much lower Biot number\* and hence a fairly uniform temperature distribution.

The coolants that have been used and/or are under consideration are air and water (and steam). The ranges for these are air for gas temperatures up to about 2100°F (1150°C), water for gas temperatures above 2400°F (1315°C), and a hybrid system for the intermediate range. In the hybrid system, water cooling is used for the highest temperature components, mainly the inlet fixed blades, and air for the remaining blades and rotor [71].

### Air Cooling

Air cooling is of three kinds: convection cooling, film or transpirational cooling, and impingement cooling. Cooling air is obtained directly from the compressor, thus bypassing the combustion chamber. In *convection cooling* the air is made to flow inside the hollow blade, entering at the leading edge, reversing direction a few times, and leaving at the trailing edge to enter the main gas stream. *Film cooling* is used in conjunction with convection cooling and never alone. Based on aerospace technology, it involves air flowing through holes or slots from the inside of the blade to the outside boundary layer to form a protective insulating film between the blade and the hot gases. Besides the cooling effect, it also helps prevent corrosion of the blades. This transpirational air must be very clean for proper effectiveness.

Figure 8-17 shows an example of air cooling on inlet fixed blades [72]. The upper vertical cross section shows air entering at the top from the stator. It then flows downward by the leading edge in two parallel paths, changes direction three or four times, and leaves at the trailing edge. The middle path includes longitudinal ribs or fins to enhance heat transfer. Other designs may include roughened internal surfaces and transverse ribs and webs. A good design should allow good heat transfer with little pressure drop.

The middle horizontal cross section through the blade (Fig. 8-17b) shows the internal paths in pure convection cooling. The lower horizontal cross section (c) shows two rows of holes A and B on the suction side of the blade for film cooling.

For the moving blades (Fig. 8-18), the cooling air enters the blade root from the rotor, flows radially through ducts in the hollow blade, changes direction, and leaves through slots from the blade trailing edge. Figure 8-18 shows three such ducts, one change of direction, and several exit slots.

The third method, *impingement cooling*, is one in which the cooling air is made to impinge on the internal surface of the blade, which provides particularly intensive cooling.

\* In transient heat transfer between a solid body and a fluid, a low Biot number ( $Bi$ ) indicates a more uniform temperature distribution within the body than a high Biot number.  $Bi$  is given by  $hL/k$ , where  $h$  is the heat-transfer coefficient,  $L$  is a characteristic length of the body, in this case the blade wall thickness, and  $k$  the thermal conductivity of the material of the body. A Biot number less than 0.1 means that all parts of the body are at the same temperature at any one instant of time and that the body can be treated as a lumped capacity in transient heat-transfer analysis.

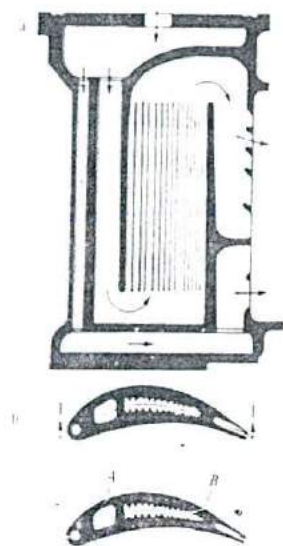


Figure 8-17 Air-cooled gas turbine fixed blade [72]

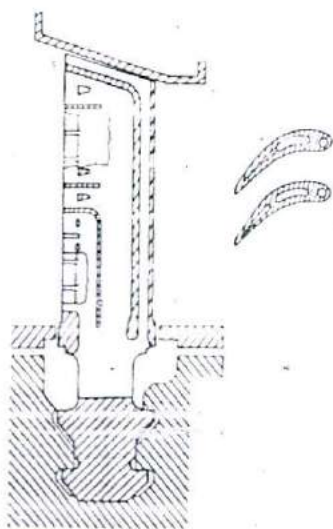


Figure 8-18 Air-cooled gas turbine moving blade [72]

A blade-cooling effectiveness  $\epsilon_{bc}$  is defined as

$$\epsilon_{bc} = \frac{T_g - T_b}{T_g - T_{a,i}} \quad (8-33)$$

where

$T_g$  = gas temperature

$T_b$  = mean blade surface temperature

$T_{a,i}$  = inlet cooling air temperature

$\epsilon_{bc}$  has been found to be a function of a dimensionless parameter  $B$ , given by

$$B = \frac{\dot{m}_a c_{p,a}}{h_g A_b}$$

where

$\dot{m}_a$  = mass-flow rate of air, lb<sub>m</sub>/h or kg/s

$c_{p,a}$  = specific heat of air, Btu/(lb<sub>m</sub> · °F) or J/(kg · °C)

$h_g$  = average heat-transfer coefficient of gas, Btu/(h · ft<sup>2</sup> · °F) or  
W/m<sup>2</sup> · °C

$A_b$  = blade surface area, ft<sup>2</sup> or m<sup>2</sup>

It is to be noted that calculation of  $h_g$  is not a simple matter, especially when film or impingement cooling is involved; the calculation requires elaborate computer programs and needs to be supplemented by experimental data. Local values between 200 and 500 Btu/(h · ft<sup>2</sup> · °F) [1.1 to 2.8 kJ/(m<sup>2</sup> · °C)] have been reported [72]. Figure 8-19 shows a plot of  $\epsilon_{bc}$  versus  $B$ . It shows that combined convection and film cooling is superior, followed by impingement and then convection cooling. It is believed that combined convection and film (transpirational) cooling offers the most promise for air-cooling schemes and permits an increase in turbine inlet-gas temperatures by about 120°F (67°C).

## Water Cooling

As gas temperatures exceed 2100°F (1150°C) or so, air cooling reaches a state of rapidly diminishing returns because of the quickly increasing demand for cooling air that bypasses the combustion chamber. Despite their additional equipment requirements, the regions of hybrid and pure water cooling are reached, with the latter holding the greatest promise for gas temperatures of 2400°F (1315°C) and beyond. The higher heat capacity and heat-transfer capability of water permit lower metal gas temperatures (for the same gas temperatures) and hence reduced hot corrosion and deposition from contaminated fuels. Water cooling also eliminates the need for air passages through the blades, as in film cooling, which would be subject to plugging by such fuels. A test program sponsored by EPRI (the Electric Power Research Institute) using heavy ash-bearing fuels showed metal temperatures below 850°F (450°C) and reduced ash accumulation on the blades with water cooling [71].

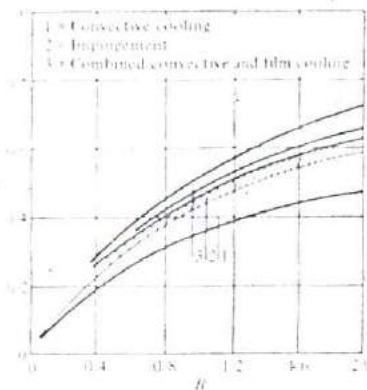


Figure 8-19 Comparison of different processes of blade cooling [72].

In designing a gas turbine for water cooling, standard aerodynamic design is followed but the hot gas paths are kept as short as possible to minimize surface areas that require cooling. The fixed blades or nozzles are hollow and contain series and parallel water-flow paths (not unlike air-cooled blades). In one turbine design [71], cooling water circulates in, through, and out of these paths in a closed loop. Heat removed from these blades is recovered in a heat exchanger for use in the steam portion of a combined-cycle plant (below). The inlet water is hot enough to prevent thermal shock and is at a pressure high enough (about 1250 psia, 86 bar) to prevent boiling and keep the water in single phase. In that design, the first-stage fixed blades are of composite construction with a core of high-strength material (Nitronic 50), a surrounding copper matrix in which water-cooling tubes are imbedded, and a covering skin, all bonded by hot isostatic pressing. Second- and third-stage fixed blades are cast IN-718 with drilled water paths. Such blades have been manufactured and successfully tested at operating conditions.

Moving blades are cooled by an open-loop water system. Water enters the blades at lower pressures and is allowed to boil, with steam ejecting from the blade tips to mix with the hot gas stream. Unvaporized water moves radially by centrifugal force and may be collected in a circumferential cavity in the casing (Fig. 8-20) [73]. Closed-loop systems are being considered but pose some design difficulties. The moving blades in the above design are forged from IN-718, with the cooling paths drilled after forging.

## Fuels

The advantages of increased gas-turbine combustion temperatures—that is, increased efficiency, power, and reduced fuel consumption—are partly negated by the increasing cost of fuels normally used by gas turbines. So far gas turbines have relied primarily on natural gas and clean liquid fuels. Natural gas now is being conserved for domestic use, and liquid hydrocarbons have increased in cost by an order of magnitude during

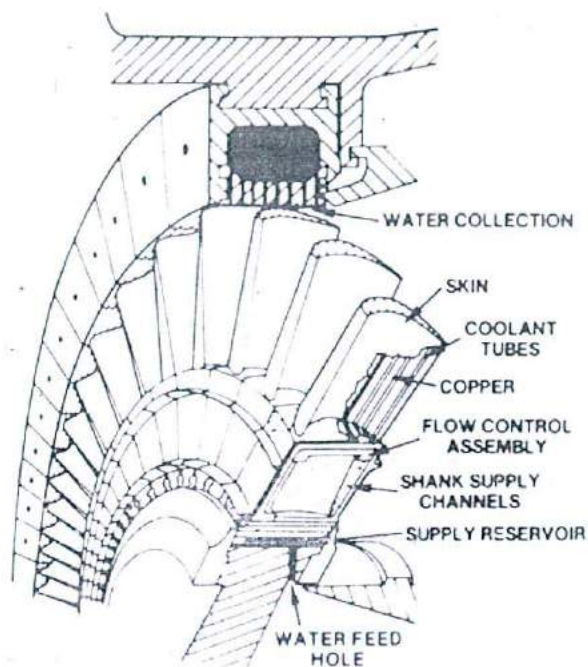


Figure 8-20 A water-cooled gas-turbine moving blade [73].

the decade of the 1970s alone. By contrast steam powerplants are making increasing use of various abundant coal-combustion systems (Chap. 5) and cheap nuclear fuels.

Residual liquid fuels, the residue left after the profitable light fractions have been extracted from the crude, have been used in gas turbines to some extent [74]. They are (1) viscous and (2) tend to polymerize (form sludge or tar) when overheated. (3) Their high carbon content leads to excessive carbon deposits in the combustion chamber. (4) Their contents of alkali metals, such as sodium, combine with sulfur to form sulfates that are corrosive. (5) They have other metals like vanadium with compounds that form during combustion also being corrosive. (6) They have a relatively high ash content that deposits mostly on the inlet fixed blades, thus reducing gas flow and power output.

The rate of corrosion increases with increasing gas temperatures. Early turbines designed for residual fuel use operated at temperatures below 1650°F (900 K) to avoid the problem. Ash deposition is not a problem with intermittent operation because of successive expansions and contractions, but it is a serious problem with steady operation.

Fortunately progress is being made at keeping gas turbines competitive by the development of systems that prepare cheaper lower-grade fuels for gas-turbine use



[75]. Washing the fuel with water and separating the mixture with centrifugal or electrostatic separators is found to remove the alkalis. Fuel additives such as magnesium have been found to neutralize vanadium. Additives and protective coatings are also used to reduce corrosion [76].

A promising scheme is pressurized-fluidized-bed combustion (PFBC) (Sec. 4-8), which makes cheap, abundant coal readily available as a gas-turbine fuel. In the PFBC, the addition of limestone will remove enough sulfur to meet environmental regulations. However, much development work remains to be done in order to reduce particulate matter from the fluidized-bed gaseous product, which can rapidly destroy turbine blading. Other alternatives (for coal use) are the use of synthetic fuels from coal gasification and liquefaction. A low-Btu gas use in a combined cycle has already been discussed in Sec. 4-11.

## 8-7 COMBINED CYCLES: GENERAL

Combined-cycle powerplants are those which have both gas and steam turbines supplying power to the network. The idea of combined cycles has grown out of the need to improve the simple Brayton-cycle efficiency by utilizing the waste heat in the turbine exhaust gases. This, as we have seen, can be done by regeneration (Sec. 8-4). Regeneration reduces the heat lost up the stack down from some 70 to 60 percent of the energy input. The sole purpose of a regenerator is to improve efficiency; it does not increase the power output. In fact, because of additional pressure losses it imposes on the plant, a regenerator reduces the turbine pressure ratio and hence the net plant output by a few percent. Aside from this small reduction in power output, regenerators with their large heat-exchange surfaces and large gas and air piping make the plant more costly. Another effect is that the optimum pressure ratio for maximum efficiency moves sharply to lower values with regeneration, resulting in reduced power as can be seen from Figs. 8-10 and 8-11.

Simple cycles operate near maximum power because they are not used in service where efficiency is the prime concern. Regenerative cycles, however, are meaningful only if they are operated near maximum efficiency. Thus they would have their output reduced from a simple cycle by a much larger percentage, perhaps 10 to 14 percent. In certain applications, an economic compromise between capital and operating costs would have to be found.

It can be seen that raising the efficiency of a gas-turbine plant by regeneration, while used for stationary applications, is costly. A means, therefore, was sought whereby both efficiency and power are increased. The solution was found in using the large quantity of energy leaving with the turbine exhaust to generate steam for a steam-turbine powerplant. This is a natural solution as the gas turbine is a relatively high-temperature machine (2000 to 3000°F, 1100 to 1650°C), whereas the steam turbine is a relatively low-temperature machine (1000 to 1200°F, 540 to 650°C). This joint operation of the gas turbine at the "hot end" and the steam turbine at the "cold end," is called a combined-cycle powerplant.

Besides both high efficiency and high power outputs, combined cycles are char-

acterized by flexibility, quick part-load starting, suitability for both base-load and cyclic operation, and a high efficiency over a wide range of loads. They have the potential of using coal [77] as well as synthetic and other fuels. Their obvious disadvantage is in their complexity, as they in essence combine two technologies in one powerplant complex.

The idea of combined cycles is not new, having been proposed as early as the beginning of this century. It was not, however, until 1950 that the first plant was installed. This was followed by a rapid rise in the number of installations, especially in the 1970s. An estimated 100 plants, with a total of 150,000-MW output, had been installed by the end of the 1970s throughout the world [78].

There have been many suggested types of combined cycles, the most important of which comprise:

1. A heat-recovery boiler with or without supplementary firing
2. A heat-recovery boiler with regeneration and/or feedwater heating
3. A heat-recovery boiler with multipressure steam cycle
4. A closed-cycle gas turbine with steam-cycle feedwater heating

Some examples of these are presented next.

## 8-8 COMBINED CYCLES WITH HEAT-RECOVERY BOILER

Figure 8-21 shows a schematic flow diagram of such a combined cycle. A simple gas-turbine cycle, consisting of air compressor (AC), combustion chamber (CC), and gas turbine (GT) is used with the turbine exhaust gas going to a *heat-recovery boiler* (HRB) to generate superheated steam. That steam is used in a standard steam cycle, which consists of turbine (ST), condenser (C), pump (CP), closed feedwater heaters (FWH), and deaerating heater (DA). The HRB consists of an economizer (EC), boiler (B), steam drum (SD), and superheater (SU). The gas leaves the HRB to the stack. Both gas and steam turbines drive electric generators (G).

The gas turbine is usually operated with a high air-fuel ratio, approximately 400 percent theoretical air, to make sufficient air available in the gas-turbine exhaust for further combustion.

For low-powered combined cycles the steam-turbine output is less than the gas-turbine output, by as much as 50 percent, and the number of feedwater heaters is small, often one deaerator and one closed-type. To increase the output for short periods during load peaks, supplementary fuel burners may be fitted to the HRB to increase the steam mass-flow rate. This can also be done on a continuous basis, but limits on the amount of fuel added are posed by the design of the HRB, which usually lacks refractory lining, water-cooled walls, etc. A limit of about 1400°F (760°C) on the gas temperatures in the HRB is common. This however, is usually sufficient to increase the steam-turbine output by perhaps 100 percent and the total cycle output by 30 percent.

In large combined-cycle plants used for base-load operation, where efficiency is

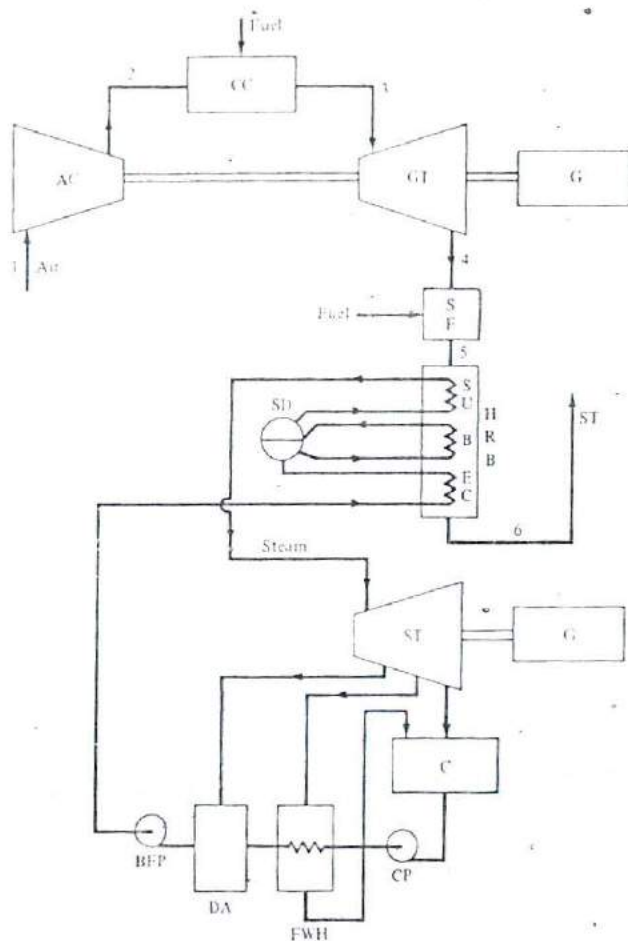


Figure 8-21 Schematic flow diagram of a combined cycle with heat-recovery boiler (HRB).

of prime importance, separate supplementary firing equipment (SF) is interposed between the gas turbine and the HRB. The steam-turbine output is usually greater than the gas-turbine output by up to 8:1. The steam cycle is therefore designed for high efficiency with reheat and a full complement of feedwater heaters. A forced-draft fan may be installed ahead of the SF to operate the steam cycle on its own when the gas turbine is cut off.

The fuel used in supplementary firing may be the same high-grade fuel used in the gas turbine. This is the simplest solution as such fuel causes few problems in the

SF and HRB. However, cheaper lower-grade fuels such as heavy oil or coal, can also be used in the SF.

**Example 8-4** A combined cycle as shown in Fig. 8-20 with supplementary firing has gas-turbine cycle fuel represented by  $\text{CH}_2_{1.45}$ , air-fuel ratio corresponding to 400 percent of theoretical air, gas-turbine inlet temperature of  $2600^\circ\text{R}$ , pressure ratio of 8, and a polytropic efficiency of 0.90. Supplementary firing using the same fuel raises the gas temperature to  $2000^\circ\text{R}$  before entering the heat-recovery boiler. The gas leaves to the stack at  $800^\circ\text{R}$ . Steam is generated at 1200 psia and  $1560^\circ\text{R}$  from feedwater at  $780^\circ\text{R}$ . Calculate the heat added in supplementary firing, Btu/lb<sub>m</sub> of air, and the mass ratio of airflow to steam flow.

**SOLUTION** Use the gas tables for 400 percent theoretical air (App. I) and refer to Fig. 8-22.

$$T_{1,3} = 2600^\circ\text{R} \quad p_{r,3} = 586.4 \quad \bar{h}_3 = 19979.7 \text{ Btu/(lb} \cdot \text{mol gas)}$$

$$p_{r,4} = \frac{p_{r,3}}{8} = 73.3 \quad T_{4,3} = 1579^\circ\text{R} \quad \bar{h}_3 = 11499.0$$

$$\eta_p = 0.9 = \frac{\bar{h}_3 - \bar{h}_4}{\bar{h}_3 - \bar{h}_{4,3}} = \frac{19979.7 - \bar{h}_4}{19979.7 - 11499.0}$$

Therefore

$$\bar{h}_4 = 12347.1 \text{ Btu/(lb} \cdot \text{mol gas)} \quad T_4 = 1685 \text{ R}$$

Assume that supplementary firing changes the mixture from 400 percent at 4 to 200 percent of theoretical air at 5 (use the gas tables for 200 percent theoretical air).

$$T_5 = 2000^\circ\text{R} \quad \bar{h}_5 = 15189.3 \text{ Btu/(lb} \cdot \text{mol gas)}$$

$$T_6 = 800^\circ\text{R} \quad \bar{h}_6 = 5676.3 \text{ Btu/(lb} \cdot \text{mol gas)}$$

From Example 8-3, the air-fuel ratio (A-F) for stoichiometric mixture of  $\text{CH}_2_{1.45}$  fuel is 14.91. The products-to-air mass ratio is  $1/(1 + 1/\text{A-F})$ . This is 1.6335 for

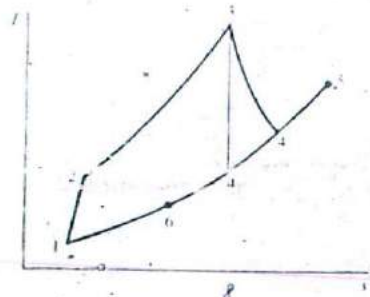


Figure 8-22  $T$ - $s$  diagram for the gas in Example 8-4.

200 percent and 1.0168 for 400 percent theoretical air. Also, the molecular masses for these products are 28.880 and 28.925, respectively. Based on 1 lb<sub>m</sub> of air

$$h_4 = \frac{12,347.1}{28.925} \times 1.0168 = 434.04 \text{ Btu/lb}_m \text{ air}$$

$$h_5 = \frac{15,189.3}{28.880} \times 1.0335 = 543.56 \text{ Btu/lb}_m \text{ air}$$

and

$$h_6 = \frac{5676.3}{28.880} \times 1.0335 = 203.13 \text{ Btu/lb}_m \text{ air}$$

Therefore, heat added in SF =  $h_5 - h_4 = 543.56 - 434.04 = 109.52$  Btu/lb<sub>m</sub> air and, heat added in HRB =  $h_5 - h_6 = 543.56 - 203.13 = 340.43$  Btu/lb<sub>m</sub> air.

For steam entering turbine,  $h = 1556.9$  Btu/lb<sub>m</sub> steam. For feedwater entering the HRB,  $h = 290.4$  Btu/lb<sub>m</sub> steam. Therefore

$$\Delta h_{\text{steam}} = 1556.9 - 290.4 = 1266.5 \text{ Btu/lb}_m \text{ steam}$$

So

$$\text{Mass ratio of air to steam} = \frac{340.43}{1266.5} = 0.269$$

Variations of the cycle shown in Fig. 8-21 are used to extract the maximum amount of energy from the gas leaving the heat-recovery boiler before exhausting it to the stack. Depending upon the temperature of that gas, it may be used for (1) partial heating (regeneration) of the compressed air leaving the compressor, (2) feedwater heating of the steam cycle in a closed-type feedwater heater, or (3) generating steam in a dual- or multipressure steam cycle. This last variation is described in Sec. 8-10.

Because gas turbines are not yet built in sizes as large as steam turbines, combined cycles are often built in combinations of more than one gas turbine plus one steam turbine. Such combinations show certain advantages, not only in higher total plant output but also in higher availability, flexibility in service, and part-load efficiency. An example is the STAG powerplant, described next.

## 8-9 THE STAG COMBINED-CYCLE POWERPLANT

The STAG (for steam and gas) 330-MW combined-cycle powerplant [79] is a cyclic plant built for the Jersey Central Power and Light Company. It is located at the Gilbert Generating Station on the Delaware River, south of Phillipsburg, N.J.

The plant was designed by the General Electric Company and is composed of four GE M801-7000 gas turbines exhausting to supplementary firing in the form of auxiliary burner sections within four heat-recovery boilers. The HRBs generate su-

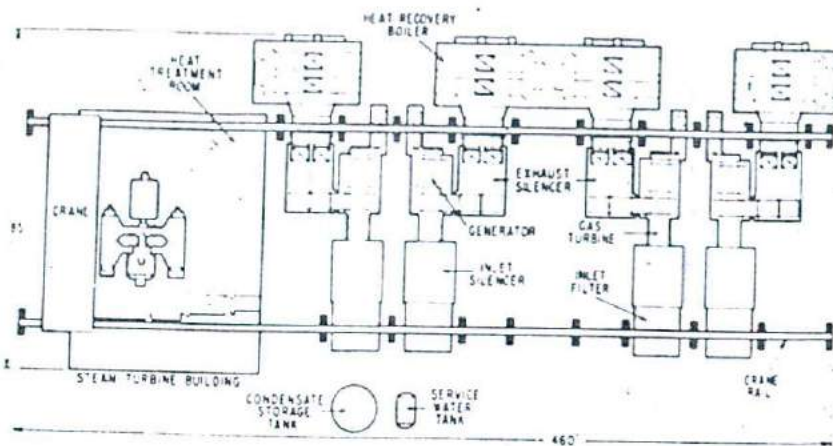


Figure 8-23 Layout of the STAG combined-cycle plant [72].

perheated steam for one steam turbine. The steam plant feedwater system includes one low-pressure closed-type feedwater heater with drain cascaded to the condenser and one open-type deaerating feedwater heater. The plant flow diagram can be schematically represented by Fig. 8-21, except that there are four gas turbines. Figure 8-23 shows the STAG plant layout. The plant data follow.

Gas turbines:	Four GE Model 7000, each rated at 49.5 MW base and 54.9 MW peak at 80°F (27°C) inlet.
Turbine exhaust:	970°F (521°C). Dampers used to bypass gas to atmosphere when operating alone, or to direct gas to the HRB when operating in combined-cycle mode. Silencers are located ahead of bypass stack and HRB.
HRB:	Four, single-pressure, burner-and-steam-generator sections are factory-assembled modules [80] for site erection. Forced-recirculation in boiler section.
Feedwater:	267°F (130°C) at economizer inlet.
Steam:	1250 psig (87 bar), 950°F (510°C), 995,200 lb <sub>m</sub> /h (125 kg/s).
Steam turbine:	One high-pressure and one double-flow low-pressure, tandem-compound sections, nonreheat, rated at 129.6 MW with 3.5 inHg (0.12 bar) back pressure.
Fuel:	No. 2 distillate oil initially. Corrosion-resistant first-stage gas-turbine materials allow future use of heavier fuel.

STAG, as most combined cycles, has operational flexibility. Each of the four gas turbines and the steam turbine may be started, controlled, and loaded independently from a centralized control room. Either one or more gas turbines may be operated,

each with or without its HRB and with its HRB supplementary fired or unfired. Gas-turbine start-ups are staggered by 30 s. Interlocks will prevent steam-turbine starting if no HRBs are operational. Steam pressures of 600, 800, 1000, and 1250 psig are used with 1, 2, 3, and 4 gas turbines and HRBs, respectively. The total gas-turbine output of 198 MW is available within 30 min and the total plant output of 330 MW within 1 hour after an overnight shutdown.

The efficiency and operational flexibility of the plant are illustrated by the heat-rate curves of Fig. 8-24. The top four short curves are indicative of operation on 1, 2, 3, 4 gas turbines, exhausting to the atmosphere, respectively. They have a heat-rate range of 13,000 to 13,500 Btu/kWh, which corresponds to thermal efficiencies of 26.3 to 25.3 percent. The curves labeled *F* are for part load combinations with the steam turbine and minimum HRB firing. Other notations are as explained in the table. It can be seen that best heat rate, at point *A*<sub>1</sub>, for peak loads and full HRB firing, is 8700 Btu/kWh corresponding to 39.2 percent efficiency.

Because STAG is partly a gas-turbine plant, the cooling-tower and circulating-water makeup requirements are about half those of a conventional steam-cyclic plant of the same output. STAG had a short lead time from order to operation and was budgeted at \$53,300,000, corresponding to about \$160/kW capital cost.

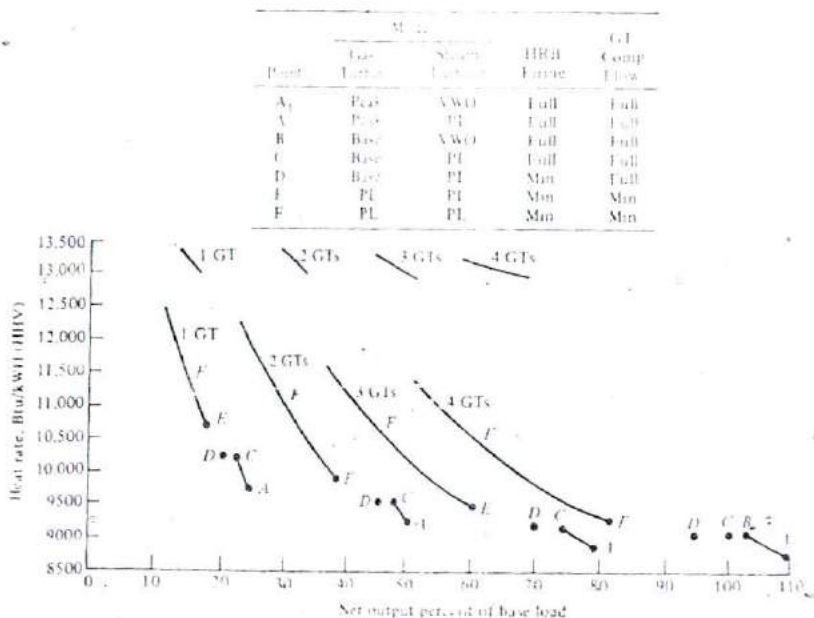


Figure 8-24 STAG combined cycle powerplant heat rates as a function of number of turbines, mode of operation and plant load. Data for 80°F air and 3.5 inHg condenser pressure [72]. VWO = very-wide-open throttle, PL = part load.

Another U.S. built combined-cycle plant is PACE, built for the St. Joseph Power and Light Company of northwestern Missouri [81].

## 8-10 COMBINED CYCLES WITH MULTIPRESSURE STEAM

A combined cycle with multipressure steam reduces the temperature of the gas leaving the heat-recovery boiler and hence results in increased efficiency of the plant as a whole. With steam cycles operating around 1300 psia (90 bar), saturation temperatures around 575°F (300°C), and feedwater into the HRB at about 265°F (130°C), the gas temperature leaving the HRB to the stack is still at about 300 to 400°F (150 to 200°C). Some of the energy leaving with that gas can be utilized in a multipressure steam cycle. The simplest such cycle is a dual-pressure\* one, although triple-pressure cycles have been considered.

A *dual-pressure cycle* (Fig. 8-25) shows a heat-recovery boiler with two steam circuits in it. One, a high-pressure circuit, feeds steam to the steam turbine at its inlet; the other, a low-pressure circuit, feeds steam to the same turbine at a lower-pressure stage. A corresponding temperature-enthalpy diagram of both gas and steam circuits in the HRB is shown in Fig. 8-26.

Exhaust gas leaving the gas turbine enters supplementary firing (SF) at 4 and the heat-recovery boiler (HRB) at 5, leaving it to the stack (ST) at 6. Condensate leaves the steam condenser (C) at 8 and enters the condensate pump (CP) and two closed-type feedwater heaters (FWH) and one open-type deaerating heater (DA). It then enters the boiler feed pump (BFP) at 9, where it is pumped to 10 to a lower pressure than that of steam maximum. Process 10-11 is feedwater heating in a low-pressure economizer, followed by evaporation to 12 and superheat to 13. Superheated low-pressure steam at 13 enters the steam turbine at a low-pressure stage.

Water from the low-pressure steam drum at 11 is pumped by a booster pump (BP) to 14 and goes to the high-pressure economizer. Evaporation occurs from 15 to 16 and superheat to 17. High-pressure superheated steam at 17 enters the steam turbine first stage.

It can be seen from the *T-H* diagram (Fig. 8-26) that low-pressure steam boils at a temperature (12) below that of high-pressure steam (16), and hence there are two pinch points between the gas line and the saturated steam lines. It can also be seen that a single high-pressure steam circuit would be represented by 10'-15-16-17 with gas leaving to the stack at 6'. Adding the low-pressure circuit allows the gas to leave at a lower temperature (6), thus extracting more energy from it and increasing the overall cycle efficiency.

An example of a dual-pressure combined cycle is the Donge-Geertruidenberg plant of PNEM in Holland [78]. It has a gas-turbine output of 76.7 MW and a steam-turbine

\* The idea is not unique to combined cycles. Low-temperature gas-cooled-reactor powerplants of the British Magnox type (Sec. 10-11) have used dual-pressure cycles for a similar purpose. An early boiling-water-reactor powerplant (Dresden I) used dual pressure, but for a different purpose [3].



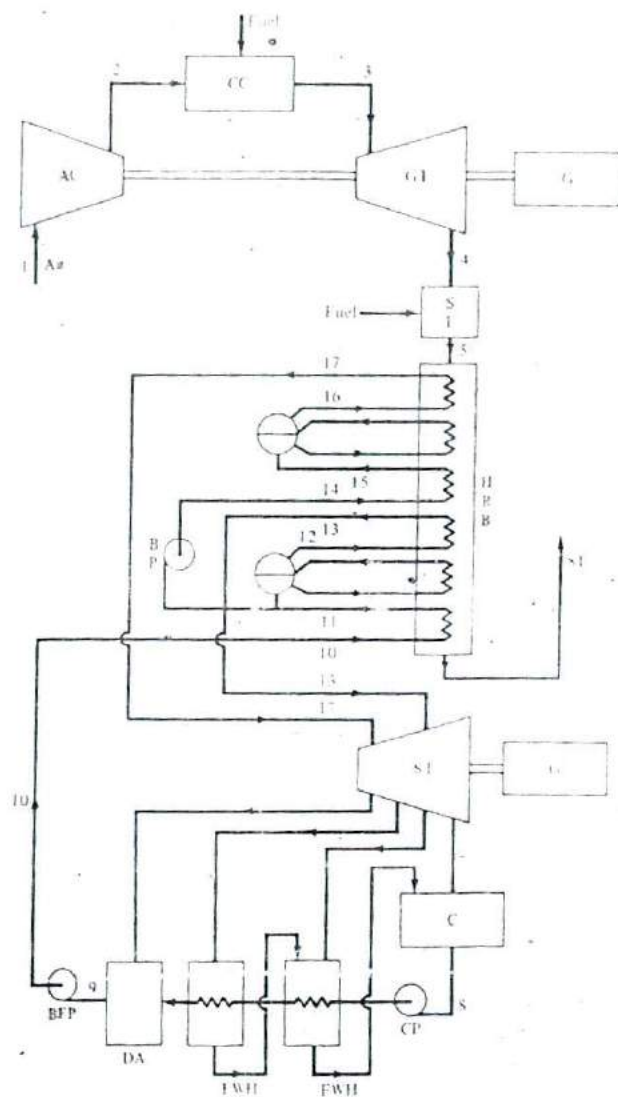


Figure 8-25 A schematic diagram for a dual-pressure combined cycle

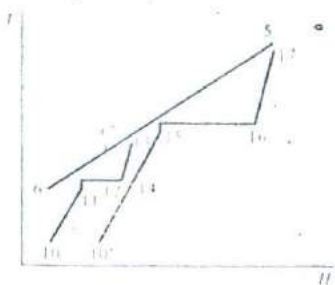


Figure 8-26 Temperature enthalpy ( $T-H$ ) diagram of the heat recovery boiler of the dual pressure combined cycle shown in Fig. 8-25.

output of 47.3 MW and attains a remarkable 46.1 percent efficiency at standard air conditions of  $15^{\circ}\text{C}$  ( $59^{\circ}\text{F}$ ) and 1 atm, with only one DA feedwater heater.

A proposed triple-pressure combined cycle generates steam at an intermediate pressure between the two steam-turbine inlets. This steam is injected into the gas-turbine combustion chamber to reduce nitrogen oxide emissions to meet  $\text{NO}_x$  rigid standards, if applicable. The water, thus lost, must of course be continually made up.

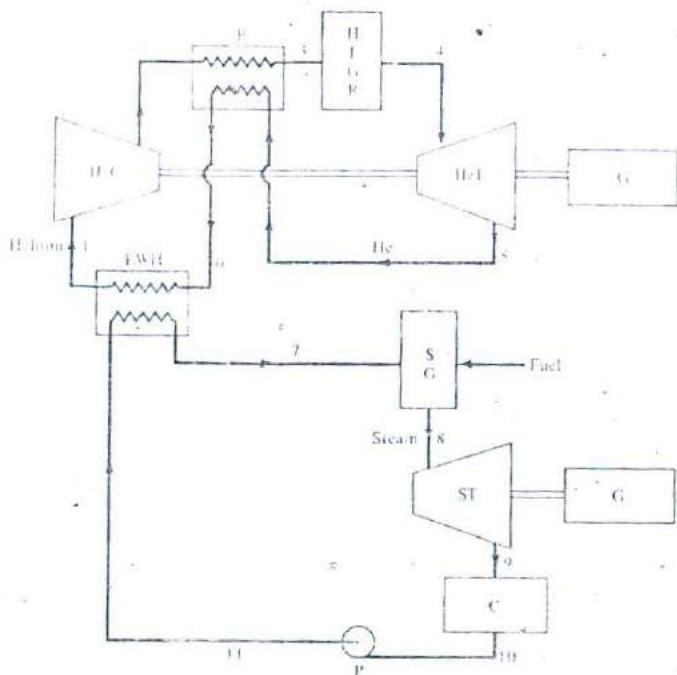


Figure 8-27 A schematic diagram of a combined cycle with a nuclear gas turbine and fossil-fuel-fired steam turbine [75].

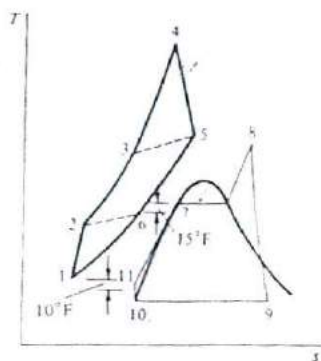


Figure 8-28  $T$ - $s$  diagrams of helium and steam cycles shown in Fig. 8-27.

## 8-11 A COMBINED CYCLE FOR NUCLEAR POWERPLANTS

A combined cycle for nuclear plants [82] presupposes that a high-temperature gas-cooled nuclear reactor (HTGR) (Sec. 10-12) is the heat source for the gas-turbine cycle. Such a reactor-turbine combination uses helium gas as the reactor coolant and gas-turbine cycle working fluid in a closed cycle.

Helium at 1 (Figs. 8-27 and 8-28) is compressed in a helium compressor (HeC) to 2. It is then preheated in a regenerator (R) to 3, enters the HTGR, and leaves at 4 at 1435 to 1470°F (780 to 800°C). It expands in the helium turbine (HeT) to 5 and enters the regenerator. The energy left in the gas at 6 is finally transferred to the steam cycle in a closed-type steam feedwater heater (FWH). The helium, back at 1, reenters the helium compressor.

The steam cycle is fairly standard. Feedwater leaves the FWH at 7, enters the fossil-fueled steam generator (SG), and leaves it as superheated steam at 8. This expands in the steam turbine (ST) and enters the condenser at 9. Condensate at 10 is pumped by pump (P), after which it enters the FWH to repeat the cycle.

It can be seen that the gas and steam cycles are coupled only by the FWH, that the heat generated in the HTGR is completely utilized in both cycles, and that heat is rejected only in the steam condenser.

## PROBLEMS

8-1 Show that the efficiency of an ideal Brayton cycle at the optimum pressure ratio is a function of minimum and maximum temperatures only, and independent of the working fluid.

8-2 It is required to compare the optimum pressure ratios and corresponding efficiencies of three ideal Brayton cycles using air, helium, and carbon dioxide as working fluids. The minimum and maximum temperatures are 10°C and 1115°C, respectively. Use properties at low temperatures.

8-3 A gas turbine cycle operates with air only with a constant specific heat of 0.24 Btu/lbm · R. The inlet air is at 14.696 psia and 60°F. The maximum cycle temperature is 1800°F. The compressor and turbine have the same pressure ratio of 8 and polytropic efficiencies of 0.85. A regenerator with 75 percent

effectiveness is considered. Calculate (a) all temperatures around the cycle, in degrees Fahrenheit, (b) the efficiency of the cycle, in percent, (c) the heat added, in Btus per hour, to produce 10-MW power, (d) the efficiency of the cycle if no regenerator is used, (e) the efficiency of a comparable ideal cycle with a perfect regenerator.

**8-4** A Brayton cycle operating on air only with a constant  $c_p = 0.24 \text{ Btu/lb}_m \cdot ^\circ\text{R}$ , has compressor and turbine polytropic efficiencies of 0.8 and 0.9, respectively, and the same pressure ratio of 6.0. The inlet and maximum temperatures are 40 and 1940°F, respectively. A regenerator with 85 percent effectiveness is used. Calculate (a) the net work, in  $\text{Btu/lb}_m$ , (b) the cycle efficiency, and (c) the air mass flow rate for a 20-MW output.

**8-5** A Brayton cycle uses helium as a working fluid with a mass flow rate of 200  $\text{lb}_m/\text{s}$ . The compressor and turbine polytropic efficiencies are 0.8 and 0.9 and their pressure ratios are 2.5 and 2.4, respectively. The inlet and maximum temperatures are 100 and 2000°F, respectively. A regenerator with 85 percent effectiveness is used. Calculate (a) the cycle efficiency, (b) the percent improvement in cycle efficiency due to regeneration, and (c) the cycle power, in megawatts.

**8-6** A helium gas turbine cycle has compressor and turbine polytropic efficiencies of 0.8 and 0.9 and pressure ratios of 2.5 and 2.4, respectively. The compressor has one stage of intercooling and the turbine has one stage of reheat. The cycle has a regenerator with 85 percent effectiveness. The cycle minimum and maximum temperatures are 100 and 2000°F, respectively. Calculate (a) the cycle efficiency, and (b) the cycle power for a helium mass flow rate of 200  $\text{lb}_m/\text{s}$ .

**8-7** Air at 14.696 psia, 40°F, and with 65 percent relative humidity enters the compressor of a gas turbine cycle. The compressor and turbine have the same pressure ratio of 6 and polytropic efficiencies of 0.80 and 0.90, respectively. Water at 60°F is injected into the compressor exit air, saturating it. Calculate (a) the air temperature after water injection, (b) the percent increase in mass flow rate due to water injection, (c) the compressor work in Btus per pound mass of original air, and (d) the compressor work if water is injected during the compression process to the same temperature as (a), in Btus per pound mass of original air. Use a constant  $c_p = 0.24 \text{ Btu/lb}_m \cdot ^\circ\text{R}$ .

**8-8** Air at 14.696 psia, 40°F, and with 65 percent relative humidity enters the compressor of a gas turbine cycle. The compressor and turbine have the same pressure ratio of 6 and polytropic efficiencies of 0.80 and 0.90, respectively. Water at 60°F is injected into the compressor exit air, saturating it. The air then goes through an 85 percent effective regenerator. The turbine inlet temperature is 1940°F. Calculate (a) the heat added, in Btus per pound mass of original air, (b) the cycle efficiency, (c) the original air mass flow rate, in pound mass per hour, for a 20-MW net cycle output, and (d) the necessary water injection rate, in pound mass per hour. For simplicity, use a constant  $c_p = 0.24 \text{ Btu/lb}_m \cdot ^\circ\text{R}$ . Compare these results with those of Prob. 8-4 that have the same data but no water injection.

**8-9** A simple Brayton cycle without regeneration, intercooling or reheat has compressor and turbine pressure ratios of 9.286 and 8.276, polytropic efficiencies of 0.862 and 0.904, and minimum and maximum temperatures of 40 and 2040°F. Air enters the compressor at the rate of  $6 \times 10^6 \text{ lb}_m/\text{h}$ . The combustion gases correspond to 400 percent theoretical air. Find the net cycle power, in megawatts, and cycle efficiency using (a) a constant specific heat of  $0.24 \text{ Btu/lb}_m \cdot ^\circ\text{R}$  and constant  $k = 1.4$ , and (b) the gas tables. The molecular weight of the combustion gases = 28.925. The ratio of products to air by mass = 1.0168.

**8-10** A 50-MW combustion gas turbine cycle using 200 percent of theoretical air has one stage of intercooling no reheat and a 79.8 percent effective regenerator. The compressor and turbine pressure ratios are 8.63 and 8.231 and have polytropic efficiencies of 90 and 90.52 percent, respectively. The inlet and maximum temperatures are 40 and 2140°F. Using the gas tables, calculate (a) the net cycle work, in Btus per pound mass air, (b) the cycle efficiency, and (c) the air mass flow rate, in pound mass per hour, if the mechanical and electrical efficiencies are 95 percent each.

**8-11** A combustion Brayton cycle uses 200 percent of theoretical air. The cycle has an inlet temperature of 500°R and a turbine inlet temperature of 2000°R. The compression ratios in the compressor and turbine are assumed equal to 9. One stage of intercooling and one stage of reheat are used. Assume that all rotary machines have efficiencies of 0.85. A 0.85 effective regenerator is used. Calculate the net work of the cycle and the overall efficiency, using the gas tables.

8-12 It is required to compare the three methods of air cooling of the blades of high-temperature combustion gas turbines: (1) convective, (2) impingement, and (3) combined convection and film (transpiration). Assume for all cases that the blades have a mean surface area of  $100 \text{ cm}^2$  and that the blade surface temperature is not to exceed  $900^\circ\text{C}$ , with a cooling air inlet temperature to the blades of  $300^\circ\text{C}$ . Assume also that the cooling air mass flow rate is  $0.02 \text{ kg/s}$  per blade and that the heat transfer coefficient is the same in all cases,  $2.0 \text{ kW/m}^2 \cdot ^\circ\text{C}$ . Estimate (a) the permissible maximum turbine gas temperature for each of three methods and (b) the net work, in kilojoules per kilogram of air, and the cycle efficiency for methods 1 and 3 only. Take  $k = 1.4$  and  $1.314$  for compressor and turbine, and  $c_p = 1.005, 1.2267$  and  $1.1057 \text{ kJ/kg} \cdot \text{K}$  for compressor, turbine, and heat addition, respectively.

8-13 Consider a combined gas-steam turbine cycle with both machines ideal. Air enters the compressor at  $1 \text{ atm}$  and  $500^\circ\text{R}$ . 200 percent theoretical air gases enter the gas turbine at  $2400^\circ\text{R}$ . The pressure ratio for both compressor and turbine is  $5.624$ . No intercooling, reheat, or regeneration are used in the gas-turbine cycle. The turbine exhaust is used directly without supplementary firing and leaves to the stack at  $1000^\circ\text{R}$ . Steam is produced at  $1000 \text{ psia}$  and  $1000^\circ\text{F}$ . The condenser pressure is  $1 \text{ psia}$ . No feedwater heating is used and the pump work may be ignored. Draw the flow and  $T$ - $s$  diagrams labeling points correspondingly, and calculate (a) the heat added, per pound mass of air, (b) the steam flow per pound mass of air, (c) the combined work, in Btus per pound mass of air, (d) the combined plant efficiency, and (e) the plant efficiency if the steam cycle is inoperative.

8-14 A combined gas-steam-turbine powerplant is designed with four  $50\text{-MW}$  gas turbines and one  $120\text{-MW}$  steam turbine. Each gas turbine operates with compressor inlet temperature  $505^\circ\text{R}$ , turbine inlet temperature  $2450^\circ\text{R}$ , pressure ratio for both compressor and turbine  $5$ , and compressor and turbine polytropic and mechanical efficiencies  $0.87$  and  $0.96$ . The gases leaving the turbines go to a heat-recovery boiler then to a regenerator with an effectiveness of  $0.87$ . The turbine gases correspond to 200 percent of theoretical air. The steam cycle has a turbine steam inlet at  $1200 \text{ psia}$  and  $1450^\circ\text{R}$ , one open-type feedwater heater (not optimally placed) with feedwater temperature to heat-recovery boiler at  $920^\circ\text{R}$ , condenser pressure  $1 \text{ psia}$ , and turbine polytropic and mechanical efficiencies  $0.87$  and  $0.96$ . All electric generator efficiencies are  $0.96$ . Supplementary firing at full load raises the gas temperature to  $3080^\circ\text{R}$ . Draw the cycle flow and  $T$ - $s$  diagrams and find (a) the required steam mass flow rate in the steam turbine in pound mass per hour, (b) the required air mass flow rate in each gas turbine in pound mass per hour, (c) the heat added in the gas cycle and in supplementary firing at full load, (d) the stack gas temperature in degrees Fahrenheit, (e) the cycle efficiency at full load, and (f) the efficiency at startup when only one gas turbine is used at its full load with no supplementary firing or regeneration. (Ignore the steam cycle pump work.)

8-15 Consider the steam generator in a combined cycle of the dual-pressure variety (Fig. 8-25). The combustion gases, corresponding to 200 percent theoretical air, leave supplementary firing at  $1500^\circ\text{R}$  and the steam generator at  $810^\circ\text{R}$ . Steam is generated at  $1000 \text{ psia}$  and  $1000^\circ\text{F}$ , and  $200 \text{ psia}$  and  $500^\circ\text{F}$ , from feedwater at  $300^\circ\text{F}$ . The high- and low-pressure steam mass flow rates are equal. Using the gas tables, calculate (a) the gas mass flow rate, in pound mass per pound mass of total steam, and (b) the gas exit temperature, in degrees Fahrenheit, if only high-pressure steam is generated, for the same gas mass flow rate. The gas molecular weight =  $28.880$ .

8-16 A combined cycle of the type shown in Fig. 8-27 uses helium in the gas turbine portion. The compressor and turbine have the same pressure ratio of  $2.0$ , the same polytropic efficiencies of  $0.85$ , and inlets at  $140$  and  $2040^\circ\text{F}$ , respectively. The regenerator effectiveness is  $0.85$ . The steam cycle operates with  $1000 \text{ psia}$  and  $1000^\circ\text{F}$  steam and condenses at  $1 \text{ psia}$ . The steam turbine polytropic efficiency is  $0.85$ . The feedwater heater has a terminal temperature difference of  $28^\circ\text{F}$ . Calculate (a) the helium mass flow rate, in pound mass per hour, for a combined output of  $200 \text{ MW}$ , and (b) the gas, steam, and combined cycle efficiencies. Ignore the steam cycle pump work.